1 2 9 0

UNIVERSIDADE D
COIMBRA

Carla Filipa Bessa Morgado de Jesus

SPLINE-BASED NUMERICAL METHODS FOR FRACTIONAL DIFFUSION EQUATIONS

Tese no âmbito do Programa Interuniversitário de Doutoramento em Matemática, orientada pela Professora Doutora Ercília Cristina da Costa e Sousa e apresentada ao Departamento de Matemática da Faculdade de Ciências e Tecnologia da Universidade de Coimbra.

Maio de 2022

Spline-based numerical methods for fractional diffusion equations

Carla Filipa Bessa Morgado de Jesus

UC|UP Joint PhD Program in Mathematics

Programa Interuniversitário de Doutoramento em Matemática

PhD Thesis | Tese de Doutoramento

May 2022

Acknowledgements

I would like to express my sincere gratitude to my supervisor, Professor Ercília Sousa, for all the discussions that we have had in the last 6 years. It was a privilege to learn from her, whose excitement about research is amazing to witness. I would also like to thank her for always finding time to help me with patience and a delightful sense of humor. The balance between pushing me to take a step further and allowing me to pursue complementary paths was of extreme importance and played a crucial role in this final work.

I would like to thank FCT for the financial support for my research through the PhD scholarships PD/BI/135311/2017 and PD/BD/142955/2018, under POCH funds, co-financed by the European Social Fund and Portuguese National Funds from MCTES. I also want to express my gratitude to the Centre for Mathematics of the University of Coimbra for the financial support and to the Department of Mathematics of the University of Coimbra, for the important contribution to my academic and personal growth.

I want to thank my PhD colleagues, namely Sara and Daniela, for all the support in my personal and academic life. They made everything easier, funnier and happier and I will always cherish the memories we have together. I would like to extend my gratitude to my friends Carolina, Dulce, Inês and Vânia for supporting me and believing in me throughout this process. Furthermore, I would like to thank Rúben for being such a good supporter, specially in the last year.

And finally, I would like to thank my whole family, but in particular my parents, who are the true loves of my life. Everything I am and everything I have ever accomplished is due to their tremendous effort and endless love and encouragement. I hope I can honor all the sacrifices they made for me.

Abstract

In this thesis we study several numerical methods, based on splines, to approximate the solution of fractional diffusion equations. These equations model anomalous diffusion that can be categorized as subdiffusion or superdiffusion, depending on the associated mean-squared displacement. In the last decades, anomalous diffusion has been a subject of intense research activity and it describes phenomena of different fields such as engineering, hydrology, physics, finance and biology.

The main tool that we use to derivate the numerical methods is splines. Splines are piecewise interpolator functions, defined by a polynomial in each interval and that differ in the degree of the polynomial and in the conditions imposed on the derivatives. The most common splines in literature are of integer degree, namely the linear spline (degree 1) and the cubic spline (degree 3). In this work, we explore splines of degree β where β is a real number between 0 and 2. For sufficiently smooth functions, we verify that the splines of degree β approximate the corresponding functions with order of convergence $\beta+1$. For functions such that $u = O(t^\gamma)$ when $t \to 0$, which are of special interest in the context of anomalous diffusion, we conclude that splines of degree β approximate these functions with convergence order of the minimum between $\beta+1$ and $\gamma+1/2$, when considering the L^2 norm. On other hand, to the L^∞ norm, we obtain the heuristic result to the order of convergence given by the minimum between $\beta+1$ and γ. After this, we approximate the fractional time integral of order α resorting to splines of degree β. For sufficiently smooth functions, the rate of convergence of this approximation is $\beta+1$, both for the L^2 and the L^∞ norms. For functions such that $u = O(t^\gamma)$ when t tends to 0, for the L^2 norm we conclude that the approximation of the integral of order α using splines of order β exhibits a rate of convergence of the minimum between $\beta+1$ and $\gamma+\alpha+1/2$. For the L^∞ norm, the order of convergence is the minimum between $\beta+1$ and $\gamma+\alpha$. In this work, we also study subdiffusion modeled by an equation involving the first derivative in time of that fractional integral. Hence, using the second order central finite difference formula, we obtain a numerical method that is second order accurate in space. Regarding the accuracy in time, the numerical method presents the same order of convergence as the approximation of the fractional integral by a fractional spline.

Concerning superdiffusion, we define a fractional integral in space that we approximate by the linear spline, that can be seen as the fractional spline of degree 1. We consider two different types of superdiffusion, depending on the value of α to be between 0 and 1 or between 1 and 2, since each of these cases originates a different equation. For $0 < \alpha < 1$, we study three numerical methods: one using a second order central approximation, other using a first order upwind approximation and another using a second order upwind approximation. From the study of the stability and consistency of the numerical methods, we conclude that the best one is the second order upwind scheme, since it is second order accurate and does not raise problems for larger meshes, as happens for the central method that presents solutions with spurious oscillations. For $1 < \alpha < 2$, we derive a numerical method for the problem of superdiffusion with a reflecting wall, based on the linear spline for the space approximation and on the Crank-Nicolson method for the time approximation. We complete the convergence analysis and conclude that the numerical method is second order convergent both in time and space.

Throughout this thesis, the stability analysis is made for the different numerical methods considering the von Neumann theory and all the conclusions stated are corroborated and illustrated by numerical methods implemented by us in MATLAB ®. From numerical experiments, we also infer the influence of the value of α regarding the processes of subdiffusion and superdiffusion.

Keywords: fractional splines, fractional differential equations, subdiffusion equation, Lévy flights, Riemann-Liouville derivatives, finite difference methods, reflecting boundary condition.

Resumo

Nesta tese estudamos vários métodos numéricos, baseados em splines, para aproximar soluções de equações de difusão com derivadas fracionárias. Estas equações modelam difusão anómala que pode classificar-se como subdifusão ou superdifusão, dependendo do momento de segunda ordem do deslocamento associado. A difusão anómala é um tema que tem despertado cada vez mais interesse ao longo das últimas décadas e que descreve fenómenos em várias áreas tais como engenharia, hidrologia, física, finanças e biologia.

Para a construção dos métodos numéricos, utilizamos como ferramenta principal os splines. Splines são funções interpoladoras segmentadas, definidas em cada intervalo por um polinómio, e que variam consoante o grau do polinómio e as condições impostas sobre as derivadas. Na literatura, os splines mais comuns são os de grau inteiro, nomeadamente os splines lineares (de grau 1) e os splines cúbicos (de grau 3). Neste trabalho, exploramos os splines de grau β, onde β é um número real entre 0 e 2. Para funções suficientemente regulares, verificamos que os splines de grau β aproximam as respetivas funções com ordem de convergência $\beta+1$. Para funções do tipo $u=O(t^\gamma)$ quando $t\rightarrow 0$, que são funções de interesse no contexto da difusão anómala, concluímos que os splines de grau β aproximam estas funções com uma ordem de convergência que é o mínimo entre $\beta+1$ e $\gamma+1/2$ para a norma L^2. Por outro lado, considerando a norma L^∞, obtemos o resultado heurístico para a ordem de convergência do mínimo entre $\beta+1$ e γ. Depois deste estudo, aproximamos integrais fracionários de ordem α com recurso aos splines de ordem β. Para funções suficientemente regulares, tanto para a norma L^2 como para a norma L^∞, obtemos uma taxa de convergência de $\beta+1$. Para funções do tipo $u=O(t^\gamma)$ quando t tende para 0, para a norma L^2 deduzimos que a aproximação do integral de ordem α baseada em splines de grau β apresenta uma taxa de convergência que é o mínimo entre $\beta+1$ e $\gamma+\alpha+1/2$. Para a norma L^∞ obtemos que a ordem de convergência é o mínimo entre $\beta+1$ e $\gamma+\alpha$. Neste trabalho estudamos também o fenómeno de subdifusão, modelado por uma equação envolvendo a derivada de primeira ordem no tempo do integral fracionário. Desse modo, recorrendo à fórmula de diferenças finitas no espaço, obtemos um método numérico de segunda ordem de convergência no espaço e provamos que, no tempo, o método apresenta a mesma ordem de convergência que a da aproximação do integral fracionário por um spline fracionário.

Para o caso da superdifusão, é definido um integral fracionário no espaço que aproximamos por um spline linear, que pode ser visto como o spline fracionário de grau 1. Consideramos dois tipos de superdifusão, dependendo se α, envolvido na derivada fracionária, está entre 0 e 1 ou entre 1 e 2, uma vez que cada um destes casos origina uma equação diferente. Para $0<\alpha<1$, estudamos três métodos numéricos, um centrado de segunda ordem, um upwind de primeira ordem e um upwind de segunda ordem. Feito o estudo da consistência e da estabilidade, concluímos que o melhor método numérico é o upwind de segunda ordem, uma vez que converge de ordem 2 e não apresenta problemas para malhas mais largas, como é o caso do método centrado de segunda ordem, que dá origem a oscilações. Para $1 < \alpha < 2$, derivamos um método numérico para o problema de superdifusão com uma parede refletora, baseado no spline linear no espaço e no método de Crank-Nicolson no tempo. Fazemos o estudo da convergência e concluímos que o método obtido é de segunda ordem tanto no espaço como no tempo.

Os estudos de estabilidade dos métodos são todos feitos segundo a teoria de von Neumann e as conclusões retiradas nesta tese são todas corroboradas e ilustradas por testes numéricos, implementados por nós em MATLAB ®. A partir de testes numéricos também se infere a influência do parâmetro α nos processos de subdifusão e superdifusão.

Palavras-chave: splines fracionários, equações com derivadas fracionárias, equação de subdifusão, voos de Lévy, derivadas de Riemann-Liouville, métodos de diferenças finitas, condição de fronteira refletora.

Table of contents

List of figures

List of tables

Chapter 1

Introduction

1.1 General introduction

The purpose of this thesis is to derive numerical methods based on splines that provide approximate solutions of fractional partial differential equations. The access to the closed form of solutions related to these equations is quite limited. Therefore, the derivation of numerical methods is of extreme importance, despite the fact that the interest on deriving numerical methods for this type of equations is rather recent. Fractional calculus comes from the XVII century although it is not usually taught in undergraduate courses. One of the first attempts to discuss derivatives of non integer order goes back to 1695, when Leibniz, in a letter to L'Hôpital, made some remarks on the possibility of considering derivatives of order $1/2$. Throughout the centuries, some of the most notable mathematicians made their contributions to the study of this subject, such as Euler, Lagrange, Laplace, Lacroix, Fourier, Abel, Liouville, De Morgan and Riemann [66].

In 1807, Fourier presented a manuscript where he demonstrated that heat propagation in a solid could be described by a partial differential equation. In the same year Laplace showed that the solution of the same equation gave an approximation to a probability event. Between 1880 and 1894, Lord Rayleigh and the economist Edgeworth formulate the stochastic diffusion equation with probability density as the dependent variable, based on Laplace's work [54]. Heat equation ended up being a special case of the diffusion equation, which in turn was derived by Fick in 1855. In his work, Fick modeled the movement of salt in liquids by analogy to the Fourier's model and verified it experimentally [55]. Nevertheless, it was Einstein who, in 1905, unified the phenomenological approach with the probability approach in his work about Brownian motion [37, 51, 54].

Anomalous diffusion takes place when some of the hypothesis considered for classical diffusion are not verified. For the classical diffusion, it was showed that the mean-squared displacement of a particle, represented by $< |x(t)|^2 >$, undergoing diffusion grows according to t. For anomalous diffusion, the second order moment grows according to a power of t that is different from 1 or even diverges. When it grows according to a power of t lower than 1, this is, $< |x(t)|^2 >\sim t^\alpha$ with $0 < \alpha < 1$, we have subdiffusion, which is a slow process in the sense of the spreading of particles compared to normal diffusion. For $< |x(t)|^2 >\sim t^\alpha$ with $\alpha > 1$, we are in the presence of superdiffusion. In the case of superdiffusion described by Lévy flights, we have $< |x(t)|^2 >\to \infty$. In this case, the diffusion is called superdiffusion because it can be characterized by their fractional moments as

$< |x(t)|^\eta > \sim t^{\eta/\alpha}$ with $0 < \eta < \alpha$. Rescaling these moments as follows $< |x(t)|^\eta >^{2/\eta} \sim t^{2/\alpha}$ for $0 < \alpha < 2$, we obtain the superdiffusive character [51]. Nowadays, anomalous diffusion appears in several fields, for instance, hydrology [21], biology [8], physics [71] and finance [11].

There are different fractional derivatives such as Caputo, Riemann-Liouville and Grünwall-Letnikov. Other definitions have appeared, but their credibility is controversial [18, 78]. In this work, we use the Riemann-Liouville derivative, which is the operator that naturally emerges from some physical problems, as we will explain later on when describing the models we study in this thesis. Fractional operators are harder to handle numerically than the classical derivatives, since they are nonlocal operators composed by singular kernels. The challenge regarding nonlocality arises when we perform the discretization of fractional operators. When the fractional operator is defined in space, to consider all the needed information we have to deal with a dense iterative matrix of the numerical method. When the fractional operator is defined in time, since at each time step we need to take into account all the previous information, we have to store the solution for all the considered instants. Hence, the numerical methods constructed to approximate solutions of equations involving this type of derivative are more demanding than the numerical methods for the classical differential equations.

1.2 Statement of the main problem

The subject of anomalous diffusion is at the moment a field rich in open problems. Our work involves the following main problems of anomalous diffusion: subdiffusion, superdiffusion and superdiffusion with a reflecting boundary.

To the best of our knowledge, the majority of the numerical methods developed for fractional differential equations that model superdiffusion were, until recently, numerical methods of order 1 (see, for example, [50, 64, 69, 73]). A numerical method with a second order approximation of the fractional derivative resorting to the linear spline was derived in [74] based on an idea developed for fractional integrals [17]. One of our main questions is to explore the possible advantages of using a fractional spline, instead of a linear one, to approximate a fractional derivative and, consequently, to approximate an anomalous diffusive model, once the fractional splines behave similarly to some solutions of fractional differential equations. Here, we show how we can use fractional splines of order $0 < \beta \leqslant 2$ to approximate a fractional integral that appears in the definition of Riemann-Liouville fractional derivative in time, used to model a subdiffusion problem. Subdiffusion is a less developed subject regarding the use of the Riemann-Liouville derivative [1, 43, 57, 63, 94]. Most of the works developed in the last years that construct numerical methods to solve subdiffusion equations consider the fractional Caputo derivative [13, 29, 34, 45, 62, 76, 87, 92]. However, the model using Caputo derivative is correct only if the diffusive coefficient does not depend on time [27, 48]. The work developed for equations involving the Riemann-Liouville derivative using splines of order $0 < \beta \leqslant 1$ has been presented in [31].

Regarding superdiffusion, the problem with $1 < \alpha < 2$ has been widely studied using, for instance, finite differences [3, 30] and finite element approaches [46], isogeometric collocation methods [88], lattice Boltzmann schemes [10], spectral-Galerkin schemes [25, 91] and discontinuous Galerkin methods [12]. None the less, there exist fewer works heeding the case when $0 < \alpha < 1$ [23, 59, 60, 86]. We derive a family of implicit numerical methods to determine the numerical solutions of the superdiffusive model for $0 < \alpha < 1$. In this work we also present the advantages and disadvantages of each method supported by some numerical computations. In this case, we use the linear spline as the basic tool to approximate the integral and upwind and central approximations to deal with the derivative. This work has been published in [32].

Despite of the Lévy flights related to the superdiffusion problem for $1 < \alpha < 2$ being subject of intense research, the inclusion of boundary conditions in this type of discussion is of special interest. Due to the long jumps, characteristic of these processes, the consideration of boundary conditions is nontrivial, neither from the physical nor the mathematical point of view. The presence of boundaries cannot be uncoupled from the fractional partial differential equation and therefore it modifies the nonlocal fractional space derivative as opposed to what happens when we consider an integer space derivative. We suggest a new approach of the problem with a reflecting boundary to add to the ones already studied in [2, 9, 15, 19, 20, 35, 40]. This work has been published in [33].

1.3 Thesis structure

This thesis is divided into four main chapters. In Chapter 2, we present the most important tool of this work: splines. All the numerical methods constructed in Chapters 4 and 5, where we study subdiffusion and superdiffusion problems, have been based on a spline approximation of a fractional integral operator.

Chapter 2 is composed by four main sections. In Section 2.1, we present the concept of fractional splines on the real line, introduced in [85]. The explicit construction of fractional B-splines, used to define the splines, is not in [85] and therefore we explain the main steps based on [84], where they establish the integer B-splines. After that, we present the fractional splines on an interval and we divide this topic into two parts that need to be treated separately: $0 < \beta \leqslant 1$ and $1 < \beta \leqslant 2$. In Section 2.2, we derive a formula for fractional splines of degree β between 0 and 1. In Section 2.3, we derive a formula for fractional splines of degree β between 1 and 2, which is a more delicate case. The final main part of Chapter 2, Section 2.4, concerns some upper bounds for the error of approximating a function by a fractional spline. The theoretical study is based on Theorem 4.1 of [85] for the L^2 norm and then we derive an upper bound for the approximation of a special type of functions. For the L^∞ norm, we present a heuristic bound for the error. We illustrate all the results with tables regarding the accuracy of these approximations.

Chapter 3 consists of two main sections and it is dedicated to the approximation of integral operators that appear in the definition of the Riemann-Liouville derivatives. In Section 3.1, we use the fractional splines of degree $0 < \beta \leqslant 2$ to approximate the integral involved in the fractional derivative in time and, similarly to Chapter 2, we determine some upper bounds for the integral approximation, using the results obtained in Section 2.4. We present some tables from numerical tests that corroborate the theoretical results. In Section 3.2, we use the linear spline to approximate the integral involved in the spacial fractional derivative, already studied in [76] and, therefore, we only present the integral approximation instead of doing the whole study.

Chapter 4 is focused on subdiffusion. In Section 4.1, we provide some insight on the mathematical model that describes that phenomenon. In Section 4.2, we construct a numerical method based on the approximation derived in Section 3.1 for $0 < \beta \leqslant 1$ and on a finite differences formula. We study the convergence by evaluating the consistency and the stability of the method and illustrate its convergence rate with numerical tests. In Section 4.3, we construct a numerical method based on a finite differences formula and on the approximation derived in Section 3.1, but now for $1 < \beta \leqslant 2$. Due to the complexity of the approximation using fractional splines with degree in this range, the stability study revealed itself to be very complicated. Hence, in this case we only present the numerical experiments that indicate the order of accuracy of the method. In the final main section of this chapter, Section 4.4, we exemplify the behaviour of the solution of the subdiffusive model given an approximation to a narrow Gaussian function as initial condition.

Chapter 5 is about superdiffusion. In Section 5.1, we explain briefly the model problem and from the model emerge two different equations, one for $0 < \alpha < 1$ and another for $1 < \alpha < 2$. Section 5.2 is dedicated to the problem for α between 0 and 1, where a linear spline is used to approximate the integral operator. We consider three ways of approximating the derivative of the integral, construct three numerical methods based on these approximations and study their consistency and stability. We end the section by presenting some numerical experiments to illustrate the rate of convergence of the method and to show the differences between the considered approaches. In Section 5.3, we explore the problem with α between 1 and 2 on the open domain, that has already been studied in [76]. In Section 5.4, we investigate a similar problem but now considering a reflecting wall at $x = 0$, leading to a problem on the semi-infinite domain. We reformulate the model and construct a numerical method for which we study the convergence utilizing results of the problem on the open domain. To conclude this chapter, we present some numerical simulations for the three superdiffusive models with the intent of analyzing the influence of various factors in Section 5.5, with initial condition an approximation of the Dirac delta function. We finish the section with a figure containing two solutions, one of the subdiffusive model and another of the superdiffusive model, illustrating some of the differences between the phenomena.

All the experimental tests have been implemented by us using MATLAB®.

Before we start the study of the problems, we want to introduce some fundamental concepts, definitions and properties that appear throughout the thesis. Hence, in the next chapters, we concentrate our attention on the challenges that arise from our problems.

1.4 Fundamental concepts

In this section, we state some basic concepts, definitions and properties that will appear through the thesis.

Let us start by giving the definition of Fourier transform and inverse Fourier transform.

Definition 1.1 ([77]). *Let $f \in L^1(\mathbb{R})$. The Fourier transform of f is defined by*

$$\hat{f}(\omega) = \int_{-\infty}^{\infty} f(t)\mathrm{e}^{\mathrm{i}\omega t} dt. \tag{1.1}$$

A function f can be in $L^1(\mathbb{R})$ and yet $\hat{f}$ may not be in $L^1(\mathbb{R})$. If $\hat{f}$ belongs to $L^1(\mathbb{R})$, we can define the inverse transform as follows.

Definition 1.2 ([77]). *Let $\hat{f} \in L^1(\mathbb{R})$. The inverse Fourier transform of $\hat{f}$ is defined by*

$$f(t) = \frac{1}{2\pi}\int_{-\infty}^{\infty} \hat{f}(\omega)\mathrm{e}^{-\mathrm{i}\omega t}d\omega. \tag{1.2}$$

In the next proposition we present a property on the Fourier transform of the convolution.

Proposition 1.3 ([77]). *If $f,g \in L^1(\mathbb{R})$, then*

$$\widehat{(f*g)}(\omega) = \hat{f}(\omega)\hat{g}(\omega) \tag{1.3}$$

where

$$(f*g)(t) = \int_{-\infty}^{\infty} f(t-y)g(y)dy.$$

We introduce the gamma function that appears in the definitions of the Riemann-Liouville derivatives and give some of its properties.

Definition 1.4 ([64]). *The gamma function is defined by*

$$\Gamma(z) = \int_0^{\infty} x^{z-1}\mathrm{e}^{-x}dx,$$

where $z > 0$.

Proposition 1.5 ([64]). *The gamma function satisfies the following properties*

$$(a)\ \Gamma(z+1) = z\Gamma(z); \tag{1.4}$$

$$(b)\ \Gamma(n+1) = n!,\ n \in \mathbb{N}_0. \tag{1.5}$$

We proceed with the definition of Riemann Liouville derivative, first in time and then in space.

Definition 1.6 ([64]). *The Riemann-Liouville derivative of order α of a function f is defined for $t > a$ by*

$$D_a^{\alpha}f(t) = \frac{1}{\Gamma(n-\alpha)}\frac{d^n}{dt^n}\int_a^t f(\tau)(t-\tau)^{n-\alpha-1}d\tau, \tag{1.6}$$

where a can be a real number or $a = -\infty$ and n is a positive integer such that $n-1 < \alpha < n$.

Definition 1.7 ([64]). *For $x \in [a,b]$, the left Riemann-Liouville derivative is defined by*

$$\frac{d^{\alpha}f}{dx^{\alpha}}(x) = \frac{1}{\Gamma(n-\alpha)}\frac{d^n}{dx^n}\int_a^x f(\xi)(x-\xi)^{n-\alpha-1}d\xi, \tag{1.7}$$

and the right Riemann-Liouville is defined by

$$\frac{d^\alpha f}{d(-x)^\alpha}(x) = \frac{1}{\Gamma(n-\alpha)}\frac{d^n}{dx^n}\int_x^b f(\xi)(x-\xi)^{n-\alpha-1}d\xi, \tag{1.8}$$

where a can be a real number or $a=-\infty$, b can be a real number or $b=\infty$ and n is a positive integer such that $n-1<\alpha<n$.

Note that the only difference between (1.6) and (1.7) is the notation. We present both cases because Definition 1.6 appears in literature related to problems defined in time and Definition 1.7 appears in literature related to problems defined in space.

We present the generalized binomial coefficients as well as some properties and then the generalized binomial theorem.

Definition 1.8 ([64]). *The generalized binomial coefficients for z and j, possibly non integers, are defined by*

$$\binom{z}{j} = \frac{\Gamma(z+1)}{\Gamma(j+1)\Gamma(z-j+1)}. \tag{1.9}$$

Proposition 1.9. *The following relation between binomial coefficients is valid for j and z, possibly non integers*

$$\binom{z}{j} + \binom{z}{j-1} = \binom{z+1}{j}.$$

Proof. Using the generalized binomial coefficients (1.9), we get

$$\binom{z}{j} + \binom{z}{j-1} = \frac{\Gamma(z+1)}{\Gamma(j+1)\Gamma(z-j+1)} + \frac{\Gamma(z+1)}{\Gamma(j)\Gamma(z-(j-1)+1)}.$$

Multiplying the numerator and denominator of the first fraction by $(z+1-j)$ and the numerator and denominator of the second fraction by j, we obtain

$$\binom{z}{j} + \binom{z}{j-1} = \frac{\Gamma(z+1)(z+1-j)}{\Gamma(j+1)\Gamma(z+1-j)(z+1-j)} + \frac{j\Gamma(z+1)}{j\Gamma(j)\Gamma(z+1-j+1)},$$

that, using the property of the gamma function (1.4), is equivalent to

$$\binom{z}{j} + \binom{z}{j-1} = \frac{\Gamma(z+2)}{\Gamma(j+1)\Gamma(z+1-j+1)} = \binom{z+1}{j}.$$

□

Proposition 1.10 ([64]). *The generalized binomial theorem states that for $z>0$,*

$$(x+y)^z = \sum_{k=0}^{\infty}\binom{z}{k}(-1)^k x^k y^{z-k}. \tag{1.10}$$

Next, we refer two properties involving integrals. The first one will be used in Theorem 3.1 Chapter 3. The second one will be used many times during the thesis.

Proposition 1.11 ([53]). *Given $f \in L^p(\Omega_1 \times \Omega_2)$, f satisfies the following generalized Minkowski's integral inequality*

$$\left(\int_{\Omega_1}\left|\int_{\Omega_2} f(x,y)dy\right|^p dx\right)^{\frac{1}{p}} \leqslant \int_{\Omega_2}\left(\int_{\Omega_1}|f(x,y)|^p\, dx\right)^{\frac{1}{p}} dy. \tag{1.11}$$

Proposition 1.12 ([81]). *For $z,\ w>0$ is valid the following equality*

$$\int_a^b (\xi-a)^{z-1}(b-\xi)^{w-1}d\xi = (b-a)^{z+w-1}\frac{\Gamma(z)\Gamma(w)}{\Gamma(z+w)}. \tag{1.12}$$

Using the last equality, we compute a fractional derivative of the power function.

Proposition 1.13. *The fractional derivative D_0^α of t^γ is given by*

$$D_0^\alpha(t^\gamma) = \frac{\Gamma(\gamma+1)}{\Gamma(\gamma-\alpha+1)}t^{\gamma-\alpha}. \tag{1.13}$$

Proof. From definition (1.6)

$$D_0^\alpha(t^\gamma) = \frac{1}{\Gamma(n-\alpha)}\frac{d^n}{dt^n}\int_0^t \tau^\gamma(t-\tau)^{n-\alpha-1}d\tau.$$

Using (1.12) we get

$$D_0^\alpha(t^\gamma) = \frac{\Gamma(\gamma+1)\Gamma(n-\alpha)}{\Gamma(n-\alpha)\Gamma(\gamma-\alpha+n+1)}\frac{d^n}{dt^n}t^{\gamma-\alpha+n}.$$

For $\gamma>-1$, taking the derivative and using (1.4), we obtain

$$\begin{aligned} D_0^\alpha(t^\gamma) &= \frac{\Gamma(\gamma+1)}{\Gamma(\gamma-\alpha+n+1)}(\gamma-\alpha+n)\frac{d^{n-1}}{dt^{n-1}}t^{\gamma-\alpha+n-1} \\ &= \frac{\Gamma(\gamma+1)}{\Gamma(\gamma-\alpha+n)}\frac{d^{n-1}}{dt^{n-1}}t^{\gamma+n-1-\alpha}. \end{aligned}$$

Repeating the procedure $(n-1)$ times, we arrive to

$$D_0^\alpha(t^\gamma) = \frac{\Gamma(\gamma+1)}{\Gamma(\gamma-\alpha+1)}t^{\gamma-\alpha}.$$

□

In what follows, we introduce the Dirac delta function and some of its properties.

Definition 1.14 ([47]). *The Dirac delta function can be expressed in distributional sense as*

$$\delta(t-x) = \frac{1}{2\pi}\int_{-\infty}^{\infty} \mathrm{e}^{\mathrm{i}\xi(x-t)}d\xi. \tag{1.14}$$

Proposition 1.15 ([47])**.** *The Dirac delta function satisfies the following properties*

(a) $\delta(x) = \delta(-x)$;

(b) $\displaystyle\int_{-\infty}^{\infty} f(t)\delta(t-T)dt = f(T)$.

We continue with the Fourier transform of the Riemann-Liouville derivatives.

Proposition 1.16 ([36])**.** *The Fourier transform satisfies*

$$\mathscr{F}\left\{\frac{d^\alpha f}{dx^\alpha}(x)\right\} = (-\mathrm{i}\omega)^\alpha \hat{f}(\omega), \quad \alpha > 0. \tag{1.15}$$

and

$$\mathscr{F}\left\{\frac{d^\alpha f}{d(-x)^\alpha}(x)\right\} = (\mathrm{i}\omega)^\alpha \hat{f}(\omega), \quad \alpha > 0. \tag{1.16}$$

We finish this chapter on introductory concepts with the computation of the Fourier transforms of the delta function and of the one-sided power function. Although the majority of the results are for functions in L^1, we will need to consider functions that do not belong to L^1. The Fourier transform in the distributional sense of a tempered distribution g satisfies

$$\int_{-\infty}^{\infty} \hat{g}(\omega)\varphi(\omega)d\omega = \int_{-\infty}^{\infty} g(t)\hat{\varphi}(t)dt, \tag{1.17}$$

where φ is a Schwartz function [77].

Proposition 1.17. *The Fourier transform of the Dirac delta function is* $\hat{\delta}(\omega) = 1$.

Proof. The Dirac function is a tempered distribution, which implies that its Fourier transform satisfies

$$\int_{-\infty}^{\infty} \hat{\delta}(\omega)\varphi(\omega)d\omega = \int_{-\infty}^{\infty} \delta(t)\hat{\varphi}(t)dt, \tag{1.18}$$

where φ is a Schwartz function. Noting that, from Proposition 1.15(b),

$$\int_{-\infty}^{\infty} \delta(t)\hat{\varphi}(t)dt = \hat{\varphi}(0)$$

and considering $\omega = 0$ in

$$\hat{\varphi}(\omega) = \int_{-\infty}^{\infty} \varphi(t)\mathrm{e}^{-\mathrm{i}\omega t}dt,$$

we get

$$\int_{-\infty}^{\infty} \delta(t)\hat{\varphi}(t)dt = \int_{-\infty}^{\infty} \varphi(\omega)d\omega.$$

From this and (1.18), we conclude that $\hat{\delta}(\omega) = 1$. □

Proposition 1.18. *The Fourier transform of the one sided power function* t_+^β *is given by*

$$\hat{t}_+^\beta(\omega) = \frac{\Gamma(\beta+1)}{(-\mathrm{i}\omega)^{\beta+1}}, \tag{1.19}$$

where

$$t_+^\beta = \begin{cases} t^\beta, & \textit{for } t \geqslant 0, \\ 0, & \textit{for } t < 0. \end{cases}$$

Proof. The Fourier transform of the one sided power function is calculated using the relation (1.15). Computing the fractional derivative of t_+^β,

$$D_{-\infty}^{\beta+1} t_+^\beta = \frac{1}{\Gamma(n-(\beta+1))} \frac{d^n}{dt^n} \int_{-\infty}^{t} \tau_+^\beta (t-\tau)^{n-(\beta+1)-1} d\tau$$

that is equivalent to

$$D_{-\infty}^{\beta+1} t_+^\beta = \frac{1}{\Gamma(n-(\beta+1))} \frac{d^n}{dt^n} \int_{0}^{t} \tau^\beta (t-\tau)^{n-(\beta+1)-1} d\tau.$$

Resorting to (1.12), we obtain

$$D_{-\infty}^{\beta+1} t_+^\beta = \frac{1}{\Gamma(n-(\beta+1))} \frac{d^n}{dt^n} t_+^{n-1} \frac{\Gamma(\beta+1)\Gamma(n-(\beta+1))}{\Gamma(n)}.$$

The $(n-2)-$th derivative of t_+^{n-1} is

$$\frac{d^{n-2}}{dt^{n-2}} t_+^{n-1} = (n-1)! t_+$$

and the weak derivative of t_+ is the Heaviside function $h(t)$ given by

$$h(t) = \begin{cases} 1, \ t > 0, \\ 0, \ t \leqslant 0. \end{cases}$$

Finally, the distributional derivative of this last function is the Dirac delta function. We conclude that the the $n-$th derivative of t_+^{n-1}, in the sense of distributions, is given by

$$\frac{d^n}{dt^n} t_+^{n-1} = (n-1)! \delta(t).$$

and therefore

$$D_{-\infty}^{\beta+1} t_+^\beta = \frac{\Gamma(\beta+1)}{\Gamma(n)} (n-1)! \delta(t).$$

As n is a positive integer, using (1.5), we have $(n-1)! = \Gamma(n)$ and therefore

$$D_{-\infty}^{\beta+1} t_{+}^{\beta} = \Gamma(\beta+1)\delta(t).$$

Consequently,

$$\widehat{D_{-\infty}^{\beta+1} t_{+}^{\beta}} = \Gamma(\beta+1)\widehat{\delta(t)}.$$

Using Proposition 1.17, we obtain

$$\widehat{D_{-\infty}^{\beta+1} t_{+}^{\beta}} = \Gamma(\beta+1)$$

Then, considering $\alpha = \beta + 1$ in (1.15), the Fourier transform of the one sided power function t_{+}^{β} can be written as

$$\hat{t}_{+}^{\beta}(\omega) = \frac{\Gamma(\beta+1)}{(-i\omega)^{\beta+1}}.$$

□

Chapter 2

Fractional splines

Splines are piecewise functions where each piece is a polynomial and the connections between pieces satisfy conditions imposed on the derivatives up to an order, depending on the type of the spline. The classical splines present in literature are made of polynomials of integer degree. Splines of degree β, $\beta \geqslant 0$, are sums of B-splines with the same degree. The "B" in the word "B-spline" stands for "basis" or "basic". The derivation of the fractional B-splines can be found in [85], where Unser and Blu resorted to the Fourier transform of the classical splines.

In the first section of this chapter, we establish the fractional splines on the real line. In the following two sections, we derive the formulation of the fractional splines on an interval $[t_0, t_M]$ for β between 0 and 1 and then for β between 1 and 2. In the fourth and last section of this chapter, we present some theoretical results for the error bounds for the fractional spline approximation in the L^2 norm and some heuristic results for the L^∞ norm.

2.1 Splines on the real line

We construct the fractional B-splines following similar ideas to the ones presented in [84] for integer B-splines. Consider the formula of the B-splines of order $n+1$ (or degree n), given by

$$B_+^0(t) = \begin{cases} 1, & 0 < t < 1, \\ 0, & \text{otherwise,} \end{cases} \qquad \text{and} \quad B_+^n(t) = \underbrace{B_+^0(t) * B_+^0(t) * \cdots * B_+^0(t)}_{(n+1) \text{ times}},$$

where " $*$ " represents the convolution operation.

Let us construct the B-splines using the Fourier transform. The Fourier transform of $B_+^0(t)$ is given by

$$\hat{B}_+^0(\omega) = \int_{-\infty}^{+\infty} B_+^0(t) \mathrm{e}^{\mathrm{i}\omega t} dt.$$

Taking into account the definition of $B_+^0(t)$, it is easy to obtain

$$\hat{B}_+^0(\omega) = \frac{1 - \mathrm{e}^{\mathrm{i}\omega}}{-\mathrm{i}\omega}.$$

Using the convolution property (1.3), we have

$$\hat{B}_+^n(\omega) = \left(\hat{B}_+^0(\omega)\right)^{n+1},$$

which leads us to

$$\hat{B}_+^n(\omega) = \left(\frac{1-\mathrm{e}^{\mathrm{i}\omega}}{-\mathrm{i}\omega}\right)^{n+1}.$$

If we generalize and replace n by a fractional number, β, we get

$$\hat{B}_+^\beta(\omega) = \left(\frac{1-\mathrm{e}^{\mathrm{i}\omega}}{-\mathrm{i}\omega}\right)^{\beta+1}.$$

Using the inverse Fourier transform of t_+^β (1.19), we can write

$$\hat{t}_+^\beta(\omega)\frac{(-\mathrm{i}\omega)^{\beta+1}}{\Gamma(\beta+1)} = 1,$$

which can be introduced in the Fourier transform of the B-spline as follows

$$\hat{B}_+^\beta(\omega) = \left(\frac{1-\mathrm{e}^{\mathrm{i}\omega}}{-\mathrm{i}\omega}\right)^{\beta+1}\frac{(-\mathrm{i}\omega)^{\beta+1}}{\Gamma(\beta+1)}\hat{t}_+^\beta(\omega).$$

Applying the generalized binomial theorem to $\left(1-\mathrm{e}^{\mathrm{i}\omega}\right)^{\beta+1}$, we get

$$\hat{B}_+^\beta(\omega) = \frac{1}{\Gamma(\beta+1)}\sum_{j=0}^{\infty}\binom{\beta+1}{j}(-1)^j\mathrm{e}^{\mathrm{i}\omega j}\hat{t}_+^\beta(\omega).$$

Let us now compute the inverse Fourier transform of $\hat{B}_+^\beta(\omega)$. Considering the formula (1.3) with $\hat{u}(\omega) = \mathrm{e}^{\mathrm{i}\omega j}$ and $\hat{v}(\omega) = \hat{t}_+^\beta(\omega)$, if we compute the inverse transform of $\hat{u}$ and do the convolution with t_+^β, we obtain the formula for the B-splines. The inverse Fourier transform of $\hat{u}$ is

$$u(t) = \frac{1}{2\pi}\int_{-\infty}^{\infty}\mathrm{e}^{\mathrm{i}\omega j}\mathrm{e}^{-\mathrm{i}\omega t}d\omega = \frac{1}{2\pi}\int_{-\infty}^{\infty}\mathrm{e}^{\mathrm{i}\omega(j-t)}d\omega = \delta(t-j),$$

using (1.14). From (1.3), the inverse Fourier of $\widehat{u}(\omega)\widehat{v}(\omega)$ is $(u*v)(t)$. Therefore,

$$t_+^\beta * \delta(t-j) = \int_{-\infty}^{\infty}\tau_+^\beta\delta(t-j-\tau)d\tau = \int_{-\infty}^{\infty}\tau_+^\beta\delta(\tau-(t-j))d\tau = (t-j)_+^\beta,$$

from Proposition 1.15. Finally, we arrive to the following formula for the fractional B-spline

$$B_+^\beta(t) = \frac{1}{\Gamma(\beta+1)}\sum_{j=0}^{\infty}(-1)^j\binom{\beta+1}{j}(t-j)_+^\beta, \tag{2.1}$$

where

$$(t-j)_+ = \begin{cases} t-j, & \text{for } t \geqslant j, \\ 0, & \text{for } t < j. \end{cases}$$

Note that, for $\beta = 1$, the linear B-spline given by (2.1) is

$$B_+^{\beta}(t) = \frac{1}{\Gamma(2)}\left(t_+ - 2(t-1)_+ + (t-2)_+\right)$$

which means that, when $0 \leqslant t < 1$,

$$B_+^{\beta}(t) = t;$$

when $1 \leqslant t < 2$,

$$B_+^{\beta}(t) = t - 2(t-1) = 2 - t;$$

and when $t \geqslant 2$,

$$B_+^{\beta}(t) = t - 2(t-1) + t - 2 = 0.$$

For $t < 0$ we have $B_+^{\beta}(t) = 0$, since none of the parcels of the B-spline is positive. Therefore, we get the classical linear B-spline as we usually see it in literature [28].

Some of the characteristics of the classical B-splines, more specifically their positivity and local support, do not hold when considering fractional B-splines. In Figure 2.1 at left, we can see an illustration of the integer B-splines from $\beta = 0$ to the cubic B-spline. At right, we observe the fractional B-splines from degree 0 to degree 3, with an interval of 0.2 between each of them. The fact that the fractional B-splines are not always nonnegative is illustrated in this figure. The nonexistence of compact support increases the need to characterize the B-splines decay. In [85] this is analyzed and it is proved that the fractional B-splines are in L^1 for $\beta > -1$ and in L^2 for $\beta > -1/2$.

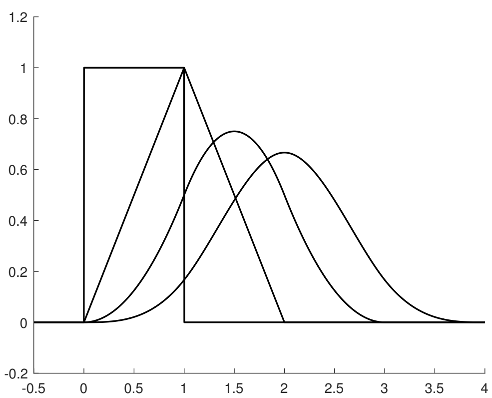

(a)

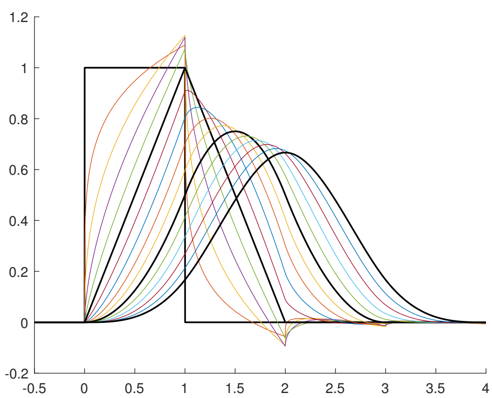

(b)

Fig. 2.1 (a) Classical B-splines (step, linear, quadratic and cubic). (b) Fractional B-splines (from $\beta = 0$ to $\beta = 3$ with a difference of 0.2). Classical B-splines are represented using a thicker line.

We can define the B-splines on the uniform grid $\Delta t\mathbb{Z}$ [28] as

$$B_{+}^{\beta}(t) = \frac{1}{\Gamma(\beta+1)} \sum_{j=0}^{\infty} (-1)^j \binom{\beta+1}{j} \left(\frac{t}{\Delta t} - j\right)_{+}^{\beta}, \tag{2.2}$$

with stepsize Δt. These functions are not centered (see Figure 2.1). Nevertheless, we can shift them and arrive to the centered B-splines (see Figure2.2), which are given by

$$B_{+}^{\beta}(t) = \frac{1}{\Gamma(\beta+1)} \sum_{j=0}^{\infty} (-1)^j \binom{\beta+1}{j} \left(\frac{t}{\Delta t} - j + \frac{\beta+1}{2}\right)_{+}^{\beta}. \tag{2.3}$$

In this work, we consider the shifted splines in order to have them centered on each interval.

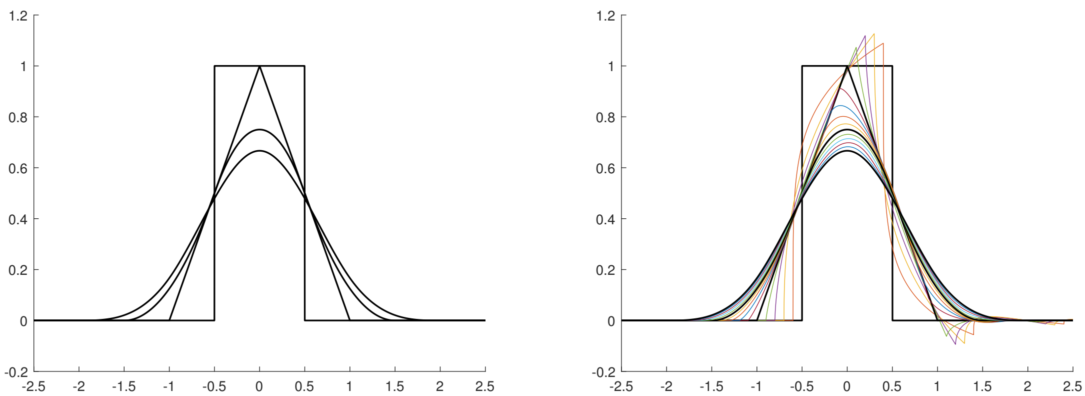

(a) (b)

Fig. 2.2 (a) Shifted classical B-splines (step, linear, quadratic and cubic). (b) Shifted fractional B-splines (from $\beta = 0$ to $\beta = 3$ with a difference of 0.2). Classical B-splines are represented using a thicker line.

Considering now a different grid, with a sequence of knots $\{t_k\}_{k\in\mathbb{Z}}$, a spline of degree β is defined by [85]

$$s_{\beta}(t) = \sum_{k\in\mathbb{Z}} c_k B_{+}^{\beta}(t - t_k). \tag{2.4}$$

Using formula (2.3) of B_{+}^{β}, we get

$$s_{\beta}(t) = \frac{1}{\Gamma(\beta+1)} \sum_{k\in\mathbb{Z}} c_k \sum_{j=0}^{+\infty} (-1)^j \binom{\beta+1}{j} \left(\frac{t-t_k}{\Delta t} - j + \frac{\beta+1}{2}\right)_{+}^{\beta}. \tag{2.5}$$

The only issue remaining is how to determine the coefficients c_k. The number of constants that need to be determined depends on the degree of the spline. However, one characteristic of splines regardless their degree is that they are interpolating functions.

In the next two sections, we explain how to approximate a function u defined in $[t_0, t_M]$ by a fractional spline in the uniform mesh. We split the cases of $0 < \beta \leqslant 1$ and $1 < \beta \leqslant 2$, because despite the logic being similar, there are some details that need to be differentiated.

2.2 Splines of degree $0 < \beta \leqslant 1$ on an interval

We consider splines of degree $0 < \beta \leqslant 1$ and, in particular, for $\beta = 1$ we obtain the classical linear spline. The B-spline of degree 1, also known as hat function, is used not only in image processing [16, 84] but also in fractional calculus [42, 63, 76] and other fields such as medicine [80].

Let us proceed with the formulation of splines of degree between 0 and 1 with $t \in [t_0, t_M]$. Let $t_{i+1} = t_i + \Delta t$ for $i = 0, \ldots, M-1$. Let us analyze

$$\left(\frac{t-t_k}{\Delta t} - j + \frac{\beta+1}{2}\right)_+^\beta .$$

We have

$$\left(\frac{t-t_k}{\Delta t} - j + \frac{\beta+1}{2}\right)_+^\beta = \begin{cases} \left(\frac{t-t_k}{\Delta t} - j + \frac{\beta+1}{2}\right)^\beta, & \text{if } \frac{t-t_k}{\Delta t} - j + \frac{\beta+1}{2} > 0 \\ 0, & \text{otherwise.} \end{cases} \tag{2.6}$$

Then, it is different from zero for

$$\frac{t-t_k}{\Delta t} - j + \frac{\beta+1}{2} > 0$$

which means that

$$t > t_k + j\Delta t - \frac{\beta+1}{2}\Delta t. \tag{2.7}$$

As t is, at most, equal to t_M, we find that the highest k satisfying (2.7) for which exists a nonzero parcel (2.6) is such that

$$t_M > t_k - \frac{\beta+1}{2}\Delta t. \tag{2.8}$$

Note that the limit case is to consider k for which t_M satisfies (2.8), but no other of the following inequalities

$$t_M > t_k - \frac{\beta+1}{2}\Delta t + j\Delta t, \quad \forall j > 0.$$

As we are considering a uniform mesh,

$$t_M > t_k - \frac{\beta+1}{2}\Delta t$$

is equivalent to

$$M + \frac{\beta+1}{2} > k$$

In this case, $0 < \beta \leqslant 1$, which means that $1/2 < (\beta+1)/2 \leqslant 1$ that gives us

$$M + \frac{1}{2} < M + \frac{\beta+1}{2} \leqslant M + 1$$

and, consequently, $k_{max} = M$.

Remember that t is at least t_0 and for $j = 0$

$$\frac{t_0 - t_k}{\Delta t} + \frac{\beta + 1}{2} > 0$$

implies

$$k < \frac{\beta + 1}{2}$$

and then $k_{min} = 0$. Therefore, we arrive to the following formula of the spline

$$s_\beta(t) = \frac{1}{\Gamma(\beta+1)} \sum_{k=0}^{M} c_k \sum_{j=0}^{+\infty} (-1)^j \binom{\beta+1}{j} \left(\frac{t - t_k}{\Delta t} - j + \frac{\beta+1}{2} \right)_+^\beta .$$

From this, we conclude that we have to determine $M+1$ coefficients c_k such that $s_\beta(t_i) = u(t_i)$ for $i = 0, \ldots, M$, which is equivalent to the system

$$\sum_{k=0}^{M} c_k \frac{1}{\Gamma(\beta+1)} \sum_{j=0}^{+\infty} (-1)^j \binom{\beta+1}{j} \left(\frac{t_i - t_k}{\Delta t} - j + \frac{\beta+1}{2} \right)_+^\beta = u(t_i),\ i = 0, \ldots, M. \tag{2.9}$$

Since $t_i - t_k = (i-k)\Delta t$, we have

$$\left(\frac{t_i - t_k}{\Delta t} - j + \frac{\beta+1}{2} \right)_+^\beta = \left(i - k - j + \frac{\beta+1}{2} \right)_+^\beta .$$

Furthermore, this term is different from 0 only for $j < i - k + (\beta+1)/2$. Then, for $i = 0, \ldots, M$, (2.9) can be written as

$$\sum_{k=0}^{M} c_k \frac{1}{\Gamma(\beta+1)} \sum_{j=0}^{i-k} (-1)^j \binom{\beta+1}{j} \left(i - k - j + \frac{\beta+1}{2} \right)^\beta = u(t_i). \tag{2.10}$$

In particular, if $\beta = 1$, the solution of (2.9) is $c_i = u(t_i),\ i = 0, \ldots, M$. Let us define the coefficients a_{i-k} as

$$a_{i-k} := \frac{1}{\Gamma(\beta+1)} \sum_{j=0}^{i-k} (-1)^j \binom{\beta+1}{j} \left(i - k - j + \frac{\beta+1}{2} \right)^\beta ,$$

for $k \leqslant i$. For $k > i$, $a_{i-k} = 0$. Using this notation in (2.10), we can write

$$\sum_{k=0}^{i} c_k a_{i-k} = u(t_i),\ i = 0, \ldots, M.$$

This system can be represented matricially by $\mathbf{A}\mathbf{c} = \mathbf{u}$ where $\mathbf{c} = [c_0\ \ldots\ c_M]^T$, $\mathbf{u} = [u(t_0)\ \ldots\ u(t_M)]^T$, and

$$\mathbf{A} = \begin{bmatrix} a_0 & 0 & 0 & \dots & 0 & 0 \\ a_1 & a_0 & 0 & \dots & 0 & 0 \\ a_2 & a_1 & a_0 & \dots & 0 & 0 \\ \vdots & \vdots & \vdots & & \vdots & \vdots \\ a_M & a_{M-1} & a_{M-2} & \dots & a_1 & a_0 \end{bmatrix},$$

with

$$a_p = \frac{1}{\Gamma(\beta+1)} \sum_{j=0}^{p} (-1)^j \binom{\beta+1}{j} \left(p - j + \frac{\beta+1}{2}\right)^{\beta}, \ p = 0, \dots, M.$$

The matrix $\mathbf{A}$ is a Toeplitz matrix. A Toeplitz matrix is a matrix where the value of each diagonal is constant. This type of matrices is very important both in theory and applications, specially in mathematical modeling of phenomena where exists shift invariance. They are also used, for example, in integral equations, signal and image processing and, as in our case, computation of spline functions. Some of the properties of Toeplitz matrices and their inversion can be seen in [7, 14, 41, 58, 82, 83]. As $\mathbf{A}$ is a lower triangular Toeplitz matrix, its inverse is also a lower triangular Toeplitz matrix. Then, we can write the coefficients c_k at the expense of $\mathbf{A^{-1}}$ and the values of u as

$$c_k = \sum_{p=0}^{k} \tilde{a}_{k-p} u(t_p),$$

where $\tilde{a}_k$ are the entries of $\mathbf{A^{-1}}$ such that

$$\mathbf{A}^{-1} = \begin{bmatrix} \tilde{a}_0 & 0 & 0 & \dots & 0 & 0 \\ \tilde{a}_1 & \tilde{a}_0 & 0 & \dots & 0 & 0 \\ \tilde{a}_2 & \tilde{a}_1 & \tilde{a}_0 & \dots & 0 & 0 \\ \vdots & \vdots & \vdots & & \vdots & \vdots \\ \tilde{a}_M & \tilde{a}_{M-1} & \tilde{a}_{M-2} & \dots & \tilde{a}_1 & \tilde{a}_0 \end{bmatrix}.$$

These entries $\tilde{a}_r, r = 0, 1, \dots, M$ can be computed recursively [83] by

$$\tilde{a}_0 = \frac{1}{a_0}, \quad \sum_{r=0}^{p} a_r \tilde{a}_{p-r} = 0, \quad p = 1, \dots, M,$$

that is,

$$\tilde{a}_0 = \frac{1}{a_0}, \qquad \tilde{a}_p = -\frac{1}{a_0} \sum_{r=1}^{p} a_r \tilde{a}_{p-r}.$$

The formulation of the case β between 0 and 1 is complete. In the next section, we do a similar formulation for β between 1 and 2.

2.3 Splines of degree $1 < \beta \leqslant 2$ on an interval

We want to approximate a function u by a fractional spline of degree between 1 and 2. Consider once again $t \in [t_0, t_M]$ and the uniform mesh $t_{i+1} - t_i = \Delta t$ for $i = 0, \dots, M-1$. It would be normal to assume that in this case we have the first sum of

$$s_\beta(t) = \frac{1}{\Gamma(\beta+1)} \sum_{k\in\mathbb{Z}} c_k \sum_{j=0}^{+\infty} (-1)^j \binom{\beta+1}{j} \left(\frac{t-t_k}{\Delta t} - j + \frac{\beta+1}{2}\right)_+^\beta$$

defined between 0 and M, as seen before. However, let us analyze this more carefully. We have

$$\frac{t-t_k}{\Delta t} - j + \frac{\beta+1}{2} > 0$$

that corresponds to

$$t > t_k + j\Delta t - \frac{\beta+1}{2}\Delta t.$$

Repeating the logic of last section, as t in $[t_0, t_M]$ is less than or equal to t_M, we have to find the highest k for which

$$t_M > t_k - \Delta t \frac{\beta+1}{2}.$$

With $1 < \beta \leqslant 2$, we arrive to $k_{max} = M+1$, this is, for $t \in [t_0, t_M]$, we have

$$s_\beta(t) = \frac{1}{\Gamma(\beta+1)} \sum_{k=0}^{M+1} c_k \sum_{j=0}^{+\infty} (-1)^j \binom{\beta+1}{j} \left(\frac{t-t_k}{\Delta t} - j + \frac{\beta+1}{2}\right)_+^\beta. \tag{2.11}$$

The step to be taken next is to determine the coefficients $c_k,\ k = 0, \ldots, M+1$, such that the spline interpolates the function u at the points $t_i,\ i = 0, \ldots, M$. To get a unique solution for the coefficients, we have to consider an additional constraint to the problem, that we will talk about later. Being the spline an interpolating function, we have the following $M+1$ equations

$$\sum_{k=0}^{M+1} c_k \frac{1}{\Gamma(\beta+1)} \sum_{j=0}^{+\infty} (-1)^j \binom{\beta+1}{j} \left(\frac{t_i-t_k}{\Delta t} - j + \frac{\beta+1}{2}\right)_+^\beta = u(t_i),\ i = 0, \ldots, M.$$

Furthermore,

$$\left(\frac{t_i-t_k}{\Delta t} - j + \frac{\beta+1}{2}\right)_+^\beta = \left(\frac{t_i-t_k}{\Delta t} - j + \frac{\beta+1}{2}\right)^\beta \text{ for } \frac{t_i-t_k}{\Delta t} - j + \frac{\beta+1}{2} > 0$$

and zero otherwise. Therefore, this is zero for $i-k+(\beta+1)/2 > j$. Since $1 < \beta \leqslant 2$ then $j \leqslant i-k+1$. Hence for $i = 0, \ldots, M$, this can be written as

$$\sum_{k=0}^{M+1} c_k \frac{1}{\Gamma(\beta+1)} \sum_{j=0}^{i-k+1} (-1)^j \binom{\beta+1}{j} \left(\frac{t_i-t_k}{\Delta t} - j + \frac{\beta+1}{2}\right)^\beta = u(t_i). \tag{2.12}$$

In order to obtain all the coefficients, we have to consider an additional constraint.

The quadratic spline, obtained using $\beta = 2$, is a continuous function with continuous derivative and that interpolates in the knots the function we want to approximate . According to [5], a spline of degree 2 can be uniquely determined using one of the extra conditions of the following theorem.

Theorem 2.1. *([5]) Given are the $M+1$ points $(t_i, u(t_i))$ where $t_0 < t_1 < \cdots < t_M$. The interpolation task can then uniquely be solved by a quadratic spline in each of the following described situations:*

- *The first derivative $s_2'(t_k) = f_k$ is given for one arbitrary k in $\{0, \ldots, M\}$.*
- *The second derivative $s_2''(t_k) = g_k$ is given for one arbitrary k in $\{0, \ldots, M-1\}$.*
- *The relationship $z \cdot s_2{}'(t_k) = s_2'(t_{k+1})$ is true for one certain k in $\{0, \ldots, M-1\}$ and $z \neq -1$.*
- *When $M+1$ is an even number, $s_2(t_0) = s_2(t_M)$ and $s_2'(t_0) = s_2'(t_M)$ are true. The spline is constructed as a periodic function with the period $t_M - t_0$. When $M+1$ is an odd number, the antiperiodicity condition $s_2'(t_0) = -s_2'(t_M)$ is true.*

One of the most common additional constraints is to consider $s'(t_0) = u'(t_0)$ or its approximation [4, 90]. However, without rearranging the terms obtained using the equalities (2.12), this condition leads to an unstable scheme [4]. Since the terms involve fractional powers, we can not easily rearrange them. Therefore we need to choose another condition such as $s_\beta'(t_M) = u'(t_M)$, which means that

$$\frac{1}{\Gamma(\beta)\Delta t} \sum_{k=0}^{M+1} c_k \sum_{j=0}^{M-k+1} (-1)^j \binom{\beta+1}{j} \left(\frac{t_M - t_k}{\Delta t} - j + \frac{\beta+1}{2} \right)^{\beta-1} = u'(t_M). \tag{2.13}$$

Let us define the coefficients a_{i-k+1}, for $k \leqslant i+1$, as

$$a_{i-k+1} := \frac{1}{\Gamma(\beta+1)} \sum_{j=0}^{i-k+1} (-1)^j \binom{\beta+1}{j} \left(i - k - j + \frac{\beta+1}{2} \right)^{\beta}$$

and, for the other values of k, $a_{i-k+1} = 0$. Furthermore, let us define

$$\overline{a}_{M-k+1} := \frac{1}{\Gamma(\beta)\Delta t} \sum_{j=0}^{M-k+1} (-1)^j \binom{\beta+1}{j} \left(M - k - j + \frac{\beta+1}{2} \right)^{\beta-1}.$$

We can write the system (2.12) as

$$\sum_{k=0}^{i+1} c_k a_{i-k+1} = u(t_i),\ i = 0, \ldots, M \tag{2.14}$$

and (2.13) as

$$\sum_{k=0}^{M+1} c_k \overline{a}_{M-k+1} = u'(t_M). \tag{2.15}$$

This can be represented matricially by $\mathbf{A_M c} = \mathbf{u}$ where $\mathbf{c} = [c_0 \ \ldots \ c_{M+1}]^T$, $\mathbf{u} = [u'(t_M)\ u(t_0)\ \ldots\ u(t_M)]^T$, and

$$\mathbf{A_M} = \begin{bmatrix} \overline{a}_{M+1} & \overline{a}_M & \overline{a}_{M-1} & \dots & \overline{a}_1 & \overline{a}_0 \\ a_1 & a_0 & 0 & \dots & 0 & 0 \\ a_2 & a_1 & a_0 & \dots & 0 & 0 \\ \vdots & \vdots & \vdots & & \vdots & \vdots \\ a_{M+1} & a_M & a_{M-1} & \dots & a_1 & a_0 \end{bmatrix}, \tag{2.16}$$

where

$$a_p = \frac{1}{\Gamma(\beta+1)} \sum_{j=0}^{p} (-1)^j \binom{\beta+1}{j} \left(p-1-j+\frac{\beta+1}{2} \right)^{\beta}, \; p = 0,\dots,M+1$$

and

$$\overline{a}_p = \frac{1}{\Gamma(\beta)\Delta t} \sum_{j=0}^{p} (-1)^j \binom{\beta+1}{j} \left(p-1-j+\frac{\beta+1}{2} \right)^{\beta-1}, \; p = 0,\dots,M+1.$$

The matrix $\mathbf{A_M}$ is no longer a Toeplitz matrix and we do not have an explicit recursive formula to obtain its inverse elements as before. A possible way to handle matrix (2.16) in order to compute its inverse is to separate the matrix as follows

$$\mathbf{A_M} = \begin{bmatrix} a_0 & 0 & 0 & \dots & 0 & 0 \\ a_1 & a_0 & 0 & \dots & 0 & 0 \\ a_2 & a_1 & a_0 & \dots & 0 & 0 \\ \vdots & \vdots & \vdots & & \vdots & \vdots \\ a_{M+1} & a_M & a_{M-1} & \dots & a_1 & a_0 \end{bmatrix} + \begin{bmatrix} \overline{a}_{M+1}-a_0 & \overline{a}_M & \overline{a}_{M-1} & \dots & \overline{a}_1 & \overline{a}_0 \\ 0 & 0 & 0 & \dots & 0 & 0 \\ 0 & 0 & 0 & \dots & 0 & 0 \\ \vdots & \vdots & \vdots & & \vdots & \vdots \\ 0 & 0 & 0 & \dots & 0 & 0 \end{bmatrix} \tag{2.17}$$

and calculate the inverse as described in [52].

In the next section, we derive the error bounds for the interpolation when using fractional splines of degree between 0 and 2.

2.4 Error bounds for the fractional spline interpolation

In this section, we discuss the order of approximation of the splines of degree between 0 and 2 both for the L^2 and L^∞ norms. As we referred at the beginning of the chapter, analyzing the rate of decay of the error as the step Δt goes to zero is specially important, since not all the splines have compact support. We start by examining the error for the L^2 norm.

2.4.1 Error bounds in the L^2 norm

Before presenting the main theorem, we introduce some definitions that can be found in [6, 56, 85].

For a positive integer m and $1 \leqslant p \leqslant \infty$, the Sobolev space $W^{m,p}$ in $\Omega \subset \mathbb{R}$ is given by

$$W^{m,p}(\Omega) = \{u \in L^p(\Omega) : D^\alpha u \in L^p(\Omega), \forall 0 \leqslant |\alpha| \leqslant m\},$$

For noninteger m, the definition is a little more complex. From [56] for $s \in (0,1)$,

$$W^{s,p}(\Omega) = \left\{ u \in L^p(\Omega) : \frac{|u(x)-u(y)|}{|x-y|^{\frac{1}{p}+s}} \in L^p(\Omega \times \Omega) \right\}.$$

When $s > 1$, with $s = m + \sigma$ with m integer and $\sigma \in (0,1)$, $W^{s,p}(\Omega)$ is defined as

$$W^{s,p}(\Omega) = \{u \in W^{m,p}(\Omega) : D^{\alpha} u \in W^{\sigma,p}(\Omega), \forall \alpha : |\alpha| = m\}.$$

In literature, we can find a theoretical result about the behavior of the fractional spline approximation error based on the Fourier domain characterization of the approximation. Therefore, we give an alternative definition of Sobolev spaces using Fourier transform [24, 56]. When $p = 2$, the Sobolev spaces can be represented by $H^r(\mathbb{R})$ and are defined as the space functions that satisfy

$$\int_{\mathbb{R}} (1+\omega^2)^r |\hat{u}(\omega)|^2 d\omega < \infty,$$

where $\hat{u}$ denotes the Fourier transform of u. For $r = 0$, we get $H^0(\mathbb{R}) = L^2(\mathbb{R})$.

We have the following result regarding the approximation of a function u by the spline defined in (2.5).

Theorem 2.2. *([85]) For all $u \in H^{\beta+1}(\mathbb{R})$, the error is bounded by*

$$||u - s_\beta||_{L^2} \leqslant C_\beta ||D_{-\infty}^{\beta+1} u||_{L^2} \Delta t^{\beta+1},$$

with $C_\beta = \sqrt{2\xi(\beta+2) - 1/2}/\pi^{\beta+1}$, where ξ is the Riemann zeta function defined by $\xi(a) = \sum_{n\geqslant 1} n^{-a}$. This means the fractional splines have a fractional order of approximation $\beta + 1$.

In the context of subdiffusion, functions of the form $u = O(t^\gamma)$ for $t \in [0, t_M]$ and zero otherwise are of special interest, since they have been considered in the context of several partial integro-differential equations with a weakly singular kernel [34, 38, 63, 79]. One important aspect that we need to pay attention is that for small values of γ the first derivative can be unbounded near zero. Therefore, consider the function defined in $[0, t_M]$ given by $u(t) = t^\gamma$. Note that $D_{-\infty}^{\beta+1}(t_+^\gamma) = D_0^{\beta+1}(t^\gamma)$ which is given by

$$D_0^{\beta+1}(t^\gamma) = \frac{1}{\Gamma(1-\beta)} \frac{d^2}{dt^2} \int_0^t \tau^\gamma (t-\tau)^{-\beta} d\tau \tag{2.18}$$

for $0 < \beta \leqslant 1$ and

$$D_0^{\beta+1}(t^\gamma) = \frac{1}{\Gamma(2-\beta)} \frac{d^3}{dt^3} \int_0^t \tau^\gamma (t-\tau)^{1-\beta} d\tau$$

for $1 < \beta \leqslant 2$. In both cases, as proved in Proposition 1.13,

$$D_0^{\beta+1}(t^\gamma) = \frac{\Gamma(\gamma+1)}{\Gamma(\gamma-\beta)} t^{\gamma-\beta-1},$$

for $0 < \beta \leqslant 2$. Hence, for values of t near 0, we have $D_0^{\beta+1}(t^\gamma) = O(t^{\gamma-\beta-1})$ and therefore $||D_0^{\beta+1}(t^\gamma)||_{L^2(0,\Delta t)} = O\left(\Delta t^{\gamma-\beta-1/2}\right)$. Then, the order of the spline approximation is dominated by the term

$$C_\beta ||D_0^{\beta+1}(t^\gamma)||_{L^2(0,\Delta t)} \Delta t^{\beta+1} = O(\Delta t^{\gamma-\beta-1/2} \Delta t^{\beta+1}) = O(\Delta t^{\gamma+1/2}).$$

Finally, combining the result of Theorem 2.2 with the previous discussion, we arrive to the following conclusion. Given a function u such that $u = O(t^\gamma)$ as $t \to 0$, the error of the spline approximation is bounded by

$$||u - s_\beta||_{L^2(0,t_M)} \leqslant C_{\gamma,\beta} \Delta t^{\min\{\beta+1,\gamma+1/2\}}, \tag{2.19}$$

with $C_{\gamma,\beta}$ a constant depending on γ and β.

To illustrate this result, we present some numerical tests that are in agreement with the predicted theoretical upper bound (2.19) for the L^2 norm. According to [22], the function $v(x) = x^\gamma$ belongs to $H^s(0,1)$ for $\gamma > s - 1/2$ with s integer. Furthermore, for $s \in (0,1)$, it can be proved that the function $v(x) = x^\gamma$ belongs to $H^s(0,1)$ for $\gamma > 1/2$. Therefore, functions of the type $u(t) = Ct^\gamma$, with C a constant, belong to $H^{\beta+1}(0,1)$ with $\beta \in (0,1)$ for $\gamma > 3/2$. When $\beta = 1$, the condition is the same. As we are aiming to show that the convergence rate of the approximation of a function using splines is $\min\{\beta+1, \gamma+1/2\}$, for the previous condition the minimum between $\beta+1$ and $\gamma+1/2$ is always $\beta+1$. Nonetheless, it is also easy to prove that $u(t) = Ct$ belongs to $H^{\beta+1}(0,1)$ for $\beta \in (0,1]$ and that $u(t) = Ct^2$ belongs to $H^{\beta+1}(0,1)$ for $\beta \in (1,2]$.

Recall that the evaluation of the numerical results is done in a discrete space. Considering a vector $f = (f(t_0), \ldots, f(t_M))$, with $t_{i+1} - t_i = \Delta t$, the discrete mesh-dependent L^2 norm is given by

$$||f||_2 = \left(\sum_{m=0}^{M} \Delta t |f^m|^2 \right)^{\frac{1}{2}}.$$

In Tables 2.1 and 2.2, we display the numerical results of the approximation of the functions $u(t) = (2t)^{1.6}$ and $u(t) = 2t$ by splines of degree β with $\beta = 0.2, 0.4, 0.6, 0.8, 1$, in order to confirm that the convergence rate is approximately of order $\min\{1+\beta, \gamma+1/2\}$. The rates presented are the mean of the rates obtained between 0.1 and 0.01 and the ones between 0.01 and 0.001.

Table 2.1 Convergence rate in the L^2 norm for the function $u(t) = (2t)^{1.60}$.

Δt	$\beta = 0.2$	$\beta = 0.4$	$\beta = 0.6$	$\beta = 0.8$	$\beta = 1$
0.1	8.3492e-02	4.5657e-02	2.0210e-02	1.3451e-02	9.3879e-03
0.01	5.2315e-03	1.8240e-03	5.0305e-04	2.1679e-04	1.0368e-04
0.001	3.2987e-04	7.2640e-05	1.2625e-05	3.4522e-06	1.0941e-06
Rate	1.20	1.40	1.60	1.80	1.97

In Table 2.1 we obtain a convergence rate of order $\beta+1$ as expected. In Table 2.2, that has the results concerning $u(t) = 2t$, the rate of convergence is $\min\{1+\beta, 1+0.5\}$, that is, for $\beta = 0.2, 0.4$ we have a rate near $\beta+1$ and for the other values of β is 1.5. In the last case, we did not present the

Table 2.2 Convergence rate in the L^2 norm for the function $u(t) = 2t$.

Δt	$\beta = 0.2$	$\beta = 0.4$	$\beta = 0.6$	$\beta = 0.8$
0.1	4.8732e-02	2.7588e-02	8.9149e-03	3.2944e-03
0.01	3.1560e-03	1.2075e-03	3.3322e-04	1.1302e-04
0.001	2.0047e-04	5.0614e-05	1.1453e-05	3.6417e-06
Rate	1.19	1.37	1.45	1.48

error for $\beta = 1$, because as we would be approximating a linear function using a linear spline, the error of approximation would be given by rounding errors.

We also computed numerical tests for functions that are not in $H^{\beta+1}$, that gave us results in concordance with (2.19). In Table 2.3 we present the convergence rate for the function $u(t) = (2t)^{0.4}$. For $\gamma = 0.4$, we display a convergence rate of order 0.9, that is, $\min\{\beta + 1, \gamma + 0.5\}$. In Table 2.4, that has the result relative to $u(t) = (2t)^{0.8}$, the rate of convergence is around $\min\{1 + \beta, 0.8 + 0.5\}$, this is, for $\beta = 0.2$ we have a rate around 1.2 and for the other values of β is around 1.3.

Table 2.3 Convergence rate in the L^2 norm for the function $u(t) = (2t)^{0.4}$.

Δt	$\beta = 0.2$	$\beta = 0.4$	$\beta = 0.6$	$\beta = 0.8$	$\beta = 1$
0.1	9.6527e-02	9.9278e-02	7.4067e-02	7.1098e-02	7.2866e-02
0.01	1.2179e-02	1.2498e-02	9.3250e-03	8.9511e-03	9.1734e-03
0.001	1.5341e-03	1.5734e-03	1.1739e-03	1.1268e-03	1.1548e-03
Rate	0.89	0.90	0.90	0.90	0.90

Table 2.4 Convergence rate in the L^2 norm for the function $u(t) = (2t)^{0.8}$.

Δt	$\beta = 0.2$	$\beta = 0.4$	$\beta = 0.6$	$\beta = 0.8$	$\beta = 1$
0.1	4.6010e-02	3.2317e-02	1.2780e-02	9.3922e-03	1.0480e-02
0.01	3.1332e-03	1.7178e-03	6.4690e-04	4.7073e-04	5.2566e-04
0.001	2.0643e-04	8.9054e-05	3.2502e-05	2.3592e-05	2.6346e-05
Rate	1.17	1.27	1.29	1.30	1.29

We continue by showing the results for $1 < \beta \leqslant 2$, using the functions $u(t) = (2t)^{\gamma}$, with $\gamma = 1.3,\ 1.5,\ 2$ and 4 as examples.

For the cases $u(t) = (2t)^{1.3}$ and $u(t) = (2t)^{1.5}$, the minimum between $\beta + 1$ and $\gamma + 0.5$ is $\gamma + 0.5$. From the observation of Tables 2.5 and 2.6, we can see that the rates of convergence for these functions of 1.8 and 2, respectively, are in agreement with the predicted theoretical results obtained for functions in $H^{\beta+1}$, despite these functions not being in $H^{\beta+1}$. For $u(t) = (2t)^2$ the expected order

Table 2.5 Convergence rate in the L^2 norm for the function $u(t) = (2t)^{1.3}$.

Δt	$\beta = 1.2$	$\beta = 1.4$	$\beta = 1.6$	$\beta = 1.8$	$\beta = 2$
0.1	2.2719e-03	8.7856e-04	3.9671e-04	3.7559e-04	4.0754e-04
0.01	3.611e-05	1.394e-05	6.315e-06	5.958e-06	6.459e-06
0.001	5.725e-07	2.210e-07	1.001e-07	9.442e-08	1.024e-07
Rate	1.80	1.80	1.80	1.80	1.80

Table 2.6 Convergence rate in the L^2 norm for the function $u(t) = (2t)^{1.5}$.

Δt	$\beta = 1.2$	$\beta = 1.4$	$\beta = 1.6$	$\beta = 1.8$	$\beta = 2$
0.1	3.5513e-03	2.0695e-03	1.4677e-03	1.1665e-03	1.0033e-03
0.01	3.650e-05	2.071e-05	1.468e-05	1.167e-05	1.003e-05
0.001	3.689e-07	2.071e-07	1.468e-07	1.167e-07	1.003e-07
Rate	1.99	2.00	2.00	2.00	2.00

Table 2.7 Convergence rate in the L^2 norm for the function $u(t) = (2t)^2$.

Δt	$\beta = 1.2$	$\beta = 1.4$	$\beta = 1.6$	$\beta = 1.8$	$\beta = 2$
0.1	5.0447e-03	2.2964e-03	1.4733e-03	1.1864e-03	1.0547e-03
0.01	3.1002e-05	9.0643e-06	4.7945e-06	3.7556e-06	3.3351e-06
0.001	1.9442e-07	3.5933e-08	1.5431e-08	1.1882e-08	1.0553e-08
Rate	2.21	2.40	2.49	2.50	2.50

Table 2.8 Convergence rate in the L^2 norm for the function $u(t) = (2t)^4$.

Δt	$\beta = 1.2$	$\beta = 1.4$	$\beta = 1.6$	$\beta = 1.8$	$\beta = 2$
0.1	6.0617e-02	2.5721e-02	1.2122e-02	5.5188e-03	2.5388e-03
0.01	3.7171e-04	9.8375e-05	2.9442e-05	8.4502e-06	2.4595e-06
0.001	2.3370e-06	3.8970e-07	7.3655e-08	1.3334e-08	2.4757e-09
Rate	2.21	2.41	2.61	2.81	3.01

of convergence would be $\beta + 1$, for $\beta = 1.2$ and 1.4 and 2.5 for the other values of β, and that was what we obtained in Table 2.7. For $u(t) = (2t)^4$, we get the $\beta + 1$ order of convergence, as shown in Table 2.8 and as predicted by the theoretical results.

2.4.2 Heuristic error bounds in the L^∞ norm

The discussion of the error bounds of the approximation using splines for the L^2 norm is complete. We present error bounds in the L^∞ norm. However, as the last section was based on a theorem that used least square approximation and since that tool has no relation to the maximum norm, a bound in the L^∞ norm is much harder to obtain than the bound in the L^2 norm. Nevertheless, the experimental tests for the L^∞ norm indicate the following result. For u sufficiently smooth and $u \in L^\infty$ we have

$$||u - s_\beta||_{L^\infty} \leqslant C_\beta \Delta t^{\beta+1} ||D^{\beta+1}_{-\infty} u||_{L^\infty}, \tag{2.20}$$

with C_β a constant depending on β.

Once again, we discuss this upper bound when we have the functions u defined in $[0, t_M]$ and such that $u = O(t^\gamma)$ when t approaches 0. The order of approximation will be dominated by the term

$$||D^{\beta+1}_0 (t^\gamma)||_{L^\infty(0,\Delta t)} \Delta t^{\beta+1} = O(\Delta t^{\gamma-\beta-1} \Delta t^{\beta+1}) = O(\Delta t^\gamma).$$

Therefore, if (2.20) holds, for a function u such that $u = O(t^\gamma)$ when $t \to 0$, the interpolation error of the spline approximation is bounded by

$$||u - s_\beta||_{L^\infty(0,t_M)} \leqslant C_{\gamma,\beta} \Delta t^{\min\{\beta+1,\gamma\}}, \tag{2.21}$$

with $C_{\gamma,\beta}$ a constant that depends on both γ and β.

In what follows, we exhibit several numerical tests done for the same type of functions presented in the previous section. This means that, for $0 < \beta \leqslant 1$, we present the results for the function $u(t) = (2t)^\gamma$ for $\gamma = 0.4, 1, 1.2, 1.6$; for $1 < \beta \leqslant 2$, we show the results when $\gamma = 2, 2.5$ and 4.

The numerical results were computed using the following discrete definition of L^∞. Considering a vector $f = (f(t_0), \ldots, f(t_M))$, with $t_{i+1} - t_i = \Delta t$, the discrete mesh-dependent L^∞ norm is given by

$$||f||_\infty = \max_{m=0,\ldots,M} |f^m|.$$

In Tables 2.9 and 2.10, we present the results when the function is $u(t) = (2t)^{0.4}$ and $u(t) = 2t$, respectively. As, in both cases, $\min\{1+\beta, \gamma\} = \gamma$, we obtained the rates of convergence of 0.4 and 1, as expected. In Table 2.11 the tests are done for the function $u(t) = (2t)^{1.6}$ and now the rate of convergence is $1+\beta$ for $\beta < 0.6$ and 1.6 for $\beta \geqslant 0.6$ as predicted by the theoretical result (2.21).

Table 2.9 Convergence rate in the L^∞ norm for the function $u(t) = (2t)^{0.4}$.

Δt	$\beta = 0.2$	$\beta = 0.4$	$\beta = 0.6$	$\beta = 0.8$	$\beta = 1$
0.1	3.0170e-01	3.0170e-01	2.0218e-01	1.7642e-01	1.7038e-01
0.01	1.2011e-01	1.2011e-01	8.0490e-02	7.0236e-02	6.7830e-02
0.001	4.7817e-02	4.7817e-02	3.2043e-02	2.7961e-02	2.7003e-02
Rate	0.40	0.40	0.40	0.40	0.40

Table 2.10 Convergence rate in the L^∞ norm for the function $u(t) = 2t$.

Δt	$\beta = 0.2$	$\beta = 0.4$	$\beta = 0.6$	$\beta = 0.8$
0.1	5.0000e-02	5.0000e-02	1.2107e-02	4.5404e-03
0.010	5.0000e-03	5.0000e-03	1.2107e-03	4.5404e-04
0.001	5.0000e-04	5.0000e-04	1.2107e-04	4.5404e-05
Rate	1.00	1.00	1.00	1.00

Table 2.11 Convergence rate in the L^∞ norm for the function $u(t) = (2t)^{1.60}$.

Δt	$\beta = 0.2$	$\beta = 0.4$	$\beta = 0.6$	$\beta = 0.8$	$\beta = 1$
0.1	7.1719e-02	3.4942e-02	1.7154e-02	1.4683e-02	1.2954e-02
0.010	4.5509e-03	1.4182e-03	4.3090e-04	3.6882e-04	3.2540e-04
0.001	2.8731e-04	5.6562e-05	1.0824e-05	9.2643e-06	8.1736e-06
Rate	1.20	1.40	1.60	1.60	1.60

In Table 2.12, we can see that the results for $u(t) = (2t)^2$ agree with the theoretical ones, since $\min\{\beta+1, 2\} = 2$. In Table 2.13, that refers to the numerical experiments with $u(t) = (2t)^{2.5}$, we get rate of convergence of $\beta+1$ for $\beta < 0.5$ and 2.5 for greater values of β. For $u(t) = (2t)^4$, we obtain $\beta+1$ for the convergence rate, as illustrated in Table 2.14.

Table 2.12 Convergence rate in the L^∞ norm for the function $u(t) = (2t)^2$.

Δt	$\beta = 1.2$	$\beta = 1.4$	$\beta = 1.6$	$\beta = 1.8$	$\beta = 2$
0.1	6.0729e-03	4.2545e-03	3.2050e-03	2.6342e-03	2.3528e-03
0.010	6.0729e-05	4.2545e-05	3.2050e-05	2.6342e-05	2.3528e-05
0.001	6.0729e-07	4.2545e-07	3.2050e-07	2.6342e-07	2.3528e-07
Rate	2.00	2.00	2.00	2.00	2.00

Table 2.13 Convergence rate in the L^∞ norm for the function $u(t) = (2t)^{2.5}$.

Δt	$\beta = 1.2$	$\beta = 1.4$	$\beta = 1.6$	$\beta = 1.8$	$\beta = 2$
0.1	9.5472e-03	3.5715e-03	1.4558e-03	1.1469e-03	9.7733e-04
0.010	6.1093e-05	1.4294e-05	4.6036e-06	3.6269e-06	3.0906e-06
0.001	3.8599e-07	5.6921e-08	1.4558e-08	1.1469e-08	9.7733e-09
Rate	2.20	2.40	2.50	2.50	2.50

Table 2.14 Convergence rate in the L^∞ norm for the function $u(t) = (2t)^4$.

Δt	$\beta = 1.2$	$\beta = 1.4$	$\beta = 1.6$	$\beta = 1.8$	$\beta = 2$
0.1	9.6447e-02	4.4402e-02	1.9671e-02	7.7228e-03	3.5727e-03
0.010	6.6291e-04	1.9261e-04	5.4002e-05	1.3431e-05	3.8933e-06
0.001	4.2175e-06	7.7321e-07	1.3696e-07	2.1781e-08	4.4750e-09
Rate	2.18	2.38	2.58	2.77	2.95

In the next chapter, we use the spline approximation to derive quadrature formulas for the integral operators involved in fractional differential equations.

Chapter 3

Fractional integrals approximations

The main goal of our work is to derive numerical methods for fractional differential equations, related not only with subdiffusion problems but also with superdiffusive models described by Lévy flights. In the next sections, we derive some approximations for the fractional integral operators that will appear later related to the fractional derivatives. In the first section, we approximate the integral operator present in the subdiffusive model using fractional splines. In the second section, we approximate the integral operator related to superdiffusion, using only the linear spline, which was used in [74, 76] and it will be an important tool for the next chapters.

3.1 Time-integral operator of order $0 < \alpha < 1$

The subdiffusive processes can be described using fractional operators with α between 0 and 1. We consider the fractional Riemann-Liouville integral of order α defined by

$$\mathscr{I}^{\alpha}u(t) = \frac{1}{\Gamma(\alpha)}\int_0^t u(\tau)(t-\tau)^{\alpha-1}d\tau, \quad 0<\alpha<1, \tag{3.1}$$

for $t \in [0,b]$. This integral exists when $u \in L^1(0,b)$. The difficulty of the approximation of the Riemann-Liouville derivative is inherent to approximate (3.1). Therefore, we focus on approximating this operator using the splines discussed in the last chapter. The general idea is to compute this integral approximating u by a fractional spline s_β, where β is the degree of the spline. Once again, we divide the cases $0 < \beta \leqslant 1$ and $1 < \beta \leqslant 2$.

Consider the discrete points t_m, $m = 0,\dots,M$, where $t_{m+1} = t_m + \Delta t$, $m = 0,\dots,M-1$. We denote the approximation of (3.1) as $I^{\alpha,\beta}u(t_m)$ defined by

$$I^{\alpha,\beta}u(t_m) = \frac{1}{\Gamma(\alpha)}\int_{t_0}^{t_m} s_\beta(\tau)(t_m-\tau)^{\alpha-1}d\tau. \tag{3.2}$$

In the following subsections, we replace the fractional spline by its explicit formula.

3.1.1 Integral approximation using splines of degree $0 < \beta \leqslant 1$

Recall the formula of the fractional spline with $0 < \beta \leqslant 1$, given by

$$s_\beta(t) = \frac{1}{\Gamma(\beta+1)} \sum_{k=0}^{M} c_k \sum_{j=0}^{+\infty} (-1)^j \binom{\beta+1}{j} \left(\frac{t-t_k}{\Delta t} - j + \frac{\beta+1}{2} \right)_+^\beta . \tag{3.3}$$

Inserting (3.3) in (3.2), we obtain the following expression

$$I^{\alpha,\beta}u(t_m) = \frac{1}{\Gamma(\alpha)} \int_{t_0}^{t_m} \left[\frac{1}{\Gamma(\beta+1)} \sum_{k=0}^{M} c_k \sum_{j=0}^{+\infty} (-1)^j \binom{\beta+1}{j} \left(\frac{\tau-t_k}{\Delta t} - j + \frac{\beta+1}{2} \right)_+^\beta \right] \times (t_m-\tau)^{\alpha-1} d\tau.$$

Note that the terms

$$\left(\frac{\tau-t_k}{\Delta t} - j + \frac{\beta+1}{2} \right)_+^\beta$$

are different from zero only for

$$\frac{\tau-t_k}{\Delta t} - j + \frac{\beta+1}{2} > 0$$

that is equivalent to

$$j < \frac{\tau-t_k}{\Delta t} + \frac{\beta+1}{2}.$$

Since $\tau \leqslant t_m$ and $1/2 < (\beta+1)/2 \leqslant 1$ this means that $j \leqslant m-k$ and we can exchange the infinite sum, that was showed to be finite, with the integral. Furthermore, as $j \geqslant 0$, we conclude that $k_{max} = m$. Hence, we arrive at

$$I^{\alpha,\beta}u(t_m) = \sum_{k=0}^{m} c_k \sum_{j=0}^{m-k} l_{j,k}, \tag{3.4}$$

where

$$l_{j,k} = \frac{1}{\Gamma(\alpha)} \frac{1}{\Gamma(\beta+1)} (-1)^j \binom{\beta+1}{j} \int_{t_0}^{t_m} \left(\frac{\tau-t_k}{\Delta t} - j + \frac{\beta+1}{2} \right)_+^\beta (t_m-\tau)^{\alpha-1} d\tau. \tag{3.5}$$

Let us now pay attention to the integral of the previous formula (3.5). Note that

$$\frac{\tau-t_k}{\Delta t} - j + \frac{\beta+1}{2} \geqslant 0$$

occurs when

$$\tau \geqslant t_k + j\Delta t - \frac{\beta+1}{2}\Delta t.$$

This means that we can consider the lower limit of the integral to be $t_k + j\Delta t - (\beta+1)\Delta t/2$, because before this value the integrand is zero, except when $(j,k) = (0,0)$. Therefore, for all $(j,k) \neq (0,0)$, we can write

$$l_{j,k} = \frac{1}{\Gamma(\alpha)} \frac{1}{\Gamma(\beta+1)} (-1)^j \binom{\beta+1}{j} \frac{1}{\Delta t^\beta} \int_{t_b}^{t_m} (\tau-t_b)^\beta (t_m-\tau)^{\alpha-1} d\tau,$$

where $t_b = t_k + j\Delta t - \Delta t(\beta+1)/2$. Since the equality (1.12) holds, we obtain

$$l_{j,k} = \frac{1}{\Gamma(\alpha)}\frac{1}{\Gamma(\beta+1)}(-1)^j\binom{\beta+1}{j}\frac{1}{\Delta t^\beta}(t_m-t_b)^{\beta+\alpha}\frac{\Gamma(\beta+1)\Gamma(\alpha)}{\Gamma(\beta+\alpha+1)},$$

which can be simplified to

$$l_{j,k} = \frac{\Delta t^\alpha}{\Gamma(\beta+\alpha+1)}(-1)^j\binom{\beta+1}{j}\left(m-k-j+\frac{\beta+1}{2}\right)^{\beta+\alpha}. \tag{3.6}$$

For the case $(j,k)=(0,0)$ we have, from (3.5),

$$l_{0,0} = \frac{1}{\Gamma(\alpha)}\frac{1}{\Gamma(\beta+1)}\int_{t_0}^{t_m}\left(\frac{\tau-t_0}{\Delta t}+\frac{\beta+1}{2}\right)^\beta (t_m-\tau)^{\alpha-1}d\tau.$$

We use the trapezoidal rule to approximate this integral as follows. The integral present in $l_{0,0}$ can be written at the expenses of two other integrals

$$\begin{aligned} l_{0,0} \quad = \quad & \frac{1}{\Gamma(\alpha)}\frac{1}{\Gamma(\beta+1)}\int_{t_0-\Delta t\frac{\beta+1}{2}}^{t_m}\left(\frac{\tau-t_0}{\Delta t}+\frac{\beta+1}{2}\right)^\beta (t_m-\tau)^{\alpha-1}d\tau \\ & -\frac{1}{\Gamma(\alpha)}\frac{1}{\Gamma(\beta+1)}\int_{t_0-\Delta t\frac{\beta+1}{2}}^{t_0}\left(\frac{\tau-t_0}{\Delta t}+\frac{\beta+1}{2}\right)^\beta (t_m-\tau)^{\alpha-1}d\tau \end{aligned}$$

The first integral can be computed as before, with $t_b = t_0 - \Delta t(\beta+1)/2$,

$$l_{0,0} = \frac{1}{\Gamma(\alpha)}\frac{1}{\Gamma(\beta+1)}\left[\frac{1}{\Delta t^\beta}(t_m-t_b)^{\beta+\alpha}\frac{\Gamma(\beta+1)\Gamma(\alpha)}{\Gamma(\beta+\alpha+1)} - \int_{t_b}^{t_0}(\tau-t_b)^\beta (t_m-\tau)^{\alpha-1}d\tau\right].$$

In order to do the computational implementation of the second integral, we approximate it with the trapezoidal rule, arriving to the following result

$$l_{0,0} \approx \frac{1}{\Gamma(\beta+\alpha+1)}\frac{1}{\Delta t^\beta}(t_m-t_b)^{\beta+\alpha} - \frac{1}{\Gamma(\alpha)\Gamma(\beta+1)}\frac{1}{\Delta t^\beta}(t_0-t_b)\left[\frac{1}{2}(t_0-t_b)^\beta (t_m-t_0)^{\alpha-1}\right].$$

Next, in order to rewrite the integral approximation (3.4), we define $b_{m,k}$, for $k=1,\dots m$, as

$$b_{m,k} = \frac{1}{\Gamma(\beta+\alpha+1)}\sum_{j=0}^{m-k}(-1)^j\binom{\beta+1}{j}\left(m-k-j+\frac{\beta+1}{2}\right)^{\beta+\alpha} \tag{3.7}$$

and for $k=0$

$$\begin{aligned} b_{m,0} = \quad & \frac{1}{\Gamma(\alpha)\Gamma(\beta+1)\Delta t^\alpha}\int_{t_0}^{t_m}\left(\frac{\tau-t_0}{\Delta t}+\frac{\beta+1}{2}\right)^\beta (t_m-\tau)^{\alpha-1}d\tau \\ & +\frac{1}{\Gamma(\beta+\alpha+1)}\sum_{j=1}^{m}(-1)^j\binom{\beta+1}{j}\left(m-j+\frac{\beta+1}{2}\right)^{\beta+\alpha}. \end{aligned} \tag{3.8}$$

that is approximately

$$b_{m,0} \approx \frac{1}{\Gamma(\beta+\alpha+1)} \sum_{j=0}^{m} (-1)^j \binom{\beta+1}{j} \left(m-j+\frac{\beta+1}{2}\right)^{\beta+\alpha} - \frac{1}{2\Gamma(\alpha)\Gamma(\beta+1)} \left(\frac{\beta+1}{2}\right)^{\beta} m^{\alpha-1}$$

By convention $b_{0,0} = 0$. We have

$$\Delta t^{\alpha} b_{m,k} = \sum_{j=0}^{m-k} l_{j,k},$$

and therefore, the approximation (3.4) can now be written as

$$I^{\alpha,\beta} u(t_m) = \Delta t^{\alpha} \sum_{k=0}^{m} c_k b_{m,k}.$$

In Chapter 2, we have seen that the coefficients c_k are given by

$$c_k = \sum_{p=0}^{k} \tilde{a}_{k-p} u(t_p),$$

with

$$\tilde{a}_0 = \frac{1}{a_0}, \qquad \tilde{a}_p = -\frac{1}{a_0} \sum_{r=1}^{p} a_r \tilde{a}_{p-r}, \quad p = 1, \dots, M, \tag{3.9}$$

and

$$a_p = \frac{1}{\Gamma(\beta+1)} \sum_{j=0}^{p} (-1)^j \binom{\beta+1}{j} \left(p-j+\frac{\beta+1}{2}\right)^{\beta}, \ p = 0, \dots, M. \tag{3.10}$$

Using this, we can write the approximation of the integral as

$$I^{\alpha,\beta} u(t_m) = \Delta t^{\alpha} \sum_{k=0}^{m} \sum_{p=0}^{k} \tilde{a}_{k-p} u(t_p) b_{m,k}.$$

Finally, rearranging the terms

$$I^{\alpha,\beta} u(t_m) = \Delta t^{\alpha} \sum_{p=0}^{m} \left(\sum_{k=p}^{m} b_{m,k} \tilde{a}_{k-p} \right) u(t_p).$$

Therefore we arrive to the quadrature formula

$$I^{\alpha,\beta} u(t_m) = \Delta t^{\alpha} \sum_{p=0}^{m} w_{m,p} u(t_p), \qquad w_{m,p} = \sum_{k=p}^{m} b_{m,k} \tilde{a}_{k-p}, \tag{3.11}$$

with $b_{m,k}$ defined by (3.7)–(3.8) and $\tilde{a}_{k-p}$ defined by (3.9).

3.1.2 Integral approximation using splines of degree $1 < \beta \leqslant 2$

In this section, we derive a formula to approximate the fractional integral using a fractional spline of degree β. This approach differs from the one taken in the previous section, because we need an additional condition to define the fractional spline.

Substituting in the integral (3.2) u by the formula of the spline (2.11), we obtain the following expression

$$I^{\alpha,\beta}u(t_m) = \frac{1}{\Gamma(\alpha)}\int_{t_0}^{t_m}\left[\frac{1}{\Gamma(\beta+1)}\sum_{k=0}^{M+1} c_k \sum_{j=0}^{+\infty}(-1)^j\binom{\beta+1}{j}\left(\frac{\tau-t_k}{\Delta t}-j+\frac{\beta+1}{2}\right)_+^{\beta}\right](t_m-\tau)^{\alpha-1}d\tau.$$

Since $t_0 \leqslant \tau \leqslant t_m$ and $2 < (\beta+1)/2 < 3/2$ the terms of interest in the infinite sum are those for which $j \leqslant m-k+1$, otherwise the term to the power of β is zero. Therefore we can, once again, interchange the integral with the sum, getting

$$I^{\alpha,\beta}u(t_m) = \sum_{k=0}^{m+1} c_k \sum_{j=0}^{m-k+1} l_{j,k}, \tag{3.12}$$

where

$$l_{j,k} = \frac{1}{\Gamma(\alpha)}\frac{1}{\Gamma(\beta+1)}(-1)^j\binom{\beta+1}{j}\int_{t_0}^{t_m}\left(\frac{\tau-t_k}{\Delta t}-j+\frac{\beta+1}{2}\right)_+^{\beta}(t_m-\tau)^{\alpha-1}d\tau.$$

We note that for all $(j,k) \neq (0,0),(0,1),(1,0)$, we have $(\tau-t_k)/\Delta t - j + (\beta+1)/2 \geqslant 0$ when $\tau \geqslant t_k + j\Delta t - (\beta+1)\Delta t/2$. Therefore, it follows that

$$l_{j,k} = \frac{\Delta t^{\alpha}}{\Gamma(1+\beta+\alpha)}(-1)^j\binom{\beta+1}{j}\left(m-k-j+\frac{\beta+1}{2}\right)^{\beta+\alpha}. \tag{3.13}$$

Let us now analyze the exceptions. For $(j,k) = (0,0)$, we have

$$l_{0,0} = \frac{1}{\Gamma(\alpha)}\frac{1}{\Gamma(\beta+1)}\int_{t_0}^{t_m}\left(\frac{\tau-t_0}{\Delta t}+\frac{\beta+1}{2}\right)^{\beta}(t_m-\tau)^{\alpha-1}d\tau$$

that we can split into

$$l_{0,0} = \frac{1}{\Gamma(\alpha)}\frac{1}{\Gamma(\beta+1)\Delta t^{\beta}}\int_{t_b}^{t_m}(\tau-t_b)^{\beta}(t_m-\tau)^{\alpha-1}d\tau - \frac{1}{\Gamma(\alpha)}\frac{1}{\Gamma(\beta+1)\Delta t^{\beta}}\int_{t_b}^{t_0}(\tau-t_b)^{\beta}(t_m-\tau)^{\alpha-1}d\tau,$$

where $t_b = t_0 - \Delta t(\beta+1)/2$. Then, using the trapezoidal rule to approximate the second integral, we get

$$l_{0,0} \approx \frac{\Delta t^{\alpha}}{\Gamma(1+\beta+\alpha)}\left(m+\frac{\beta+1}{2}\right)^{\beta+\alpha} - \frac{\Delta t^{\alpha}}{2\Gamma(\beta+1)\Gamma(\alpha)}\left(\frac{\beta+1}{2}\right)^{\beta+1} m^{\alpha-1}.$$

For the case $(j,k)=(1,0)$ we have, from (3.13),

$$l_{1,0}=-\frac{\beta+1}{\Gamma(\alpha)}\frac{1}{\Gamma(\beta+1)}\int_{t_0}^{t_m}\left(\frac{\tau-t_0}{\Delta t}-1+\frac{\beta+1}{2}\right)^{\beta}(t_m-\tau)^{\alpha-1}d\tau.$$

Using the same strategy as before, we arrive to

$$l_{1,0}\approx-\frac{\Delta t^{\alpha}(\beta+1)}{\Gamma(1+\beta+\alpha)}\left(m-1+\frac{\beta+1}{2}\right)^{\beta+\alpha}+\frac{\Delta t^{\alpha}(\beta+1)}{2\Gamma(\beta+1)\Gamma(\alpha)}\left(\frac{\beta+1}{2}-1\right)^{\beta+1}m^{\alpha-1}.$$

For the case $(j,k)=(0,1)$ we have

$$l_{0,1}=\frac{1}{\Gamma(\alpha)}\frac{1}{\Gamma(\beta+1)}\int_{t_0}^{t_m}\left(\frac{\tau-t_1}{\Delta t}+\frac{\beta+1}{2}\right)^{\beta}(t_m-\tau)^{\alpha-1}d\tau$$

that leads us to

$$l_{0,1}\approx\frac{\Delta t^{\alpha}}{\Gamma(1+\beta+\alpha)}\left(m-1+\frac{\beta+1}{2}\right)^{\beta+\alpha}-\frac{\Delta t^{\alpha}}{2\Gamma(\beta+1)\Gamma(\alpha)}\left(\frac{\beta+1}{2}-1\right)^{\beta+1}m^{\alpha-1}.$$

We define $b_{m,k}$ for $1<\beta\leqslant 2$ such that

$$\Delta t^{\alpha}b_{m,k}=\sum_{j=0}^{m-k+1}l_{j,k},$$

For $k=1,\dots m+1$ and $m=1,\dots,M$ we have

$$b_{m,k}=\frac{1}{\Gamma(1+\beta+\alpha)}\sum_{j=0}^{m-k+1}(-1)^j\binom{\beta+1}{j}\left(m-k-j+\frac{\beta+1}{2}\right)^{\beta+\alpha}.$$

Considering $b_{0,0}=0$ by convention, for $k=0$ we have

$$\begin{aligned}b_{m,0}\ &\approx\ -\frac{1}{2\Gamma(\beta+1)\Gamma(\alpha)}\left[\left(\frac{\beta+1}{2}\right)^{\beta+1}-(\beta+1)\left(\frac{\beta+1}{2}-1\right)^{\beta+1}\right]m^{\alpha-1}\\&\quad+\frac{1}{\Gamma(1+\beta+\alpha)}\sum_{j=0}^{m+1}(-1)^j\binom{\beta+1}{j}\left(m-j+\frac{\beta+1}{2}\right)^{\beta+\alpha}\end{aligned}$$

and for $k=1$ we have

$$\begin{aligned}b_{m,1}\ &\approx\ -\frac{1}{2\Gamma(\beta+1)\Gamma(\alpha)}\left(\frac{\beta+1}{2}-1\right)^{\beta+1}m^{\alpha-1}\\&\quad+\frac{1}{\Gamma(1+\beta+\alpha)}\sum_{j=0}^{m}(-1)^j\binom{\beta+1}{j}\left(m-1-j+\frac{\beta+1}{2}\right)^{\beta+\alpha}.\end{aligned}$$

We arrive to the following approximation of (3.12)

$$I^{\alpha,\beta}u(t_m) = \Delta t^{\alpha} \sum_{k=0}^{m+1} c_{k,m} b_{m,k}, \quad c_{k,m} = \tilde{a}^m_{k,0} u'(t_m) + \sum_{s=1}^{m+1} \tilde{a}^m_{k,s} u(t_{s-1}),$$

with $\tilde{a}^m_{k,s}$ being the entries of the matrix $\tilde{A}_m = [\tilde{a}^m_{k,s}],\ k = 0,\ldots,m+1,\ s = 0,\ldots,m+1$ which is the inverse of A_m (2.16).

Note that, in order to obtain $c_{k,m}$, we need to have access to the derivative of u at the knots. As we will see in the next chapter, sometimes this type of information is not available. Therefore, in order to approximate the first derivative of u, we use the approximation given by [39]

$$\frac{D_{-}u(t_m)}{\Delta t} + c_1 \frac{D^2_{-}u(t_m)}{\Delta t} + c_2 \frac{D^3_{-}u(t_m)}{\Delta t} \approx u'(t_m)$$

with

$$D_{-}u(t_m) = u(t_m) - u(t_{m-1}).$$

The general formula can be written as

$$\begin{aligned} &\frac{D_{-}u(t_m)}{\Delta t} + c_1 \frac{D^2_{-}u(t_m)}{\Delta t} + c_2 \frac{D^3_{-}u(t_m)}{\Delta t} = \\ &= \frac{u(t_m) - u(t_{m-1})}{\Delta t} + c_1 \frac{u(t_m) - 2u(t_{m-1}) + u(t_{m-2})}{\Delta t} + c_2 \frac{u(t_m) - 3u(t_{m-1}) + 3u(t_{m-2}) - u(t_{m-3})}{\Delta t} \end{aligned}$$

that can be rearranged as

$$\begin{aligned} &\frac{D_{-}u(t_m)}{\Delta t} + c_1 \frac{D^2_{-}u(t_m)}{\Delta t} + c_2 \frac{D^3_{-}u(t_m)}{\Delta t} = \\ &= \frac{1}{\Delta t}\Big((1 + c_1 + c_2)u(t_m) - (1 + 2c_1 + 3c_2)u(t_{m-1}) + (c_1 + 3c_2)u(t_{m-2}) - c_2 u(t_{m-3})\Big). \end{aligned} \tag{3.14}$$

Ideally, we would use $c_1 = -1/2$ and $c_2 = 1/3$, which is a third order accurate approximation. However, that is only possible for $m > 2$ because, for $m = 1$ and $m = 2$, we would need the values $u(t_{-2})$ and $u(t_{-1})$. Therefore, for $m = 1$, we use $c_1, c_2 = 0$, which is a first order accurate approximation. For $m = 2$, we use $c_1 = -1/2$ and $c_2 = 0$, which is a second order accurate approximation.

In the next section, we derive error bounds for the fractional integral approximation. We also present some numerical simulations using the exact value of $u'(t_m)$ and using the approximation (3.14) of $u'(t_m)$.

3.1.3 Error bounds for the fractional integral approximation

In this section we discuss the error bounds, in the L^2 norm and the L^{∞} norm, for the approximation of the fractional integral when we use fractional splines of degree β. In order to do it, we resort to the result obtained in Chapter 2 for $\beta \in (0,2]$. We also display some numerical tests to confirm the theoretical results.

We denote by $\tilde{H}^{\beta+1}(\Omega)$ the set of functions u whose extension by zero to $\tilde{u}$ is in $H^{\beta+1}(\mathbb{R})$.

Theorem 3.1. *For all $u \in \tilde{H}^{\beta+1}(\Omega)$, $\Omega = [0,T]$, the error of the integral approximation is bounded by*

$$||\mathscr{I}^{\alpha}u - I^{\alpha,\beta}u||_{L^2(\Omega)} \leqslant \frac{T^{\alpha}}{\Gamma(1+\alpha)} C_{\beta} ||D_0^{\beta+1}u||_{L^2(\Omega)} \Delta t^{\beta+1},$$

with C_{β} a constant depending on β and $D_0^{\beta+1}$ the Riemann-Liouville derivative (1.6).

Proof. We have that

$$\mathscr{I}^{\alpha}u(t) - I^{\alpha,\beta}u(t) = \frac{1}{\Gamma(\alpha)} \int_0^t (u(\xi) - s_{\beta}(\xi))(t-\xi)^{\alpha-1} d\xi.$$

Considering $\Omega = (0,T)$, let us do the change of variables $\tau = t - \xi$. We get

$$\mathscr{I}^{\alpha}u(t) - I^{\alpha,\beta}u(t) = -\frac{1}{\Gamma(\alpha)} \int_t^0 (u(t-\tau) - s_{\beta}(t-\tau))\tau^{\alpha-1} d\tau$$

that is equivalent to

$$\mathscr{I}^{\alpha}u(t) - I^{\alpha,\beta}u(t) = \frac{1}{\Gamma(\alpha)} \int_0^t (u(t-\tau) - s_{\beta}(t-\tau))\tau^{\alpha-1} d\tau.$$

Therefore,

$$\left|\mathscr{I}^{\alpha}u(t) - I^{\alpha,\beta}u(t)\right| \leqslant \frac{1}{\Gamma(\alpha)} \int_0^T \left|(u(t-\tau) - s_{\beta}(t-\tau))\right| |\tau|^{\alpha-1} d\tau.$$

Taking the L^2 norm,

$$||\mathscr{I}^{\alpha}u - I^{\alpha,\beta}u||_{L^2(\Omega)} = \left(\int_0^T \left|\mathscr{I}^{\alpha}u(t) - I^{\alpha,\beta}u(t)\right|^2 dt\right)^{\frac{1}{2}},$$

we can write

$$||\mathscr{I}^{\alpha}u - I^{\alpha,\beta}u||_{L^2(\Omega)} \leqslant \left(\int_0^T \left(\frac{1}{\Gamma(\alpha)} \int_0^T \left|u(t-\tau) - s_{\beta}(t-\tau)\right| |\tau|^{\alpha-1} d\tau\right)^2 dt\right)^{\frac{1}{2}}.$$

Using the generalized Minkowski's inequality (1.11), we obtain

$$||\mathscr{I}^{\alpha}u - I^{\alpha,\beta}u||_{L^2(\Omega)} \leqslant \frac{1}{\Gamma(\alpha)} \int_0^T \left(\int_0^T \left|u(t-\tau) - s_{\beta}(t-\tau)\right|^2 |\tau|^{2\alpha-2} dt\right)^{\frac{1}{2}} d\tau$$

and, consequently,

$$||\mathscr{I}^{\alpha}u - I^{\alpha,\beta}u||_{L^2(\Omega)} \leqslant \frac{1}{\Gamma(\alpha)} \int_0^T \left(\int_0^T \left|u(t-\tau) - s_{\beta}(t-\tau)\right|^2 dt\right)^{\frac{1}{2}} |\tau|^{\alpha-1} d\tau.$$

Doing the change of variable $z = t - \tau$, we get

$$||\mathscr{I}^{\alpha}u - I^{\alpha,\beta}u||_{L^2(\Omega)} \leqslant \frac{1}{\Gamma(\alpha)} \int_0^T \left(\int_{-\tau}^{T-\tau} \left|u(z) - s_{\beta}(z)\right|^2 dz\right)^{\frac{1}{2}} |\tau|^{\alpha-1} d\tau.$$

Considering that $u(z) - s_\beta(z) = 0$ for $z \leqslant 0$, it follows

$$||\mathscr{I}^\alpha u - I^{\alpha,\beta} u||_{L^2(\Omega)} \leqslant \frac{1}{\Gamma(\alpha)} \int_0^T \left(\int_0^{T-\tau} \left| u(z) - s_\beta(z) \right|^2 dz \right)^{\frac{1}{2}} |\tau|^{\alpha-1} d\tau.$$

Furthermore, τ is between 0 and T, so we arrive to

$$||\mathscr{I}^\alpha u - I^{\alpha,\beta} u||_{L^2(\Omega)} \leqslant \frac{1}{\Gamma(\alpha)} \int_0^T |\tau|^{\alpha-1} d\tau \left(\int_0^T \left| u(z) - s_\beta(z) \right|^2 dz \right)^{\frac{1}{2}}$$

which means that

$$||\mathscr{I}^\alpha u - I^{\alpha,\beta} u||_{L^2(\Omega)} \leqslant \frac{1}{\Gamma(\alpha)} ||u - s_\beta||_{L^2(\Omega)} ||K||_{L^1(\Omega)},$$

where $K(t) := t^{\alpha-1}$. Therefore by Theorem 2.2 of Chapter 2, we obtain

$$||\mathscr{I}^\alpha u - I^{\alpha,\beta} u||_{L^2(\Omega)} \leqslant C_\beta \frac{\Delta t^{\beta+1}}{\Gamma(\alpha+1)} T^\alpha ||D_0^{\beta+1} u||_{L^2(\Omega)}.$$

□

From this discussion, we expect to have an order of approximation of $\beta + 1$ for functions under the conditions of the previous theorem. We also note that this order of convergence is mainly controlled by the spline approximation, because it is the approximation we have done to compute the integral.

Consider the functions of interest, as in the previous subsections, that behave like $u = O(t^\gamma)$ when t tends to 0. Recalling that

$$||D_0^{\beta+1}(t^\gamma)||_{L^2(0,\Delta t)} = C_{\gamma,\beta} \Delta t^{\gamma-\beta-1/2}$$

from Theorem 3.1, we can conclude the following result.

If $u = O(t^\gamma)$ when t is close to zero then the error of the integral approximation is bounded by

$$||\mathscr{I}^\alpha u - I^{\alpha,\beta} u||_{L^2(\Omega)} \leqslant C_{\gamma,\beta,\alpha} \Delta t^{\min\{\beta+1,\gamma+1/2+\alpha\}},$$

with $C_{\gamma,\beta,\alpha}$ a constant depending on γ, β and α. From this result we infer that the order of the integral, α, may affect the order of convergence.

For the L^∞ norm, we assume that we have (2.20), that says

$$||u - s_\beta||_{L^\infty(\Omega)} \leqslant C_\beta \Delta t^{\beta+1} ||D_{-\infty}^{\beta+1} u||_{L^\infty(\Omega)},$$

which leads us to the following result. And, for functions that vanish outside Ω,

$$||u - s_\beta||_{L^\infty(\Omega)} \leqslant C_\beta \Delta t^{\beta+1} ||D_0^{\beta+1} u||_{L^\infty(\Omega)}.$$

Theorem 3.2. *Let u be a function sufficiently smooth, $u \in L^\infty(\Omega)$ and*

$$||u - s_\beta||_{L^\infty(\Omega)} \leqslant C_\beta \Delta t^{\beta+1} ||D_0^{\beta+1} u||_{L^\infty(\Omega)},$$

with C_β a constant depending on β. Then

$$||\mathscr{I}^\alpha u - I^{\alpha,\beta}u||_{L^\infty(\Omega)} \leqslant \frac{t^\alpha}{\Gamma(\alpha+1)} C_\beta ||D_0^{\beta+1}u||_{L^\infty(\Omega)} \Delta t^{\beta+1}.$$

Recalling that

$$||D_0^{\beta+1}(t^\gamma)||_{L^\infty(0,\Delta t)} = O(\Delta t^\gamma),$$

in the cases where we have a function $u = O(t^\gamma)$ when $t \to 0$, the error of the integral approximation is bounded by

$$||\mathscr{I}^\alpha u - I^{\alpha,\beta}u||_{L^\infty(\Omega)} \leqslant C_{\gamma,\beta,\alpha} \Delta t^{\min\{\beta+1,\gamma+\alpha\}},$$

with $C_{\gamma,\beta,\alpha}$ a constant depending on γ, β and α.

We present some numerical tests for the same type of functions we have considered in the discussions of the order of the spline approximation. In the next tables the numerical results are obtained for the functions $u(t) = (2t)^\gamma$, with $\gamma = 1$, $\gamma = 1.6$ and $\gamma = 2$, for β and α between 0 and 1.

In Table 3.1, we show the results for the case $\gamma = 1$, for $\beta = 0.4$ and $\alpha = 0.9$ and for $\beta = 0.8$ and $\alpha = 0.1$. In the first case the minimum between $\beta+1$ and $\gamma+\alpha+0.5$ or $\gamma+\alpha$ is the former one, this is, 1.4. In the second case the minimum between $\beta+1$ and $\gamma+\alpha+0.5$ or $\gamma+\alpha$ is the latter ones, this is, $\gamma+\alpha = 1.1$ for the L^∞ norm and $\gamma+\alpha+0.5 = 1.6$ for the L^2 norm. From the numerical results we conclude the same, since we obtain approximately the expected order of convergence.

Table 3.1 Convergence rate for the integral using $u(t) = 2t$, $(\beta,\alpha) = (0.4, 0.9)$ and $(\beta,\alpha) = (0.8, 0.1)$, in the L^2 norm and L^∞ norm.

	$\beta = 0.4,\ \alpha = 0.9$				$\beta = 0.8,\ \alpha = 0.1$			
Δt	$\|\|\cdot\|\|_\infty$	Rate	$\|\|\cdot\|\|_2$	Rate	$\|\|\cdot\|\|_\infty$	Rate	$\|\|\cdot\|\|_2$	Rate
0.1	2.7904e-03		1.8259e-03		5.3336e-04		4.0248e-04	
0.01	1.4794e-04	1.28	1.0135e-04	1.26	4.2366e-05	1.10	1.4890e-05	1.43
0.001	6.3113e-06	1.37	4.4217e-06	1.36	3.3653e-06	1.10	4.3798e-07	1.53

In Table 3.2, we display the results for the case $\gamma = 1.6$. In both cases considered, $(\beta,\alpha) = (0.8, 0.1)$ and $(\beta,\alpha) = (1, 0.2)$, we obtain the order of convergence around $\beta+1$ for the L^2 norm, which is the minimum between $\beta+1$ and $\gamma+\alpha+0.5$. For the L^∞ norm, we obtain the order of convergence around $\gamma+\alpha$, this is, 1.7 in the first case and 1.8 in the second case, which are the minimum between $\beta+1$ and $\gamma+\alpha$.

In Table 3.3, we show the results for the function $u(t) = (2t)^2$. From the information of the table, we conclude that the order of convergence is $\beta+1$ for both norms as established in the theoretical results. Note that, as $\gamma = 2$, $\beta+1$ is always lower than $\gamma+\alpha$ and, consequently, lower than $\gamma+\alpha+0.5$.

We present some numerical results for $\beta \in (1,2]$ and $\alpha \in (0,1)$, using the exact value for $u'(t_m)$, for the functions $u(t) = (2t)^\gamma$, with $\gamma = 2$ and $\gamma = 4$.

In Table 3.4, we present the numerical results regarding $\gamma = 2$, for $(\beta,\alpha) = (1.2, 0.4)$ and $(\beta,\alpha) = (1.8, 0.2)$. In the first case, the order of convergence is $\beta+1$ for both norms, since 2.2 is lower than $\gamma+\alpha = 2.4$. For the second pair of values, the rate of convergence for the L^2 norm is

Table 3.2 Convergence rate for the integral using $u(t) = (2t)^{1.6}$, $(\beta,\alpha) = (0.8,0.1)$ and $(\beta,\alpha) = (1,0.2)$, in the L^2 norm and L^∞ norm.

	$\beta = 0.8,\ \alpha = 0.1$				$\beta = 1,\ \alpha = 0.2$			
Δt	$\|\|\cdot\|\|_\infty$	Rate	$\|\|\cdot\|\|_2$	Rate	$\|\|\cdot\|\|_\infty$	Rate	$\|\|\cdot\|\|_2$	Rate
0.1	2.1487e-03		2.0909e-03		2.6355e-03		2.3361e-03	
0.01	4.3221e-05	1.70	4.2761e-05	1.69	4.1770e-05	1.80	2.9172e-05	1.90
0.001	8.6236e-07	1.70	8.0681e-07	1.72	6.6201e-07	1.80	3.3121e-07	1.94

Table 3.3 Convergence rate for the integral using $u(t) = (2t)^2$, $(\beta,\alpha) = (0.2,0.6)$ and $(\beta,\alpha) = (0.6,0.8)$, in the L^2 norm and L^∞ norm.

	$\beta = 0.2,\ \alpha = 0.6$				$\beta = 0.6,\ \alpha = 0.8$			
Δt	$\|\|\cdot\|\|_\infty$	Rate	$\|\|\cdot\|\|_2$	Rate	$\|\|\cdot\|\|_\infty$	Rate	$\|\|\cdot\|\|_2$	Rate
0.1	1.7949e-02		1.0902e-02		1.1871e-02		7.1376e-03	
0.01	7.6772e-04	1.37	4.0830e-04	1.43	2.7971e-04	1.63	1.5350e-04	1.67
0.001	4.3623e-05	1.25	2.2547e-05	1.26	6.9662e-06	1.60	3.7829e-06	1.61

Table 3.4 Convergence rate for the integral using $u(t) = (2t)^2$, $(\beta,\alpha) = (1.2,0.4)$ and $(\beta,\alpha) = (1.8,0.2)$, in the L^2 norm and L^∞ norm.

	$\beta = 1.2,\ \alpha = 0.4$				$\beta = 1.8,\ \alpha = 0.2$			
Δt	$\|\|\cdot\|\|_\infty$	Rate	$\|\|\cdot\|\|_2$	Rate	$\|\|\cdot\|\|_\infty$	Rate	$\|\|\cdot\|\|_2$	Rate
0.1	1.8170e-03		1.4141e-03		5.1520e-04		1.8982e-04	
0.01	1.1900e-05	2.18	9.5472e-06	2.17	3.2507e-06	2.20	3.9689e-07	2.68
0.001	7.6495e-08	2.19	6.3222e-08	2.18	2.0510e-08	2.20	8.0730e-10	2.69

Table 3.5 Convergence rate for the integral using $u(t) = (2t)^4$, $(\beta,\alpha) = (1.4,0.6)$ and $(\beta,\alpha) = (1.6,0.8)$, in the L^2 norm and L^∞ norm.

	$\beta = 1.4,\ \alpha = 0.6$				$\beta = 1.6,\ \alpha = 0.8$			
Δt	$\|\|\cdot\|\|_\infty$	Rate	$\|\|\cdot\|\|_2$	Rate	$\|\|\cdot\|\|_\infty$	Rate	$\|\|\cdot\|\|_2$	Rate
0.1	9.8791e-03		3.9999e-03		2.8656e-03		1.1099e-03	
0.01	4.1781e-05	2.37	1.7116e-05	2.37	7.5325e-06	2.58	3.1250e-06	2.55
0.001	1.6707e-07	2.40	7.0877e-08	2.38	1.8929e-08	2.60	8.0864e-09	2.59

$\gamma + \alpha + 0.5 = 2.7$ and for the L^∞ norm is $\gamma + \alpha = 2.2$, since $\beta + 1 = 2.8$. In Table 3.5, we show the results of the numerical tests done with $u(t) = (2t)^4$. We got an order of convergence of $\beta + 1$ for both cases and both norms, as expected by the theoretical results.

In Table 3.6, we present a numerical test for the case $u(t) = (2t)^2$ considered in Table 3.4, but instead of using the exact value of $u'(t_m)$, we use the approximation (3.14). When $(\beta,\alpha) = (1.2,0.4)$, we obtain a convergence rate around $\beta+1$ for both norms. When $(\beta,\alpha) = (1.8,0.2)$, we obtain a convergence rate around $2+\alpha$ for both norms.

Table 3.6 Convergence rate for the integral using $u(t) = (2t)^2$, $(\beta,\alpha) = (1.2,0.4)$ and $(\beta,\alpha) = (1.8,0.2)$, in the L^2 norm and L^∞ norm, resorting to the approximation (3.14).

	$\beta = 1.2,\ \alpha = 0.4$				$\beta = 1.8,\ \alpha = 0.2$			
Δt	$\|\|\cdot\|\|_\infty$	Rate	$\|\|\cdot\|\|_2$	Rate	$\|\|\cdot\|\|_\infty$	Rate	$\|\|\cdot\|\|_2$	Rate
0.1	3.4727e-03		4.4484e-03		3.4113e-03		3.9807e-03	
0.01	1.9175e-05	2.26	2.3916e-05	2.27	2.1524e-05	2.20	2.4360e-05	2.21
0.001	1.0953e-07	2.24	1.3502e-07	2.25	1.3581e-07	2.20	1.5223e-07	2.20

We conclude that the numerical tests are according to the theoretical results and, for some cases, the order of approximation is influenced by the value of α as expected. Furthermore, it is affected by the approximation of the derivative $u'(t_m)$, needed when β is between 1 and 2.

3.2 Space-integral operator of order $0 < \alpha < 2,\ \alpha \neq 1$

Superdiffusive phenomena can be modeled via fractional operators not only with α between 1 and 2 but also with α between 0 and 1. In this section, we describe the approximation of the left and right fractional integrals of order α with $n-1 < \alpha < n$ defined, respectively, by

$$\mathscr{I}^l u(x) = \frac{1}{\Gamma(n-\alpha)} \int_{-\infty}^{x} u(\xi)(x-\xi)^{n-1-\alpha} d\xi \tag{3.15}$$

and

$$\mathscr{I}^r u(x) = \frac{1}{\Gamma(n-\alpha)} \int_{x}^{\infty} u(\xi)(\xi-x)^{n-1-\alpha} d\xi. \tag{3.16}$$

These integrals are related to the definition of the fractional derivatives that will appear during in Chapter 5.

3.2.1 Integral approximation using the linear spline

Consider the uniform discretization of the real line $x_k = x_{k-1} + \Delta x,\ k \in \mathbb{Z}$. We begin by approximating the integral $\mathscr{I}^l u(x_j)$ using the linear spline. As seen in Chapter 1, the linear spline is given by

$$s(x) := s_1(x) = \sum_{k\in\mathbb{Z}} u(x_k) B_+^1(x-x_k),$$

with

$$B_+^1(x-x_k) = \frac{1}{\Gamma(2)} \sum_{j=0}^{+\infty} (-1)^j \binom{2}{j} \left(\frac{x-x_k}{\Delta x} - j + 1 \right)_+ .$$

It is easy to see that $B^1_+(x-x_k)$ is equal to

$$B^1_+(x-x_k) = \begin{cases} \dfrac{x-x_{k-1}}{\Delta x}, & x_{k-1} < x \leqslant x_k, \\ \dfrac{x_{k+1}-x}{\Delta x}, & x_k < x \leqslant x_{k+1}, \\ 0, & \text{otherwise} \end{cases}$$

for $k < j$ and, for $k = j$,

$$B^1_+(x-x_j) = \begin{cases} \dfrac{x_j-x}{\Delta x}, & x_{j-1} \leqslant x \leqslant x_j, \\ 0, & \text{otherwise.} \end{cases}$$

Then, the spline that approximates a function u is given by

$$s(x) = \sum_{k=-\infty}^{j} u(x_k) B^1_+(x-x_k).$$

Substituting u by s in (3.15),

$$\begin{aligned} I^l u(x_j) &= \frac{1}{\Gamma(n-\alpha)} \int_{-\infty}^{x_j} s(\xi)(x_j-\xi)^{n-1-\alpha} d\xi \\ &= \frac{1}{\Gamma(n-\alpha)} \sum_{k=-\infty}^{j} \int_{-\infty}^{x_j} u(x_k) B^1_+(\xi-x_k)(x_j-\xi)^{n-1-\alpha} d\xi, \end{aligned}$$

provided that u is bounded.

For $k < j$, the integral is given by

$$I^l u(x_j) = \frac{1}{\Gamma(n-\alpha)} \sum_{k=-\infty}^{j} u(x_k) \int_{x_{k-1}}^{x_{k+1}} B^1_+(\xi-x_k)(x_j-\xi)^{n-1-\alpha} d\xi$$

and

$$\int_{x_{k-1}}^{x_{k+1}} B^1_+(\xi-x_k)(x_j-\xi)^{n-1-\alpha} d\xi = \int_{x_{k-1}}^{x_k} \frac{\xi-x_{k-1}}{\Delta x}(x_j-\xi)^{n-1-\alpha} d\xi + \int_{x_k}^{x_{k+1}} \frac{x_{k+1}-\xi}{\Delta x}(x_j-\xi)^{n-1-\alpha} d\xi.$$

Integrating by parts,

$$\begin{aligned} \int_{x_{k-1}}^{x_{k+1}} B^1_+(\xi-x_k)(x_j-\xi)^{n-1-\alpha} d\xi &= \left[\frac{(x_j-\xi)^{n-\alpha}(\xi-x_{k-1})}{(\alpha-n)\Delta x}\right]_{x_{k-1}}^{x_k} + \int_{x_{k-1}}^{x_k} \frac{(x_j-\xi)^{n-\alpha}}{(n-\alpha)\Delta x} d\xi \\ &+ \left[\frac{(x_j-\xi)^{n-\alpha}(x_{k+1}-\xi)}{(\alpha-n)\Delta x}\right]_{x_k}^{x_{k+1}} - \int_{x_k}^{x_{k+1}} \frac{(x_j-\xi)^{n-\alpha}}{(n-\alpha)\Delta x} d\xi, \end{aligned}$$

that is equivalent to

$$\int_{x_{k-1}}^{x_{k+1}} B_+^1(\xi - x_k)(x_j-\xi)^{n-1-\alpha}d\xi = -\frac{(x_j-x_k)^{n-\alpha}(x_k-x_{k-1})}{(n-\alpha)\Delta x} - \left[\frac{(x_j-\xi)^{n+1-\alpha}}{(n-\alpha)(n+1-\alpha)\Delta x}\right]_{x_{k-1}}^{x_k}$$
$$+\frac{(x_j-x_k)^{n-\alpha}(x_{k+1}-x_k)}{(n-\alpha)\Delta x} + \left[\frac{(x_j-\xi)^{n+1-\alpha}}{(n-\alpha)(n+1-\alpha)\Delta x}\right]_{x_k}^{x_{k+1}}.$$

Recalling that $x_i - x_{i-1} = \Delta x$,

$$\int_{x_{k-1}}^{x_{k+1}} B_+^1(\xi - x_k)(x_j-\xi)^{n-1-\alpha}d\xi = \frac{(j-k+1)^{n+1-\alpha} - 2(j-k)^{n+1-\alpha} + (j-k-1)^{n+1-\alpha}}{(n+1-\alpha)(n-\alpha)}\Delta x^{n-\alpha}.$$

For $k = j$, due to the support of the B-spline, we have

$$I^l u(x_j) = \frac{1}{\Gamma(n-\alpha)}\sum_{k=-\infty}^{j} u(x_k)\int_{x_{j-1}}^{x_j} B_+^1(\xi - x_k)(x_j-\xi)^{n-1-\alpha}d\xi$$

with

$$\int_{x_{j-1}}^{x_j} B_+^1(\xi - x_j)(x_j-\xi)^{n-1-\alpha}d\xi = \int_{x_{j-1}}^{x_j} \frac{\xi - x_{j-1}}{\Delta x}(x_j-\xi)^{n-1-\alpha}d\xi = \frac{\Gamma(2)\Gamma(n-\alpha)}{\Gamma(n+2-\alpha)}\Delta x^{n-\alpha}.$$

Finally, we arrive to the following approximation of $\mathscr{I}^l u(x_j)$

$$I^l u(x_j) = \frac{\Delta x^{n-\alpha}}{\Gamma(n+2-\alpha)}\sum_{k=-\infty}^{j} u(x_k)a^l_{j,k},$$

where

$$\begin{aligned} a^l_{j,k} &= (j-k-1)^{n+1-\alpha} - 2(j-k)^{n+1-\alpha} + (j-k+1)^{n+1-\alpha}, \quad k \leqslant j-1,\\ a^l_{j,j} &= 1. \end{aligned}$$

The approximation of the right integral follows similarly. We obtain the following approximation of $\mathscr{I}^r u(x_j)$

$$I^r u(x_j) = \frac{\Delta x^{n-\alpha}}{\Gamma(n+2-\alpha)}\sum_{k=j}^{\infty} u(x_k)a^r_{j,k},$$

where

$$\begin{aligned} a^r_{j,k} &= (k+1-j)^{n+1-\alpha} - 2(k-j)^{n+1-\alpha} + (k-1-j)^{n+1-\alpha}, \quad k \geqslant j+1,\\ a^r_{j,j} &= 1. \end{aligned}$$

Considering $m = j-k$, we can rewrite the integrals as

$$I^l u(x_j) = \frac{\Delta x^{n-\alpha}}{\Gamma(n+2-\alpha)}\sum_{m=0}^{\infty} a_m u(x_{j-m}, t) \tag{3.17}$$

and

$$I^r u(x_j) = \frac{\Delta x^{n-\alpha}}{\Gamma(n+2-\alpha)} \sum_{m=0}^{\infty} a_m u(x_{j+m}), \tag{3.18}$$

where the coefficients, that are equal for both quadratures, are given by

$$\begin{aligned} a_0 &= 1, \\ a_m &= (m+1)^{n+1-\alpha} - 2m^{n+1-\alpha} + (m-1)^{n+1-\alpha}, \text{ for } m \geqslant 1. \end{aligned} \tag{3.19}$$

The error bounds for these integrals can be obtained in a similar way to what has been done in Section 2.4, considering $\beta = 1$.

In the next chapters, we develop numerical methods for fractional differential equations that can model subdiffusion and superdiffusion, based on the discussion presented in this chapter.

Chapter 4

Subdiffusion problem

In the first section of this chapter, we describe briefly the deduction of the fractional differential equation that models subdiffusion based on the continuous time random walk. A continuous time random walk (CTRW) differs from the Brownian random walk in the waiting times. While in the latter the waiting times are constant, in the CTRW they are given by a function. In the second section, we derive a numerical method to approximate the solution of the subdiffusive problem resorting to splines of degree β between 0 and 1. We study the stability and the convergence of the method, illustrating the convergence rate with some numerical computations. In the third section, we formulate a numerical method to approximate the same problem but now using splines of degree β between 1 and 2. As this is a much more difficult problem, the stability of the method is yet to be studied. Nevertheless, we give some numerical examples that indicate the order of accuracy of the method. In the last section, we present some figures to illustrate the phenomena of subdiffusion when the initial condition is an approximation of the Dirac delta function.

4.1 Model problem

The CTRW model is the basis for the fractional equation used in subdiffusion derived by Metzler and Klafter in [51]. Consider a probability density function (pdf), ψ, that characterizes the length of a jump and the waiting time between two consecutive jumps. The jump length pdf, λ, and the waiting time pdf, w, can be determined respectively by

$$\lambda(x) = \int_0^\infty \psi(x,t)dt \qquad \text{and} \qquad \nu(t) = \int_{-\infty}^\infty \psi(x,t)dx.$$

When the waiting time and the length of the jumps are independent, ψ can be written as $\psi(x,t) = \lambda(x)\nu(t)$. It can be proved that, in the Fourier-Laplace space, the pdf u that represents the probability of being in position x at time t, obeys to [44, 51]

$$\hat{u}(\omega,s) = \frac{1-\hat{\nu}(s)}{s}\frac{\hat{u}_0(\omega)}{1-\hat{\psi}(\omega,s)},$$

where $\hat{u}_0(\omega)$ denotes the Fourier transform of the initial condition $u_0(x)$. Note that $\hat{f}(\omega)$ and $\hat{f}(s)$ denote the Fourier transform and the Laplace transform of f, respectively. Furthermore, $\hat{f}(\omega,s)$

represents the Fourier transform of the function of the first variable and a Laplace transform of the second variable.

CTRW processes can be classified according to the characteristic waiting time, T, and the jump length variance, σ^2, given by

$$T = \int_0^\infty t\nu(t)dt, \qquad \sigma^2 = \int_{-\infty}^\infty x^2\lambda(x)dx.$$

being finite or divergent. When T and σ^2 are finite, we are in the presence of the Brownian motion. Consider that T diverges, but σ^2 remains finite with a waiting time pdf that obeys

$$\nu(t) \sim A_\alpha(\tau/t)^{1-\alpha},$$

for $0 < \alpha < 1$, with the Laplace transform behaving as

$$\hat{\nu}(s) \sim 1-(s\tau)^\alpha.$$

For the jump length pdf, choosing the Gaussian behaviour, the Fourier transform of λ is characterized by

$$\hat{\lambda}(\omega) \sim 1-\sigma^2\omega^2+O(\omega^4).$$

Then, the pdf u can be written in the Fourier-Laplace space as

$$\hat{u}(\omega,s) = \frac{[\hat{u}_0(\omega)/s]}{1+K_\alpha s^{-\alpha\omega^2}}.$$

Computing the inverse Fourier-Laplace transform, this leads us to the fractional integral equation

$$u(x,t)-u_0(x) = K_\alpha \frac{\partial^2}{\partial x^2}\left[\frac{1}{\Gamma(\alpha)}\int_0^t (t-\tau)^{\alpha-1}u(x,\tau)d\tau\right]$$

Applying the first derivative in time, we get

$$\frac{\partial u}{\partial t}(x,t) = K_\alpha \frac{\partial^2}{\partial x^2} D_0^{1-\alpha}u(x,t),$$

where $D_0^{1-\alpha}u$ is the fractional Riemann-Liouville derivative operator is given by

$$D_0^{1-\alpha}u(t) = \frac{d}{dt}\mathscr{I}^\alpha u(t)$$

with

$$\mathscr{I}^\alpha u(t) = \frac{1}{\Gamma(\alpha)}\int_0^t u(\tau)(t-\tau)^{\alpha-1}d\tau, \quad 0<\alpha<1.$$

A similar, more general, fractional equation related to subdiffusion processes [27] is given by

$$\frac{\partial u}{\partial t}(x,t) = \frac{\partial^2}{\partial x^2}\Big(d(x,t)D_0^{1-\alpha}u(x,t)\Big)+g(x,t), \quad (x,t)\in[a,b]\times[0,T] \tag{4.1}$$

where $d(x,t)$ is the positive diffusive coefficient and $g(x,t)$ is a source term. Additionally, we consider an initial condition and, for simplicity, we assume homogeneous Dirichlet boundary conditions $u(a,t) = u(b,t) = 0$, for $t \in [0,T]$. Other boundary conditions can be easily considered.

In the next section, we derive a numerical method to approximate the solution of this problem, using the approximations presented in Chapters 2 and 3.

4.2 Numerical method using splines of degree $0 < \beta \leqslant 1$

In the following sections, we construct a numerical method based on the integral approximation using splines of degree $0 < \beta \leqslant 1$ derived in Section 3.1.1. We proceed with its convergence analysis and with numerical experiments that illustrate the order of convergence of the numerical method.

4.2.1 Finite differences method

The goal is to construct a numerical method based on fractional splines to solve equation (4.1) defined in the domain $[a,b] \times [t_0,T]$. In order to evaluate the method, let us start by discretize the interval $[t_0,T]$ with a uniform grid $t_{m+1} = t_m + \Delta t$, $m = 0,1,\ldots,M-1$ with time step $\Delta t = (t_M - t_0)/M$, $t_0 = 0$ and $t_M = T$.

We start by integrating (4.1) over an interval of time (t_{m-1},t_m), similarly to what has been done in [63], obtaining

$$u(x,t_m) - u(x,t_{m-1}) = \int_{t_{m-1}}^{t_m} \frac{\partial^2}{\partial x^2}\Big(d(x,t)\,{}_0D_t^{1-\alpha}u(x,t)\Big)dt + \int_{t_{m-1}}^{t_m} g(x,t)dt.$$

Approximating $d(x,t)$ in each interval by the second order approximation $d^{m+\frac{1}{2}}(x) = (d(x,t_m) + d(x,t_{m-1}))/2$, we get

$$u(x,t_m) - u(x,t_{m-1}) \approx \frac{\partial^2}{\partial x^2}\Big(d^{m+\frac{1}{2}}(x)\int_{t_{m-1}}^{t_m} \frac{\partial}{\partial t}\mathscr{I}^{\alpha}u(x,t)\Big)dt + \int_{t_{m-1}}^{t_m} g(x,t)dt$$

that leads to

$$u(x,t_m) - u(x,t_{m-1}) \approx \frac{\partial^2}{\partial x^2}\Big(d^{m+\frac{1}{2}}(x)\left(\mathscr{I}^{\alpha}u(x,t_m) - \mathscr{I}^{\alpha}u(x,t_{m-1})\right)\Big) + \int_{t_{m-1}}^{t_m} g(x,t)dt. \qquad (4.2)$$

Recall that in Chapter 3 we presented the approximation (3.11) of $\mathscr{I}^{\alpha}u(x,t_m)$, given by

$$I^{\alpha,\beta}u(x,t_m) = \Delta t^{\alpha}\sum_{p=0}^{m} w_{m,p}u(x,t_p),$$

where

$$w_{m,p} = \sum_{k=p}^{m} b_{m,k}\tilde{a}_{k-p}. \qquad (4.3)$$

Replacing $\mathscr{I}^{\alpha}u(x,t_m)$ by $I^{\alpha,\beta}u(x,t_m)$ for each x, we obtain

$$u(x,t_m)-u(x,t_{m-1}) \approx \frac{\partial^2}{\partial x^2}\left(d^{m+\frac{1}{2}}(x)\Delta t^{\alpha}\left(\sum_{k=0}^{m} w_{m,k}u(x,t_k)-\sum_{k=0}^{m-1} w_{m-1,k}u(x,t_k)\right)\right)+\int_{t_{m-1}}^{t_m} g(x,t)dt.$$

We proceed with the space discretization in order to approximate the second order derivative in space. Consider the set of spatial discrete points $x_j = a + j\Delta x,\ j = 0,1,\ldots,N$ with $\Delta x = (b-a)/N$ and the central second order operator $\delta^2 u(x_j,t) = u(x_{j+1},t)-2u(x_j,t)+u(x_{j-1},t)$. We obtain the following numerical method

$$U_j^m - U_j^{m-1} = \mu_\alpha \delta^2\left(d_j^{m+\frac{1}{2}}\left(\sum_{k=0}^{m} w_{m,k}U_j^k - \sum_{k=0}^{m-1} w_{m-1,k}U_j^k\right)\right)+\int_{t_{m-1}}^{t_m} g(x_j,t)dt,$$

where we denote U_j^m the approximation of $u(x_j,t_m)$, $d_j^{m+\frac{1}{2}} := d^{m+\frac{1}{2}}(x_j)$ and $\mu_\alpha = \Delta t^{\alpha}/\Delta x^2$. Aggregating the terms,

$$U_j^m - U_j^{m-1} = \mu_\alpha \sum_{k=0}^{m-1}(w_{m,k}-w_{m-1,k})\delta^2(d_j^{m+\frac{1}{2}}U_j^k)+\mu_\alpha w_{m,m}\delta^2(d_j^{m+\frac{1}{2}}U_j^m)+\int_{t_{m-1}}^{t_m} g(x_j,t)dt. \quad (4.4)$$

The matricial form of this method is

$$(\mathbf{I}-\mu_\alpha w_{m,m}\mathbf{D}^m)\mathbf{U}^m = \mathbf{I}\mathbf{U}^{m-1}+\mu_\alpha\sum_{k=0}^{m-1}(w_{m,k}-w_{m-1,k})\mathbf{D}^m\mathbf{U}^k+\mathbf{G}^m, \quad (4.5)$$

where $\mathbf{I}$ is the identity matrix, $\mathbf{U}^m$ is the solution vector $\mathbf{U}^m = [U_1^m,\ldots,U_{N-1}^m]^T$, $\mathbf{D}^m$ is a tridiagonal matrix with entries $\mathbf{D}^m_{j,j-1} = d_{j-1}^{m+\frac{1}{2}}$, $\mathbf{D}^m_{j,j} = -2d_j^{m+\frac{1}{2}}$ and $\mathbf{D}^m_{j,j+1} = d_{j+1}^{m+\frac{1}{2}}$ and $\mathbf{G}^m$ contains the values of the integral of the source term.

In the next section, we discuss the convergence of the numerical method using von Neumann analysis.

4.2.2 Convergence analysis

In this section, we discuss the consistency of the numerical method based on the error bounds derived in Section 3.1.3. After that, we prove the stability of the numerical method using the von Neumann approach.

In terms of consistency, from (4.2) we can state that the spatial accuracy of the method is based on the approximation of the second order derivative in space. As we use a second order central finite differences formula, we conclude that the method is second order accurate in space. The accuracy of the method in time is based on the approximation of the integrals present in (4.2). Hence, we conclude that the accuracy of the numerical method in time is the minimum between $\alpha+\gamma$ and $\beta+1$ for the L^{∞} norm and is the minimum between $\alpha+\gamma+0.5$ and $\beta+1$ for the L^2 norm, when considering functions that behave as $u = O(t^{\gamma})$ when t tends to 0. Note that to compute (3.8), we use the trapezoidal rule, which does not affect the order of accuracy of the method once it is a second order accurate approximation.

In order to study the stability of the method, we start by giving properties regarding the coefficients $w_{m,p}$ that appear in the formula of the numerical method (4.5).

Proposition 4.1. *The coefficients* $w_{m,p}$ (4.3) *verify*

$$w_{m,p} = w_{n,q}, \text{ for } m-p = n-q, \ p,q \neq 0.$$

For $p=0$, *we have* $w_{k-p,0} \leqslant w_{k,p}$.

Proof. Recall that the coefficients $w_{m,p}$ that appear in (4.5) are given by

$$w_{m,p} = \sum_{k=p}^{m} b_{m,k}\tilde{a}_{k-p}, \quad \text{and} \quad w_{n,q} = \sum_{k=q}^{n} b_{n,k}\tilde{a}_{k-q}. \tag{4.6}$$

For $k>0$, $b_{m,k}$ is defined as

$$b_{m,k} = \frac{1}{\Gamma(\beta+\alpha+1)} \sum_{j=0}^{m-k} (-1)^j \binom{\beta+1}{j} \left(m-k-j+\frac{\beta+1}{2}\right)^{\beta+\alpha}.$$

Doing a change of variables in (4.6), we get

$$w_{m,p} = \sum_{s=0}^{m-p} b_{m,s+p}\tilde{a}_s, \quad \text{and} \quad w_{n,q} = \sum_{s=0}^{n-q} b_{n,s+q}\tilde{a}_s.$$

Having

$$b_{m,s+p} = \frac{1}{\Gamma(\beta+\alpha+1)} \sum_{j=0}^{m-(s+p)} (-1)^j \binom{\beta+1}{j} \left(m-(s+p)-j+\frac{\beta+1}{2}\right)^{\beta+\alpha}$$

and

$$b_{n,s+q} = \frac{1}{\Gamma(\beta+\alpha+1)} \sum_{j=0}^{n-(s+q)} (-1)^j \binom{\beta+1}{j} \left(n-(s+q)-j+\frac{\beta+1}{2}\right)^{\beta+\alpha}$$

equivalent, respectively, to

$$b_{m,s+p} = \frac{1}{\Gamma(\beta+\alpha+1)} \sum_{j=0}^{(m-p)-s} (-1)^j \binom{\beta+1}{j} \left((m-p)-s-j+\frac{\beta+1}{2}\right)^{\beta+\alpha}$$

and

$$b_{n,s+q} = \frac{1}{\Gamma(\beta+\alpha+1)} \sum_{j=0}^{(n-q)-s} (-1)^j \binom{\beta+1}{j} \left((n-q)-s-j+\frac{\beta+1}{2}\right)^{\beta+\alpha},$$

we arrive to the result. □

Furthermore, these coefficients obey

$$w_{m,p} \geqslant 0,\ p = 0,1,\dots,m-1,m, \quad w_{m,p+1} \geqslant w_{m,p},\ p = 0,1,\dots,m-2. \tag{4.7}$$

We plot in Figure 4.1 $w_{m,p}$ for $m = 1000$ and $p = 0,1,\dots,m-1$ for β between 0 and 1 and for $\alpha = 0.1,\ 0.2,\dots,\ 0.9$.

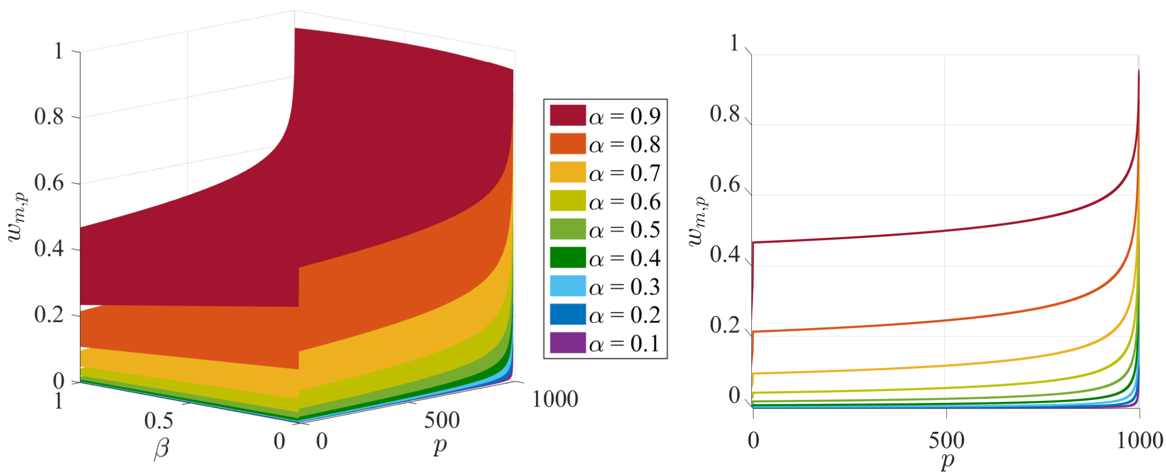

Fig. 4.1 Two different views of the coefficients $w_{m,p}$ defined in (3.11) for β between 0 and 1 and α changing from 0.1 to 0.9.

We can simplify the formulation (4.5) and also improve the performance of the numerical method if we define the coefficients as

$$q_{m,k} = w_{m,k} - w_{m-1,k}, \quad k = 0,1,\dots,m-1. \tag{4.8}$$

Using the definition of $w_{m,k}$, we arrive to the following.

Proposition 4.2. *The coefficients* $q_{m,k}$ (4.8) *can be rewritten as*

$$q_{m,k} = \sum_{p=k}^{m-1} (b_{m,p} - b_{m-1,p})\tilde{a}_{p-k} + b_{m,m}\tilde{a}_{m-k}. \tag{4.9}$$

For $p = 1,\dots,m-1,$

$$b_{m,p} - b_{m-1,p} = \frac{1}{\Gamma(\beta+\alpha+1)} \sum_{j=0}^{m-p} (-1)^j \binom{\beta+2}{j} \left(m-p-j+\frac{\beta+1}{2}\right)^{\beta+\alpha} \tag{4.10}$$

and, for $p = 0,$

$$\begin{aligned} b_{m,0} - b_{m-1,0} &= \frac{1}{\Gamma(\beta+\alpha+1)} \sum_{j=0}^{m} (-1)^j \binom{\beta+2}{j} \left(m - j + \frac{\beta+1}{2}\right)^{\beta+\alpha} \\ &+ \frac{\Delta t^{-\alpha-\beta}}{\Gamma(\alpha)\Gamma(\beta+1)} \int_{t_b}^{t_0} (\tau - t_b)^\beta [(t_{m-1}-\tau)^{\alpha-1} - (t_m - \tau)^{\alpha-1}] d\tau \end{aligned}$$

where $t_b = t_0 - \Delta t(\beta+1)/2$.

Proof. From (4.8), using (4.6) is easy to obtain (4.9). Let us show how we arrived to the formula (4.10). Using the definition of $b_{m,k}$,

$$\begin{aligned} b_{m,p} - b_{m-1,p} &= \frac{1}{\Gamma(\beta+\alpha+1)} \sum_{j=0}^{m-p} (-1)^j \binom{\beta+1}{j} \left(m - p - j + \frac{\beta+1}{2}\right)^{\beta+\alpha} \\ &- \frac{1}{\Gamma(\beta+\alpha+1)} \sum_{j=0}^{m-1-p} (-1)^j \binom{\beta+1}{j} \left(m - 1 - p - j + \frac{\beta+1}{2}\right)^{\beta+\alpha} \end{aligned}$$

that is equivalent to

$$\begin{aligned} b_{m,p} - b_{m-1,p} &= \frac{1}{\Gamma(\beta+\alpha+1)} \sum_{j=0}^{m-p} (-1)^j \binom{\beta+1}{j} \left(m - p - j + \frac{\beta+1}{2}\right)^{\beta+\alpha} \\ &+ \frac{1}{\Gamma(\beta+\alpha+1)} \sum_{j=0}^{m-1-p} (-1)^{j+1} \binom{\beta+1}{j} \left(m - p - (j+1) + \frac{\beta+1}{2}\right)^{\beta+\alpha}. \end{aligned}$$

Considering $s = j+1$ in the second sum, we get

$$\begin{aligned} b_{m,p} - b_{m-1,p} &= \frac{1}{\Gamma(\beta+\alpha+1)} \sum_{j=0}^{m-p} (-1)^j \binom{\beta+1}{j} \left(m - p - j + \frac{\beta+1}{2}\right)^{\beta+\alpha} \\ &+ \frac{1}{\Gamma(\beta+\alpha+1)} \sum_{s=1}^{m-p} (-1)^s \binom{\beta+1}{s-1} \left(m - p - s + \frac{\beta+1}{2}\right)^{\beta+\alpha}. \end{aligned}$$

which can be written as

$$\begin{aligned} b_{m,p} - b_{m-1,p} = & \frac{1}{\Gamma(\beta+\alpha+1)} \sum_{j=1}^{m-p} (-1)^j \left[\binom{\beta+1}{j} + \binom{\beta+1}{j-1}\right] \left(m - p - j + \frac{\beta+1}{2}\right)^{\beta+\alpha} \\ & + \frac{1}{\Gamma(\beta+\alpha+1)} (-1)^0 \binom{\beta+1}{0} \left(m - p + \frac{\beta+1}{2}\right)^{\beta+\alpha}. \end{aligned} \tag{4.11}$$

Note that, using Proposition 1.9,

$$\binom{\beta+1}{j} + \binom{\beta+1}{j-1} = \binom{\beta+2}{j}$$

and as

$$\binom{\beta+1}{0} = 1 = \binom{\beta+2}{0},$$

we can rewrite (4.11) as follows

$$b_{m,p}-b_{m-1,p}=\frac{1}{\Gamma(\beta+\alpha+1)}\sum_{j=0}^{m-p}(-1)^j\binom{\beta+2}{j}\left(m-p-j+\frac{\beta+1}{2}\right)^{\beta+\alpha}.$$

For $p=0$, we use the same strategy applied to (3.8). □

In the next lemma we present some properties satisfied by the coefficients of the quadrature formula that approximate the fractional integral.

Lemma 4.3. *For $w_{m,p}$ satisfying* (4.7) *and $q_{m,p}$ defined by* (4.8) *we have the following properties.*

(a) $-1<q_{m,m-1}<1,\quad q_{m,p}\leqslant 0,\quad p=0,1,\ldots,m-2.$

(b) If $q_{m,m-1}$ is negative or zero then $\displaystyle\sum_{k=0}^{m-1}|q_{m,k}|\leqslant w_{m,m}$.

(c) If $q_{m,m-1}$ is positive then $\displaystyle -q_{m,m-1}+\sum_{k=0}^{m-2}|q_{m,k}|\leqslant w_{m,m}$.

Proof. (a) We have that

$$q_{m,p}=w_{m,p}-w_{m-1,p}=w_{m,p}-w_{m,p+1}\leqslant 0,\ p=1,\ldots,m-2.$$

In particular we have that $q_{m,0}=w_{m,0}-w_{m,1}\leqslant 0$ since $w_{m,1}\geqslant w_{m,0}$.

The definition of $q_{m,m-1}$ is

$$q_{m,m-1}=(b_{m,m-1}-b_{m-1,m-1})\tilde{a}_0+b_{m,m}\tilde{a}_1 \tag{4.12}$$

Resorting to $\tilde{a}_0=1/a_0$ and $\tilde{a}_1=-a_1/a_0^2$,

$$q_{m,m-1}=(b_{m,m-1}-b_{m-1,m-1})\frac{1}{a_0}-b_{m,m}\frac{a_1}{a_0^2}$$

that is equivalent to

$$q_{m,m-1}=\frac{\Gamma(\beta+1)}{\Gamma(\beta+\alpha+1)}\left[\left(1+\frac{\beta+1}{2}\right)^{\beta+\alpha}-(\beta+2)\left(\frac{\beta+1}{2}\right)^{\beta+\alpha}\right]\left(\frac{\beta+1}{2}\right)^{-\beta}$$
$$-\frac{1}{\Gamma(\beta+\alpha+1)}\left(\frac{\beta+1}{2}\right)^{\beta+\alpha}\frac{\Gamma(\beta+1)^2}{\Gamma(\beta+1)}\left[\left(1+\frac{\beta+1}{2}\right)^{\beta}-(\beta+1)\left(\frac{\beta+1}{2}\right)^{\beta}\right]\left(\frac{\beta+1}{2}\right)^{-2\beta},$$

which can be simplified to

$$q_{m,m-1}=\frac{\Gamma(\beta+1)}{\Gamma(\beta+\alpha+1)}\left(\frac{\beta+1}{2}\right)^{\alpha}\left[\left(1+\frac{2}{\beta+1}\right)^{\beta+\alpha}-1-\left(1+\frac{2}{\beta+1}\right)^{\beta}\right].$$

As $0 < \alpha < 1$ and $0 < \beta \leqslant 1$, we conclude that $-1 < q_{m,m-1} < 1$.

(b) Using (a), for $p = 0, 1, \ldots, m-1$ we have $q_{m,p} \leqslant 0$, then $|q_{m,p}| = -q_{m,p}$. Furthermore, if $q_{m,m-1}$ is nonpositive, we have

$$\sum_{k=0}^{m-1} |q_{m,k}| = -q_{m,0} - q_{m,1} - q_{m,2} - \cdots - q_{m,m-2} - q_{m,m-1}.$$

As $q_{m,k} = w_{m,k} - w_{m-1,k} = w_{m,k} - w_{m,k+1}$,

$$\sum_{k=0}^{m-1} |q_{m,k}| = -\sum_{p=0}^{m-1} (w_{m,p} - w_{m,p+1}) = -w_{m,0} + w_{m,m} \leqslant w_{m,m}.$$

Since $w_{m,k} \geqslant 0$, $k = 0, 1, \ldots, m$, we get

$$\sum_{k=0}^{m-1} |q_{m,k}| = -w_{m,0} + w_{m,m} \leqslant w_{m,m}.$$

(c) Provided $q_{m,m-1} > 0$,

$$-q_{m,m-1} + \sum_{k=0}^{m-2} |q_{m,k}| = -q_{m,0} - q_{m,1} - q_{m,2} - \cdots - q_{m,m-2} - q_{m,m-1}$$

Following the same logic as before, we get

$$-q_{m,m-1} + \sum_{k=0}^{m-2} |q_{m,k}| \leqslant w_{m,m}.$$

□

To prove the stability of the method, consider e_j^m such that $e_j^m = U_j^m - u_j^m$, where u_j^m is the exact solution of the discretized equation $u(x_j, t_m)$ and U_j^m is the computed solution. Then, e_j^m satisfies

$$e_j^m - \mu_\alpha w_{m,m} \delta^2 (d_j^{m+\frac{1}{2}} e_j^m) = e_j^{m-1} + \mu_\alpha \sum_{k=0}^{m-1} q_{m,k} \delta^2 (d_j^{m+\frac{1}{2}} e_j^k). \tag{4.13}$$

We assume that $d_j^{m+\frac{1}{2}}$ is locally constant and denote it by d [26]. That is, freezing the coefficients at their value at a certain point, we apply the von Neumann method to obtain a local stability condition.

Theorem 4.4. *Let* $0 < \beta \leqslant 1$, $0 < \alpha < 1$ *and* $\mu_d^\alpha = d\Delta t^\alpha / \Delta x^2$.

(a) Let α *be such that* $q_{m,m-1} \leqslant 0$. *The* β*-method* (4.4) *is unconditionally von Neumann stable.*

(b) Let α *be such that* $q_{m,m-1} > 0$. *If* $\mu_d^\alpha \leqslant 1/(4q_{m,m-1})$ *then the* β*-method* (4.4) *is von Neumann stable.*

Proof. We start this proof with a general approach and then we proceed according to the sign of $q_{m,m-1}$.

Following the von Neumann stability analysis [65, 70, 72], a numerical solution of (4.13) can be decomposed into a Fourier series as

$$e_j^m = \sum_{p=-M}^{M} \kappa_p^m \mathrm{e}^{i\xi_p j\Delta x},$$

where κ_p is the p-th harmonic and $\xi_p \Delta x = p\pi/M$, which is called the phase angle, covers the domain $[-\pi/\pi]$ in steps of π/M. The time evolution of the solution can determined by just one parcel $\kappa^m \mathrm{e}^{ij\phi}$. Then, replacing e_j^m by $\kappa^m \mathrm{e}^{ij\phi}$, we get

$$\kappa^m \mathrm{e}^{ij\phi} - \mu_d^\alpha w_{m,m} \delta^2(\kappa^m \mathrm{e}^{ij\phi}) = \kappa^{m-1} \mathrm{e}^{ij\phi} + \mu_d^\alpha \sum_{k=0}^{m-1} q_{m,k} \delta^2(\kappa^k \mathrm{e}^{ij\phi}). \tag{4.14}$$

The purpose of the stability Fourier analysis is to prove that the amplification factor is less than one. Following an idea presented in [89], we define $\kappa^m = G\kappa^{m-1}$, that means

$$|G(\phi)| = \left| \frac{\kappa^m}{\kappa^{m-1}} \right| \leqslant 1, \quad \text{for all } \phi.$$

Dividing (4.14) by κ^{m-1}, we obtain

$$\frac{\kappa^m}{\kappa^{m-1}} \mathrm{e}^{ij\phi} - \mu_d^\alpha w_{m,m} \frac{\kappa^m}{\kappa^{m-1}} \delta^2(\mathrm{e}^{ij\phi}) = \mathrm{e}^{ij\phi} + \mu_d^\alpha \sum_{k=0}^{m-1} q_{m,k} \delta^2(\mathrm{e}^{ij\phi}) \frac{\kappa^k}{\kappa^{m-1}}.$$

Applying $\kappa^{m-1} = G\kappa^{m-2}$ iteratively, $\kappa^{m-1} = G^2\kappa^{m-3} = \cdots = G^{m-1-k}\kappa^k$. Then, we have

$$G\mathrm{e}^{ij\phi} - \mu_d^\alpha w_{m,m} G \delta^2(\mathrm{e}^{ij\phi}) = \mathrm{e}^{ij\phi} + \mu_d^\alpha \sum_{k=0}^{m-1} q_{m,k} \delta^2(\mathrm{e}^{ij\phi}) G^{k-m+1}.$$

Furthermore,

$$\delta^2(\mathrm{e}^{ij\phi}) = \mathrm{e}^{ij\phi}\left(\mathrm{e}^{-i\phi} + \mathrm{e}^{i\phi} - 2\right) = 2\mathrm{e}^{ij\phi}(\cos\phi - 1) = -4\sin^2(\phi/2)\mathrm{e}^{ij\phi}.$$

Thus, considering $s^2 = 4\sin^2(\phi/2)$, we can write

$$G\mathrm{e}^{ij\phi} + G\mu_d^\alpha w_{m,m} s^2 \mathrm{e}^{ij\phi} = \mathrm{e}^{ij\phi} - \mu_d^\alpha \sum_{k=0}^{m-1} q_{m,k} \mathrm{e}^{ij\phi} s^2 G^{k-m+1}.$$

Dividing by $\mathrm{e}^{ij\phi}$ and multiplying by G^{m-1} we have

$$G^m(1 + \mu_d^\alpha w_{m,m} s^2) = G^{m-1} - \mu_d^\alpha \sum_{k=0}^{m-1} q_{m,k} s^2 G^k.$$

Therefore we have the polynomial in G

$$(1+\mu_d^\alpha w_{m,m}s^2)G^m - (1-\mu_d^\alpha q_{m,m-1}s^2)G^{m-1} + \mu_d^\alpha s^2 \sum_{k=0}^{m-2} q_{m,k}G^k = 0$$

or, equivalently,

$$G^m - \frac{1-\mu_d^\alpha q_{m,m-1}s^2}{1+\mu_d^\alpha w_{m,m}s^2}G^{m-1} + \frac{\mu_d^\alpha s^2}{1+\mu_d^\alpha w_{m,m}s^2}\sum_{k=0}^{m-2} q_{m,k}G^k = 0. \tag{4.15}$$

We want to prove that the solutions of (4.15) are less than 1. The roots G^* of the polynomial verify [49]

$$|G^*| \leqslant \max\left\{1, \frac{\left|1-\mu_d^\alpha q_{m,m-1}s^2\right|}{1+\mu_d^\alpha w_{m,m}s^2} + \frac{\mu_d^\alpha s^2}{1+\mu_d^\alpha w_{m,m}s^2}\sum_{k=0}^{m-2} |q_{m,k}|\right\}.$$

Let us analyze for which conditions the roots G^* are less or equal to 1, this means, for which parameters

$$\frac{1}{1+\mu_d^\alpha w_{m,m}s^2}\left(\left|1-\mu_d^\alpha q_{m,m-1}s^2\right| + \mu_d^\alpha s^2 \sum_{k=0}^{m-2}|q_{m,k}|\right) \leqslant 1.$$

(a) If $q_{m,m-1}$ is nonpositive , then

$$\left|1-\mu_d^\alpha q_{m,m-1}s^2\right| = 1-\mu_d^\alpha q_{m,m-1}s^2 = 1+\mu_d^\alpha(-q_{m,m-1})s^2 = 1+\mu_d^\alpha |q_{m,m-1}|s^2$$

and, consequently,

$$\left|1-\mu_d^\alpha q_{m,m-1}s^2\right| + \mu_d^\alpha s^2\sum_{k=0}^{m-2}|q_{m,k}| = 1+\mu_d^\alpha|q_{m,m-1}|s^2 + \mu_d^\alpha s^2\sum_{k=0}^{m-2}|q_{m,k}| = 1+\mu_d^\alpha s^2\sum_{k=0}^{m-1}|q_{m,k}|.$$

From Lemma 4.3(b), $\sum_{k=0}^{m-1}|q_{m,k}| \leqslant w_{m,m}$ and therefore

$$\begin{aligned}\frac{1}{1+\mu_d^\alpha w_{m,m}s^2}\left(\left|1-\mu_d^\alpha q_{m,m-1}s^2\right| + \mu_d^\alpha s^2\sum_{k=0}^{m-2}|q_{m,k}|\right) &= \frac{1}{1+\mu_d^\alpha w_{m,m}s^2}\left(1+\mu_d^\alpha s^2\sum_{k=0}^{m-1}|q_{m,k}|\right)\\ &\leqslant \frac{1+\mu_d^\alpha s^2 w_{m,m}}{1+\mu_d^\alpha w_{m,m}s^2} = 1.\end{aligned}$$

Finally, we conclude $|G^*| \leqslant 1$.

(b) For $q_{m,m-1}$ positive,

$$\left|1-\mu_d^\alpha q_{m,m-1}s^2\right| = 1-\mu_d^\alpha q_{m,m-1}s^2, \quad \text{if } \mu_d^\alpha q_{m,m-1}s^2 \leqslant 1.$$

As $s^2 = 4\sin^2(\phi/2) \leqslant 4$,

$$\left|1-\mu_d^\alpha q_{m,m-1}s^2\right| = 1-\mu_d^\alpha q_{m,m-1}s^2, \quad \text{for } \mu_d^\alpha q_{m,m-1} \leqslant 1/4.$$

Therefore

$$\left|1-\mu_d^\alpha q_{m,m-1}s^2\right| + \mu_d^\alpha s^2 \sum_{k=0}^{m-2} |q_{m,k}| = 1 + \mu_d^\alpha s^2 \left(-q_{m,m-1} + \sum_{k=0}^{m-2} |q_{m,k}| \right),$$

and, as from Lemma 4.3 (c)

$$-q_{m,m-1} + \sum_{k=0}^{m-2} |q_{m,k}| \leqslant w_{m,m},$$

we obtain

$$1 + \mu_d^\alpha s^2 \left(-q_{m,m-1} + \sum_{k=0}^{m-2} |q_{m,k}| \right) \leqslant 1 + \mu_d^\alpha s^2 w_{m,m}.$$

Hence, we arrive to $|G^*| \leqslant 1$ provided $\mu_d^\alpha \leqslant 1/(4q_{m,m-1})$. □

Remark. We have that $q_{m,m-1} = 0$ for α and β such that

$$\left(1+\frac{2}{\beta+1}\right)^{\beta+\alpha} - 1 - \left(1+\frac{2}{\beta+1}\right)^{\beta} = 0. \tag{4.16}$$

That is, for $0 < \beta \leqslant 1$, $q_{m,m-1} = 0$ for α such that

$$\alpha = \frac{\log(1+(1+2/(\beta+1))^{-\beta})}{\log(1+2/(\beta+1))},$$

and it is represented in Figure 4.2 in red. We also note that the condition on the statement of Theorem 4.4 (b) is not very restrictive since $q_{m,m-1} < 1$. Actually, observing Figure 4.2, the greater $q_{m,m-1}$ is near 0.5.

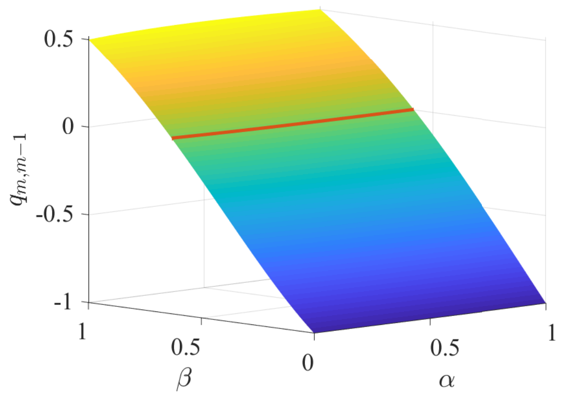

Fig. 4.2 Value of $q_{m,m-1}$, with α and β between 0 and 1. Red line represents $q_{m,m-1} = 0$.

4.2.3 Numerical experiments

In this section we compute the numerical solutions of equation (4.1) in the domain $[a,b]\times[0,T]$. As before, we consider a uniform mesh in space and time, that is, $x_j = a + j\Delta x$, for $j = 0,\dots,N$, with

$x_N = b$ and $t_m = t_{m-1} + \Delta t,\ m = 0, \ldots, M$, with $t_M = T$. To discuss the accuracy of the approximation, we define two types of error that take in consideration the discrete L^∞ norm in time and the discrete L^2 norm in time discussed in the previous chapter.

We define the error, related to the discrete L^∞ norm in time, as

$$E_\infty = \max_{m=1,\ldots,M} \left(\Delta x \sum_{j=1}^{N-1} \left(U_j^m - u(x_j, t_m) \right)^2 \right)^{\frac{1}{2}} \tag{4.17}$$

and the error related to the discrete L^2 norm in time as

$$E_2 = \left(\Delta t \Delta x \sum_{m=1}^{M} \sum_{j=1}^{N-1} \left(U_j^m - u(x_j, t_m) \right)^2 \right)^{\frac{1}{2}}. \tag{4.18}$$

The value U_j^m is the numerical approximation of the exact solution $u(x_j, t_m)$. The test problems we consider in what follows are similar to the ones presented in [43, 63]. For all problems, the rate of convergence of the numerical method are denoted respectively by R_∞ and R_2, with respect to the two norms.

Problem 1. Let $[a, b] = [0, 2]$, $T = 1$ and $d(x, t) = x$. The source term $g(x, t)$ and the initial condition $u_0(x)$ are defined such that the exact solution of the problem is $u(x, t) = t^{2+\alpha} x^4 (2 - x)^4$. The regularity of the solution is $C^2([0, T])$ in time. Furthermore, note that u belongs to $H^{\beta+1}([0, T])$.

Despite our focus being on the convergence in time, for this problem we illustrate the rate of convergence in space in Tables 4.1 and 4.2 with respect to the two norms for different values of β and $\alpha = 0.2$ and $\alpha = 0.8$. As expected, the numerical method is second accurate in space. For other values of α we obtain similar results. We also note that the linear spline, $\beta = 1$, is not necessarily the one that performs better considering the magnitude of the error.

The order of convergence in time is shown in Table 4.3 and Table 4.4, $\alpha = 0.2$ and $\alpha = 0.8$, respectively. Regarding both errors, we obtain $1 + \beta$ as expected. The solution seems to be regular enough near $t = 0$, to the order of convergence is not be affected by the behaviour of the solution near this point. In the next example we decrease the regularity of the solution and discuss if and how it affects the order of convergence.

Problem 2. Let $[a, b] = [0, 2]$, $T = 1$ and now $d(x, t) = 1$. Once again, the source term $g(x, t)$ and the initial condition $u_0(x)$ are defined such that the exact solution of this problem is given by $u(x, t) = t^{1+\alpha} 4x^2 (2 - x)^2$. The regularity of the solution in time is $C^1([0, T])$, which is lower compared to the previous problem. Furthermore, there may exist some value of α for which $u \notin H^{\beta+1}(0, T)$.

We display the order of convergence in time for a small Δx, from Table 4.5 to Table 4.8 for $\alpha = 0.2, 0.4, 0.6, 0.8$, respectively. From the error bounds discussed in the previous chapters, the order of convergence, regarding the error E_∞, would be of $\min\{1 + \beta, 1 + 2\alpha\}$ and, regarding the error E_2, is expected to be $\min\{1 + \beta, 3/2 + 2\alpha\}$. For $\alpha = 0.2$, $\min\{1 + \beta, 1 + 2\alpha\}$ is 1.2 for $\beta = 0.2$ and 1.4 for the other values of β and $\min\{1 + \beta, 3/2 + 2\alpha\} = 1 + \beta$ except for $\beta = 1$, for which the minimum

Table 4.1 Results concerning Problem 1. Convergence rate (R_∞ and R_2) in space for different values of β with α=0.2 and $\Delta t = 1/5000$, for the errors (4.17) and (4.18), respectively.

Δx	$\beta = 0.2$	R_∞	$\beta = 0.4$	R_∞	$\beta = 0.6$	R_∞	$\beta = 0.8$	R_∞	$\beta = 1$	R_∞
2^{-3}	1.007e-02		1.008e-02		1.008e-02		1.008e-02		1.008e-02	
2^{-4}	2.487e-03	2.02	2.488e-03	2.02	2.488e-03	2.02	2.488e-03	2.02	2.488e-03	2.02
2^{-5}	6.195e-04	2.01	6.200e-04	2.00	6.202e-04	2.00	6.202e-04	2.00	6.203e-04	2.00
2^{-6}	1.542e-04	2.01	1.547e-04	2.00	1.549e-04	2.00	1.550e-04	2.00	1.550e-04	2.00
2^{-7}	3.795e-05	2.02	3.851e-05	2.01	3.869e-05	2.00	3.873e-05	2.00	3.874e-05	2.00
2^{-8}	8.967e-06	2.08	9.455e-06	2.03	9.633e-06	2.01	9.671e-06	2.00	9.684e-06	2.00
2^{-9}	2.048e-06	2.13	2.215e-06	2.09	2.370e-06	2.02	2.407e-06	2.01	2.420e-06	2.00
		R_2		R_2		R_2		R_2		R_2
2^{-3}	4.319e-03		4.319e-03		4.319e-03		4.319e-03		4.319e-03	
2^{-4}	1.066e-03	2.02	1.067e-03	2.02	1.067e-03	2.02	1.067e-03	2.02	1.067e-03	2.02
2^{-5}	2.655e-04	2.01	2.658e-04	2.00	2.659e-04	2.00	2.659e-04	2.00	2.660e-04	2.00
2^{-6}	6.601e-05	2.01	6.632e-05	2.00	6.642e-05	2.00	6.644e-05	2.00	6.645e-05	2.00
2^{-7}	1.618e-05	2.03	1.648e-05	2.01	1.658e-05	2.00	1.660e-05	2.00	1.661e-05	2.00
2^{-8}	3.776e-06	2.10	4.022e-06	2.03	4.120e-06	2.01	4.144e-06	2.00	4.152e-06	2.00
2^{-9}	9.399e-07	2.01	9.298e-07	2.11	1.006e-06	2.03	1.030e-06	2.01	1.037e-06	2.00

Table 4.2 Results concerning Problem 1. Convergence rate (R_∞ and R_2) in space for different values of β with α=0.8 and $\Delta t = 1/5000$, for the errors (4.17) and (4.18), respectively.

Δx	$\beta = 0.2$	R_∞	$\beta = 0.4$	R_∞	$\beta = 0.6$	R_∞	$\beta = 0.8$	R_∞	$\beta = 1$	R_∞
2^{-3}	9.147e-03		9.148e-03		9.148e-03		9.148e-03		9.148e-03	
2^{-4}	2.265e-03	2.01	2.266e-03	2.01	2.266e-03	2.01	2.266e-03	2.01	2.266e-03	2.01
2^{-5}	5.647e-04	2.00	5.653e-04	2.00	5.656e-04	2.00	5.656e-04	2.00	5.657e-04	2.00
2^{-6}	1.404e-04	2.01	1.411e-04	2.00	1.413e-04	2.00	1.414e-04	2.00	1.414e-04	2.00
2^{-7}	3.441e-05	2.03	3.501e-05	2.01	3.526e-05	2.00	3.533e-05	2.00	3.535e-05	2.00
2^{-8}	7.975e-06	2.11	8.499e-06	2.04	8.747e-06	2.01	8.816e-06	2.00	8.835e-06	2.00
2^{-9}	1.801e-06	2.15	1.919e-06	2.15	2.120e-06	2.04	2.186e-06	2.01	2.205e-06	2.00
		R_2		R_2		R_2		R_2		R_2
2^{-3}	3.486e-03		3.486e-03		3.486e-03		3.486e-03		3.486e-03	
2^{-4}	8.637e-04	2.01	8.640e-04	2.01	8.641e-04	2.01	8.642e-04	2.01	8.642e-04	2.01
2^{-5}	2.153e-04	2.00	2.156e-04	2.00	2.157e-04	2.00	2.157e-04	2.00	2.157e-04	2.00
2^{-6}	5.349e-05	2.01	5.377e-05	2.00	5.389e-05	2.00	5.393e-05	2.00	5.393e-05	2.00
2^{-7}	1.305e-05	2.04	1.332e-05	2.01	1.344e-05	2.00	1.348e-05	2.00	1.348e-05	2.00
2^{-8}	2.982e-06	2.13	3.210e-06	2.05	3.325e-06	2.02	3.360e-06	2.00	3.370e-06	2.00
2^{-9}	7.217e-07	2.05	7.129e-07	2.17	7.981e-07	2.06	8.308e-07	2.02	8.403e-07	2.00

is 1.9. We are getting an order of 1.3 for the E_∞ and for the E_2 norm when $\beta = 1$, we observe the order approaching 1.8 instead of 1.9, although these values are still very near to the expected order. Considering $\alpha = 0.4$, for the error E_2 we have $\min\{1+\beta, 1+2\alpha\} = 1+\beta$ for $\beta = 0.2, 0.4, 0.6, 0.8$

Table 4.3 Results concerning Problem 1. Convergence rate (R_∞ and R_2) in time for different values of β with α=0.2 and $\Delta x = 1/5000$, for the errors (4.17) and (4.18), respectively.

Δt	$\beta = 0.2$	R_∞	$\beta = 0.4$	R_∞	$\beta = 0.6$	R_∞	$\beta = 0.8$	R_∞	$\beta = 1$	R_∞
2^{-3}	4.632e-03		3.471e-03		2.566e-03		1.855e-03		1.302e-03	
2^{-4}	1.889e-03	1.29	1.313e-03	1.40	8.791e-04	1.55	5.660e-04	1.71	3.498e-04	1.90
2^{-5}	7.803e-04	1.28	4.994e-04	1.39	3.001e-04	1.55	1.710e-04	1.73	9.271e-05	1.92
2^{-6}	3.256e-04	1.26	1.904e-04	1.39	1.021e-04	1.56	5.126e-05	1.74	2.432e-05	1.93
2^{-7}	1.369e-04	1.25	7.266e-05	1.39	3.457e-05	1.56	1.525e-05	1.75	6.320e-06	1.94
2^{-8}	5.784e-05	1.24	2.772e-05	1.39	1.166e-05	1.57	4.507e-06	1.76	1.624e-06	1.96
2^{-9}	2.454e-05	1.24	1.057e-05	1.39	3.914e-06	1.57	1.319e-06	1.77	4.088e-07	1.99
		R_2		R_2		R_2		R_2		R_2
2^{-3}	2.988e-03		2.308e-03		1.781e-03		1.364e-03		1.034e-03	
2^{-4}	1.160e-03	1.36	8.361e-04	1.46	5.896e-04	1.60	4.067e-04	1.75	2.747e-04	1.91
2^{-5}	4.661e-04	1.32	3.108e-04	1.43	1.981e-04	1.57	1.218e-04	1.74	7.276e-05	1.92
2^{-6}	1.914e-04	1.28	1.171e-04	1.41	6.689e-05	1.57	3.643e-05	1.74	1.915e-05	1.93
2^{-7}	7.972e-05	1.26	4.443e-05	1.40	2.260e-05	1.57	1.086e-05	1.75	5.005e-06	1.94
2^{-8}	3.350e-05	1.25	1.691e-05	1.39	7.626e-06	1.57	3.218e-06	1.75	1.297e-06	1.95
2^{-9}	1.416e-05	1.24	6.438e-06	1.39	2.564e-06	1.57	9.473e-07	1.76	3.318e-07	1.97

Table 4.4 Results concerning Problem 1. Convergence rate (R_∞ and R_2) in time for different values of β with α=0.8 and $\Delta x = 1/5000$, for the errors (4.17) and (4.18), respectively.

Δt	$\beta = 0.2$	R_∞	$\beta = 0.4$	R_∞	$\beta = 0.6$	R_∞	$\beta = 0.8$	R_∞	$\beta = 1$	R_∞
2^{-3}	6.421e-03		6.282e-03		5.573e-03		4.661e-03		3.734e-03	
2^{-4}	2.257e-03	1.51	2.156e-03	1.54	1.759e-03	1.66	1.321e-03	1.82	9.381e-04	1.99
2^{-5}	8.544e-04	1.40	7.706e-04	1.48	5.661e-04	1.64	3.766e-04	1.81	2.351e-04	2.00
2^{-6}	3.413e-04	1.32	2.824e-04	1.45	1.842e-04	1.62	1.077e-04	1.81	5.887e-05	2.00
2^{-7}	1.413e-04	1.27	1.050e-04	1.43	6.030e-05	1.61	3.087e-05	1.80	1.472e-05	2.00
2^{-8}	5.974e-05	1.24	3.938e-05	1.42	1.980e-05	1.61	8.846e-06	1.80	3.673e-06	2.00
2^{-9}	2.558e-05	1.22	1.483e-05	1.41	6.509e-06	1.61	2.530e-06	1.81	9.092e-07	2.01
		R_2		R_2		R_2		R_2		R_2
2^{-3}	3.690e-03		3.610e-03		3.265e-03		2.815e-03		2.348e-03	
2^{-4}	1.194e-03	1.63	1.151e-03	1.65	9.677e-04	1.75	7.572e-04	1.89	5.658e-04	2.05
2^{-5}	4.278e-04	1.48	3.940e-04	1.55	3.008e-04	1.69	2.100e-04	1.85	1.388e-04	2.03
2^{-6}	1.653e-04	1.37	1.410e-04	1.48	9.607e-05	1.65	5.921e-05	1.83	3.437e-05	2.01
2^{-7}	6.709e-05	1.30	5.176e-05	1.45	3.115e-05	1.62	1.684e-05	1.81	8.551e-06	2.01
2^{-8}	2.806e-05	1.26	1.927e-05	1.42	1.018e-05	1.61	4.810e-06	1.81	2.130e-06	2.01
2^{-9}	1.194e-05	1.23	7.233e-06	1.41	3.339e-06	1.61	1.374e-06	1.81	5.285e-07	2.01

and 1.8 for $\beta = 1$. For the error E_∞, we have that $\min\{1+\beta, 3/2+2\alpha\}$ is $1+\beta$. From observing the Table 4.6, the results are closer to the expected compared to $\alpha = 0.2$. Furthermore note that the results for E_∞ are more tuned with the theoretical ones. For $\alpha = 0.6$ and $\alpha = 0.8$, for both errors the

Table 4.5 Results concerning Problem 2. Convergence rate (R_∞ and R_2) in time for different values of β with α=0.2 and $\Delta x = 1/5000$, for the error (4.17) and (4.18), respectively.

Δt	$\beta = 0.2$	R_∞	$\beta = 0.4$	R_∞	$\beta = 0.6$	R_∞	$\beta = 0.8$	R_∞	$\beta = 1$	R_∞
2^{-3}	9.234e-03		7.390e-03		6.012e-03		4.944e-03		4.093e-03	
2^{-4}	3.806e-03	1.28	3.045e-03	1.28	2.476e-03	1.28	2.036e-03	1.28	1.685e-03	1.28
2^{-5}	1.562e-03	1.28	1.249e-03	1.29	1.016e-03	1.29	8.349e-04	1.29	6.910e-04	1.29
2^{-6}	6.477e-04	1.27	5.103e-04	1.29	4.148e-04	1.29	3.409e-04	1.29	2.821e-04	1.29
2^{-7}	2.749e-04	1.24	2.076e-04	1.30	1.687e-04	1.30	1.387e-04	1.30	1.147e-04	1.30
2^{-8}	1.169e-04	1.23	8.412e-05	1.30	6.835e-05	1.30	5.616e-05	1.30	4.646e-05	1.30
2^{-9}	4.984e-05	1.23	3.396e-05	1.31	2.758e-05	1.31	2.266e-05	1.31	1.874e-05	1.31
		R_2		R_2		R_2		R_2		R_2
2^{-3}	8.709e-03		6.245e-03		4.362e-03		2.938e-03		1.910e-03	
2^{-4}	3.627e-03	1.26	2.452e-03	1.35	1.586e-03	1.46	9.830e-04	1.58	5.911e-04	1.69
2^{-5}	1.520e-03	1.26	9.566e-04	1.36	5.669e-04	1.48	3.223e-04	1.61	1.801e-04	1.71
2^{-6}	6.395e-04	1.25	3.710e-04	1.37	1.998e-04	1.50	1.039e-04	1.63	5.421e-05	1.73
2^{-7}	2.701e-04	1.24	1.431e-04	1.37	6.957e-05	1.52	3.301e-05	1.65	1.615e-05	1.75
2^{-8}	1.145e-04	1.24	5.499e-05	1.38	2.398e-05	1.54	1.035e-05	1.67	4.769e-06	1.76
2^{-9}	4.863e-05	1.24	2.105e-05	1.39	8.185e-06	1.55	3.207e-06	1.69	1.394e-06	1.77

Table 4.6 Results concerning Problem 2. Convergence rate (R_∞ and R_2) in time for different values of β with α=0.4 and $\Delta x = 1/5000$, for the errors (4.17) and (4.18), respectively.

Δt	$\beta = 0.2$	R_∞	$\beta = 0.4$	R_∞	$\beta = 0.6$	R_∞	$\beta = 0.8$	R_∞	$\beta = 1$	R_∞
2^{-3}	1.220e-02		9.776e-03		8.817e-03		8.067e-03		7.465e-03	
2^{-4}	4.811e-03	1.34	3.482e-03	1.49	2.887e-03	1.61	2.640e-03	1.61	2.442e-03	1.61
2^{-5}	1.939e-03	1.31	1.297e-03	1.43	9.314e-04	1.63	8.515e-04	1.63	7.874e-04	1.63
2^{-6}	7.944e-04	1.29	4.849e-04	1.42	2.969e-04	1.65	2.713e-04	1.65	2.509e-04	1.65
2^{-7}	3.299e-04	1.27	1.819e-04	1.41	9.374e-05	1.66	8.565e-05	1.66	7.917e-05	1.66
2^{-8}	1.384e-04	1.25	6.836e-05	1.41	3.081e-05	1.61	2.684e-05	1.67	2.481e-05	1.67
2^{-9}	5.851e-05	1.24	2.569e-05	1.41	1.023e-05	1.59	8.370e-06	1.68	7.735e-06	1.68
		R_2		R_2		R_2		R_2		R_2
2^{-3}	1.139e-02		9.218e-03		7.153e-03		5.391e-03		4.016e-03	
2^{-4}	4.282e-03	1.41	3.302e-03	1.48	2.355e-03	1.60	1.608e-03	1.75	1.085e-03	1.89
2^{-5}	1.665e-03	1.36	1.206e-03	1.45	7.793e-04	1.60	4.769e-04	1.75	2.894e-04	1.91
2^{-6}	6.652e-04	1.32	4.456e-04	1.44	2.582e-04	1.59	1.406e-04	1.76	7.643e-05	1.92
2^{-7}	2.712e-04	1.29	1.659e-04	1.43	8.548e-05	1.59	4.120e-05	1.77	1.999e-05	1.93
2^{-8}	1.123e-04	1.27	6.207e-05	1.42	2.827e-05	1.60	1.200e-05	1.78	5.175e-06	1.95
2^{-9}	4.701e-05	1.26	2.328e-05	1.41	9.322e-06	1.60	3.467e-06	1.79	1.320e-06	1.97

theoretical results point to an order of convergence of $\beta + 1$, as illustrated in Tables 4.7 and 4.8. Note that, when the order of convergence is supposed to be $\beta + 1$, the numerical experiments are more in agreement with the theoretical results.

Table 4.7 Results concerning Problem 2. Convergence rate (R_∞ and R_2) in time for different values of β with α=0.6 and $\Delta x = 1/5000$, for the errors (4.17) and (4.18), respectively.

Δt	$\beta = 0.2$	R_∞	$\beta = 0.4$	R_∞	$\beta = 0.6$	R_∞	$\beta = 0.8$	R_∞	$\beta = 1$	R_∞
2^{-3}	1.378e-02		1.210e-02		9.312e-03		7.383e-03		7.117e-03	
2^{-4}	5.265e-03	1.39	4.384e-03	1.46	3.041e-03	1.61	1.954e-03	1.92	1.803e-03	1.98
2^{-5}	2.095e-03	1.33	1.616e-03	1.44	9.971e-04	1.61	5.633e-04	1.79	4.484e-04	2.01
2^{-6}	8.584e-04	1.29	6.014e-04	1.43	3.277e-04	1.61	1.622e-04	1.80	1.102e-04	2.02
2^{-7}	3.589e-04	1.26	2.253e-04	1.42	1.078e-04	1.60	4.669e-05	1.80	2.685e-05	2.04
2^{-8}	1.520e-04	1.24	8.468e-05	1.41	3.544e-05	1.60	1.342e-05	1.80	6.789e-06	1.98
2^{-9}	6.498e-05	1.23	3.188e-05	1.41	1.161e-05	1.61	3.846e-06	1.80	1.716e-06	1.98
		R_2		R_2		R_2		R_2		R_2
2^{-3}	1.150e-02		1.030e-02		8.548e-03		6.771e-03		5.225e-03	
2^{-4}	4.081e-03	1.49	3.531e-03	1.54	2.689e-03	1.67	1.913e-03	1.82	1.314e-03	1.99
2^{-5}	1.543e-03	1.40	1.260e-03	1.49	8.649e-04	1.64	5.463e-04	1.81	3.311e-04	1.99
2^{-6}	6.113e-04	1.34	4.602e-04	1.45	2.815e-04	1.62	1.567e-04	1.80	8.339e-05	1.99
2^{-7}	2.501e-04	1.29	1.706e-04	1.43	9.213e-05	1.61	4.498e-05	1.80	2.096e-05	1.99
2^{-8}	1.046e-04	1.26	6.373e-05	1.42	3.023e-05	1.61	1.290e-05	1.80	5.242e-06	2.00
2^{-9}	4.432e-05	1.24	2.392e-05	1.41	9.923e-06	1.61	3.683e-06	1.81	1.294e-06	2.02

Table 4.8 Results concerning Problem 2. Convergence rate (R_∞ and R_2) in time for different values of β with α=0.8 and $\Delta x = 1/5000$, for the error (4.17) and (4.18), respectively.

Δt	$\beta = 0.2$	R_∞	$\beta = 0.4$	R_∞	$\beta = 0.6$	R_∞	$\beta = 0.8$	R_∞	$\beta = 1$	R_∞
2^{-3}	1.473e-02		1.433e-02		1.191e-02		8.999e-03		6.374e-03	
2^{-4}	5.567e-03	1.40	5.150e-03	1.48	3.858e-03	1.63	2.575e-03	1.81	1.593e-03	2.00
2^{-5}	2.223e-03	1.32	1.894e-03	1.44	1.260e-03	1.61	7.381e-04	1.80	3.986e-04	2.00
2^{-6}	9.198e-04	1.27	7.061e-04	1.42	4.135e-04	1.61	2.117e-04	1.80	9.970e-05	2.00
2^{-7}	3.889e-04	1.24	2.651e-04	1.41	1.360e-04	1.60	6.072e-05	1.80	2.491e-05	2.00
2^{-8}	1.665e-04	1.22	9.989e-05	1.41	4.472e-05	1.60	1.737e-05	1.81	6.206e-06	2.01
2^{-9}	7.176e-05	1.21	3.770e-05	1.41	1.468e-05	1.61	4.932e-06	1.82	1.532e-06	2.02
		R_2		R_2		R_2		R_2		R_2
2^{-3}	1.089e-02		1.065e-02		9.333e-03		7.683e-03		6.080e-03	
2^{-4}	3.770e-03	1.53	3.586e-03	1.57	2.882e-03	1.70	2.128e-03	1.85	1.493e-03	2.03
2^{-5}	1.423e-03	1.41	1.272e-03	1.50	9.182e-04	1.65	6.003e-04	1.83	3.704e-04	2.01
2^{-6}	5.692e-04	1.32	4.647e-04	1.45	2.974e-04	1.63	1.709e-04	1.81	9.229e-05	2.00
2^{-7}	2.361e-04	1.27	1.726e-04	1.43	9.716e-05	1.61	4.884e-05	1.81	2.303e-05	2.00
2^{-8}	1.000e-04	1.24	6.468e-05	1.42	3.187e-05	1.61	1.397e-05	1.81	5.734e-06	2.01
2^{-9}	4.286e-05	1.22	2.435e-05	1.41	1.046e-05	1.61	3.988e-06	1.81	1.413e-06	2.02

Problem 3. In this example we further reduce the regularity of the solution in time. We consider $[a,b] = [0,\pi]$, $T = 1$ and $d(x,t) = 1$. The source term $g(x,t)$ and the initial condition $u_0(x)$ are

defined such that the exact solution of this problem is given by

$$u(x,t) = \left(1 + \frac{t^{\alpha}}{\Gamma(1+\alpha)}\right)\sin(x).$$

The regularity of the solution is only $C[0,T]$ in time, since $u_t = O(t^{\alpha-1})$.

We display the numerical results from Table 4.9 to Table 4.12 for $\alpha = 0.2, 0.4, 0.6, 0.8$. For the E_∞ error we obtain, in general, the expected order of convergence α. However, for the E_2 error, we obtain a smaller order of convergence than the expected $\alpha + 0.5$, where greater values of β display better results in refined meshes. To better illustrate the rate of accuracy, we have introduced additional time steps in the tables of this example.

Table 4.9 Results concerning Problem 3. Convergence rate (R_∞ and R_2) in time for different values of β with α=0.2 and $\Delta x = \pi/2500$, for the errors (4.17) and (4.18), respectively.

Δt	$\beta = 0.2$	R_∞	$\beta = 0.4$	R_∞	$\beta = 0.6$	R_∞	$\beta = 0.8$	R_∞	$\beta = 1$	R_∞
2^{-3}	1.720e-02		2.281e-02		3.093e-02		4.243e-02		5.789e-02	
2^{-4}	1.137e-02	0.60	1.606e-02	0.51	2.316e-02	0.42	3.343e-02	0.34	4.737e-02	0.29
2^{-5}	6.891e-03	0.72	1.081e-02	0.57	1.702e-02	0.44	2.617e-02	0.35	3.871e-02	0.29
2^{-6}	4.798e-03	0.52	6.795e-03	0.67	1.222e-02	0.48	2.036e-02	0.36	3.161e-02	0.29
2^{-7}	4.891e-03	-0.03	4.975e-03	0.45	8.509e-03	0.52	1.574e-02	0.37	2.580e-02	0.29
2^{-8}	4.874e-03	0.01	4.855e-03	0.04	5.673e-03	0.58	1.209e-02	0.38	2.107e-02	0.29
2^{-9}	4.910e-03	-0.01	4.717e-03	0.04	3.537e-03	0.68	9.220e-03	0.39	1.722e-02	0.29
2^{-10}	4.825e-03	0.03	4.538e-03	0.06	3.321e-03	0.09	6.979e-03	0.40	1.409e-02	0.29
2^{-11}	4.650e-03	0.05	4.352e-03	0.06	3.124e-03	0.09	5.240e-03	0.41	1.154e-02	0.29
2^{-12}	4.412e-03	0.08	4.146e-03	0.07	2.927e-03	0.09	3.898e-03	0.43	9.476e-03	0.28
2^{-13}	4.134e-03	0.09	3.898e-03	0.09	2.728e-03	0.10	2.869e-03	0.44	7.798e-03	0.28
2^{-14}	3.833e-03	0.11	3.624e-03	0.11	2.535e-03	0.11	2.086e-03	0.46	6.434e-03	0.28
		R_2		R_2		R_2		R_2		R_2
2^{-3}	6.384e-03		8.331e-03		1.102e-02		1.537e-02		2.177e-02	
2^{-4}	4.024e-03	0.67	5.093e-03	0.71	6.167e-03	0.84	8.568e-03	0.84	1.276e-02	0.77
2^{-5}	3.245e-03	0.31	3.929e-03	0.37	3.993e-03	0.63	4.849e-03	0.82	7.433e-03	0.78
2^{-6}	2.850e-03	0.19	3.436e-03	0.19	3.132e-03	0.35	2.941e-03	0.72	4.315e-03	0.78
2^{-7}	2.500e-03	0.19	3.064e-03	0.17	2.716e-03	0.21	2.029e-03	0.54	2.501e-03	0.79
2^{-8}	2.164e-03	0.21	2.707e-03	0.18	2.407e-03	0.17	1.594e-03	0.35	1.449e-03	0.79
2^{-9}	1.859e-03	0.22	2.369e-03	0.19	2.126e-03	0.18	1.346e-03	0.24	8.390e-04	0.79
2^{-10}	1.594e-03	0.22	2.062e-03	0.20	1.865e-03	0.19	1.168e-03	0.20	4.862e-04	0.79
2^{-11}	1.368e-03	0.22	1.790e-03	0.20	1.629e-03	0.20	1.019e-03	0.20	2.820e-04	0.79
2^{-12}	1.178e-03	0.22	1.553e-03	0.20	1.420e-03	0.20	8.897e-04	0.20	1.638e-04	0.78
2^{-13}	1.017e-03	0.21	1.349e-03	0.20	1.236e-03	0.20	7.760e-04	0.20	9.534e-05	0.78
2^{-14}	8.808e-04	0.21	1.172e-03	0.20	1.075e-03	0.20	6.761e-04	0.20	5.561e-05	0.78

We note that the fractional splines that perform better for larger time steps, regarding the size of the error, are the splines of degree β, with β closer to α as illustrated in Tables 4.9–4.12. For $\alpha = 0.2$, the spline of degree $\beta = 0.2$ presents the smallest error and for $\alpha = 0.4$, are the splines of degree

Table 4.10 Results concerning Problem 3. Convergence rate (R_∞ and R_2) in time for different values of β with α=0.4 and $\Delta x = \pi/2500$, for the errors (4.17) and (4.18), respectively.

Δt	$\beta = 0.2$	R_∞	$\beta = 0.4$	R_∞	$\beta = 0.6$	R_∞	$\beta = 0.8$	R_∞	$\beta = 1$	R_∞
2^{-3}	1.027e-02		6.519e-03		1.320e-02		2.645e-02		4.258e-02	
2^{-4}	1.036e-02	-0.01	7.094e-03	-0.12	5.444e-03	1.28	1.589e-02	0.74	2.870e-02	0.57
2^{-5}	1.050e-02	-0.02	6.972e-03	0.02	3.159e-03	0.79	9.353e-03	0.76	1.945e-02	0.56
2^{-6}	9.915e-03	0.08	6.393e-03	0.13	3.228e-03	-0.03	5.393e-03	0.79	1.329e-02	0.55
2^{-7}	8.727e-03	0.18	5.740e-03	0.16	3.058e-03	0.08	3.038e-03	0.83	9.175e-03	0.53
2^{-8}	7.353e-03	0.25	5.086e-03	0.17	2.714e-03	0.17	1.664e-03	0.87	6.407e-03	0.52
2^{-9}	6.018e-03	0.29	4.297e-03	0.24	2.306e-03	0.24	8.770e-04	0.92	4.528e-03	0.50
2^{-10}	4.826e-03	0.32	3.520e-03	0.29	1.901e-03	0.28	6.432e-04	0.45	3.236e-03	0.48
2^{-11}	3.814e-03	0.34	2.823e-03	0.32	1.534e-03	0.31	5.367e-04	0.26	2.337e-03	0.47
2^{-12}	2.982e-03	0.35	2.231e-03	0.34	1.230e-03	0.32	4.376e-04	0.29	1.704e-03	0.46
2^{-13}	2.314e-03	0.37	1.744e-03	0.36	9.831e-04	0.32	3.512e-04	0.32	1.252e-03	0.44
2^{-14}	1.785e-03	0.37	1.353e-03	0.37	7.746e-04	0.34	2.778e-04	0.34	9.258e-04	0.44
		R_2		R_2		R_2		R_2		R_2
2^{-3}	5.945e-03		3.865e-03		4.826e-03		9.665e-03		1.630e-02	
2^{-4}	5.375e-03	0.15	3.692e-03	0.07	2.260e-03	1.09	4.091e-03	1.24	7.947e-03	1.04
2^{-5}	4.074e-03	0.40	3.064e-03	0.27	1.761e-03	0.36	1.758e-03	1.22	3.866e-03	1.04
2^{-6}	2.833e-03	0.52	2.283e-03	0.42	1.447e-03	0.28	8.916e-04	0.98	1.885e-03	1.04
2^{-7}	1.881e-03	0.59	1.606e-03	0.51	1.110e-03	0.38	5.859e-04	0.61	9.246e-04	1.03
2^{-8}	1.219e-03	0.63	1.099e-03	0.55	8.139e-04	0.45	4.348e-04	0.43	4.572e-04	1.02
2^{-9}	7.821e-04	0.64	7.463e-04	0.56	5.842e-04	0.48	3.272e-04	0.41	2.282e-04	1.00
2^{-10}	5.035e-04	0.64	5.093e-04	0.55	4.174e-04	0.49	2.442e-04	0.42	1.150e-04	0.99
2^{-11}	3.284e-04	0.62	3.522e-04	0.53	2.997e-04	0.48	1.813e-04	0.43	5.854e-05	0.97
2^{-12}	2.187e-04	0.59	2.479e-04	0.51	2.171e-04	0.46	1.345e-04	0.43	3.007e-05	0.96
2^{-13}	1.494e-04	0.55	1.775e-04	0.48	1.589e-04	0.45	1.000e-04	0.43	1.557e-05	0.95
2^{-14}	1.046e-04	0.51	1.292e-04	0.46	1.174e-04	0.44	7.468e-05	0.42	8.120e-06	0.94

$\beta = 0.4$ and $\beta = 0.6$. Similarly, for $\alpha = 0.6$ the splines that lead to smaller errors for larger time steps are for $\beta = 0.6$ and $\beta = 0.8$ and for $\alpha = 0.8$ are the splines of degree $\beta = 0.8$ and $\beta = 1$.

Overall, the errors in this example have a less regular behaviour when compared with the previous examples, as presented in Tables 4.9 and 4.10 for $\alpha = 0.2$ and $\alpha = 0.4$. In Table 4.9, although we observe for $\alpha = 0.2$ and $\beta = 0.2$ some oscillations in the error E_∞, it becomes smaller as we refine the time step. Still for $\alpha, \beta = 0.2$, at the beginning the rates of convergence R_2 and R_∞ are higher than expected but then slow down and stabilize. This last aspect can also be observed in Table 4.10 for $\beta = 0.6$ and $\beta = 0.8$.

Regarding the stability of the numerical method, when running the experiments we observed that the method converges even when the stability condition presented in Theorem 4.4 (b) is not satisfied.

Table 4.11 Results concerning Problem 3. Convergence rate (R_∞ and R_2) in time for different values of β with α=0.6 and $\Delta x = \pi/2500$, for the errors (4.17) and (4.18), respectively.

Δt	$\beta = 0.2$	R_∞	$\beta = 0.4$	R_∞	$\beta = 0.6$	R_∞	$\beta = 0.8$	R_∞	$\beta = 1$	R_∞
2^{-3}	2.634e-02		1.704e-02		7.312e-03		6.280e-03		2.092e-02	
2^{-4}	2.041e-02	0.37	1.410e-02	0.27	6.725e-03	0.12	1.941e-03	1.69	1.208e-02	0.79
2^{-5}	1.493e-02	0.45	1.068e-02	0.40	5.678e-03	0.24	1.347e-03	0.53	7.141e-03	0.76
2^{-6}	1.053e-02	0.50	7.685e-03	0.47	4.325e-03	0.39	1.183e-03	0.19	4.325e-03	0.72
2^{-7}	7.260e-03	0.54	5.364e-03	0.52	3.118e-03	0.47	9.282e-04	0.35	2.678e-03	0.69
2^{-8}	4.930e-03	0.56	3.670e-03	0.55	2.176e-03	0.52	6.832e-04	0.44	1.688e-03	0.67
2^{-9}	3.315e-03	0.57	2.480e-03	0.57	1.488e-03	0.55	4.836e-04	0.50	1.078e-03	0.65
2^{-10}	2.215e-03	0.58	1.662e-03	0.58	1.005e-03	0.57	3.340e-04	0.53	6.958e-04	0.63
2^{-11}	1.473e-03	0.59	1.108e-03	0.59	6.734e-04	0.58	2.270e-04	0.56	4.523e-04	0.62
2^{-12}	9.772e-04	0.59	7.360e-04	0.59	4.488e-04	0.59	1.527e-04	0.57	2.954e-04	0.61
2^{-13}	6.470e-04	0.59	4.877e-04	0.59	2.980e-04	0.59	1.021e-04	0.58	1.936e-04	0.61
2^{-14}	4.279e-04	0.60	3.227e-04	0.60	1.975e-04	0.59	6.791e-05	0.59	1.272e-04	0.61
2^{-15}	2.828e-04	0.60	2.133e-04	0.60	1.307e-04	0.60	4.505e-05	0.59	8.364e-05	0.60
		R_2		R_2		R_2		R_2		R_2
2^{-3}	1.363e-02		9.419e-03		4.478e-03		2.259e-03		8.309e-03	
2^{-4}	8.665e-03	0.65	6.290e-03	0.58	3.481e-03	0.36	9.125e-04	1.31	3.502e-03	1.25
2^{-5}	5.152e-03	0.75	3.840e-03	0.71	2.299e-03	0.60	7.299e-04	0.32	1.488e-03	1.24
2^{-6}	2.938e-03	0.81	2.229e-03	0.78	1.402e-03	0.71	5.385e-04	0.44	6.405e-04	1.22
2^{-7}	1.630e-03	0.88	1.254e-03	0.83	8.186e-04	0.78	3.547e-04	0.60	2.800e-04	1.19
2^{-8}	8.880e-04	0.88	6.931e-04	0.86	4.660e-04	0.81	2.192e-04	0.69	1.243e-04	1.17
2^{-9}	4.781e-04	0.89	3.790e-04	0.87	2.619e-04	0.83	1.309e-04	0.74	5.591e-05	1.15
2^{-10}	2.556e-04	0.90	2.063e-04	0.88	1.465e-04	0.84	7.693e-05	0.77	2.541e-05	1.13
2^{-11}	1.362e-04	0.91	1.124e-04	0.88	8.214e-05	0.84	4.498e-05	0.77	1.164e-05	1.13
2^{-12}	7.257e-05	0.91	6.154e-05	0.87	4.639e-05	0.82	2.638e-05	0.77	5.365e-06	1.12
2^{-13}	3.882e-05	0.90	3.403e-05	0.85	2.649e-05	0.81	1.560e-05	0.76	2.483e-06	1.11
2^{-14}	2.092e-05	0.89	1.906e-05	0.84	1.534e-05	0.79	9.341e-06	0.74	1.153e-06	1.11
2^{-15}	1.139e-05	0.88	1.087e-05	0.81	8.934e-06	0.78	5.709e-06	0.71	5.526e-07	1.06

4.3 Numerical method using splines of degree $1 < \beta \leqslant 2$

In the next sections, we construct a numerical method based on finite differences and on the integral approximation using splines of degree $1 < \beta \leqslant 2$ obtained in Section 3.1.2. This approach presented more challenges than we anticipated. The analysis regarding the stability and consistency of the method has hard details and we have decided to leave it as an open problem. However, since we find it an interesting approach, we describe the numerical method and present some numerical experiments that illustrates its order of convergence.

4.3.1 Finite differences method

We construct the numerical method that intends to obtain an approximate solution for (4.1), but now using splines of degree $1 < \beta \leqslant 2$ and for a constant diffusion coefficient $d(x,t) := d$. Following the

Table 4.12 Results concerning Problem 3. Convergence rate (R_∞ and R_2) in time for different values of β with α=0.8 and $\Delta x = \pi/2500$, for the errors (4.17) and (4.18), respectively.

Δt	$\beta=0.2$	R_∞	$\beta=0.4$	R_∞	$\beta=0.6$	R_∞	$\beta=0.8$	R_∞	$\beta=1$	R_∞
2^{-3}	3.293e-02		2.471e-02		1.541e-02		4.822e-03		7.197e-03	
2^{-4}	2.024e-02	0.70	1.536e-02	0.69	9.804e-03	0.65	3.479e-03	0.47	3.711e-03	0.96
2^{-5}	1.210e-02	0.74	9.231e-03	0.73	5.969e-03	0.72	2.249e-03	0.63	1.981e-03	0.91
2^{-6}	7.110e-03	0.77	5.443e-03	0.76	3.545e-03	0.75	1.378e-03	0.71	1.086e-03	0.87
2^{-7}	4.139e-03	0.78	3.174e-03	0.78	2.075e-03	0.77	8.208e-04	0.75	6.066e-04	0.84
2^{-8}	2.395e-03	0.79	1.839e-03	0.79	1.205e-03	0.78	4.812e-04	0.77	3.426e-04	0.82
2^{-9}	1.382e-03	0.79	1.062e-03	0.79	6.965e-04	0.79	2.796e-04	0.78	1.948e-04	0.81
2^{-10}	7.957e-04	0.80	6.115e-04	0.80	4.015e-04	0.79	1.617e-04	0.79	1.112e-04	0.81
2^{-11}	4.577e-04	0.80	3.518e-04	0.80	2.311e-04	0.80	9.322e-05	0.79	6.368e-05	0.80
2^{-12}	2.631e-04	0.80	2.023e-04	0.80	1.329e-04	0.80	5.366e-05	0.80	3.651e-05	0.80
2^{-13}	1.512e-04	0.80	1.162e-04	0.80	7.637e-05	0.80	3.086e-05	0.80	2.094e-05	0.80
2^{-14}	8.686e-05	0.80	6.678e-05	0.80	4.388e-05	0.80	1.774e-05	0.80	1.202e-05	0.80
2^{-15}	4.989e-05	0.80	3.836e-05	0.80	2.521e-05	0.80	1.019e-05	0.80	6.902e-06	0.80
		R_2		R_2		R_2		R_2		R_2
2^{-3}	1.776e-02		1.341e-02		8.442e-03		3.028e-03		2.995e-03	
2^{-4}	9.675e-03	0.88	7.331e-03	0.87	4.697e-03	0.85	1.914e-03	0.66	1.133e-03	1.40
2^{-5}	5.118e-03	0.92	3.869e-03	0.92	2.504e-03	0.91	1.099e-03	0.80	4.337e-04	1.38
2^{-6}	2.653e-03	0.95	1.997e-03	0.95	1.302e-03	0.94	5.999e-04	0.87	1.686e-04	1.36
2^{-7}	1.356e-03	0.97	1.017e-03	0.97	6.666e-04	0.97	3.179e-04	0.92	6.647e-05	1.34
2^{-8}	6.869e-04	0.98	5.129e-04	0.99	3.383e-04	0.98	1.655e-04	0.94	2.648e-05	1.33
2^{-9}	3.457e-04	0.99	2.574e-04	0.99	1.708e-04	0.99	8.518e-05	0.96	1.063e-05	1.32
2^{-10}	1.732e-04	1.00	1.287e-04	1.00	8.592e-05	0.99	4.355e-05	0.97	4.285e-06	1.31
2^{-11}	8.657e-05	1.00	6.426e-05	1.00	4.316e-05	0.99	2.217e-05	0.97	1.733e-06	1.31
2^{-12}	4.318e-05	1.00	3.205e-05	1.00	2.166e-05	0.99	1.125e-05	0.98	7.036e-07	1.30
2^{-13}	2.150e-05	1.01	1.597e-05	1.00	1.086e-05	1.00	5.702e-06	0.98	2.882e-07	1.29
2^{-14}	1.070e-05	1.01	7.953e-06	1.01	5.433e-06	1.00	2.886e-06	0.98	1.266e-07	1.19
2^{-15}	5.310e-06	1.01	3.961e-06	1.01	2.662e-06	1.03	1.486e-06	0.96	9.273e-08	0.45

same steps as last section, from (4.1), we arrive at

$$u(x,t_m) - u(x,t_{m-1}) \approx d\frac{\partial^2}{\partial x^2}\Big((\mathscr{I}^\alpha u(x,t_m) - \mathscr{I}^\alpha u(x,t_{m-1}))\Big) + \int_{t_{m-1}}^{t_m} g(x,t)dt.$$

In Chapter 3, we have seen that the integral $\mathscr{I}^\alpha u(x,t)$ could be approximated using splines of degree between 1 and 2 given by

$$I^{\alpha,\beta}u(x,t_m) = \Delta t^\alpha \sum_{k=0}^{m+1} c_{k,m} b_{m,k}, \quad c_{k,m} = \tilde{a}^m_{k,0}\frac{\partial u}{\partial t}(x,t_m) + \sum_{s=1}^{m+1} \tilde{a}^m_{k,s} u(x,t_{s-1}),$$

with $\tilde{A}_m = [\tilde{a}^m_{k,s}],\ k = 0,\ldots,m+1,\ s = 0,\ldots,m+1$ the inverse matrix of A_m (2.16). Therefore,

$$\begin{aligned} u(x,t_m) - u(x,t_{m-1}) \approx\ & d\frac{\partial^2}{\partial x^2}\Delta t^{\alpha}\left(\sum_{k=0}^{m+1}\left(\tilde{a}^m_{k,0}(x,t_m) + \sum_{s=1}^{m+1}\tilde{a}^m_{k,s}u(x,t_{s-1})\right)b_{m,k}\right. \\ & \left. - \sum_{k=0}^{m}\left(\tilde{a}^{m-1}_{k,0}\frac{\partial u}{\partial t}(x,t_{m-1}) + \sum_{s=1}^{m}\tilde{a}^{m-1}_{k,s}u(x,t_{s-1})\right)b_{m-1,k}\right) + \int_{t_{m-1}}^{t_m} g(x,t)dt. \end{aligned}$$

Doing the space discretization as before and applying the approximation (3.14) of $u'(t_m)$, we obtain the following numerical method

$$\begin{aligned} U^m_j - U^{m-1}_j =\ & d\frac{\Delta t^{\alpha}}{\Delta x^2}\delta^2\left(\sum_{k=0}^{m+1}\left(\frac{\tilde{a}^m_{k,0}}{\Delta t}\Big((1+c_1+c_2)U^m_j - (1+2c_1+3c_2)U^{m-1}_j\right.\right. \\ & \left. +(c_1+3c_2)U^{m-2}_j - c_2U^{m-3}_j\Big) + \sum_{s=1}^{m+1}\tilde{a}^m_{k,s}U^{s-1}_j\right)b_{m,k} - \sum_{k=0}^{m}\left(\frac{\tilde{a}^{m-1}_{k,0}}{\Delta t}\Big((1+d_1)U^{m-1}_j\right. \\ & \left.\left. -(1+2d_1)U^{m-2}_j + d_1U^{m-3}_j + \sum_{s=1}^{m}\tilde{a}^{m-1}_{k,s}U^{s-1}_j\right)b_{m-1,k}\right) + \int_{t_{m-1}}^{t_m} g(x_j,t)dt \end{aligned}$$

where we denote U^m_j the approximation of $u(x_j,t_m)$. At this point, a difficulty arises because we do not have enough points at the first time steps to implement such numerical method. Therefore, we need to do different approaches for $m = 1$, $m = 2$ and $m \geqslant 3$. For the first time step, $m = 1$, as we would need the values of U^{-1}_j and U^{-2}_j, we consider $c_1, c_2, d_1 = 0$. For $m = 2$, we would need the values of U^{-1}_j, therefore we define $c_1 = -1/2$ and $c_2, d_1 = 0$; for $m \geqslant 3$, we consider $c_1 = -1/2$, $c_2 = 1/3$ and $d_1 = -1/2$.

Let $\mu_\alpha = d\Delta t^{\alpha}/\Delta x^2$. We can write

$$\begin{aligned} & \left(1 - \mu_\alpha\delta^2\sum_{k=0}^{m+1}\left(\tilde{a}^m_{k,m+1} + \frac{\tilde{a}^m_{k,0}}{\Delta t}(1+c_1+c_2)\right)b_{m,m+1}\right)U^m_j = U^{m-1}_j \\ & +\mu_\alpha\delta^2\left(\sum_{k=0}^{m+1}\left(-\frac{\tilde{a}^m_{k,0}}{\Delta t}(1+2c_1+3c_2) + \tilde{a}^m_{k,m}\right)b_{m,k} - \sum_{k=0}^{m}\left(-\frac{\tilde{a}^{m-1}_{k,0}}{\Delta t}(1+d_1) + \tilde{a}^{m-1}_{k,m}\right)b_{m-1,k}\right)U^{m-1}_j \\ & +\mu_\alpha\delta^2\left(\sum_{k=0}^{m+1}\left(\frac{\tilde{a}^m_{k,0}}{\Delta t}(c_1+3c_2) + \tilde{a}^m_{k,m-1}\right)b_{m,k} - \sum_{k=0}^{m}\left(-\frac{\tilde{a}^{m-1}_{k,0}}{\Delta t}(1+2d_1) + \tilde{a}^{m-1}_{k,n-1}\right)b_{m-1,k}\right)U^{m-2}_j \quad (4.19) \\ & +\mu_\alpha\delta^2\left(\sum_{k=0}^{m+1}\left(-\frac{\tilde{a}^m_{k,0}}{\Delta t}c_2 + \tilde{a}^m_{k,m-2}\right)b_{m,k} - \sum_{k=0}^{m}\left(\frac{\tilde{a}^m_{k,0}}{\Delta t}d_1 + \tilde{a}^{m-1}_{k,m-2}\right)b_{m-1,k}\right)U^{m-3}_j \\ & +\mu_\alpha\delta^2\sum_{s=1}^{m-3}\left(\sum_{k=0}^{m+1}\tilde{a}^m_{k,s}b_{m,k} - \sum_{k=0}^{m}\tilde{a}^{m-1}_{k,s}b_{m-1,k}\right)U^{s-1}_j + \int_{t_{m-1}}^{t_m} g(x_j,t)dt \end{aligned}$$

It can be written in the matricial form as

$$\left(\mathbf{I}-\mu_\alpha\sum_{k=0}^{m+1}\left(\tilde{a}^m_{k,m+1}+\frac{\tilde{a}^m_{k,0}}{\Delta t}(1+c_1+c_2)\right)b_{m,m+1}\right)\mathbf{D}\mathbf{U}^m=\mathbf{I}\mathbf{U}^{m-1}$$
$$+\mu_\alpha\left(\sum_{k=0}^{m+1}\left(-\frac{\tilde{a}^m_{k,0}}{\Delta t}(1+2c_1+3c_2)+\tilde{a}^m_{k,m}\right)b_{m,k}-\sum_{k=0}^{m}\left(-\frac{\tilde{a}^{m-1}_{k,0}}{\Delta t}(1+d_1)+\tilde{a}^{m-1}_{k,m}\right)b_{m-1,k}\right)\mathbf{D}\mathbf{U}^{m-1}$$
$$+\mu_\alpha\left(\sum_{k=0}^{m+1}\left(\frac{\tilde{a}^m_{k,0}}{\Delta t}(c_1+3c_2)+\tilde{a}^m_{k,m-1}\right)b_{m,k}-\sum_{k=0}^{m}\left(-\frac{\tilde{a}^{m-1}_{k,0}}{\Delta t}(1+2d_1)+\tilde{a}^{m-1}_{k,m-1}\right)b_{m-1,k}\right)\mathbf{D}\mathbf{U}^{m-2}$$
$$+\mu_\alpha\left(\sum_{k=0}^{m+1}\left(-\frac{\tilde{a}^m_{k,0}}{\Delta t}c_2+\tilde{a}^m_{k,m-2}\right)b_{m,k}-\sum_{k=0}^{m}\left(\frac{\tilde{a}^m_{k,0}}{\Delta t}d_1+\tilde{a}^{m-1}_{k,m-2}\right)b_{m-1,k}\right)\mathbf{D}\mathbf{U}^{m-3}$$
$$+\mu_\alpha\sum_{s=1}^{m-3}\left(\sum_{k=0}^{m+1}\tilde{a}^m_{k,s}b_{m,k}-\sum_{k=0}^{m}\tilde{a}^{m-1}_{k,s}b_{m-1,k}\right)\mathbf{D}\mathbf{U}^{s-1}+\mathbf{G}^m,$$

where $\mathbf{I}$ is the identity matrix, $\mathbf{U}^m$ is the solution vector $\mathbf{U}^m=[U^m_1,\dots,U^m_{N-1}]^T$, $\mathbf{D}$ is a tridiagonal matrix with entries $\mathbf{D}_{j,j-1}=1$, $\mathbf{D}_{j,j}=-2$ and $\mathbf{D}_{j,j+1}=1$ and $\mathbf{G}^m$ contains the values of the integral of the source term.

We proceed with one numerical test that may indicate the convergence rate of this method.

4.3.2 Numerical experiments

Consider the same conditions as in Section 4.2.3. We present an example of an approximate solution of the fractional differential equation (4.1) obtained by the numerical method constructed resorting to splines of degree $1<\beta\leqslant 2$.

Let $[a,b]=[0,2]$, $T=1$ and $d=1$. The source term $g(x,t)$ and the initial condition $u_0(x)$ are defined such that the exact solution of the problem is $u(x,t)=t^4x^4(2-x)^4$.

In Tables 4.13–4.15 we present the results and now we analyze them to try to identify the trend, or rule, of the convergence order that the method obeys. By observation of the tables, we see that both errors E_2 and E_∞ follow the same tendency. For $\alpha=0.2$, we observe an order of accuracy of around 2.2. For $\alpha=0.4$, we see that the order of accuracy is about 2.2 for $\beta=1.2$ and around 2.4 for the other values of β. And finally, for $\alpha=0.8$, we note that the order of accuracy is around 2.2 for $\beta=1.2$, 2.6 for $\beta=1.4$ and between 2.8 and 2.9 for $\beta=1.8$ and $\beta=2$. Then, heuristically, the experimental results of this problem point out that the order of accuracy of this method is the minimum between $\beta+1$ and $2+\alpha$, for sufficiently smooth solutions.

At the end of this and the next chapters, we present some figures that illustrate the evolution of the solution along time for different values of α.

Table 4.13 Convergence rate (R_∞ and R_2) in time for different values of β with α=0.2 and $\Delta x = 2/10000$, for the errors (4.17) and (4.18), respectively.

Δt	$\beta = 1.2$	R_∞	$\beta = 1.4$	R_∞	$\beta = 1.6$	R_∞	$\beta = 1.8$	R_∞	$\beta = 2$	R_∞
2^{-3}	2.959e-03		2.645e-03		2.624e-03		2.676e-03		2.732e-03	
2^{-4}	7.059e-04	2.07	6.003e-04	2.14	5.948e-04	2.14	6.107e-04	2.13	6.267e-04	2.12
2^{-5}	1.636e-04	2.11	1.325e-04	2.18	1.315e-04	2.18	1.360e-04	2.17	1.401e-04	2.16
2^{-6}	3.729e-05	2.13	2.882e-05	2.20	2.873e-05	2.19	2.991e-05	2.18	3.091e-05	2.18
2^{-7}	8.400e-06	2.15	6.213e-06	2.21	6.233e-06	2.20	6.531e-06	2.20	6.765e-06	2.19
2^{-8}	1.871e-06	2.17	1.327e-06	2.23	1.342e-06	2.22	1.415e-06	2.21	1.468e-06	2.20
2^{-9}	4.084e-07	2.20	2.761e-07	2.27	2.818e-07	2.25	2.998e-07	2.24	3.111e-07	2.24
		R_2		R_2		R_2		R_2		R_2
2^{-3}	1.522e-03		1.375e-03		1.366e-03		1.391e-03		1.419e-03	
2^{-4}	3.418e-04	2.16	2.943e-04	2.22	2.917e-04	2.23	2.989e-04	2.22	3.064e-04	2.21
2^{-5}	7.691e-05	2.15	6.313e-05	2.22	6.261e-05	2.22	6.462e-05	2.21	6.651e-05	2.20
2^{-6}	1.728e-05	2.15	1.354e-05	2.22	1.347e-05	2.22	1.400e-05	2.21	1.446e-05	2.20
2^{-7}	3.869e-06	2.16	2.899e-06	2.22	2.902e-06	2.21	3.035e-06	2.21	3.142e-06	2.20
2^{-8}	8.609e-07	2.17	6.185e-07	2.23	6.238e-07	2.22	6.564e-07	2.21	6.808e-07	2.21
2^{-9}	1.889e-07	2.19	1.297e-07	2.25	1.320e-07	2.24	1.400e-07	2.23	1.453e-07	2.23

Table 4.14 Convergence rate (R_∞ and R_2) in time for different values of β with α=0.4 and $\Delta x = 2/10000$, for the errors (4.17) and (4.18), respectively.

Δt	$\beta = 1.2$	R_∞	$\beta = 1.4$	R_∞	$\beta = 1.6$	R_∞	$\beta = 1.8$	R_∞	$\beta = 2$	R_∞
2^{-3}	3.774e-03		3.131e-03		3.017e-03		3.055e-03		3.121e-03	
2^{-4}	8.271e-04	2.19	6.279e-04	2.32	5.952e-04	2.34	6.052e-04	2.34	6.215e-04	2.33
2^{-5}	1.779e-04	2.22	1.227e-04	2.36	1.146e-04	2.38	1.171e-04	2.37	1.208e-04	2.36
2^{-6}	3.795e-05	2.23	2.365e-05	2.38	2.179e-05	2.40	2.238e-05	2.39	2.317e-05	2.38
2^{-7}	8.059e-06	2.24	4.517e-06	2.39	4.110e-06	2.41	4.245e-06	2.40	4.408e-06	2.39
2^{-8}	1.703e-06	2.24	8.518e-07	2.41	7.658e-07	2.42	7.956e-07	2.42	8.284e-07	2.41
2^{-9}	3.530e-07	2.27	1.530e-07	2.48	1.356e-07	2.50	1.419e-07	2.49	1.482e-07	2.48
		R_2		R_2		R_2		R_2		R_2
2^{-3}	1.959e-03		1.656e-03		1.602e-03		1.621e-03		1.654e-03	
2^{-4}	4.040e-04	2.28	3.140e-04	2.40	2.990e-04	2.42	3.037e-04	2.42	3.114e-04	2.41
2^{-5}	8.420e-05	2.26	5.973e-05	2.39	5.602e-05	2.42	5.715e-05	2.41	5.888e-05	2.40
2^{-6}	1.767e-05	2.25	1.136e-05	2.39	1.051e-05	2.41	1.077e-05	2.41	1.114e-05	2.40
2^{-7}	3.723e-06	2.25	2.157e-06	2.40	1.970e-06	2.42	2.031e-06	2.41	2.107e-06	2.40
2^{-8}	7.845e-07	2.25	4.069e-07	2.41	3.673e-07	2.42	3.809e-07	2.42	3.962e-07	2.41
2^{-9}	1.635e-07	2.26	7.440e-08	2.45	6.630e-08	2.47	6.918e-08	2.46	7.218e-08	2.46

Table 4.15 Convergence rate (R_∞ and R_2) in time for different values of β with α=0.8 and $\Delta x = 2/10000$, for the errors (4.17) and (4.18), respectively.

Δx	$\beta=1.2$	R_∞	$\beta=1.4$	R_∞	$\beta=1.6$	R_∞	$\beta=1.8$	R_∞	$\beta=2$	R_∞
2^{-3}	3.307e-03		2.234e-03		1.921e-03		1.864e-03		1.886e-03	
2^{-4}	6.678e-04	2.31	3.742e-04	2.58	2.946e-04	2.70	2.800e-04	2.73	2.834e-04	2.73
2^{-5}	1.367e-04	2.29	6.265e-05	2.58	4.433e-05	2.73	4.110e-05	2.77	4.163e-05	2.77
2^{-6}	2.841e-05	2.27	1.058e-05	2.57	6.608e-06	2.75	5.958e-06	2.79	6.037e-06	2.79
2^{-7}	5.977e-06	2.25	1.806e-06	2.55	9.756e-07	2.76	8.513e-07	2.81	8.627e-07	2.81
2^{-8}	1.263e-06	2.24	3.062e-07	2.56	1.375e-07	2.83	1.150e-07	2.89	1.166e-07	2.89
2^{-9}	2.630e-07	2.26	4.877e-08	2.65	1.917e-08	2.84	1.641e-08	2.81	1.711e-08	2.77
		R_2		R_2		R_2		R_2		R_2
2^{-3}	1.713e-03		1.202e-03		1.054e-03		1.027e-03		1.039e-03	
2^{-4}	3.219e-04	2.41	1.899e-04	2.66	1.537e-04	2.78	1.470e-04	2.80	1.488e-04	2.80
2^{-5}	6.326e-05	2.35	3.075e-05	2.63	2.254e-05	2.77	2.108e-05	2.80	2.135e-05	2.80
2^{-6}	1.284e-05	2.30	5.091e-06	2.59	3.318e-06	2.76	3.022e-06	2.80	3.062e-06	2.80
2^{-7}	2.667e-06	2.27	8.586e-07	2.57	4.880e-07	2.77	4.310e-07	2.81	4.368e-07	2.81
2^{-8}	5.604e-07	2.25	1.455e-07	2.56	6.988e-08	2.80	5.942e-08	2.86	6.024e-08	2.86
2^{-9}	1.170e-07	2.26	2.359e-08	2.62	9.288e-09	2.91	7.627e-09	2.96	7.905e-09	2.93

4.4 Numerical approximations of the fundamental solutions

To conclude this chapter, we want to illustrate the process of subdiffusion for different values of α. We consider equation (4.1) without source term and with initial condition

$$u_0(x) = \delta_\varepsilon(x), \quad \text{with} \quad \delta_\varepsilon(x) = \frac{1}{\varepsilon\sqrt{\pi}} e^{-x^2/\varepsilon^2}, \tag{4.20}$$

for a small value of ε, that can be seen as an approximation of the Dirac delta function.

In Figure 4.3 we plot the numerical solution of our method, for $\beta = 1$ and $\alpha = 0.1, 0.5, 0.9$ from $t = 1$ to $t = 2$. We can see that, as α grows, the shape of the solution tends to be less sharp. Furthermore, the variation of the maximum value of the solution is more accentuated for $\alpha = 0.9$, pointing out that the phenomenon of (anomalous) diffusion is faster for bigger values of α. We finish the study of subdiffusion with Figure 4.4, where we plot the solutions for $t = 2$ and α between 0.1 and 0.9 that corroborates the conclusions already stated.

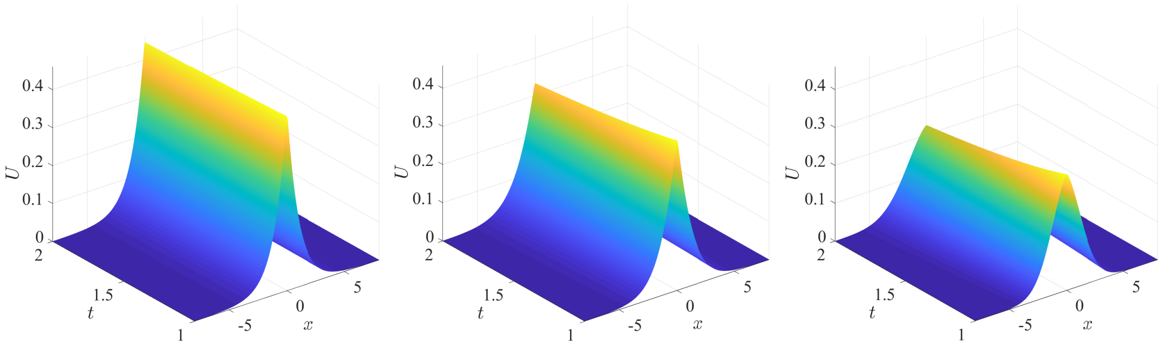

Fig. 4.3 Numerical solutions when the initial condition is (4.20) and $D = 1$, as time changes from 1 to 2. Left: $\alpha = 0.1$. Center: $\alpha = 0.5$. Right: $\alpha = 0.9$.

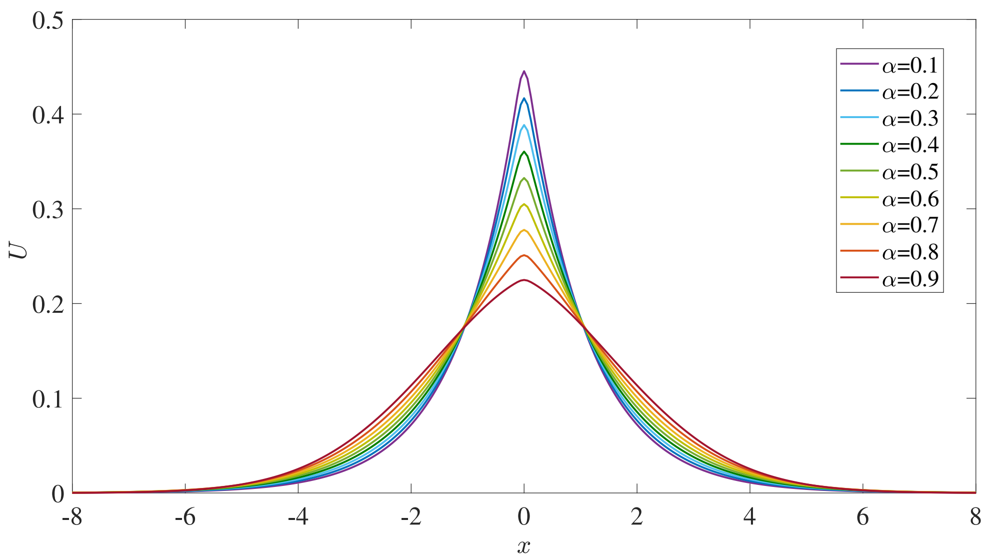

Fig. 4.4 Numerical solutions when the initial condition is (4.20) for $t = 2$, $D = 1$ and α changing from 0.1 to 0.9.

Chapter 5

Superdiffusion problem

In parallel to what we have done in the previous chapter, the first section of Chapter 5 is dedicated to the deduction of the fractional differential equation that models superdiffusion, related to Lévy flights when $0 < \alpha < 2$ $(\alpha \neq 1)$. We separate the cases when $0 < \alpha < 1$ and $1 < \alpha < 2$, since the fractional partial differential equation must be solved differently for each case. For the first one, this is, α between 0 and 1, there are less studies. Here, we present three different approaches to the approximation of the fractional derivative involved in this superdiffusive problem. We construct three numerical methods based on these approximations and study their convergence. Numerical experiments are done to support the theoretical results. For the case when α is between 1 and 2, more studied in literature, we present a numerical method on the open domain [76] and adapt this approach to solve a problem that includes a reflecting boundary. For the reflecting case, we study the convergence properties of the method in detail. At the end of the chapter, we display and analyze some computational simulations for all the considered cases of superdiffusion and we finish with an example that juxtaposes one solution of the subdiffusive model and one solution of the superdiffusive model.

5.1 Model problem

The class of Lévy stable processes that we consider is the class for which the Fourier transform of the jump distribution [68] is described by the characteristic function ψ,

$$\psi(\omega, \alpha, p) = \exp\left[(-1)^n Dt \left(\frac{1+p}{2}(-\mathrm{i}\omega)^\alpha + \frac{1-p}{2}(\mathrm{i}\omega)^\alpha\right)\right], \tag{5.1}$$

where $n = [\alpha] + 1$, D is a positive constant, α is the characteristic exponent that describes the tail of the distribution and $-1 \leqslant p \leqslant 1$ is the skewness and specifies if the distribution is skewed to the left ($p < 0$), right ($p > 0$) of if it is symmetric ($p = 0$). According to [67], the probability density function is positive if we have $0 < \alpha \leqslant 2$, with $\alpha = 2$ corresponding to the Gaussian case. For $0 < \alpha < 2$, it describes Lévy flights where the jumps are typically very large.

The characteristic function (5.1), when $0 < \alpha < 2$ and $\alpha \neq 1$, is the solution of the equation

$$\frac{\partial \hat{u}(\omega,t)}{\partial t} = (-1)^n D \left(\frac{1+p}{2}(-\mathrm{i}\omega)^\alpha + \frac{1-p}{2}(\mathrm{i}\omega)^\alpha \right) \hat{u}(\omega,t). \tag{5.2}$$

Applying the inverse Fourier transform, we can write

$$\frac{\partial u(x,t)}{\partial t} = (-1)^n D \left(\frac{1+p}{2}\mathscr{F}^{-1}\left\{(-\mathrm{i}\omega)^\alpha \hat{u}(\omega,t)\right\} + \frac{1-p}{2}\mathscr{F}^{-1}\left\{(\mathrm{i}\omega)^\alpha \hat{u}(\omega,t)\right\} \right).$$

Using the properties present in Proposition 1.16

$$\frac{\partial^\alpha u}{\partial x^\alpha}(x,t) := \mathscr{F}^{-1}\left\{(-\mathrm{i}\omega)^\alpha \hat{u}(\omega,t)\right\} \quad \text{and} \quad \frac{\partial^\alpha u}{\partial (-x)^\alpha}(x,t) := \mathscr{F}^{-1}\left\{(\mathrm{i}\omega)^\alpha \hat{u}(\omega,t)\right\},$$

we arrive at the final equation, for $0 < \alpha < 2$ ($\alpha \neq 1$),

$$\frac{\partial u}{\partial t}(x,t) = (-1)^n D \nabla_\alpha^p u(x,t), \tag{5.3}$$

where

$$\nabla_\alpha^p u(x,t) = \frac{1+p}{2}\frac{\partial^\alpha u}{\partial x^\alpha}(x,t) + \frac{1-p}{2}\frac{\partial^\alpha u}{\partial (-x)^\alpha}(x,t), \tag{5.4}$$

for $-1 \leqslant p \leqslant 1$, where D is the diffusion coefficient.

For $0 < \alpha < 1$, described in Section 5.2, we construct and compare three different numerical methods to approximate the solution of equation

$$\frac{\partial u(x,t)}{\partial t} = -D \nabla_\alpha^p u(x,t) + g(x,t), \quad x \in \mathbb{R},\ t > 0, \tag{5.5}$$

where we have introduced a source term, $g(x,t)$. Additionally, we consider an initial condition and

$$\lim_{|x| \to \infty} u(x,t) = 0. \tag{5.6}$$

For $1 < \alpha < 2$, described in Section 5.3, we present the numerical method considered in [76] to approximate the solution of equation

$$\frac{\partial u(x,t)}{\partial t} = D \nabla_\alpha^p u(x,t) + g(x,t), \quad x \in \mathbb{R},\ t > 0, \tag{5.7}$$

and in Section 5.4 we propose an approach when a reflecting wall is at $x = 0$.

5.2 Superdiffusion when $0 < \alpha < 1$

In the next sections we present three ways of approximating the Riemann-Liouville derivatives, which for $0 < \alpha < 1$, as seen before, are the first derivative of integral operators. First, to approximate the integral, we use the linear spline approximation. Then, we use three different ways of approximating the derivative outside the integral: a central difference method, a first order upwind method and a second order upwind method. We construct a family of implicit methods and discuss their consistency and stability. Furthermore, we present numerical experiments to illustrate the theoretical results and to show the disadvantages of the central approximation in comparison with the upwind approaches.

5.2.1 Fractional derivative approximations

In this section we describe how we approximate the left and right fractional Riemann-Liouville derivatives, that are defined by the first derivative of a fractional integral. For the integral, we use the approximation derived in Section 3.2. For the first order derivative, we build three types of approximation.

Fractional derivative approximation

In this section, we approximate the left and right Riemann-Liouville derivatives

$$\frac{\partial}{\partial x}\mathscr{I}^l u(x,t), \quad -\frac{\partial}{\partial x}\mathscr{I}^r u(x,t) \tag{5.8}$$

using a central and two upwind approximations of the derivative and the linear spline approximation of the integral developed in Section 3.2 for $\alpha \in (0,1)$. Recall that, resorting to the linear spline and considering the uniform domain discretization $x_j = x_{j-1} + \Delta x,\ j \in \mathbb{Z}$, the integrals $\mathscr{I}^l u(x,t)$ and $\mathscr{I}^r u(x,t)$ can be approximated by

$$I^l u(x_j,t) = \frac{\Delta x^{1-\alpha}}{\Gamma(3-\alpha)} \sum_{k=0}^{\infty} a_k u(x_{j-k},t), \tag{5.9}$$

$$I^r u(x_j,t) = \frac{\Delta x^{1-\alpha}}{\Gamma(3-\alpha)} \sum_{k=0}^{\infty} a_k u(x_{j+k},t), \tag{5.10}$$

respectively, with the coefficients of both quadratures given by (3.19).

We proceed with the derivative approximation.

Fractional derivative central approximation

We start by considering the left Riemann-Liouville derivative; the steps for the right derivative are similar. This type of approximation was done in [75]. The central approximation for the first order derivative of the integral is given by

$$\frac{\partial}{\partial x}\mathscr{I}^l u(x_j,t) \approx \frac{\mathscr{I}^l u(x_{j+1},t) - \mathscr{I}^l u(x_{j-1},t)}{2\Delta x}$$

and, furthermore,

$$\frac{\partial}{\partial x}\mathscr{I}^l u(x_j,t) \approx \frac{I^l u(x_{j+1},t) - I^l u(x_{j-1},t)}{2\Delta x}.$$

Using (5.9), we obtain

$$\frac{\partial}{\partial x}\mathscr{I}^l u(x_j,t) \approx \frac{\Delta x^{1-\alpha}}{2\Delta x \Gamma(3-\alpha)} \left(\sum_{k=0}^{\infty} a_k u(x_{j+1-k},t) - \sum_{k=0}^{\infty} a_k u(x_{j-1-k},t) \right)$$

and, considering $k' = k-1$ in the first sum and $k' = k+1$ in the second sum,

$$\frac{\partial}{\partial x}\mathscr{I}^l u(x_j,t) \approx \frac{\Delta x^{1-\alpha}}{2\Delta x\Gamma(3-\alpha)}\left(\sum_{k'=-1}^{\infty} a_{k'+1}u(x_{j-k'},t) - \sum_{k'=1}^{\infty} a_{k'-1}u(x_{j-k'},t)\right).$$

Finally, we can combine the terms as follows

$$\frac{\partial}{\partial x}\mathscr{I}^l u(x_j,t) \approx \frac{\Delta x^{-\alpha}}{2\Gamma(3-\alpha)}\left(a_0 u(x_{j+1},t) + a_1 u(x_j,t) + \sum_{k=1}^{\infty}(a_{k+1}-a_{k-1})u(x_{j-k},t)\right).$$

Therefore, we conclude that the left fractional derivative $\partial\mathscr{I}^l u(x_j,t)/\partial x$ can be approximated by $\delta_c^l u(x_j,t)/\Delta x^\alpha$ with $\delta_c^l u$ defined as

$$\delta_c^l u(x_j,t) = \frac{1}{2\Gamma(3-\alpha)}\sum_{k=-1}^{\infty} b_{k,c}u(x_{j-k},t),$$

where

$$b_{-1,c} = a_0, \quad b_{0,c} = a_1, \quad b_{k,c} = a_{k+1} - a_{k-1}, \quad k \geqslant 1. \tag{5.11}$$

Replicating the same steps using (5.10), for the right Riemann-Liouville derivative we obtain

$$-\frac{\partial}{\partial x}\mathscr{I}^r u(x_j,t) \approx \frac{\Delta x^{1-\alpha}}{2\Delta x\Gamma(3-\alpha)}\sum_{k=-1}^{\infty} b_{k,c}u(x_{j+k},t), \tag{5.12}$$

and then the right fractional Riemann-Liouville derivative $-\partial\mathscr{I}^r u(x_j,t)/\partial x$ can be approximated by $\delta_c^r u(x_j,t)/\Delta x^\alpha$ with $\delta_c^r u$ defined as

$$\delta_c^r u(x_j,t) = \frac{1}{2\Gamma(3-\alpha)}\sum_{k=-1}^{\infty} b_{k,c}u(x_{j+k},t),$$

where the coefficients $b_{k,c}$ are defined in (5.11).

Therefore, we can define the general operator $\nabla_\alpha^p u$, for $0 < \alpha < 1$ and $-1 \leqslant p \leqslant 1$, can be approximated by the operator $\delta_{\alpha,c}^p u(x_j,t)/\Delta x^\alpha$ where the operator $\delta_{\alpha,c}^p u$ is given by

$$\delta_{\alpha,c}^p u(x_j,t) = \frac{1+p}{2}\delta_c^l u(x_j,t) + \frac{1-p}{2}\delta_c^r u(x_j,t). \tag{5.13}$$

The reason why we want to derive alternative approximations is the fact that, using this approach, we may obtain spurious numerical oscillations, although we are in the presence of a second order accurate scheme. We show some examples in Section 5.2.5. Even though we did not present the numerical method using this approximation yet, in Figure 5.1 we plot the solution of the central method considering $\alpha = 0.1, 0.3, 0.5, 0.7, 0.9$ for $p = -0.8$ at left, $p = 0$ at center and $p = 0.8$ at right. We can observe that, in the asymmetric cases $p = -0.8, 0.8$, as α grows more severe oscillations appear. For $p = -0.8$ they emerge at the left side of the solution and for $p = 0.8$ they emerge at the right side. For the symmetric case, there are no oscillations, regardless of the value of α.

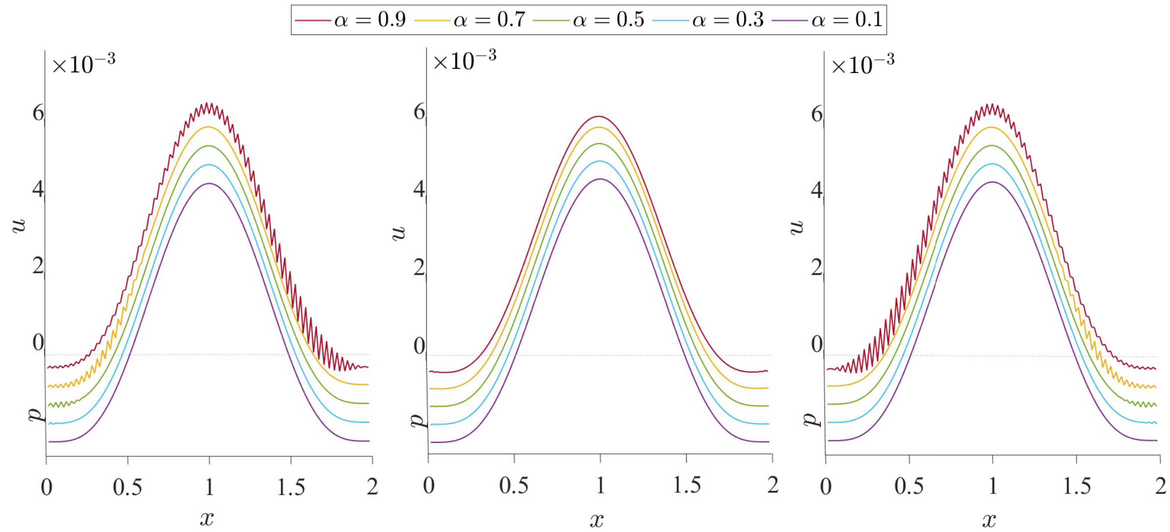

Fig. 5.1 Numerical solution with the central method for $\alpha = 0.1, 0.3, 0.5, 0.7, 0.9$. Left: $p = -0.8$. Center: $p = 0$. Right:$p = 0.8$.

Therefore, in the next two sections we resort to a first order and a second order upwind discretizations to approximate the fractional derivative in an attempt to obtain solutions without oscillations.

Fractional derivative upwind first order approximation

In this section, we approximate the derivative of the fractional integral by a first order upwind approximation. In the case of the left fractional derivative, it uses a two-point backward difference and, in the case of the right fractional derivative, a two-point forward difference. This is a natural consequence of the fact that the left and right derivatives have opposite signs for $0 < \alpha < 1$.

The first order upwind approximation [61] is given by

$$c\frac{\partial u}{\partial x}(x_j) \approx \begin{cases} c\dfrac{u(x_j) - u(x_{j-1})}{\Delta x}, & \text{for } c > 0, \\ c\dfrac{u(x_{j+1}) - u(x_j)}{\Delta x}, & \text{for } c < 0. \end{cases}$$

For the left fractional derivative we have

$$\frac{\partial}{\partial x}\mathscr{I}^l u(x_j,t) \approx \frac{I^l u(x_j,t) - I^l u(x_{j-1},t)}{\Delta x} = \frac{\Delta x^{1-\alpha}}{\Gamma(3-\alpha)\Delta x}\left(\sum_{k=0}^{\infty} a_k u(x_{j-k},t) - \sum_{k=0}^{\infty} a_k u(x_{j-1-k},t)\right).$$

Considering $k' = k+1$ in the second sum and aggregating the terms,

$$\begin{aligned} \frac{\partial}{\partial x}\mathscr{I}^l u(x_j,t) &\approx \frac{1}{\Gamma(3-\alpha)\Delta x^{\alpha}}\left(\sum_{k=0}^{\infty} a_k u(x_{j-k},t) - \sum_{k'=1}^{\infty} a_{k'-1} u(x_{j-k'},t)\right) \\ &= \frac{1}{\Gamma(3-\alpha)\Delta x^{\alpha}}\left(a_0 u(x_j,t) + \sum_{k=1}^{\infty}(a_k - a_{k-1}) u(x_{j-k},t)\right). \end{aligned}$$

We arrive to

$$\frac{\partial}{\partial x}\mathscr{I}^l u(x_j,t) \approx \frac{1}{\Gamma(3-\alpha)\Delta x^\alpha}\sum_{k=0}^{\infty} b_{k,1}u(x_{j-k},t),$$

where

$$b_{0,1} = a_0, \quad b_{k,1} = a_k - a_{k-1},\ k \geqslant 1. \tag{5.14}$$

For the right fractional derivative, it follows

$$\begin{aligned} -\frac{\partial}{\partial x}\mathscr{I}^r u(x_j,t) &\approx -\frac{I^r u(x_{j+1},t) - I^r u(x_j,t)}{\Delta x} \\ &= -\frac{\Delta x^{1-\alpha}}{\Gamma(3-\alpha)\Delta x}\left(\sum_{k=0}^{\infty} a_k u(x_{j+1+k},t) - \sum_{k=0}^{\infty} a_k u(x_{j+k},t)\right). \end{aligned}$$

Once again, considering $k' = k+1$ in the first sum and aggregating the terms, we get

$$\begin{aligned} -\frac{\partial}{\partial x}\mathscr{I}^r u(x_j,t) &\approx -\frac{1}{\Gamma(3-\alpha)\Delta x^\alpha}\left(\sum_{k'=1}^{\infty} a_{k'-1} u(x_{j+k'},t) - \sum_{k=0}^{\infty} a_k u(x_{j+k},t)\right) \\ &= \frac{1}{\Gamma(3-\alpha)\Delta x^\alpha}\left(\sum_{k=1}^{\infty} (a_k - a_{k-1}) u(x_{j+k},t) + a_0 u(x_j,t)\right). \end{aligned}$$

Therefore, we obtain

$$-\frac{\partial}{\partial x}\mathscr{I}^r u(x_j,t) \approx \frac{1}{\Gamma(3-\alpha)\Delta x^\alpha}\sum_{k=0}^{\infty} b_{k,1}u(x_{j+k},t),$$

where $b_{k,1}$ are defined in (5.14). Then, the left and right fractional derivatives, $\partial\mathscr{I}^l u(x_j,t)/\partial x$ and $-\partial\mathscr{I}^r u(x_j,t)/\partial x$, can be approximated respectively by $\delta_1^l u(x_j,t)/\Delta x^\alpha$ and $\delta_1^r u(x_j,t)/\Delta x^\alpha$, such that

$$\delta_1^l u(x_j,t) = \frac{1}{\Gamma(3-\alpha)}\sum_{k=0}^{\infty} b_{k,1}u(x_{j-k},t), \quad \delta_1^r u(x_j,t) = \frac{1}{\Gamma(3-\alpha)}\sum_{k=0}^{\infty} b_{k,1}u(x_{j+k},t).$$

Therefore, the general operator $\nabla_\alpha^p u$, for $0 < \alpha < 1$ and $-1 \leqslant p \leqslant 1$, will be approximated by the operator $\delta_{\alpha,1}^p u(x_j,t)/\Delta x^\alpha$ where $\delta_{\alpha,1}^p u$ is given by

$$\delta_{\alpha,1}^p u(x_j,t) = \frac{1+p}{2}\delta_1^l u(x_j,t) + \frac{1-p}{2}\delta_1^r u(x_j,t). \tag{5.15}$$

Fractional derivative upwind second order approximation

Similarly to what we have done in the previous section, we build a new approximation for the derivative of the fractional integrals by a second order upwind approximation. It consists in a three-point backward finite difference for the left fractional derivative and in a three-point forward finite difference for the right fractional derivative.

The second order upwind approximation is defined as

$$c\frac{\partial u}{\partial x}(x_j) \approx \begin{cases} c\dfrac{3u(x_j)-4u(x_{j-1})+u(x_{j-2})}{\Delta x}, & \text{for } c>0, \\[2ex] c\dfrac{-3u(x_j)+4u(x_{j+1})-u(x_{j+2})}{\Delta x}, & \text{for } c<0. \end{cases}$$

Thus, for the left fractional derivative we have

$$\begin{aligned} \frac{\partial}{\partial x}\mathscr{I}^l u(x_j,t) &\approx \frac{3I^l u(x_j,t)-4I^l u(x_{j-1},t)+I^l u(x_{j-2},t)}{2\Delta x} \\ &= \frac{\Delta x^{1-\alpha}}{2\Gamma(3-\alpha)\Delta x}\left(3\sum_{k=0}^{\infty}a_k u(x_{j-k},t)-4\sum_{k=0}^{\infty}a_k u(x_{j-1-k},t)+\sum_{k=0}^{\infty}a_k u(x_{j-2-k},t)\right). \end{aligned}$$

Doing $k' = k+1$ in the second sum and $k' = k+2$ in the third one and rearranging the terms,

$$\begin{aligned} \frac{\partial}{\partial x}\mathscr{I}^l u(x_j,t) &\approx \frac{1}{2\Gamma(3-\alpha)\Delta x^\alpha}\left(3\sum_{k=0}^{\infty}a_k u(x_{j-k},t)-4\sum_{k'=1}^{\infty}a_{k'-1}u(x_{j-k'},t)+\sum_{k'=2}^{\infty}a_{k'-2}u(x_{j-k'},t)\right) \\ &= \frac{1}{2\Gamma(3-\alpha)\Delta x^\alpha}\left(3a_0 u(x_j,t)+(3a_1-4a_0)u(x_{j-1},t)+\sum_{k=2}^{\infty}(3a_k-4a_{k-1}+a_{k-2})u(x_{j-k},t)\right). \end{aligned}$$

Then, the approximation can be written as

$$\frac{\partial}{\partial x}\mathscr{I}^l u(x_j,t) \approx \frac{1}{2\Gamma(3-\alpha)\Delta x^\alpha}\sum_{k=0}^{\infty}b_{k,2}u(x_{j-k},t), \tag{5.16}$$

where

$$b_{0,2} = 3a_0, \quad b_{1,2} = 3a_1-4a_0, \quad b_{k,2} = 3a_k-4a_{k-1}+a_{k-2},\ k \geqslant 2. \tag{5.17}$$

Similarly, for the right derivative we have

$$\begin{aligned} -\frac{\partial}{\partial x}\mathscr{I}^r u(x_j,t) &\approx -\frac{-3I^r u(x_j,t)+4I^r u(x_{j+1},t)-I^r u(x_{j+2},t)}{2\Delta x} \\ &= \frac{-\Delta x^{1-\alpha}}{2\Gamma(3-\alpha)\Delta x}\left(-3\sum_{k=0}^{\infty}a_k u(x_{j+k},t)+4\sum_{k=0}^{\infty}a_k u(x_{j+1+k},t)-\sum_{k=0}^{\infty}a_k u(x_{j+2+k},t)\right). \end{aligned}$$

Using the same strategy as before,

$$\begin{aligned} -\frac{\partial}{\partial x}\mathscr{I}^r u(x_j,t) &\approx \frac{-1}{2\Gamma(3-\alpha)\Delta x^\alpha}\left(-3\sum_{k=0}^{\infty}a_k u(x_{j+k},t)+4\sum_{k=1}^{\infty}a_{k-1}u(x_{j+k},t)-\sum_{k=2}^{\infty}a_{k-2}u(x_{j+k},t)\right) \\ &= \frac{1}{2\Gamma(3-\alpha)\Delta x^\alpha}\left(3a_0 u(x_j,t)+(3a_1-4a_0)u(x_{j+1},t)+\sum_{=2}^{\infty}(3a_k-4a_{k-1}+a_{k-2})u(x_{j+k},t)\right). \end{aligned}$$

We arrive to

$$-\frac{\partial}{\partial x}\mathscr{I}^r u(x_j,t) \approx \frac{1}{2\Gamma(3-\alpha)\Delta x^\alpha}\sum_{k=0}^{\infty}b_{k,2}u(x_{j+k},t). \tag{5.18}$$

Finally, we conclude that the left and right fractional derivatives, $\partial \mathscr{I}^l u(x_j,t)/\partial x$ and $-\partial \mathscr{I}^r u(x_j,t)/\partial x$, can be approximated respectively by $\delta_2^l u(x_j,t)/\Delta x^\alpha$ and $\delta_2^r u(x_j,t)/\Delta x^\alpha$ with $\delta_2^l u$ and $\delta_2^r u$ defined as

$$\delta_2^l u(x_j,t) = \frac{1}{2\Gamma(3-\alpha)} \sum_{k=0}^{\infty} b_{k,2} u(x_{j-k},t), \quad \delta_2^r u(x_j,t) = \frac{1}{2\Gamma(3-\alpha)} \sum_{k=0}^{\infty} b_{k,2} u(x_{j+k},t),$$

with the coefficients $b_{k,2}$ given by (5.17). The general operator $\nabla_\alpha^p u$, for $0 < \alpha < 1$ and $-1 \leqslant p \leqslant 1$, will be approximated by the operator $\delta_{\alpha,2}^p u(x_j,t)/\Delta x^\alpha$ where $\delta_{\alpha,2}^p u$ is given by

$$\delta_{\alpha,2}^p u(x_j,t) = \frac{1+p}{2} \delta_2^l u(x_j,t) + \frac{1-p}{2} \delta_2^r u(x_j,t). \tag{5.19}$$

Concluded the three approaches, we proceed with the construction of the numerical method with an even more general operator.

5.2.2 Numerical methods

We present a numerical method for the equation (5.5). Let us consider a uniform mesh in time $t_{m+1} = t_m + \Delta t$, with $t_0 = 0$ and $t_M = T$, for $m = 0, \ldots, M-1$. In space, consider the uniform mesh in the real line defined as $x_j = x_{j-1} + \Delta x$, for $j \in \mathbb{Z}$.

Note that the three operators (5.13), (5.15) and (5.19) are defined similarly. Therefore, we can consider a general operator that represents each of the three operators given previously, $\delta_{\alpha,c}^p u$, $\delta_{\alpha,1}^p u$ or $\delta_{\alpha,2}^p u$, and we denote it by $\delta_{\alpha,*}^p u$.

The explicit and implicit Euler numerical methods are given respectively by

$$\frac{U_j^{m+1} - U_j^m}{\Delta t} = -\frac{D}{\Delta x^\alpha} \delta_{\alpha,*}^p U_j^m + g_j^m, \qquad \frac{U_j^{m+1} - U_j^m}{\Delta t} = -\frac{D}{\Delta x^\alpha} \delta_{\alpha,*}^p U_j^{m+1} + g_j^{m+1}.$$

The Crank-Nicolson scheme is given by the average of the last two methods, this is,

$$\frac{U_j^{m+1} - U_j^m}{\Delta t} = -\frac{D}{\Delta x^\alpha} \frac{1}{2} \delta_{\alpha,*}^p U_j^m - \frac{D}{\Delta x^\alpha} \frac{1}{2} \delta_{\alpha,*}^p U_j^{m+1} + g_j^{m+1/2},$$

where $g_j^{m+1/2} = (g_j^{m+1} + g_j^m)/2$, that is,

$$\left(1 + \frac{D}{2\Delta x^\alpha} \Delta t \delta_{\alpha,*}^p\right) U_j^{m+1} = \left(1 - \frac{D}{2\Delta x^\alpha} \Delta t \delta_{\alpha,*}^p\right) U_j^m + g_j^{m+1/2}.$$

Let $\mu_\alpha = D\Delta t/\Delta x^\alpha$. The numerical method can be rewritten as

$$\left(1 + \frac{1}{2} \mu_\alpha \delta_{\alpha,*}^p\right) U_j^{m+1} = \left(1 - \frac{1}{2} \mu_\alpha \delta_{\alpha,*}^p\right) U_j^m + g_j^{m+1/2}. \tag{5.20}$$

All the three schemes can also be written in a matricial form. When the problem is defined in the real line we assume natural boundary conditions given by (5.6). Hence, for the implementation of the numerical method, if we consider N large enough, that is, N such that the condition $u(x,t) \approx 0$, for $x \notin [x_0, x_N]$, the numerical boundary conditions do not interfere with the accuracy of the numerical solutions. Therefore, assume the nodal points are U_j^m, $j = -N, ..., N$ such that $U_k = 0$ for $k < -N$ and $k > N$. Introducing the vector $\mathbf{U^m} = [U_{-N}^m, ..., U_N^m]^T$, the schemes may be written as matrix equations

$$\left(\mathbf{I} + \frac{1}{2}\mu_\alpha \mathbf{B}_{\alpha,*}^p\right)\mathbf{U^{m+1}} = \left(\mathbf{I} - \frac{1}{2}\mu_\alpha \mathbf{B}_{\alpha,*}^p\right)\mathbf{U^m} + \mathbf{G^{m+1/2}},$$

where $\mathbf{I}$ is the identity matrix, $\mathbf{U}^m$ is the solution vector $\mathbf{U}^m = [U_{-N}^m, \ldots, U_N^m]^T$, $\mathbf{G}^m$ contains the values of the source term and $\mathbf{B}_{\alpha,*}^p$ is defined such that

$$\mathbf{B}_{\alpha,*}^p = \frac{1+p}{2}\mathbf{B}_{\alpha,*} + \frac{1-p}{2}\mathbf{B}_{\alpha,*}^T, \tag{5.21}$$

with $\mathbf{B}_{\alpha,*}$, the matrix associated with the operators $\delta_{\alpha,c}^p u$, $\delta_{\alpha,1}^p u$ and $\delta_{\alpha,2}^p u$ and given by

$$\mathbf{B_{\alpha,c}} = \frac{1}{2\Gamma(3-\alpha)} \begin{bmatrix} b_{0,c} & b_{-1,c} & 0 & \ldots & 0 & 0 \\ b_{1,c} & b_{0,c} & b_{-1,c} & \ldots & 0 & 0 \\ b_{2,c} & b_{1,c} & b_{0,c} & \ldots & 0 & 0 \\ \vdots & \vdots & \vdots & & \vdots & \vdots \\ b_{2N,c} & b_{2N-1,c} & b_{2N-2,c} & \ldots & b_{1,c} & b_{0,c} \end{bmatrix} \tag{5.22}$$

in the first case,

$$\mathbf{B_{\alpha,1}} = \frac{1}{\Gamma(3-\alpha)} \begin{bmatrix} b_{0,1} & 0 & 0 & \ldots & 0 & 0 \\ b_{1,1} & b_{0,1} & 0 & \ldots & 0 & 0 \\ b_{2,1} & b_{1,1} & b_{0,1} & \ldots & 0 & 0 \\ \vdots & \vdots & \vdots & & \vdots & \vdots \\ b_{2N,1} & b_{2N-1,1} & b_{2N-2,1} & \ldots & b_{1,1} & b_{0,1} \end{bmatrix} \tag{5.23}$$

in the second case and

$$\mathbf{B_{\alpha,2}} = \frac{1}{2\Gamma(3-\alpha)} \begin{bmatrix} b_{0,2} & 0 & 0 & \ldots & 0 & 0 \\ b_{1,2} & b_{0,2} & 0 & \ldots & 0 & 0 \\ b_{2,2} & b_{1,2} & b_{0,2} & \ldots & 0 & 0 \\ \vdots & \vdots & \vdots & & \vdots & \vdots \\ b_{2N,2} & b_{2N-1,2} & b_{2N-2,2} & \ldots & b_{1,2} & b_{0,2} \end{bmatrix} \tag{5.24}$$

in the last case. Note that $\mathbf{B}_{\alpha,*}$ is a Toeplitz matrix, a type of matrices that we have already seen in Section 2.2. Furthermore, $\mathbf{B}_{\alpha,*}$ for $* = 1,2$ is, additionally, a lower triangular matrix.

In the next section, we study the convergence of the three numerical methods obtained specifying the operator in equation (5.20).

5.2.3 Convergence analysis

In order to analyze the convergence of the proposed numerical methods, in this section we study their consistency and stability. In our analysis, we assume we are dealing with functions that vanish at infinity, since our problems are defined in the whole real line. We start by presenting some results regarding the consistency and then present the stability analysis.

Consistency analysis

We discuss the truncation errors of the fractional derivative approximations and, for the sake of clarity, we omit the variable t. Furthermore, we present the results only for the left fractional derivative since the ones for the right fractional derivative can be obtained in a similar manner.

We start by presenting a known result for the central approximation.

Theorem 5.1 (Central approximation, [75]). *Let $0 < \alpha < 1$, $u \in C^3(\mathbb{R})$ and such that the third-order derivative, $u^{(3)}$, has compact support. We have that*

$$\frac{\partial^\alpha u}{\partial x^\alpha}(x_j) - \frac{\delta_c^l u}{\Delta x^\alpha}(x_j) = \varepsilon(x_j), \quad |\varepsilon(x_j)| \leqslant C\Delta x^2,$$

where C does not depend on Δx.

Before moving to the next method, we present a result of great use for the next consistency theorems.

Lemma 5.2. *Consider $\xi \in [x_{k-1}, x_k]$ and*

$$s_k(\xi) = \frac{x_k - \xi}{\Delta x} u(x_{k-1}) + \frac{\xi - x_{k-1}}{\Delta x} u(x_k). \tag{5.25}$$

(a) For $u \in C^2(\mathbb{R})$, we have

$$u(\xi) - s_k(\xi) = -\frac{1}{2} u^{(2)}(\sigma_k) l_{k,2}(\xi), \quad \sigma_k \in [x_{k-1}, x_k].$$

(b) For $u \in C^3(\mathbb{R})$, we have

$$u(\xi) - s_k(\xi) = -\frac{1}{2} u^{(2)}(\eta_k) l_{k,2}(\xi) - \frac{1}{3!}\left(u^{(3)}(\eta_k) \frac{x_k - \xi}{\Delta x}(x_{k-1} - \xi)^3 + u^{(3)}(\zeta_k)(x_k - \xi)^3 \frac{\xi - x_{k-1}}{\Delta x} \right),$$

for $\eta_k \in [x_{k-1}, \xi]$ and $\zeta_k \in [\xi, x_k]$.

In both lines, $l_{k,2}(\xi) = (x_k - \xi)\Delta x - (x_k - \xi)^2$.

Proof. (a) We follow the proof presented in [76]. For $\xi \in [x_{k-1}, x_k]$, doing the Taylor expansions of $u(x_{k-1})$ and $u(x_k)$ around ξ,

$$u(x_{k-1}) = u(\xi) + u'(\xi)(x_{k-1} - \xi) + \frac{1}{2!} u^{(2)}(\eta_k)(x_{k-1} - \xi)^2, \ \eta_k \in [x_{k-1}, \xi],$$

$$u(x_k) = u(\xi) + u'(\xi)(x_k - \xi) + \frac{1}{2!} u^{(2)}(\zeta_k)(x_k - \xi)^2, \ \zeta_k \in [\xi, x_k].$$

Replacing $u(x_{k-1})$ and $u(x_k)$ in (5.25) by the previous expansions,

$$\begin{aligned} s_k(\xi) &= \frac{x_k-\xi}{\Delta x}\left(u(\xi)+u'(\xi)(x_{k-1}-\xi)+\frac{1}{2!}u^{(2)}(\eta_k)(x_{k-1}-\xi)^2\right) \\ &\quad +\frac{\xi-x_{k-1}}{\Delta x}\left(u(\xi)+u'(\xi)(x_k-\xi)+\frac{1}{2!}u^{(2)}(\zeta_k)(x_k-\xi)^2\right). \end{aligned}$$

that is equivalent to

$$s_k(\xi)=u(\xi)+\frac{1}{2}u^{(2)}(\sigma_k)\left(\frac{x_k-\xi}{\Delta x}(x_{k-1}-\xi)^2+(x_k-\xi)^2\frac{\xi-x_k+\Delta x}{\Delta x}\right)$$

with $\sigma_k \in [x_{k-1},x_k]$, since $u^{(2)}$ is continuous and the coefficients of $u^{(2)}$ have the same sign.

Then, we can write

$$u(\xi)-s_k(\xi)=-\frac{1}{2}u^{(2)}(\sigma_k)l_{k,2}(\xi), \quad \sigma_k \in [x_{k-1},x_k],$$

with

$$l_{k,2}(\xi)=(x_k-\xi)\Delta x-(x_k-\xi)^2. \tag{5.26}$$

(b) Following the same ideas of the previous proof, doing the Taylor expansions of $u(x_{k-1})$ and $u(x_k)$ around ξ,

$$u(x_{k-1})=u(\xi)+u'(\xi)(x_{k-1}-\xi)+\frac{1}{2!}u^{(2)}(\xi)(x_{k-1}-\xi)^2+\frac{1}{3!}u^{(3)}(\eta_k)(x_{k-1}-\xi)^3,\ \eta_k \in [x_{k-1},\xi],$$

$$u(x_k)=u(\xi)+u'(\xi)(x_k-\xi)+\frac{1}{2!}u^{(2)}(\xi)(x_k-\xi)^2+\frac{1}{3!}u^{(3)}(\zeta_k)(x_k-\xi)^3,\ \zeta_k \in [\xi,x_k]$$

and replacing $u(x_{k-1})$ and $u(x_k)$ in (5.25) by the previous expansions,

$$\begin{aligned} s_k(\xi) &= \frac{x_k-\xi}{\Delta x}\left(u(\xi)+u'(\xi)(x_{k-1}-\xi)+\frac{1}{2!}u^{(2)}(\xi)(x_{k-1}-\xi)^2+\frac{1}{3!}u^{(3)}(\eta_k)(x_{k-1}-\xi)^3\right) \\ &\quad +\frac{\xi-x_{k-1}}{\Delta x}\left(u(\xi)+u'(\xi)(x_k-\xi)+\frac{1}{2!}u^{(2)}(\xi)(x_k-\xi)^2+\frac{1}{3!}u^{(3)}(\zeta_k)(x_k-\xi)^3\right). \end{aligned}$$

Gathering the terms according to the derivative of u, we obtain

$$\begin{aligned} s_k(\xi) &= u(\xi)+\frac{1}{2}u^{(2)}(\xi)\left(\frac{x_k-\xi}{\Delta x}(x_{k-1}-\xi)^2+(x_k-\xi)^2\frac{\xi-x_k+\Delta x}{\Delta x}\right) \\ &\quad +\frac{1}{3!}\left(u^{(3)}(\eta_k)\frac{x_k-\xi}{\Delta x}(x_{k-1}-\xi)^3+u^{(3)}(\zeta_k)(x_k-\xi)^3\frac{\xi-x_k+\Delta x}{\Delta x}\right). \end{aligned}$$

In this case, despite $u^{(3)}$ being continuous, one coefficient is positive and the other is negative. Therefore,

$$u(\xi)-s_k(\xi)=-\frac{1}{2}u^{(2)}(\xi)l_{k,2}(\xi)-\frac{1}{3!}\left(u^{(3)}(\eta_k)\frac{x_k-\xi}{\Delta x}(x_{k-1}-\xi)^3+u^{(3)}(\zeta_k)(x_k-\xi)^3\frac{\xi-x_k+\Delta x}{\Delta x}\right)$$

with $\eta_k \in [x_{k-1},\xi]$, $\zeta_k \in [\xi,x_k]$ and $l_{k,2}$ defined in (5.26).

□

We present the result for the upwind first order approximation.

Theorem 5.3 (Upwind first order approximation)**.** *Let* $0 < \alpha < 1$, $u \in C^2(\mathbb{R})$ *and such that the spatial derivatives vanish at infinity in an appropriate manner, that is, there exists an* x_a *such that*

$$\int_{-\infty}^{x_a} u^{(2)}(\xi)(x_j-\xi)^{-\alpha} d\xi < C_I \Delta x^3. \tag{5.27}$$

Then, we have that

$$\frac{\partial^\alpha u}{\partial x^\alpha}(x_j) - \frac{\delta_1^l u}{\Delta x^\alpha}(x_j) = \varepsilon(x_j), \quad |\varepsilon(x_j)| \leqslant C\Delta x,$$

where C *does not depend on* Δx*.*

Proof. For the first order upwind approximation, we have

$$\frac{\partial}{\partial x}\mathscr{I}^l u(x_j) = \frac{\mathscr{I}^l u(x_j) - \mathscr{I}^l u(x_{j-1})}{\Delta x} + \varepsilon_1(x_j)$$

where $\varepsilon_1(x_j) = O(\Delta x)$. Considering now the approximation of $\mathscr{I}^l u(x_j)$ by $I^l u(x_j)$, we can write

$$\frac{\partial}{\partial x}\mathscr{I}^l u(x_j) = \frac{\delta_1^l u}{\Delta x}(x_j) + \varepsilon_2(x_j) + \varepsilon_1(x_j)$$

where

$$\varepsilon_2(x_j) = \frac{1}{\Delta x}\left(\left[\mathscr{I}^l u(x_j) - I^l u(x_j)\right] - \left[\mathscr{I}^l u(x_{j-1}) - I^l u(x_{j-1})\right]\right).$$

Recall that the approximation $I^l u(x_j)$ is obtained substituting u by the linear spline s

$$s(x) = \sum_{k=-\infty}^{j} u(x_k) B_+^1(x-x_k),$$

where, for $k < j$

$$B_+^1(x-x_k) = \begin{cases} \dfrac{x-x_{k-1}}{\Delta x}, & x_{k-1} < x \leqslant x_k, \\ \dfrac{x_{k+1}-x}{\Delta x}, & x_k < x \leqslant x_{k+1}, \\ 0, & \text{otherwise} \end{cases} \quad \text{and} \quad B_+^1(x-x_j) = \begin{cases} \dfrac{x_j-x}{\Delta x}, & x_{j-1} \leqslant x \leqslant x_j, \\ 0, & \text{otherwise.} \end{cases}$$

Then, we can rewrite the spline as

$$s(x) = \sum_{k=-\infty}^{j} s_k(x),$$

with

$$s_k(\xi) = \frac{x_k-\xi}{\Delta x} u(x_{k-1}) + \frac{\xi - x_{k-1}}{\Delta x} u(x_k), \quad \text{for } k \leqslant j.$$

Hence,

$$\mathscr{I}^l u(x_j) - I^l u(x_j) = \frac{1}{\Gamma(3-\alpha)} \int_{-\infty}^{x_j} \left(u(\xi) - s(\xi)\right)(x_j-\xi)^{-\alpha} d\xi \tag{5.28}$$

can be written as

$$\mathscr{I}^l u(x_j) - I^l u(x_j) = \frac{1}{\Gamma(3-\alpha)} \sum_{k=-\infty}^{j} \int_{x_{k-1}}^{x_k} (u(\xi) - s_k(\xi))(x_j - \xi)^{-\alpha} d\xi$$

Therefore

$$\varepsilon_2(x_j) = \frac{1}{\Delta x} \frac{1}{\Gamma(3-\alpha)} \left(\sum_{k=-\infty}^{j} \int_{x_{k-1}}^{x_k} (u(\xi) - s_k(\xi))(x_j - \xi)^{-\alpha} d\xi - \sum_{k=-\infty}^{j-1} \int_{x_{k-1}}^{x_k} (u(\xi) - s_k(\xi))(x_{j-1} - \xi)^{-\alpha} d\xi \right).$$

From Lemma 5.2(a),

$$u(\xi) - s_k(\xi) = -\frac{1}{2} u^{(2)}(\eta_k) l_{k,2}(\xi), \ \eta_k \in [x_{k-1}, x_k], \tag{5.29}$$

where

$$l_{k,2}(\xi) = (x_k - \xi)\Delta x - (x_k - \xi)^2$$

and therefore, $|l_{k,2}(\xi)| \leqslant \Delta x^2$. Using (5.29),

$$\varepsilon_2(x_j) = \frac{-1}{\Delta x \Gamma(3-\alpha)} \left(\sum_{k=-\infty}^{j} \int_{x_{k-1}}^{x_k} u^{(2)}(\eta_k) l_{k,2}(\xi)(x_j - \xi)^{-\alpha} d\xi - \sum_{k=-\infty}^{j-1} \int_{x_{k-1}}^{x_k} u^{(2)}(\eta_k) l_{k,2}(\xi)(x_{j-1} - \xi)^{-\alpha} d\xi \right).$$

For the second integral, by doing a change of variable $\xi = \xi - \Delta x$,

$$\sum_{k=-\infty}^{j-1} \int_{x_{k-1}}^{x_k} u^{(2)}(\eta_k) l_{k,2}(\xi)(x_{j-1} - \xi)^{-\alpha} d\xi = \sum_{k=-\infty}^{j-1} \int_{x_k}^{x_{k+1}} u^{(2)}(\eta_{k-1}) l_{k,2}(\xi - \Delta x)(x_j - \xi)^{-\alpha} d\xi.$$

Noting that

$$\begin{aligned} l_{k,2}(\xi - \Delta x) &= (x_k - \xi + \Delta x)\Delta x - (x_k - \xi + \Delta x)^2 \\ &= (x_{k+1} - \xi)\Delta x - (x_{k+1} - \xi)^2 \\ &= l_{k+1,2}(\xi), \end{aligned}$$

we obtain

$$\sum_{k=-\infty}^{j-1} \int_{x_{k-1}}^{x_k} u^{(2)}(\eta_k) l_{k,2}(\xi)(x_{j-1} - \xi)^{-\alpha} d\xi = \sum_{k=-\infty}^{j-1} \int_{x_k}^{x_{k+1}} u^{(2)}(\eta_{k-1}) l_{k+1,2}(\xi)(x_j - \xi)^{-\alpha} d\xi.$$

that is equivalent to

$$\sum_{k=-\infty}^{j-1} \int_{x_{k-1}}^{x_k} u^{(2)}(\eta_k) l_{k,2}(\xi)(x_{j-1} - \xi)^{-\alpha} d\xi = \sum_{k=-\infty}^{j} \int_{x_{k-1}}^{x_k} u^{(2)}(\eta_{k-1}) l_{k,2}(\xi)(x_j - \xi)^{-\alpha} d\xi.$$

Additionally, if we assume that the function u and its derivatives behave as (5.27), then we can write

$$\begin{aligned}\varepsilon_2(x_j) &= \frac{1}{\Delta x}\frac{1}{\Gamma(3-\alpha)}\sum_{k=[x_a/\Delta x]}^{j}\int_{x_{k-1}}^{x_k} u^{(2)}(\eta_{k-1})l_{k,2}(\xi)(x_j-\xi)^{-\alpha}d\xi \\ &\quad -\frac{1}{\Delta x}\frac{1}{\Gamma(3-\alpha)}\sum_{k=[x_a/\Delta x]}^{j}\int_{x_{k-1}}^{x_k} u^{(2)}(\eta_k)l_{k,2}(\xi)(x_j-\xi)^{-\alpha}d\xi + O(\Delta x^2).\end{aligned}$$

Therefore we can obtain the following upper bound for $\varepsilon_2(x_j)$

$$|\varepsilon_2(x_j)| \leqslant \frac{2}{\Delta x\Gamma(3-\alpha)}||u^{(2)}||_\infty \Delta x^2\frac{(x_j-x_a)^{1-\alpha}}{1-\alpha} + C_I\Delta x^2.$$

We conclude that this approximation is a first order approximation for the fractional derivative. □

We finish this section with the result regarding the accuracy of the upwind second order approximation.

Theorem 5.4 (Upwind second order approximation)**.** *Let* $0<\alpha<1$*,* $u\in C^3(\mathbb{R})$ *and such that the spatial derivatives vanish at infinity in an appropriate manner as in* (5.27)*. We have that*

$$\frac{\partial^\alpha u}{\partial x^\alpha}(x_j) - \frac{\delta_2^l u}{\Delta x^\alpha}(x_j) = \varepsilon(x_j), \quad |\varepsilon(x_j)| \leqslant C\Delta x^2,$$

where C *does not depend on* Δx*.*

Proof. For the second order upwind approximation, we have

$$\frac{\partial}{\partial x}\mathscr{I}^l u(x_j) = \frac{3\mathscr{I}^l u(x_j) - 4\mathscr{I}^l u(x_{j-1}) + \mathscr{I}^l u(x_{j-2})}{2\Delta x} + \varepsilon_1(x_j)$$

where $\varepsilon_1(x_j) = O(\Delta x^2)$. Then, using the spline approximation of the integral, we can write

$$\frac{\partial}{\partial x}\mathscr{I}^l u(x_j) = \frac{\delta_2^l u}{\Delta x}(x_j) + \varepsilon_2(x_j) + \varepsilon_1(x_j)$$

where

$$\varepsilon_2(x_j) = \frac{1}{2\Delta x}\left(3(\mathscr{I}^l u(x_j) - I^l u(x_j)) - 4(\mathscr{I}^l u(x_{j-1}) - I^l u(x_{j-1})) + (\mathscr{I}^l u(x_{j-2}) - I^l u(x_{j-2}))\right).$$

From Lemma 5.2(b),

$$u(\xi) - s_k(\xi) = -\frac{1}{2}u^{(2)}(\xi)l_{k,2}(\xi) - \frac{1}{3!}c_k(\xi,\eta_k,\zeta_k)$$

with $l_{k,2}$ given by (5.26) and $c_k(\xi,\eta_k,\zeta_k)$ given by

$$c_k(\xi,\eta_k,\zeta_k) = u^{(3)}(\eta_k)\frac{x_k-\xi}{\Delta x}(x_{k-1}-\xi)^3 + u^{(3)}(\zeta_k)(x_k-\xi)^3\frac{\xi-x_k+\Delta x}{\Delta x}.$$

Therefore we can write

$$\varepsilon_2(x_j) = -\frac{1}{2}\varepsilon_{2,2}(x_j) - \frac{1}{3!}\varepsilon_{2,3}(x_j)$$

with

$$\begin{aligned}\varepsilon_{2,2}(x_j) &= \frac{1}{2\Delta x}\frac{3}{\Gamma(3-\alpha)}\sum_{k=-\infty}^{j}\int_{x_{k-1}}^{x_k} l_{k,2}(\xi)u^{(2)}(\xi)(x_j-\xi)^{-\alpha}d\xi \\ &-\frac{1}{2\Delta x}\frac{4}{\Gamma(3-\alpha)}\sum_{k=-\infty}^{j-1}\int_{x_{k-1}}^{x_k} l_{k,2}(\xi)u^{(2)}(\xi)(x_{j-1}-\xi)^{-\alpha}d\xi \\ &+\frac{1}{2\Delta x}\frac{1}{\Gamma(3-\alpha)}\sum_{k=-\infty}^{j-2}\int_{x_{k-1}}^{x_k} l_{k,2}(\xi)u^{(2)}(\xi)(x_{j-2}-\xi)^{-\alpha}d\xi\end{aligned}$$

and

$$\begin{aligned}\varepsilon_{2,3}(x_j) &= \frac{1}{2\Delta x}\frac{3}{\Gamma(3-\alpha)}\sum_{k=-\infty}^{j}\int_{x_{k-1}}^{x_k} c_k(\xi,\eta_k,\zeta_k)(x_j-\xi)^{-\alpha}d\xi \\ &-\frac{1}{2\Delta x}\frac{4}{\Gamma(3-\alpha)}\sum_{k=-\infty}^{j-1}\int_{x_{k-1}}^{x_k} c_k(\xi,\eta_k,\zeta_k)(x_{j-1}-\xi)^{-\alpha}d\xi \\ &+\frac{1}{2\Delta x}\frac{1}{\Gamma(3-\alpha)}\sum_{k=-\infty}^{j-2}\int_{x_{k-1}}^{x_k} c_k(\xi,\eta_k,\zeta_k)(x_{j-2}-\xi)^{-\alpha}d\xi.\end{aligned}$$

We continue with the simplification of the term $\varepsilon_{2,2}(x_j)$. By doing the change of variables $\xi = \xi - \Delta x$ in the second integral and $\xi = \xi - 2\Delta x$ in the third one, we obtain

$$\begin{aligned}\varepsilon_{2,2}(x_j) &= \frac{3}{2\Delta x}\frac{1}{\Gamma(3-\alpha)}\sum_{k=-\infty}^{j}\int_{x_{k-1}}^{x_k} l_{k,2}(\xi)u^{(2)}(\xi)(x_j-\xi)^{-\alpha}d\xi \\ &-\frac{4}{2\Delta x}\frac{1}{\Gamma(3-\alpha)}\sum_{k=-\infty}^{j-1}\int_{x_{k-1}+\Delta x}^{x_k+\Delta x} l_{k,2}(\xi-\Delta x)u^{(2)}(\xi-\Delta x)(x_j-\xi)^{-\alpha}d\xi \\ &+\frac{1}{2\Delta x}\frac{1}{\Gamma(3-\alpha)}\sum_{k=-\infty}^{j-2}\int_{x_{k-1}+2\Delta x}^{x_k+2\Delta x} l_{k,2}(\xi-2\Delta x)u^{(2)}(\xi-2\Delta x)(x_j-\xi)^{-\alpha}d\xi.\end{aligned}$$

Since $l_{k,2}(\xi-\Delta x) = l_{k+1,2}(\xi)$, as we seen in the last theorem, it follows that

$$\varepsilon_{2,2}(x_j) = \frac{1}{2\Delta x\Gamma(3-\alpha)}\sum_{k=-\infty}^{j}\int_{x_{k-1}}^{x_k} l_{k,2}(\xi)(3u^{(2)}(\xi)-4u^{(2)}(\xi-\Delta x)+u^{(2)}(\xi-2\Delta x))(x_j-\xi)^{-\alpha}d\xi.$$

Note that

$$3u^{(2)}(\xi)-4u^{(2)}(\xi-\Delta x)+u^{(2)}(\xi-2\Delta x)=3\left(u^{(2)}(\xi)-u^{(2)}(\xi-\Delta x)\right)-\left(u^{(2)}(\xi-\Delta x)-u^{(2)}(\xi-2\Delta x)\right). \tag{5.30}$$

Doing a Taylor expansion of $u^{(2)}(\xi-\Delta x)$ around ξ and a Taylor expansion of $u^{(2)}(\xi-2\Delta x)$ around $\xi-\Delta x$,

$$\begin{array}{rcll} u^{(2)}(\xi-\Delta x) & = & u^{(2)}(\xi)-\Delta x u^{(3)}(\xi_1), & \xi_1\in[\xi-\Delta x,\xi], \\ u^{(2)}(\xi-2\Delta x) & = & u^{(2)}(\xi-\Delta x)-\Delta x u^{(3)}(\xi_2), & \xi_2\in[\xi-2\Delta x,\xi-\Delta x] \end{array}$$

and therefore, (5.30) can be written as

$$3u^{(2)}(\xi)-4u^{(2)}(\xi-\Delta x)+u^{(2)}(\xi-2\Delta x)=\left(3u^{(3)}(\xi_1)-u^{(3)}(\xi_2)\right)\Delta x.$$

Thus, assuming that the derivatives of u vanish in an appropriate manner as in (5.27) so that there exists x_a such that

$$\varepsilon_{2,2}(x_j)=\frac{1}{2\Delta x\Gamma(3-\alpha)}\sum_{k=[x_a/\Delta x]}^{j}\int_{x_{k-1}}^{x_k} l_{k,2}(\xi)(3\Delta x u^{(3)}(\xi_1)-\Delta x u^{(3)}(\xi_2))(x_j-\xi)^{-\alpha}d\xi+C_I\Delta x^2,$$

we obtain

$$|\varepsilon_{2,2}(x_j)|\leqslant\frac{4}{2\Gamma(3-\alpha)}\Delta x^2||u^{(3)}||_\infty\frac{(x_j-x_a)^{1-\alpha}}{1-\alpha}+C_I\Delta x^2.$$

Similarly, for the term $\varepsilon_{2,3}$, by doing a change of variables and assuming that the derivatives of u vanish in an appropriate manner as in (5.27) we have that there exists x_a such that

$$\begin{aligned}\varepsilon_{2,3}(x_j)=&\frac{1}{2\Delta x}\frac{3}{\Gamma(3-\alpha)}\sum_{k=x_a}^{j}\int_{x_{k-1}}^{x_k} c_k(\xi,\eta_k,\zeta_k)(x_j-\xi)^{-\alpha}d\xi\\ &-\frac{4}{2\Delta x}\frac{1}{\Gamma(3-\alpha)}\sum_{k=x_a}^{j}\int_{x_{k-1}}^{x_k} c_k(\xi-\Delta x,\eta_{k-1},\zeta_{k-1})(x_j-\xi)^{-\alpha}d\xi\\ &+\frac{1}{2\Delta x}\frac{1}{\Gamma(3-\alpha)}\sum_{k=x_a}^{j}\int_{x_{k-1}}^{x_k} c_k(\xi-2\Delta x,\eta_{k-2},\zeta_{k-2})(x_j-\xi)^{-\alpha}d\xi+C_I\Delta x^2.\end{aligned}$$

Therefore

$$|\varepsilon_{2,3}(x_j)|\leqslant\frac{8}{2\Gamma(3-\alpha)}\Delta x^2||u^{(3)}||_\infty\frac{(x_j-x_a)^{1-\alpha}}{1-\alpha}+C_I\Delta x^2.$$

It follows from the bounds of $\varepsilon_{2,2}(x_j)$ and $\varepsilon_{2,3}(x_j)$ that the bound of $\varepsilon_2(x_j)$ is of second order. □

In the next section, we discuss the stability of the methods described previously.

Stability analysis

We present the stability results using the von Neumann analysis, regarding the central, the upwind first order and the upwind second order methods. The study of the three implicit methods is done in the same way. For each method, we present a lemma that involves properties of the coefficients that will be needed to prove the main theorem on stability.

We start with the implicit central method given by

$$U_j^{m+1}+\frac{1}{2}\mu_\alpha\delta^p_{\alpha,c}U_j^{m+1}=U_j^m-\frac{1}{2}\mu_\alpha\delta^p_{\alpha,c}U_j^m+g_j^{m+1/2}, \tag{5.31}$$

where the operator $\delta^p_{\alpha,c}u$ is defined by (5.13).

The next lemma concerns the coefficients that appear in the operator (5.13) that already appeared in the literature.

Lemma 5.5 ([75]). *The coefficients $b_{k,c}$, defined by* (5.11), *verify*

(a) $|b_{k+1,c}| < |b_{k,c}|,\ k \geqslant 1, \qquad \lim_{k\to\infty} b_{k,c} = 0,$

(b) $\sum_{k=-1}^{\infty} b_{k,c}\cos(k\phi) \geqslant 0,\ \sum_{k=-1}^{\infty} b_{k,c} = 0,\ \sum_{k=-1}^{\infty} b_{k,c}(-1)^k = 0.$

The main stability result for the method involving the central approximation is presented next.

Theorem 5.6 (Central method)**.** *The implicit central method is unconditionally stable.*

Proof. As described in section 4.2.2, the Fourier analysis can be done, in brief, substituting the error in equation

$$e_j^{m+1} + \frac{1}{2}\mu_\alpha \delta^p_{\alpha,c} e_j^{m+1} = e_j^m - \frac{1}{2}\mu_\alpha \delta^p_{\alpha,c} e_j^m, \tag{5.32}$$

by $\kappa^m e^{ij\phi}$ and verifying if the amplification factor κ is not larger than 1, for all $\phi \in [0,\pi]$. Using the formula of the operator $\delta^p_{\alpha,c}u$

$$\kappa^{m+1}e^{ij\phi} + \frac{1}{2}\mu_\alpha\kappa^{m+1}\left[\frac{1+p}{2}\frac{1}{2\Gamma(3-\alpha)}\sum_{k=-1}^{\infty} b_{k,c}e^{i(j-k)\phi} + \frac{1-p}{2}\frac{1}{2\Gamma(3-\alpha)}\sum_{k=-1}^{\infty} b_{k,c}e^{i(j+k)\phi}\right] =$$
$$= \kappa^m e^{ij\phi} - \frac{1}{2}\mu_\alpha\kappa^m\left[\frac{1+p}{2}\frac{1}{2\Gamma(3-\alpha)}\sum_{k=-1}^{\infty} b_{k,c}e^{i(j-k)\phi} + \frac{1-p}{2}\frac{1}{2\Gamma(3-\alpha)}\sum_{k=-1}^{\infty} b_{k,c}e^{i(j+k)\phi}\right].$$

Simplifying $\kappa^m e^{ij\phi}$ on both sides we obtain

$$\kappa\left(1 + \frac{1}{2}\mu_\alpha\left[\frac{1+p}{2}\frac{1}{2\Gamma(3-\alpha)}\sum_{k=-1}^{\infty} b_{k,c}e^{-ik\phi} + \frac{1-p}{2}\frac{1}{2\Gamma(3-\alpha)}\sum_{k=-1}^{\infty} b_{k,c}e^{ik\phi}\right]\right) =$$
$$= 1 - \frac{1}{2}\mu_\alpha\left[\frac{1+p}{2}\frac{1}{2\Gamma(3-\alpha)}\sum_{k=-1}^{\infty} b_{k,c}e^{-ik\phi} + \frac{1-p}{2}\frac{1}{2\Gamma(3-\alpha)}\sum_{k=-1}^{\infty} b_{k,c}e^{ik\phi}\right].$$

Since $\mu_\alpha > 0$, if the real part of

$$\frac{1+p}{2}\sum_{k=-1}^{\infty} b_{k,c}e^{-ik\phi} + \frac{1-p}{2}\sum_{k=-1}^{\infty} b_{k,c}e^{ik\phi}$$

is positive or zero then $|\kappa(\phi)| \leqslant 1$, as explained in the remark after this proof. The real part is given by

$$\frac{1+p}{2}\sum_{k=-1}^{\infty} b_{k,c}\cos(k\phi) + \frac{1-p}{2}\sum_{k=-1}^{\infty} b_{k,c}\cos(k\phi)$$

that is equal to

$$\sum_{k=-1}^{\infty} b_{k,c}\cos(k\phi).$$

By the previous lemma we can conclude that it is nonnegative.

□

Remark. Consider three complex numbers z_1, z_2 and z_3 such that $z_2 = 1 - a - \mathrm{i}b$, $z_3 = 1 + a + \mathrm{i}b$ and $z_1 = z_2/z_3$. In polar coordinates, we have $z_k = r_k e^{\mathrm{i}\phi_k}$ for $k = 1,2,3$ where $|z_k| = r_k$. Then, we can write

$$z_1 = \frac{z_2}{z_3} = \frac{r_2}{r_3} e^{\mathrm{i}(\phi_2 - \phi_3)}$$

that implies that

$$|z_1| = \frac{\sqrt{(1-a)^2 + b^2}}{\sqrt{(1+a)^2 + b^2}}.$$

In order to have $|z_1| \leqslant 1$, it requires that $(1-a)^2 \leqslant (1+a)^2$ and therefore we just have to guarantee that $a \geqslant 0$.

Let us now consider the implicit upwind first order method given by

$$U_j^{m+1} + \frac{1}{2}\mu_\alpha \delta_{\alpha,1}^p U_j^{m+1} = U_j^m - \frac{1}{2}\mu_\alpha \delta_{\alpha,1}^p U_j^m + g_j^{m+1/2}, \tag{5.33}$$

where the operator $\delta_{\alpha,1}^p u$ is defined by (5.15).

Lemma 5.7. *The coefficients $b_{k,1}$, defined by* (5.14)*, verify:*

(a) $\lim_{k\to\infty} b_{k,1} = 0, \quad b_{k,1} \leqslant 0,\ k \geqslant 2\,,$

(b) $\sum_{k=0}^{\infty} b_{k,1} = 0,\ \sum_{k=0}^{\infty} b_{k,1}\cos(k\phi) \geqslant 0.$

Proof. (a) Recall that $b_{k,1}$ is defined by (5.14) as

$$b_{0,1} = a_0, \quad b_{k,1} = a_k - a_{k-1},\ m \geqslant 1,$$

with

$$a_0 = 1, \quad a_k = (k+1)^{2-\alpha} - 2k^{2-\alpha} + (k-1)^{2-\alpha},\ \text{for } k \geqslant 1.$$

Then, $b_{0,1} > 0$, $b_{1,1} = 2^{2-\alpha} - 3$ can be positive, negative or 0 and, for $k \geqslant 2$, we have $b_{k,1} \leqslant 0$. The coefficient $b_{1,1}$ is positive for $\alpha \leqslant \ln(4/3)/\ln(2) \simeq 0,415$ and negative otherwise.

The coefficients $b_{k,1}$ can be written for $k > 1$ in the form

$$b_{k,1} = (k+1)^{2-\alpha} - 3k^{2-\alpha} + 3(k-1)^{2-\alpha} - (k-2)^{2-\alpha},$$

that is equivalent to

$$b_{k,1} = k^{2-\alpha}\left[\left(1+\frac{1}{k}\right)^{2-\alpha} - 3 + 3\left(1-\frac{1}{k}\right)^{2-\alpha} - \left(1-\frac{2}{k}\right)^{2-\alpha}\right].$$

Using the generalized binomial theorem,

$$b_{k,1} = k^{2-\alpha}\left(-3 + \sum_{j=0}^{+\infty}\binom{2-\alpha}{j}\left(1+(-1)^j 3 - (-1)^j 2^j\right)\left(\frac{1}{k}\right)^j\right).$$

In the series, the first three terms are given by

$$(1+3-1) = 3, \quad (2-\alpha)(1-3+2)\frac{1}{k} = 0, \quad \binom{2-\alpha}{2}\left(1+3-2^2\right)\left(\frac{1}{k}\right)^2 = 0$$

and therefore we can arrive to

$$b_{k,1} = \sum_{j=3}^{\infty}\binom{2-\alpha}{j}\frac{c_j}{k^{j+\alpha-2}}, \tag{5.34}$$

where $c_j = 1+(-1)^j(3-2^j)$.It follows from (5.34) that, for $0 < \alpha < 1$, we have $\lim_{k\to\infty} b_{k,1} = 0$.

(b) Note that $\sum_{k=0}^{+\infty} b_{k,1}$ can be seen as $\lim_{N\to\infty}\sum_{k=0}^{N} b_{k,1}$. Then, let us consider $s_N = \sum_{k=0}^{N} b_{k,1}$. We have that

$$\begin{aligned} s_N &= b_{0,1} + b_{1,1} + \cdots + b_{N-1,1} + b_{N,1} \\ &= a_0 + a_1 - a_0 + \cdots + a_{N-1,1} - a_{N-2,1} + a_{N,1} - a_{N-1,1} \\ &= a_{N,1} \end{aligned}$$

that is equivalent to

$$s_N = (N+1)^{2-\alpha} - 2N^{2-\alpha} + (N-1)^{2-\alpha} = \sum_{j=2}^{\infty}\binom{2-\alpha}{j}\frac{1+(-1)^j}{N^{\alpha-2+j}}.$$

Therefore $\lim_{N\to\infty} s_N = 0$ and we have

$$\sum_{k=0}^{\infty} b_{k,1} = 0. \tag{5.35}$$

Regarding the cosine series, we denote it by $s(\phi)$, that is,

$$s(\phi) := \sum_{k=0}^{\infty} b_{k,1}\cos(k\phi). \tag{5.36}$$

Since

$$b_{0,1} = -b_{1,1} + \sum_{k=2}^{\infty}(-b_{k,1})$$

we have

$$s(\phi) = b_{0,1} + b_{1,1}\cos\phi + \sum_{k=2}^{\infty} b_{k,1}\cos(k\phi) = -b_{1,1}(1-\cos\phi) + \sum_{k=2}^{\infty}(-b_{k,1})(1-\cos(k\phi)).$$

The series is nonnegative, once $b_{k,1} \leqslant 0$ for $k > 1$ and $0 \leqslant 1-\cos(k\phi) \leqslant 2$. However, the term $-b_{1,1}(1-\cos\phi)$ can be either positive or negative, depending on the sign of $b_{1,1}$. For the values of α such that $b_{1,1} \leqslant 0$, we can conclude immediately that $s(\phi) \geqslant 0$. If $b_{1,1} \geqslant 0$ we proceed differently. From the definition of $s(\phi)$ we conclude that it is a continuous function for $\phi \in [0,\pi]$ and, from (5.35), $s(0) = 0$. Furthermore, $s(\phi)$ is positive, since $s(\pi/2) > 0$ and $s(\phi) \neq 0$ for all $\phi \neq 0$ as can be seen in Figure 5.2. □

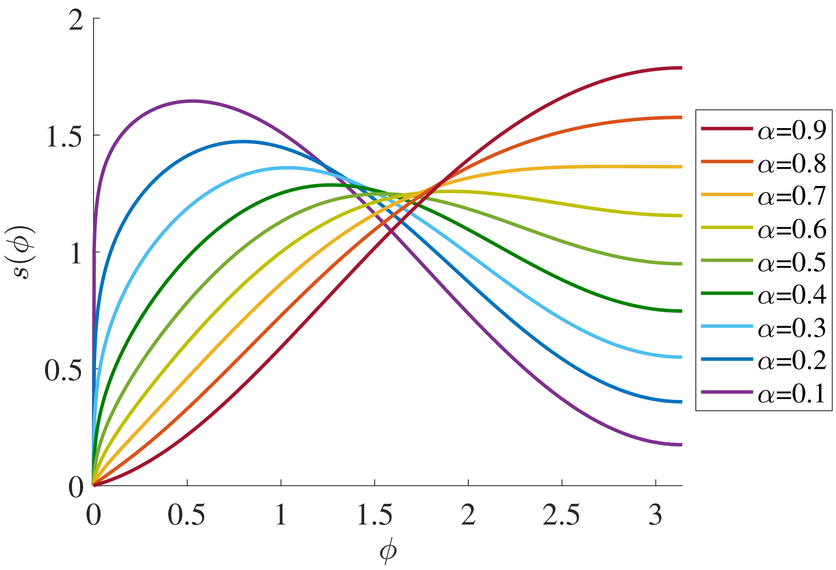

Fig. 5.2 Plot of the series function of cosines $s(\phi)$ given by (5.36) when $\phi \in [0,\pi]$ and for different values of α changing from 0.1 to 0.9.

The main stability result for the method involving the first order upwind approximation is presented next.

Theorem 5.8 (Upwind first order method)**.** *The implicit upwind first order method is unconditionally stable.*

Proof. Similarly to the last theorem, the von Neumann analysis can be done replacing the error in equation

$$e_j^{m+1} + \frac{1}{2}\mu_\alpha \delta_{\alpha,1}^p e_j^{m+1} = e_j^m - \frac{1}{2}\mu_\alpha \delta_{\alpha,1}^p e_j^m, \tag{5.37}$$

by $\kappa^m \mathrm{e}^{ij\phi}$ and verifying if the amplification factor κ is less than or equal to 1, for all $\phi \in [0,\pi]$. Using the formula of the operator $\delta_{\alpha,1}^2 u$ and dividing the whole equation by $\kappa^m \mathrm{e}^{ij\phi}$,

$$\kappa\left(1 + \frac{\mu_\alpha}{2\Gamma(3-\alpha)}\left[\frac{1+p}{2}\sum_{k=0}^{\infty} b_{k,1}\mathrm{e}^{-ik\phi} + \frac{1-p}{2}\sum_{k=0}^{\infty} b_{k,1}\mathrm{e}^{ik\phi}\right]\right)$$
$$= 1 - \frac{\mu_\alpha}{2\Gamma(3-\alpha)}\left[\frac{1+p}{2}\sum_{k=0}^{\infty} b_{k,1}\mathrm{e}^{-ik\phi} + \frac{1-p}{2}\sum_{k=0}^{\infty} b_{k,1}\mathrm{e}^{ik\phi}\right].$$

If the real part of

$$\frac{1+p}{2}\sum_{k=0}^{\infty} b_{k,1}e^{-ik\phi} + \frac{1-p}{2}\sum_{k=0}^{\infty} b_{k,1}e^{ik\phi}$$

is positive or zero then $|\kappa(\phi)| \leqslant 1$ as seen before. The real part is given by

$$\frac{1+p}{2}\sum_{k=0}^{\infty} b_{k,1}\cos(k\phi) + \frac{1-p}{2}\sum_{k=0}^{\infty} b_{k,1}\cos(k\phi).$$

By the previous lemma we can conclude that it is nonnegative. □

The implicit upwind second order method is given by

$$U_j^{m+1} + \frac{1}{2}\mu_\alpha \delta^p_{\alpha,2} U_j^{m+1} = U_j^m - \frac{1}{2}\mu_\alpha \delta^p_{\alpha,2} U_j^m + g_j^{m+1/2}, \tag{5.38}$$

where the operator $\delta^p_{\alpha,2}u$ is defined by (5.19).

Lemma 5.9. *The coefficients $b_{k,2}$, defined by (5.17), verify:*

(a) $\lim_{k\to\infty} b_{k,2} = 0, \quad b_{k,2} \leqslant 0,\ k \geqslant 4,$

(b) $\sum_{k=0}^{\infty} b_{k,2} = 0,\ \sum_{k=0}^{\infty} b_{k,2}\cos(k\phi) \geqslant 0.$

Proof. The proof can be done following the same steps of Lemma 5.7.

(a) From (5.17), we have

$$b_{0,2} = 3a_0, \quad b_{1,2} = 3a_1 - 4a_0, \quad b_{k,2} = 3a_k - 4a_{k-1} + a_{k-2},\ k \geqslant 2.$$

It is easy to check that, for all $k \geqslant 4$, we have $b_{k,2} \leqslant 0$. For $k = 0$, we have $b_{0,2} = 3 > 0$. For $k = 1$, $b_{1,2} = 3 \times 2^{2-\alpha} - 10$ is positive for $\alpha \leqslant \ln(6/5)/\ln(2) \simeq 0,263$ and negative otherwise. For $k = 2, 3$, we have that $b_{2,k}$ can be positive or negative, once again depending on the value of α.

For $k \geqslant 3$, the coefficients $b_{k,2}$ can be written as

$$b_{k,2} = 3(k+1)^{2-\alpha} - 10k^{2-\alpha} + 12(k-1)^{2-\alpha} - 6(k-2)^{2-\alpha} + (k-3)^{2-\alpha},$$

that leads us

$$b_{k,2} = k^{2-\alpha}\left[3\left(1+\frac{1}{k}\right)^{2-\alpha} - 10 + 12\left(1-\frac{1}{k}\right)^{2-\alpha} - 6\left(1-\frac{2}{k}\right)^{2-\alpha} + \left(1-\frac{3}{k}\right)^{2-\alpha}\right].$$

Applying the generalized binomial theorem,

$$b_{k,2} = k^{2-\alpha}\left(-10 + \sum_{j=0}^{+\infty}\binom{2-\alpha}{j}\left(3 + 12\times(-1)^j - 6\times(-1)^j 2^j + (-1)^j 3^j\right)\left(\frac{1}{k}\right)^j\right).$$

Note that, the first three terms of the series are given by

$$3+12-6+1=10, \quad (3-12+6\times 2-3)\frac{1}{k}=0, \quad (3+12-6\times 4+9)\frac{1}{k^2}=0.$$

Therefore, we can write that the coefficients $b_{k,2}$ are defined by the series

$$b_{k,2}=\sum_{j=3}^{\infty}\binom{2-\alpha}{j}\frac{3c_j}{k^{j+\alpha-2}}, \tag{5.39}$$

for $k>2$, with $c_j=1+(-1)^j(4-2^{j+1}+3^{j-1})$. It follows from (5.39) that, for $0<\alpha<1$, we have $\lim_{k\to\infty} b_{k,2}=0$.

(b) Considering $s_N=\sum_{k=0}^{N} b_{k,2}$, we can write $\lim_{N\to\infty} s_N=\sum_{k=0}^{\infty} b_{k,2}$. Using the definition of $b_{k,2}$, for s_N we have

$$\begin{aligned} s_N &= b_{0,2}+b_{1,2}+b_{2,2}+\cdots+b_{N,2}\\ &= 3a_0+3a_1-4a_0+3a_2-4a_1+a_0\cdots+3a_{N-1}-4a_{N-2}+a_{N-3}+3a_N-4a_{N-1}+a_{N-2}\\ &= 3a_{N,1}-a_{N-1,1}, \end{aligned}$$

which is equivalent to

$$s_N=3\left((N+1)^{2-\alpha}-2N^{2-\alpha}+(N-1)^{2-\alpha}\right)-\left(N^{2-\alpha}-2(N-1)^{2-\alpha}+(N-2)^{2-\alpha}\right)$$

and then

$$s_N=3(N+1)^{2-\alpha}-7N^{2-\alpha}+5(N-1)^{2-\alpha}-(N-2)^{2-\alpha}.$$

Using once again the generalized binomial theorem, we obtain

$$s_N=\sum_{j=2}^{\infty}\binom{2-\alpha}{j}\frac{d_j}{N^{\alpha-2+j}},$$

where $d_j=3+(-1)^j(5-2^j)$. Therefore $\lim_{N\to\infty} s_N=0$ and

$$\sum_{k=0}^{\infty} b_{k,2}=0. \tag{5.40}$$

Regarding the cosine series, that we denote it by $s(\phi)$,

$$s(\phi):=\sum_{k=0}^{\infty} b_{k,2}\cos(k\phi), \tag{5.41}$$

and, from (5.40), we have that $s(0)=0$. Furthermore, $s(\phi)$ is positive, since it is a continuous function $s(\pi/2)>0$ and $s(\phi)\neq 0$ for all $\phi\neq 0$ as can be seen in Figure 5.3.

□

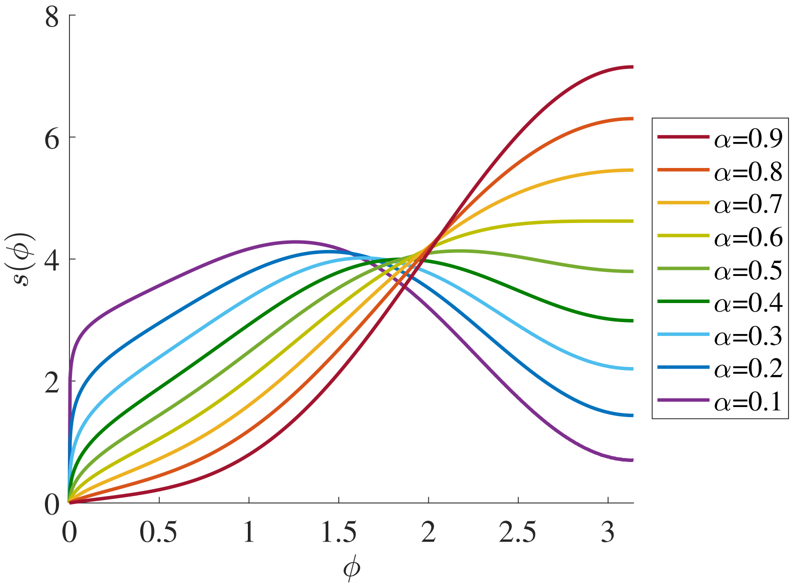

Fig. 5.3 Plot of the series function of cosines $s(\phi)$ given by (5.41) when $\phi \in [0, \pi]$ and for different values of α changing from 0.1 to 0.9.

The main stability result for the method involving the second order upwind approximation is presented next.

Theorem 5.10 (Upwind second order method)**.** *The implicit upwind second order method is unconditionally stable.*

Proof. The proof is similar to the proof of Theorem 5.8. By replacing the error in equation

$$e_j^{m+1} + \frac{1}{2}\mu_\alpha \delta_{\alpha,2}^p e_j^{m+1} = e_j^m - \frac{1}{2}\mu_\alpha \delta_{\alpha,2}^p e_j^m, \tag{5.42}$$

by a single mode $\kappa^m \mathrm{e}^{ij\phi}$ and simplifying $\kappa^m \mathrm{e}^{ij\phi}$ on both sides we obtain

$$\kappa\left(1+\frac{\mu_\alpha}{4}\left[\frac{1+p}{2}\frac{1}{\Gamma(3-\alpha)}\sum_{k=0}^{\infty} b_{k,2}\mathrm{e}^{-ik\phi}+\frac{1-p}{2}\frac{1}{\Gamma(3-\alpha)}\sum_{k=0}^{\infty} b_{k,2}\mathrm{e}^{ik\phi}\right]\right)$$
$$=1-\frac{\mu_\alpha}{4}\left(\frac{1+p}{2}\frac{1}{\Gamma(3-\alpha)}\sum_{k=0}^{\infty} b_{k,2}\mathrm{e}^{-ik\phi}+\frac{1-p}{2}\frac{1}{\Gamma(3-\alpha)}\sum_{k=0}^{\infty} b_{k,2}\mathrm{e}^{ik\phi}\right).$$

If the real part of

$$\frac{1+p}{2}\sum_{k=0}^{\infty} b_{k,2}\mathrm{e}^{-ik\phi}+\frac{1-p}{2}\sum_{k=0}^{\infty} b_{k,2}\mathrm{e}^{ik\phi}$$

is non-negative then $|\kappa(\phi)| \leqslant 1$. The real part is given by

$$\frac{1+p}{2}\sum_{k=0}^{\infty} b_{k,2}\cos(k\phi)+\frac{1-p}{2}\sum_{k=0}^{\infty} b_{k,2}\cos(k\phi)$$

and, by Lemma 5.9(b), we can conclude that it is positive or zero. □

In the next sections we present some experiments with the three numerical methods discussed previously.

5.2.4 Numerical experiments

Consider equation (5.5), with $D = 1$, source term $g(x,t)$ and initial condition $u_0(x)$ are defined in order to the exact solution of the problem be $u(x,t) = \mathrm{e}^{-t}x^4(2-x)^4$. Moreover, consider the following domain $[0,2] \times [0,1]$, discretized uniformly.

In the next tables we determine the discrete L^∞ norm and the discrete L^2 norm of error for an instant of time $t_M = M\Delta t$, as follows

$$||u^M - U^M||_\infty = \max_{j=1,\ldots,N-1} \left|u(x_j,t_M) - U_j^M\right| \tag{5.43}$$

and

$$||u^M - U^M||_2 = \left(\Delta x \sum_{j=1}^{N-1} \left|u(x_j,t_M) - U_j^M\right|^2\right)^{1/2}. \tag{5.44}$$

We present the convergence in space, for different values of α and for $p = -1,0,1$, for the three numerical methods suggested previously.

Table 5.1 Results concerning the central approximation for $p = 1$, $\Delta t = 0.001$ and different values of α. Convergence rates R_∞ for the error (5.43) and R_2 for the error (5.44).

Δx	$\alpha = 0.1$	R_∞	$\alpha = 0.3$	R_∞	$\alpha = 0.5$	R_∞	$\alpha = 0.7$	R_∞	$\alpha = 0.9$	R_∞
2^{-6}	1.923e-04		2.227e-04		2.606e-04		2.998e-04		4.132e-04	
2^{-7}	4.805e-05	2.00	5.567e-05	2.00	6.538e-05	2.00	7.569e-05	1.99	1.049e-04	1.98
2^{-8}	1.199e-05	2.00	1.390e-05	2.00	1.637e-05	2.00	1.907e-05	1.99	2.659e-05	1.98
2^{-9}	2.975e-06	2.01	3.455e-06	2.01	4.080e-06	2.00	4.783e-06	2.00	6.756e-06	1.98
		R_2		R_2		R_2		R_2		R_2
2^{-6}	1.514e-04		1.766e-04		2.079e-04		2.400e-04		2.565e-04	
2^{-7}	3.783e-05	2.00	4.416e-05	2.00	5.213e-05	2.00	6.062e-05	1.99	6.490e-05	1.98
2^{-8}	9.447e-06	2.00	1.104e-05	2.00	1.306e-05	2.00	1.528e-05	1.99	1.641e-05	1.98
2^{-9}	2.352e-06	2.01	2.752e-06	2.00	3.266e-06	2.00	3.844e-06	1.99	4.142e-06	1.99

In Tables 5.1–5.9 we have the results for the three methods, for $p = 1,0$ and -1. In Tables 5.1–5.3 we exhibit the results for the central approximation; in Tables 5.4–5.6 we exhibit the results for the first order upwind approximation; and in Tables 5.7–5.9 we exhibit the results for the second order upwind approximation. By observing the tables, we conclude that the methods using the central approximation and the second order upwind approximation are second order accurate while the first order accuracy is attained by the first order upwind scheme. All the results are according to the theoretical results.

Table 5.2 Results concerning the central approximation for $p = 0$, $\Delta t = 0.001$ and different values of α. Convergence rates R_∞ for the error (5.43) and R_2 for the error (5.44).

Δx	$\alpha = 0.1$	R_∞	$\alpha = 0.3$	R_∞	$\alpha = 0.5$	R_∞	$\alpha = 0.7$	R_∞	$\alpha = 0.9$	R_∞
2^{-6}	1.902e-04		2.029e-04		2.046e-04		1.907e-04		1.226e-04	
2^{-7}	4.753e-05	2.00	5.069e-05	2.00	5.109e-05	2.00	4.760e-05	2.00	3.057e-05	2.00
2^{-8}	1.186e-05	2.00	1.265e-05	2.00	1.275e-05	2.00	1.187e-05	2.00	7.604e-06	2.01
2^{-9}	2.942e-06	2.01	3.140e-06	2.01	3.163e-06	2.01	2.940e-06	2.01	1.867e-06	2.03
		R_2		R_2		R_2		R_2		R_2
2^{-6}	1.498e-04		1.612e-04		1.642e-04		1.556e-04		1.032e-04	
2^{-7}	3.742e-05	2.00	4.027e-05	2.00	4.102e-05	2.00	3.883e-05	2.00	2.572e-05	2.00
2^{-8}	9.344e-06	2.00	1.006e-05	2.00	1.024e-05	2.00	9.694e-06	2.00	6.413e-06	2.00
2^{-9}	2.326e-06	2.01	2.505e-06	2.01	2.552e-06	2.00	2.414e-06	2.01	1.592e-06	2.01

Table 5.3 Results concerning the central approximation for $p = -1$, $\Delta t = 0.001$ and different values of α. Convergence rates R_∞ for the error (5.43) and R_2 for the error (5.44).

Δx	$\alpha = 0.1$	R_∞	$\alpha = 0.3$	R_∞	$\alpha = 0.5$	R_∞	$\alpha = 0.7$	R_∞	$\alpha = 0.9$	R_∞
2^{-6}	1.923e-04		2.227e-04		2.606e-04		2.998e-04		4.132e-04	
2^{-7}	4.805e-05	2.00	5.567e-05	2.00	6.538e-05	2.00	7.569e-05	1.99	1.049e-04	1.98
2^{-8}	1.199e-05	2.00	1.390e-05	2.00	1.637e-05	2.00	1.907e-05	1.99	2.659e-05	1.98
2^{-9}	2.975e-06	2.01	3.455e-06	2.01	4.080e-06	2.00	4.783e-06	2.00	6.756e-06	1.98
		R_2		R_2		R_2		R_2		R_2
2^{-6}	1.514e-04		1.766e-04		2.079e-04		2.400e-04		2.565e-04	
2^{-7}	3.783e-05	2.00	4.416e-05	2.00	5.213e-05	2.00	6.062e-05	1.99	6.490e-05	1.98
2^{-8}	9.447e-06	2.00	1.104e-05	2.00	1.306e-05	2.00	1.528e-05	1.99	1.641e-05	1.98
2^{-9}	2.352e-06	2.01	2.752e-06	2.00	3.266e-06	2.00	3.844e-06	1.99	4.142e-06	1.99

Table 5.4 Results concerning the upwind first order approximation for $p = 1$, $\Delta t = 0.001$ and different values of α. Convergence rates R_∞ for the error (5.43) and R_2 for the error (5.44).

Δx	$\alpha = 0.1$	R_∞	$\alpha = 0.3$	R_∞	$\alpha = 0.5$	R_∞	$\alpha = 0.7$	R_∞	$\alpha = 0.9$	R_∞
2^{-6}	2.166e-02		2.278e-02		2.346e-02		2.840e-02		4.084e-02	
2^{-7}	1.083e-02	1.00	1.140e-02	1.00	1.176e-02	1.00	1.424e-02	1.00	2.054e-02	0.99
2^{-8}	5.415e-03	1.00	5.703e-03	1.00	5.890e-03	1.00	7.132e-03	1.00	1.030e-02	1.00
2^{-9}	2.708e-03	1.00	2.852e-03	1.00	2.947e-03	1.00	3.569e-03	1.00	5.158e-03	1.00
		R_2		R_2		R_2		R_2		R_2
2^{-6}	5.194e-03		5.930e-03		6.969e-03		8.447e-03		1.063e-02	
2^{-7}	2.599e-03	1.00	2.974e-03	1.00	3.507e-03	0.99	4.269e-03	0.98	5.411e-03	0.97
2^{-8}	1.300e-03	1.00	1.490e-03	1.00	1.759e-03	1.00	2.146e-03	0.99	2.731e-03	0.99
2^{-9}	6.501e-04	1.00	7.455e-04	1.00	8.810e-04	1.00	1.076e-03	1.00	1.372e-03	0.99

Table 5.5 Results concerning the upwind first order approximation for $p = 0$, $\Delta t = 0.001$ and different values of α. Convergence rates R_∞ for the error (5.43) and R_2 for the error (5.44).

Δx	$\alpha = 0.1$	R_∞	$\alpha = 0.3$	R_∞	$\alpha = 0.5$	R_∞	$\alpha = 0.7$	R_∞	$\alpha = 0.9$	R_∞
2^{-6}	3.356e-03		1.252e-02		2.593e-02		4.702e-02		8.402e-02	
2^{-7}	1.788e-03	0.91	6.400e-03	0.97	1.318e-02	0.98	2.392e-02	0.98	4.300e-02	0.97
2^{-8}	9.219e-04	0.96	3.235e-03	0.98	6.647e-03	0.99	1.206e-02	0.99	2.175e-02	0.98
2^{-9}	4.679e-04	0.98	1.626e-03	0.99	3.337e-03	0.99	6.056e-03	0.99	1.093e-02	0.99
		R_2		R_2		R_2		R_2		R_2
2^{-6}	6.650e-04		2.554e-03		5.077e-03		9.088e-03		1.789e-02	
2^{-7}	3.674e-04	0.86	1.321e-03	0.95	2.602e-03	0.96	4.664e-03	0.96	9.272e-03	0.95
2^{-8}	1.926e-04	0.93	6.715e-04	0.98	1.317e-03	0.98	2.363e-03	0.98	4.722e-03	0.97
2^{-9}	9.852e-05	0.97	3.385e-04	0.99	6.627e-04	0.99	1.189e-03	0.99	2.383e-03	0.99

Table 5.6 Results concerning the upwind first order approximation for $p = -1$, $\Delta t = 0.001$ and different values of α. Convergence rates R_∞ for the error (5.43) and R_2 for the error (5.44).

Δx	$\alpha = 0.1$	R_∞	$\alpha = 0.3$	R_∞	$\alpha = 0.5$	R_∞	$\alpha = 0.7$	R_∞	$\alpha = 0.9$	R_∞
2^{-6}	2.152e-02		2.269e-02		2.509e-02		3.025e-02		4.282e-02	
2^{-7}	1.076e-02	1.00	1.135e-02	1.00	1.259e-02	0.99	1.531e-02	0.98	2.224e-02	0.95
2^{-8}	5.379e-03	1.00	5.679e-03	1.00	6.309e-03	1.00	7.707e-03	0.99	1.135e-02	0.97
2^{-9}	2.689e-03	1.00	2.840e-03	1.00	3.158e-03	1.00	3.866e-03	1.00	5.735e-03	0.98
		R_2		R_2		R_2		R_2		R_2
2^{-6}	5.194e-03		5.930e-03		6.969e-03		8.447e-03		1.063e-02	
2^{-7}	2.599e-03	1.00	2.974e-03	1.00	3.507e-03	0.99	4.269e-03	0.98	5.411e-03	0.97
2^{-8}	1.300e-03	1.00	1.490e-03	1.00	1.759e-03	1.00	2.146e-03	0.99	2.731e-03	0.99
2^{-9}	6.501e-04	1.00	7.455e-04	1.00	8.810e-04	1.00	1.076e-03	1.00	1.372e-03	0.99

Table 5.7 Results concerning the upwind second order approximation for $p = 1$, $\Delta t = 0.001$ and different values of α. Convergence rates R_∞ for the error (5.43) and R_2 for the error (5.44).

Δx	$\alpha = 0.1$	R_∞	$\alpha = 0.3$	R_∞	$\alpha = 0.5$	R_∞	$\alpha = 0.7$	R_∞	$\alpha = 0.9$	R_∞
2^{-6}	7.649e-04		8.042e-04		8.310e-04		8.321e-04		1.292e-03	
2^{-7}	2.036e-04	1.91	2.135e-04	1.91	2.213e-04	1.91	2.207e-04	1.91	3.187e-04	2.02
2^{-8}	5.280e-05	1.95	5.548e-05	1.94	5.744e-05	1.95	5.700e-05	1.95	7.881e-05	2.02
2^{-9}	1.359e-05	1.96	1.420e-05	1.97	1.468e-05	1.97	1.454e-05	1.97	1.956e-05	2.01
		R_2		R_2		R_2		R_2		R_2
2^{-6}	1.512e-04		1.770e-04		2.129e-04		2.674e-04		3.539e-04	
2^{-7}	3.784e-05	2.00	4.427e-05	2.00	5.312e-05	2.00	6.636e-05	2.01	8.816e-05	2.01
2^{-8}	9.473e-06	2.00	1.107e-05	2.00	1.326e-05	2.00	1.647e-05	2.01	2.188e-05	2.01
2^{-9}	2.378e-06	1.99	2.776e-06	2.00	3.314e-06	2.00	4.093e-06	2.01	5.426e-06	2.01

Table 5.8 Results concerning the upwind second order approximation for $p = 0$, $\Delta t = 0.001$ and different values of α. Convergence rates R_∞ for the error (5.43) and R_2 for the error (5.44).

Δx	$\alpha = 0.1$	R_∞	$\alpha = 0.3$	R_∞	$\alpha = 0.5$	R_∞	$\alpha = 0.7$	R_∞	$\alpha = 0.9$	R_∞
2^{-6}	7.822e-04		8.302e-04		8.085e-04		8.064e-04		1.079e-03	
2^{-7}	2.115e-04	1.89	2.230e-04	1.90	2.082e-04	1.96	2.097e-04	1.94	2.743e-04	1.98
2^{-8}	5.499e-05	1.94	5.756e-05	1.95	5.232e-05	1.99	5.290e-05	1.99	6.809e-05	2.01
2^{-9}	1.404e-05	1.97	1.459e-05	1.98	1.296e-05	2.01	1.319e-05	2.00	1.681e-05	2.02
		R_2		R_2		R_2		R_2		R_2
2^{-6}	1.508e-04		1.662e-04		1.750e-04		1.767e-04		1.517e-04	
2^{-7}	3.761e-05	2.00	4.097e-05	2.02	4.244e-05	2.04	4.155e-05	2.09	3.186e-05	2.25
2^{-8}	9.394e-06	2.00	1.017e-05	2.01	1.044e-05	2.02	1.006e-05	2.05	7.207e-06	2.14
2^{-9}	2.356e-06	2.00	2.540e-06	2.00	2.598e-06	2.01	2.481e-06	2.02	1.717e-06	2.07

Table 5.9 Results concerning the upwind second order approximation for $p = -1$, $\Delta t = 0.001$ and different values of α. Convergence rates R_∞ for the error (5.43) and R_2 for the error (5.44).

Δx	$\alpha = 0.1$	R_∞	$\alpha = 0.3$	R_∞	$\alpha = 0.5$	R_∞	$\alpha = 0.7$	R_∞	$\alpha = 0.9$	R_∞
2^{-6}	8.248e-04		8.904e-04		8.877e-04		9.327e-04		1.184e-03	
2^{-7}	2.186e-04	1.92	2.324e-04	1.94	2.269e-04	1.97	2.360e-04	1.98	2.978e-04	1.99
2^{-8}	5.646e-05	1.95	5.894e-05	1.98	5.730e-05	1.99	5.908e-05	2.00	7.426e-05	2.00
2^{-9}	1.439e-05	1.97	1.484e-05	1.99	1.436e-05	2.00	1.471e-05	2.01	1.841e-05	2.01
		R_2		R_2		R_2		R_2		R_2
2^{-6}	1.512e-04		1.770e-04		2.129e-04		2.674e-04		3.539e-04	
2^{-7}	3.784e-05	2.00	4.427e-05	2.00	5.312e-05	2.00	6.636e-05	2.01	8.816e-05	2.01
2^{-8}	9.473e-06	2.00	1.107e-05	2.00	1.326e-05	2.00	1.647e-05	2.01	2.188e-05	2.01
2^{-9}	2.378e-06	1.99	2.776e-06	2.00	3.314e-06	2.00	4.093e-06	2.01	5.426e-06	2.01

Furthermore note that, by analyzing all the tables, in general the values of the error are higher for larger values of α, as it is illustrated by some figures displayed in the next section. Moreover, from Tables 5.1–5.3 we can see that the values of the error for the central method are smaller for the symmetric case $p = 0$. From Tables 5.4–5.6 we confirm that for larger values of α, namely $\alpha = 0.5, 0.7, 0.9$, the upwind first order method presents higher values for the error when $p = 0$ comparing with $p = -1$ and $p = 1$. These features are also highlighted by figures in the next section.

One computational advantage of using the upwind numerical method is the lack of need of extending the computational domain to the right-hand side, as in the central method case, when $p = 1$ since the numerical method only uses interpolation points on the left, for the left fractional derivative. Similarly, for the right fractional derivative, for $p = -1$ we do not have to extend the computational domain to the left-hand side since the numerical method only uses interpolation points on the right.

Furthermore, the main advantage of the upwind methods over the central method is going to be explored in the next section and is related to oscillations.

5.2.5 Central method versus upwind methods: numerical behaviour

It is known that some high-order finite differences methods may trigger spurious oscillations, including the central differences scheme [93]. We have used a second-order central difference to approximate the derivative outside the integral that appears in the left and right fractional derivatives of order $0 < \alpha < 1$. In what follows, we present examples for which spurious oscillations arise when using the central discretization and do not occur when using an upwind approximation for the fractional derivatives.

Consider equation (5.5) defined in the domain $[0,2] \times [0,T]$ and the following uniform space and time discretizations $x_j = j\Delta x,\ j = 0,\ldots,N$ with $x_N = 2$ and $t_m = t_{m-1} + m\Delta t,\ m = 1,\ldots,M$ with $t_M = T$. Also consider the diffusion coefficient $D = 1$ and the source term $g(x,t)$ and the initial condition $u_0(x)$ such that the exact solution of the problem is $u(x,t) = \mathrm{e}^{-t}x^4(2-x)^4$. Note that the problem can be interpreted as defined on the real line with $u(x,t) = 0,\ x \notin (0,2)$. Then, the regularity of the solution in space is $C^3(\mathbb{R})$.

In the following, we present several numerical tests with space step $\Delta x = 2/125$, for $T = 5$ and, since we have implicit methods one of the advantages would be to be able to choose a large time step, and therefore we chose $\Delta t = 0.1$.

In Figures 5.4–5.6, we plot the numerical solutions versus the exact solution for different values of $p = -0.8, -0.4, 0, 0.4, 0.8$ and $\alpha = 0.8$ (left) and $\alpha = 0.2$ (right), for the three methods. The experiments using the central method in Figure 5.4 show, once again, the influence of p in where appear the oscillations, specially for $\alpha = 0.8$. For $\alpha = 0.2$, we can still spot some oscillations for the more extreme cases $p = -0.8$ and $p = 0.8$, signalized with black ellipses. In Figure 5.5, we plot

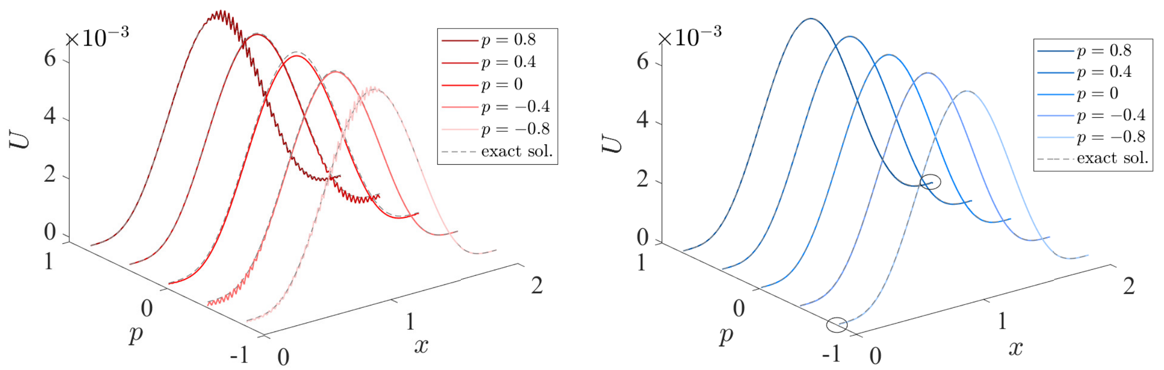

Fig. 5.4 Numerical solution with the central method for $p = -0.8, -0.4, 0, 0.4, 0.8$. Left: $\alpha = 0.8$. Right: $\alpha = 0.2$.

the numerical solutions obtained using the second order upwind method. In this case, we no longer observe the spurious oscillations for any values of p and α. In Figure 5.5, we present the numerical solutions obtained using the first order upwind method. Despite not having the oscillations observed previously, for $\alpha = 0.8$ the method does not approximate the exact solution as effectively as the second order upwind method, specially for $p = 0$ and closer values.

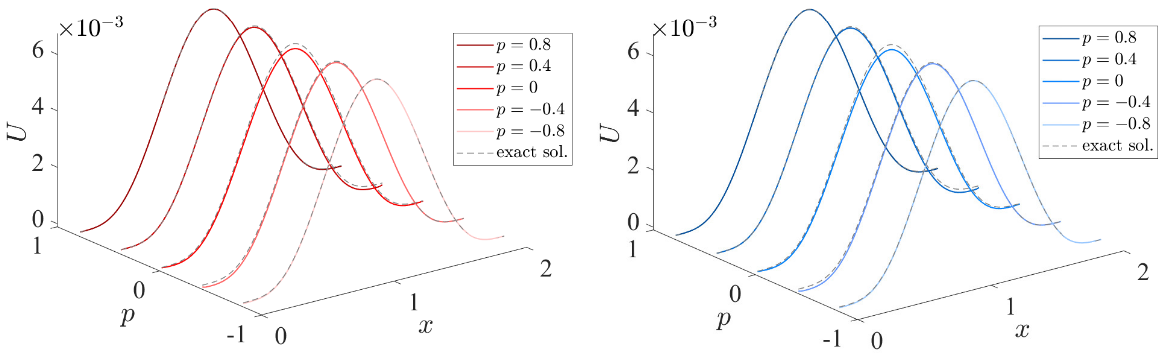

Fig. 5.5 Numerical solution with the upwind second order method for $p = -0.8, -0.4, 0, 0.4, 0.8$. Left: $\alpha = 0.8$. Right: $\alpha = 0.2$.

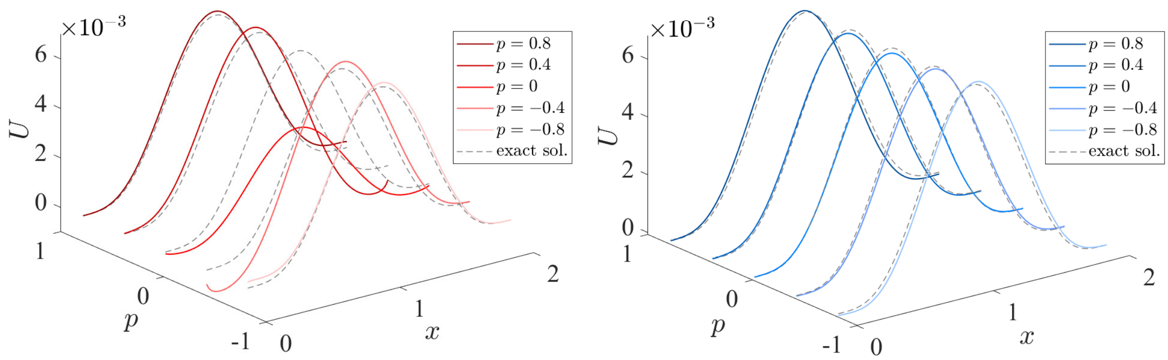

Fig. 5.6 Numerical solution with the upwind first order method for $p = -0.8, -0.4, 0, 0.4, 0.8$. Left: $\alpha = 0.8$. Right: $\alpha = 0.2$.

Note that, by observing the three Figures 5.4, 5.5 and 5.6, all the methods seems to perform better for $\alpha = 0.2$, when considering $\Delta t = 0.1$. None the less, as we have seen in the last section, as we refine the mesh the three methods approximate accurately the solution as expected by the theoretical analysis for all values of α.

5.3 Superdiffusion when $1 < \alpha < 2$

In this section, we present the numerical method derived in [76] for the real line and then we suggest an approach to the case with a reflecting boundary at $x = 0$. Hence, the only purpose of including this section is to turn the next one more clear, this is, to better expose the difference between not having a boundary and having a reflecting boundary. Therefore, for all the results presented in this section, the proofs are omitted.

As described at the beginning of the chapter, in Section 5.1 we saw that Lévy flights can be represented by the fractional equation

$$\frac{\partial u(x,t)}{\partial t} = d(x)\nabla_\alpha^p u(x,t) + g(x,t), \quad x \in \mathbb{R},\ t > 0, \tag{5.45}$$

where

$$\nabla_\alpha^p u(x,t) = \frac{1+p}{2}\frac{\partial^\alpha u}{\partial x^\alpha}(x,t) + \frac{1-p}{2}\frac{\partial^\alpha u}{\partial(-x)^\alpha}(x,t),$$

for $1 < \alpha < 2$, $-1 \leqslant p \leqslant 1$, $x \in \mathbb{R}$, where $d(x) > 0$ is the diffusion coefficient and $g(x,t)$ is the source term. Furthermore, we start by considering an initial condition and

$$\lim_{|x|\to\infty} u(x,t) = 0.$$

The Riemann-Liouville derivatives are given by (1.7) and (1.8) for $1 < \alpha < 2$, this is, for $x \in [a,b]$, the left and right Riemann-Liouville derivatives are defined by

$$\frac{\partial^\alpha u}{\partial x^\alpha}(x,t) = \frac{1}{\Gamma(2-\alpha)}\frac{d^2}{dx^2}\int_a^x u(\xi,t)(x-\xi)^{1-\alpha}d\xi \tag{5.46}$$

and

$$\frac{\partial^\alpha u}{\partial(-x)^\alpha}(x,t) = \frac{1}{\Gamma(2-\alpha)}\frac{d^2}{dx^2}\int_x^b u(\xi,t)(x-\xi)^{1-\alpha}d\xi. \tag{5.47}$$

In order to approximate these derivatives, we use the integral approximation derived in Section 3.2 and the central second order finite differences to approximate the second order derivative.

5.3.1 Numerical method

In this section we develop the approximations to the fractional derivatives.

Consider the uniform domain discretization $x_j = x_{j-1} + \Delta x,\ j \in \mathbb{Z}$. As we saw in Section 3.2, to approximate

$$\mathscr{I}^l(x,t) = \frac{1}{\Gamma(2-\alpha)}\int_a^x u(\xi,t)(x-\xi)^{1-\alpha}d\xi \quad \text{and} \quad \mathscr{I}^r(x,t) = \frac{1}{\Gamma(2-\alpha)}\int_x^b u(\xi,t)(x-\xi)^{1-\alpha}d\xi \tag{5.48}$$

using the linear spline approximation, we obtain the following formulas

$$I^l u(x_j,t) = \frac{\Delta x^{2-\alpha}}{\Gamma(4-\alpha)}\sum_{k=0}^{\infty} a_k u(x_{j-k},t), \quad I^r u(x_j,t) = \frac{\Delta x^{2-\alpha}}{\Gamma(4-\alpha)}\sum_{k=0}^{\infty} a_k u(x_{j+k},t), \tag{5.49}$$

respectively, where the coefficients of both quadratures are given by (3.19).

Considering the second order centered finite differences

$$\delta^2 f(x_j) = f(x_{j+1}) - 2f(x_j) + f(x_{j-1}),$$

we obtain, for the left Riemann-Liouville derivative

$$\frac{\partial^\alpha u}{\partial x^\alpha}(x,t) = \frac{d^2}{dx^2}\mathscr{I}^l(x,t)$$

the following

$$\begin{aligned}\frac{\partial^\alpha u}{\partial x^\alpha}(x,t) &\approx \frac{I^l(x_{j+1},t)-2I^l(x_j,t)+I^l(x_{j-1},t)}{\Delta x^2}\\ &= \frac{1}{\Delta x^\alpha \Gamma(4-\alpha)}\left[\sum_{k=0}^{\infty} a_k u(x_{j-1-k},t) - 2\sum_{k=0}^{\infty} a_k u(x_{j-k},t) + \sum_{k=0}^{\infty} a_k u(x_{j+1-k},t)\right].\end{aligned}$$

Considering $k' = k+1$ in the first sum and $k' = k-1$ in the last sum, we have

$$\frac{\partial^\alpha u}{\partial x^\alpha}(x,t) \approx \frac{1}{\Delta x^\alpha \Gamma(4-\alpha)}\left[\sum_{k'=1}^{\infty} a_{k'-1} u(x_{j-k'},t) - 2\sum_{k=0}^{\infty} a_k u(x_{j-k},t) + \sum_{k'=-1}^{\infty} a_{k'+1} u(x_{j-k'},t)\right]$$

that is equivalent to

$$\frac{\partial^\alpha u}{\partial x^\alpha}(x,t) \approx \frac{1}{\Delta x^\alpha \Gamma(4-\alpha)}\sum_{k=-1}^{\infty} q_k u(x_{j-k},t),$$

with

$$q_{-1} = a_0, \quad q_0 = -2a_0 + a_1, \quad q_k = a_{k-1} - 2a_k + a_{k+1}, \text{ for } k \geqslant 1. \tag{5.50}$$

For the right Riemann-Liouville derivative, we obtain similarly

$$\frac{\partial^\alpha u}{\partial(-x)^\alpha}(x,t) \approx \frac{1}{\Delta x^\alpha \Gamma(4-\alpha)}\sum_{k=-1}^{\infty} q_k u(x_{j+k},t),$$

with q_k defined in (5.50).

We construct a numerical method based on these approximations, but before we need to do the time discretization. In [46], they use the $\theta-$method but here we take into account only the Crank-Nicolson method. Consider a uniform mesh $0 \leqslant t_m \leqslant t_M$ with time step Δt, $d_j = d(x_j)$, $g_j^m = g(x_j,t_m)$ and the operators $\delta_l^\alpha U^m/\Delta x^\alpha$ and $\delta_r^\alpha U^m/\Delta x^\alpha$ given by

$$\frac{\delta_\alpha^l U_j^m}{\Delta x^\alpha} = \frac{1}{\Delta x^\alpha \Gamma(4-\alpha)}\sum_{k=-1}^{\infty} q_k U_{j-k}^m \tag{5.51}$$

and

$$\frac{\delta_\alpha^r U_j^m}{\Delta x^\alpha} = \frac{1}{\Delta x^\alpha \Gamma(4-\alpha)}\sum_{k=-1}^{\infty} q_k U_{j+k}^m, \tag{5.52}$$

with q_k defined in (5.50).

We arrive to the numerical method

$$\left(1 - \frac{1}{2}\mu_\alpha \delta_\alpha^p\right) U_j^{m+1} = \left(1 + \frac{1}{2}\mu_\alpha \delta_\alpha^p\right) U_j^m + g^{m+1/2}, \tag{5.53}$$

where $g_j^{m+1/2} = (g_j^{m+1} + g_j^m)/2$, $\mu^\alpha = \Delta t/\Delta x^\alpha$ and

$$\delta_\alpha^p U_j^m = \frac{1+p}{2}\delta_\alpha^l U_j^m + \frac{1-p}{2}\delta_\alpha^r U_j^m. \tag{5.54}$$

If we assume U_j^m, $j = -N, ..., N$ such that $U_k = 0$ for $k < -N$ and $k > N$, we can rewrite the scheme in the matricial form

$$\left(\mathbf{I} + \frac{1}{2}\mu_\alpha \mathbf{Q}_\alpha^p\right)\mathbf{U^{m+1}} = \left(\mathbf{I} - \frac{1}{2}\mu_\alpha \mathbf{Q}_\alpha^p\right)\mathbf{U^m} + \mathbf{G^{m+1/2}},$$

where $\mathbf{U^m} = [U_{-N}^m, ..., U_N^m]^T$ is the solution vector, $\mathbf{I}$ is the identity matrix and $\mathbf{G}^m$ contains the values of the source term. The matrix $\mathbf{Q}_\alpha^p$ is given by

$$\mathbf{Q}_\alpha^p = \frac{1+p}{2}\mathbf{Q}_\alpha + \frac{1-p}{2}\mathbf{Q}_\alpha^T, \tag{5.55}$$

with $\mathbf{Q}_\alpha$ defined as

$$\mathbf{Q}_\alpha = \frac{1}{\Gamma(4-\alpha)}\begin{bmatrix} q_0 & q_{-1} & 0 & \dots & 0 & 0 \\ q_1 & q_0 & q_{-1} & \dots & 0 & 0 \\ q_2 & q_1 & q_0 & \dots & 0 & 0 \\ \vdots & \vdots & \vdots & & \vdots & \vdots \\ q_{2N} & q_{2N-1} & q_{2N-2} & \dots & q_1 & q_0 \end{bmatrix}. \tag{5.56}$$

In the next section we state the results regarding the accuracy and the stability of the numerical method.

5.3.2 Convergence analysis

In this section, we do not provide the proofs because they are very similar with the ones done in Section 5.2.3 and can also be seen in [76]. Once again, for the sake of clarity, we omit the variable t.

Theorem 5.11 ([76])**.** *Let $u \in C^4(\mathbb{R})$ and such that $u^{(4)}(x) = 0$, for $x \leqslant a$, being a a real constant. We have that*

$$\frac{\partial^\alpha u}{\partial x^\alpha}(x_j) - \frac{\delta^\alpha u}{\Delta x^\alpha}(x_j) = \varepsilon(x_j),$$

where $|\varepsilon(x_j)| \leqslant C\Delta x^2$ and C is a constant independent of Δx.

Using this result, we are able to prove the following consistency result.

Theorem 5.12 ([76])**.** *The truncation error of the weighted numerical method* (5.53) *is of order $O(\Delta x^2)+O(\Delta t^2)$.*

We proceed with the study of the stability of the method using the von Neumann approach. We start by presenting some results on the coefficients (5.50).

Lemma 5.13. *Consider the coefficients q_k defined by* (5.50)*. Then*

(a) $q_{-1} = 1,\ q_0 \leqslant 0,\ q_k \geqslant 0$ *for* $k \geqslant 2,\ \lim_{k\to\infty} q_k = 0$ *and* $q_{k+1} \leqslant q_k \leqslant q_2$,

(b) $\sum_{k=2}^{\infty} q_k = -3 + 3 \times 2^{3-\alpha} - 3^{3-\alpha}$,

(c) $\sum_{k=-1}^{\infty} q_k = 0$,

(d) $\sum_{k=-1}^{\infty} q_k \cos(k\phi) \leqslant 0$.

Using this lemma, it can be proved that the numerical method is unconditionally von Neumann stable. It can also be concluded that the numerical method (5.53) is second order convergent both in time and space [76].

5.4 Superdiffusion with a reflecting boundary

The problem of including boundary conditions in nonlocal problems is very interesting and challenging. It also ables us to simulate different phenomena. The two types of conditions that appear more frequently related to Lévy flights are the absorbing and the reflecting boundary conditions. For the absorbing boundary conditions it is considered that, at the bounds of an interval, the probability of a particle to be there or anywhere out of the interval is zero. In other words, if we consider a mass from which a particle jumps to outside the domain (or to the boundaries), then the mass of the system decreases, once the particle is absorbed. This can be represented by homogeneous Dirichlet boundary conditions [2]. For the reflecting condition, in a porous medium, such boundary may represent a wall permeable to the fluid but impermeable to the tracer: the particle hits the wall and is bounced back, which means that if it would reach the position $x = -a$ with $a > 0$, then it will end at $x = a$ [40]. The imposition of boundary conditions changes the fractional differential equation as we are going to see during this section.

We start by formulating the superdiffusive problem with a left reflecting wall. The chosen reflecting boundary is according to [40], where a symmetric diffusion on a semi-infinite domain is considered, this is, the particles are restricted to a semi-infinite domain limited by a reflecting wall. Mathematically, we have a problem defined by equation (5.45)

$$\frac{\partial u(x,t)}{\partial t} = D\nabla^p_\alpha u(x,t) + g(x,t),$$

where

$$\nabla^p_\alpha u(x,t) = \frac{1+p}{2}\frac{\partial^\alpha u}{\partial x^\alpha}(x,t) + \frac{1-p}{2}\frac{\partial^\alpha u}{\partial(-x)^\alpha}(x,t),$$

for $-1 \leqslant p \leqslant 1$, $x \in \mathbb{R}$, where $D > 0$ is the diffusion coefficient and $g(x,t)$ is the source term. This equation is subjected to the wall condition, suggested in [40], $u(x,t) = u(-x,t)$, for $x < 0$ and illustrated in Figure 5.7.

The left Riemann-Liouville fractional derivative for $x > 0$

$$\frac{\partial^\alpha u}{\partial x^\alpha}(x,t) = \frac{1}{\Gamma(2-\alpha)}\frac{\partial^2}{\partial x^2}\int_{-\infty}^{0} u(\xi,t)(x-\xi)^{1-\alpha}d\xi + \frac{1}{\Gamma(2-\alpha)}\frac{\partial^2}{\partial x^2}\int_{0}^{x} u(\xi,t)(x-\xi)^{1-\alpha}d\xi$$

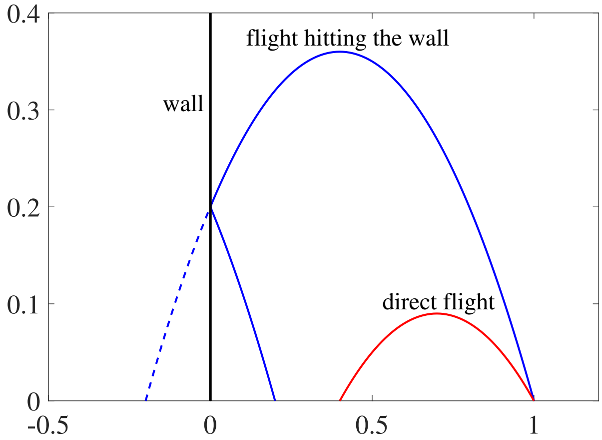

Fig. 5.7 Illustration of the reflecting boundary condition at $x = 0$.

is affected by this condition $u(x,t) = u(-x,t)$ for $x < 0$ as follows

$$\frac{\partial^\alpha u}{\partial x^\alpha}(x,t) = \frac{1}{\Gamma(2-\alpha)}\frac{\partial^2}{\partial x^2}\int_{-\infty}^{0} u(-\xi,t)(x-\xi)^{1-\alpha}d\xi + \frac{1}{\Gamma(2-\alpha)}\frac{\partial^2}{\partial x^2}\int_{0}^{x} u(\xi,t)(x-\xi)^{1-\alpha}d\xi.$$

By doing a change of variables, we obtain what we define as the reflecting left Riemann-Liouville fractional derivative, for $x > 0$,

$$\frac{\partial^\alpha_{ref} u}{\partial x^\alpha}(x,t) := \frac{1}{\Gamma(2-\alpha)}\frac{\partial^2}{\partial x^2}\int_{0}^{\infty} u(\xi,t)(x+\xi)^{1-\alpha}d\xi + \frac{1}{\Gamma(2-\alpha)}\frac{\partial^2}{\partial x^2}\int_{0}^{x} u(\xi,t)(x-\xi)^{1-\alpha}d\xi. \tag{5.57}$$

The right Riemann-Liouville derivative is not affected by the reflecting wall and remains defined by (5.47).

Formally, when subjected to a reflecting wall, we are considering the following problem

$$\frac{\partial u}{\partial t}(x,t) = D\left(\frac{1+p}{2}\frac{\partial^\alpha_{ref} u}{\partial x^\alpha}(x,t) + \frac{1-p}{2}\frac{\partial^\alpha u}{\partial(-x)^\alpha}(x,t)\right) + g(x,t), \quad x > 0, \tag{5.58}$$

$$u(x,t) = u(-x,t), \quad \text{for all} \quad x < 0, \tag{5.59}$$

with an initial condition $u(x,0) = u_0(x)$, $x \geqslant 0$.

In the next section, we derive a similar numerical method to the one described in Section 5.3.1.

5.4.1 Numerical method

When we have a reflecting boundary condition at $x = 0$, since the left fractional derivative is modified to (5.57), the modified left fractional integral is defined by

$$\mathscr{I}^l_{ref} u(x_j,t) = \frac{1}{\Gamma(2-\alpha)}\int_{0}^{\infty} u(\xi,t)(x+\xi)^{1-\alpha}d\xi + \frac{1}{\Gamma(2-\alpha)}\int_{0}^{x} u(\xi,t)(x-\xi)^{1-\alpha}d\xi. \tag{5.60}$$

Following a similar approach as in the open domain, where u inside the integral is approximated by a linear spline, we obtain the following approximation for the left fractional integral (5.60),

$$I^l_{ref}u(x_j,t) = \frac{\Delta x^{2-\alpha}}{\Gamma(4-\alpha)}\sum_{k=j+1}^{\infty} a_k u(x_{k-j},t) + \frac{\Delta x^{2-\alpha}}{\Gamma(4-\alpha)}\sum_{k=0}^{j} a_k u(x_{j-k},t). \tag{5.61}$$

Once again, we use the central second order finite difference to discretize the second order derivative involved in the modified left Riemann-Liouville derivative $\partial^2 \mathscr{I}^l_{ref}u(x,t)/\partial x^2$ and in the right Riemann-Liouville derivative $\partial^2 \mathscr{I}^r u(x,t)/\partial x^2$. For the modified left Riemann-Liouville derivative, it follows

$$\frac{\partial^2}{\partial x^2}\mathscr{I}^l_{ref}u(x_j,t) \approx \frac{1}{\Delta x^\alpha \Gamma(4-\alpha)}\sum_{k=-1}^{j} q_k u(x_{j-k},t) + \frac{1}{\Delta x^\alpha \Gamma(4-\alpha)}\sum_{k=j+1}^{\infty} q_k u(x_{k-j},t),$$

with q_k defined in (5.50). For the right Riemann-Liouville derivative, we use the approximation given by (5.52).

We assume a uniform mesh in time and space with $t_{m+1} = t_m + \Delta t$, $m = 0,\dots,M-1$, $x_j = x_{j-1} + \Delta x$, $j \in \mathbb{N}$. Let U_j^m be the approximated solution of $u(x_j,t_m)$ and define $\mu_\alpha = D\Delta t/\Delta x^\alpha$. Consider the Crank-Nicolson scheme to approximate equation (5.45) given by

$$\left(1 - \frac{1}{2}\mu_\alpha \delta^p_{\alpha,ref}\right) U_j^{m+1} = \left(1 + \frac{1}{2}\mu_\alpha \delta^p_{\alpha,ref}\right) U_j^m + g_j^{m+1/2} \tag{5.62}$$

where $g_j^{m+1/2} = (g_j^{m+1} + g_j^m)/2$ and

$$\delta^p_{\alpha,ref}U_j^m = \frac{1+p}{2}\delta^l_{\alpha,ref}U_j^m + \frac{1-p}{2}\delta^r_\alpha U_j^m \tag{5.63}$$

and

$$\frac{\delta^l_{\alpha,ref}U_j^m}{\Delta x^\alpha} = \frac{1}{\Delta x^\alpha \Gamma(4-\alpha)}\sum_{k=-1}^{j} q_k U^m_{j-k} + \frac{1}{\Delta x^\alpha \Gamma(4-\alpha)}\sum_{k=j+1}^{\infty} q_k U^m_{k-j}. \tag{5.64}$$

Consider the nodal points U_j^m, $j = 0,\dots,N$ such that $U_k^m \approx 0$ for $k > N$. The numerical method can be written matricially as

$$\left(\mathbf{I} + \frac{1}{2}\mu_\alpha \mathbf{Q}^p_{\alpha,ref}\right)\mathbf{U^{m+1}} = \left(\mathbf{I} - \frac{1}{2}\mu_\alpha \mathbf{Q}^p_{\alpha,ref}\right)\mathbf{U^m} + \mathbf{G^{m+1/2}},$$

where $\mathbf{U^m} = [U_0^m,\dots,U_N^m]^T$ is the solution vector, $\mathbf{I}$ is the identity matrix and $\mathbf{G}^m$ contains the values of the source term. The matrix $\mathbf{Q}^p_{\alpha,ref}$ is given by

$$\mathbf{Q}^p_{\alpha,ref} = \frac{1+p}{2}\mathbf{Q}^l_{\alpha,ref} + \frac{1-p}{2}\mathbf{Q}^r_{\alpha,ref}, \tag{5.65}$$

with $\mathbf{Q}^l_{\alpha,ref}$ defined by

$$\mathbf{Q}^l_{\alpha,ref} = \frac{1}{\Gamma(4-\alpha)} \begin{bmatrix} q_0 & q_{-1}+q_1 & q_2 & \cdots & q_{N-1} & q_N \\ q_1 & q_0+q_2 & q_{-1}+q_3 & \cdots & q_N & q_{N+1} \\ q_2 & q_1+q_3 & q_0+q_4 & \cdots & q_{N+1} & q_{N+2} \\ \vdots & \vdots & \vdots & & \vdots & \vdots \\ q_N & q_{N-1}+q_{N+1} & q_{N-2}+q_{N+2} & \cdots & q_1+q_{2N-1} & q_0+q_{2N} \end{bmatrix}. \tag{5.66}$$

Note that as we are considering the positive semi-infinite domain $(0,\infty)$, for the right derivative at U_0^m we have, from (5.52),

$$\delta^r_\alpha U_0^m = \frac{1}{\Gamma(4-\alpha)} \sum_{k=-1}^{\infty} q_k U_k^m = \frac{1}{\Gamma(4-\alpha)} \left(q_{-1}U_{-1}^m + \sum_{k=0}^{\infty} q_k U_k^m \right)$$

and using the fact that $U_{-1}^m = U_1^m$ we obtain

$$\delta^r_\alpha U_0^m = \frac{1}{\Gamma(4-\alpha)} \left(q_0 U_0^m + (q_{-1}+q_1)U_1^m + \sum_{k=2}^{\infty} q_k U_k^m \right).$$

Hence

$$\mathbf{Q}^r_{\alpha,ref} = \frac{1}{\Gamma(4-\alpha)} \begin{bmatrix} q_0 & q_{-1}+q_1 & q_2 & \cdots & q_{N-1} & q_N \\ q_{-1} & q_0 & q_1 & \cdots & q_{N-2} & q_{N-1} \\ 0 & q_{-1} & q_0 & \cdots & q_{N-1} & q_{N-2} \\ \vdots & \vdots & \vdots & & \vdots & \vdots \\ 0 & 0 & 0 & \cdots & q_{-1} & q_0 \end{bmatrix}. \tag{5.67}$$

We continue with the study of the convergence of the method.

5.4.2 Convergence analysis

The dependency on t is omitted in the following results in the sake of clarity and simplicity. The results on the open domain are present in Section 5.3.2. The approach to the convergence analysis is similar to the ones taken previously.

The next result determines the truncation error for the approximation (5.64) of the modified left Riemann-Liouville derivative.

Theorem 5.14. *Let $u \in C^4(\mathbb{R})$ and such that verifies (5.59). Additionally, let the spatial derivatives vanish at infinity in an appropriate manner. Then*

$$\frac{\partial^\alpha_{ref} u}{\partial x^\alpha}(x_j) - \frac{\delta^l_{\alpha,ref} u}{\Delta x^\alpha}(x_j) = \varepsilon_{ref,l}(x_j), \quad |\varepsilon_{ref,l}(x_j)| \leqslant C_{ref,l}\Delta x^2,$$

where $C_{ref,l}$ does not depend on Δx.

Proof. We start by focusing our attention on the difference $\mathscr{I}_{ref}^{l}u(x_j)-I_{ref}^{l}u(x_j)$. For exact value of the integral, $\mathscr{I}_{ref}^{l}u(x_j)$, by doing a change of variable we have

$$\begin{aligned}\mathscr{I}_{ref}^{l}u(x_j) &= \int_0^{x_j}u(\xi)(x_j-\xi)^{1-\alpha}d\xi+\int_0^{\infty}u(\xi)(x_j+\xi)^{1-\alpha}d\xi\\ &= \int_0^{x_j}u(\xi)(x_j-\xi)^{1-\alpha}d\xi-\int_0^{-\infty}u(-\xi)(x_j-\xi)^{1-\alpha}d\xi\end{aligned}$$

and, taking in consideration the reflecting condition (5.59),

$$\begin{aligned}\mathscr{I}_{ref}^{l}u(x_j) &= \int_0^{x_j}u(\xi)(x_j-\xi)^{1-\alpha}d\xi+\int_{-\infty}^{0}u(\xi)(x_j-\xi)^{1-\alpha}d\xi\\ &= \frac{1}{\Gamma(4-\alpha)}\sum_{k=-\infty}^{j}\int_{x_{k-1}}^{x_k}u(\xi)(x_j-\xi)^{1-\alpha}d\xi.\end{aligned}$$

For the approximation of the integral, we have

$$I_{ref}^{l}u(x_j)=\frac{\Delta x^{2-\alpha}}{\Gamma(4-\alpha)}\sum_{k=0}^{j}a_k u(x_{j-k})+\frac{\Delta x^{2-\alpha}}{\Gamma(4-\alpha)}\sum_{k=j+1}^{\infty}a_k u(x_{k-j})$$

and, taking into account (5.59),

$$\begin{aligned}I_{ref}^{l}u(x_j) &= \frac{\Delta x^{2-\alpha}}{\Gamma(4-\alpha)}\sum_{k=0}^{j}a_k u(x_{j-k})+\frac{\Delta x^{2-\alpha}}{\Gamma(4-\alpha)}\sum_{k=j+1}^{\infty}a_k u(x_{j-k})\\ &= \frac{\Delta x^{2-\alpha}}{\Gamma(4-\alpha)}\sum_{k=0}^{\infty}a_k u(x_{j-k}).\end{aligned}$$

Therefore, we have that

$$\mathscr{I}_{ref}^{l}u(x_j)-I_{ref}^{l}u(x_j) = \frac{1}{\Gamma(4-\alpha)}\sum_{k=-\infty}^{j}\int_{x_{k-1}}^{x_k}(u(\xi)-s_k(\xi))(x_j-\xi)^{1-\alpha}d\xi,$$

where

$$s_k(\xi)=\frac{x_k-\xi}{\Delta x}u(x_{k-1})+\frac{\xi-x_{k-1}}{\Delta x}u(x_k).$$

From this point on, the proof follows the same steps as the proof of Theorem 5.11 that can be seen in [76]. □

In the next theorem, we study the stability of the numerical method, based on the von Neumann analysis, resorting to Lemma 5.13.

Theorem 5.15. *The numerical method* (5.62) *is unconditionally stable.*

Proof. The difference operator defined in (5.63)

$$\delta^p_{\alpha,ref}U^m_j = \frac{1+p}{2}\left[\frac{1}{\Gamma(4-\alpha)}\sum_{k=-1}^{j} q_k U^m_{j-k} + \frac{1}{\Gamma(4-\alpha)}\sum_{k=j+1}^{\infty} q_k U^m_{k-j}\right] + \frac{1-p}{2}\frac{1}{\Gamma(4-\alpha)}\sum_{k=-1}^{\infty} q_k U^m_{j+k}$$

can be rewritten as

$$\delta^p_{\alpha,ref}U^m_j = \frac{1+p}{2}\left[\frac{1}{\Gamma(4-\alpha)}\sum_{k=-1}^{j} q_k U^m_{j-k} + \frac{1}{\Gamma(4-\alpha)}\sum_{k=j+1}^{\infty} q_k U^m_{j-k}\right] + \frac{1-p}{2}\frac{1}{\Gamma(4-\alpha)}\sum_{k=-1}^{\infty} q_k U^m_{j+k},$$

since $U^m_{k-j} = U^m_{j-k}$ for $k > j$.

As seen previously, we can do the von Neumann analysis by inserting a single mode $\kappa^m \mathrm{e}^{ij\phi}$ into the numerical scheme (5.62), neglecting the source term. Taking in consideration the previous equality for the reflecting operator, then

$$\begin{aligned}&\kappa^{m+1}\mathrm{e}^{ij\phi} - \frac{1}{2}\mu_\alpha \kappa^{m+1}\left[\frac{1+p}{2}\frac{1}{\Gamma(4-\alpha)}\sum_{k=-1}^{\infty} q_k \mathrm{e}^{i(j-k)\phi} + \frac{1-p}{2}\frac{1}{\Gamma(4-\alpha)}\sum_{k=-1}^{\infty} q_k \mathrm{e}^{i(j+k)\phi}\right]\\ &= \kappa^{m}\mathrm{e}^{ij\phi} + \frac{1}{2}\mu_\alpha \kappa^{m}\left[\frac{1+p}{2}\frac{1}{\Gamma(4-\alpha)}\sum_{k=-1}^{\infty} q_k \mathrm{e}^{i(j-k)\phi} + \frac{1-p}{2}\frac{1}{\Gamma(4-\alpha)}\sum_{k=-1}^{\infty} q_k \mathrm{e}^{i(j+k)\phi}\right].\end{aligned}$$

Dividing the whole equality by $\kappa^m \mathrm{e}^{ij\phi}$, we obtain

$$\begin{aligned}&\kappa\left(1 - \frac{1}{2}\mu_\alpha\left[\frac{1+p}{2}\frac{1}{\Gamma(4-\alpha)}\sum_{k=-1}^{\infty} q_k \mathrm{e}^{-ik\phi} + \frac{1-p}{2}\frac{1}{\Gamma(4-\alpha)}\sum_{k=-1}^{\infty} q_k \mathrm{e}^{ik\phi}\right]\right)\\ &= 1 + \frac{1}{2}\mu_\alpha\left[\frac{1+p}{2}\frac{1}{\Gamma(4-\alpha)}\sum_{k=-1}^{\infty} q_k \mathrm{e}^{-ik\phi} + \frac{1-p}{2}\frac{1}{\Gamma(4-\alpha)}\sum_{k=-1}^{\infty} q_k \mathrm{e}^{ik\phi}\right].\end{aligned}$$

If the real part of

$$\frac{1+p}{2}\sum_{k=-1}^{\infty} q_k \mathrm{e}^{-ik\phi} + \frac{1-p}{2}\sum_{k=-1}^{\infty} q_k \mathrm{e}^{ik\phi}$$

is negative or zero then $|\kappa(\phi)| \leqslant 1$ (see remark of Theorem 5.6). The real part is given by

$$\frac{1+p}{2}\sum_{k=-1}^{\infty} q_k \cos(k\phi) + \frac{1-p}{2}\sum_{k=-1}^{\infty} q_k \cos(k\phi)$$

and by Lemma 5.13 we can conclude that it is nonpositive. □

In the next section we present a numerical test that illustrates the order of accuracy of the method.

5.4.3 Numerical experiments

Let U^m_j and $u(x_j,t_m)$ be the approximate solution and the exact solution, respectively, at $x_j = j\Delta x$, $j \in \mathbb{N}_0$, and $t_m = m\Delta t$, $m = 0,\ldots,M$.

Consider the problem with a reflecting wall at $x = 0$ and with source term and initial condition defined such that the solution $u(x,t) = 4\mathrm{e}^{-t}(2+x)^2(2-x)^2$ is the exact solution of the equation

(5.58), for $0 < x < 2$. In Tables 5.10–5.12, we illustrate the order of accuracy of the method for $\alpha = 1.1, 1.4, 1.5, 1.7, 1.9$ resorting to the L^2 discrete norm and the L^∞ discrete norm given, respectively, by (5.44) and (5.43). Table 5.10 refers to the use of $p = 1$, the results displayed in Table 5.10 have to do with $p = 0$ and in Table 5.10 are the results for $p = -1$. As predicted by the theoretical result, the numerical method is second order accurate.

Table 5.10 Results concerning problem with a reflecting boundary, for $u(x,t) = 4e^{-t}(2+x)^2(2-x)^2$ and $p = 1$ for different values of α and $\Delta t = 0.0001$. Convergence rates in space R_∞ for the error (5.43) and R_2 for the error (5.44).

Δx	$\alpha = 1.1$	R_∞	$\alpha = 1.3$	R_∞	$\alpha = 1.5$	R_∞	$\alpha = 1.7$	R_∞	$\alpha = 1.9$	R_∞
2^{-7}	3.163e-03		2.638e-03		2.416e-03		2.209e-03		1.666e-03	
2^{-8}	7.908e-04	2.00	6.599e-04	2.00	6.063e-04	1.99	5.588e-04	1.98	4.2547e-04	1.97
2^{-9}	1.977e-04	2.00	1.651e-04	2.00	1.519e-04	2.00	1.410e-04	1.99	1.0847e-04	1.97
2^{-10}	4.942e-05	2.00	4.127e-05	2.00	3.804e-05	2.00	3.549e-05	1.99	2.7595e-05	1.97
2^{-11}	1.235e-05	2.00	1.031e-05	2.00	9.510e-06	2.00	8.911e-06	1.99	6.9979e-06	1.98
		R_2		R_2		R_2		R_2		R_2
2^{-7}	3.257e-03		2.961e-03		2.713e-03		2.412e-03		1.7824e-03	
2^{-8}	8.139e-04	2.00	7.399e-04	2.00	6.797e-04	2.00	6.088e-04	1.99	4.544e-04	1.97
2^{-9}	2.034e-04	2.00	1.849e-04	2.00	1.702e-04	2.00	1.534e-04	1.99	1.157e-04	1.97
2^{-10}	5.084e-05	2.00	4.622e-05	2.00	4.260e-05	2.00	3.860e-05	1.99	2.942e-05	1.98
2^{-11}	1.270e-05	2.00	1.154e-05	2.00	1.065e-05	2.00	9.690e-06	1.99	7.460e-06	1.98

Table 5.11 Results concerning problem with a reflecting boundary, for $u(x,t) = 4e^{-t}(2+x)^2(2-x)^2$ and $p = 0$ for different values of α and $\Delta t = 0.0001$. Convergence rates in space R_∞ for the error (5.43) and R_2 for the error (5.44).

Δx	$\alpha = 1.1$	R_∞	$\alpha = 1.3$	R_∞	$\alpha = 1.5$	R_∞	$\alpha = 1.7$	R_∞	$\alpha = 1.9$	R_∞
2^{-7}	1.610e-03		1.516e-03		1.184e-03		1.137e-03		1.194e-03	
2^{-8}	4.268e-04	1.92	4.036e-04	1.91	3.225e-04	1.88	2.829e-04	2.01	3.0107e-04	1.99
2^{-9}	1.121e-04	1.93	1.059e-04	1.93	8.637e-05	1.90	7.027e-05	2.01	7.5773e-05	1.99
2^{-10}	2.910e-05	1.95	2.749e-05	1.95	2.283e-05	1.92	1.742e-05	2.01	1.9035e-05	1.99
2^{-11}	7.479e-06	1.96	7.077e-06	1.96	5.976e-06	1.93	4.373e-06	1.99	4.7642e-06	2.00
		R_2		R_2		R_2		R_2		R_2
2^{-7}	7.296e-04		1.076e-03		1.059e-03		1.039e-03		1.1292e-03	
2^{-8}	1.946e-04	1.91	2.821e-04	1.93	2.754e-04	1.94	2.629e-04	1.98	2.821e-04	2.00
2^{-9}	5.072e-05	1.94	7.305e-05	1.95	7.120e-05	1.95	6.662e-05	1.98	7.053e-05	2.00
2^{-10}	1.304e-05	1.96	1.875e-05	1.96	1.831e-05	1.96	1.688e-05	1.98	1.762e-05	2.00
2^{-11}	3.322e-06	1.97	4.781e-06	1.97	4.685e-06	1.97	4.272e-06	1.98	4.393e-06	2.00

We proceed with some numerical simulations involving the three cases of superdiffusion considered previously: superdiffusion on the open domain for $0 < \alpha < 1$, superdiffusion on the open domain for $1 < \alpha < 2$ and superdiffusion considering a reflecting wall for $1 < \alpha < 2$. We complete

Table 5.12 Results concerning problem with a reflecting boundary, for $u(x,t) = 4e^{-t}(2+x)^2(2-x)^2$ and $p = -1$ for different values of α and $\Delta t = 0.0001$. Convergence rates in space R_∞ for the error (5.43) and R_2 for the error (5.44).

Δx	$\alpha = 1.1$	R_∞	$\alpha = 1.3$	R_∞	$\alpha = 1.5$	R_∞	$\alpha = 1.7$	R_∞	$\alpha = 1.9$	R_∞
2^{-7}	5.535e-03		3.550e-03		2.345e-03		1.449e-03		8.618e-04	
2^{-8}	1.355e-03	2.03	8.601e-04	2.05	5.752e-04	2.03	3.815e-04	1.93	2.1583e-04	2.00
2^{-9}	3.316e-04	2.03	2.090e-04	2.04	1.416e-04	2.02	9.950e-05	1.94	5.4033e-05	2.00
2^{-10}	8.113e-05	2.03	5.098e-05	2.04	3.496e-05	2.02	2.575e-05	1.95	1.3513e-05	2.00
2^{-11}	1.987e-05	2.03	1.248e-05	2.03	8.661e-06	2.01	6.625e-06	1.96	3.4147e-06	1.98
		R_2		R_2		R_2		R_2		R_2
2^{-7}	2.117e-03		1.659e-03		1.368e-03		1.080e-03		7.8427e-04	
2^{-8}	5.316e-04	1.99	4.211e-04	1.98	3.497e-04	1.97	2.820e-04	1.94	1.999e-04	1.97
2^{-9}	1.332e-04	2.00	1.060e-04	1.99	8.861e-05	1.98	7.285e-05	1.95	5.109e-05	1.97
2^{-10}	3.336e-05	2.00	2.662e-05	1.99	2.235e-05	1.99	1.868e-05	1.96	1.306e-05	1.97
2^{-11}	8.359e-06	2.00	6.675e-06	2.00	5.622e-06	1.99	4.765e-06	1.97	3.335e-06	1.97

the simulations presenting a final experiment focused on illustrating the main differences between superdiffusion and subdiffusion.

5.5 Numerical approximations of the fundamental solutions

Similar to what has been done in the last chapter, we illustrate the process of superdiffusion for different values of α. We also compare different values of p. We consider the approximations of the solution of equation (5.5) defined for $0 < \alpha < 1$ and the solutions of (5.45) defined for $1 < \alpha < 2$ without source term. The initial condition is an approximation of the Dirac delta function, this is,

$$u_0(x) = \delta_\varepsilon(x), \quad \text{with} \quad \delta_\varepsilon(x) = \frac{1}{\varepsilon\sqrt{\pi}} \mathrm{e}^{-(x-x_0)^2/\varepsilon^2}, \tag{5.68}$$

for a small $\varepsilon > 0$. For all figures, we have considered $D = 1$, $\varepsilon = 0.1$, $x_0 = 0$ and $p = -0.8, 0, 0.8$.

In Figures 5.8, 5.9, 5.10 and 5.11 we show the evolution of the solution along time for $\alpha = 0.2, 0.8, 1.2$ and 1.8, respectively, for different values of p. Overall, we observe the asymmetry taking place as we evolve in time, being more prominent for α near 1, both for $0 < \alpha < 1$ and $1 < \alpha < 2$. We can also see that, as α increases the solution is more diffusive. Therefore the peak values of the solutions are higher for smaller values of α, illustrating the increasing speed of the (anomalous) diffusion with the increase of α. Recall that the initial condition and the final instant are the same for all the involved experiments.

In Figures 5.12 and 5.13, we show the evolution of the numerical solution along time for the reflecting problem given by (5.58) and (5.59) with initial condition (5.68) for $\alpha = 1.2$ and 1.8, respectively, and for different values of p. The parameters considered were $D = 1$, $\varepsilon = 0.1$, $x_0 = 0.7$ and $p = -0.8, 0, 0.8$. The solutions exhibit similar behaviour as the solutions for α between 1 and 2

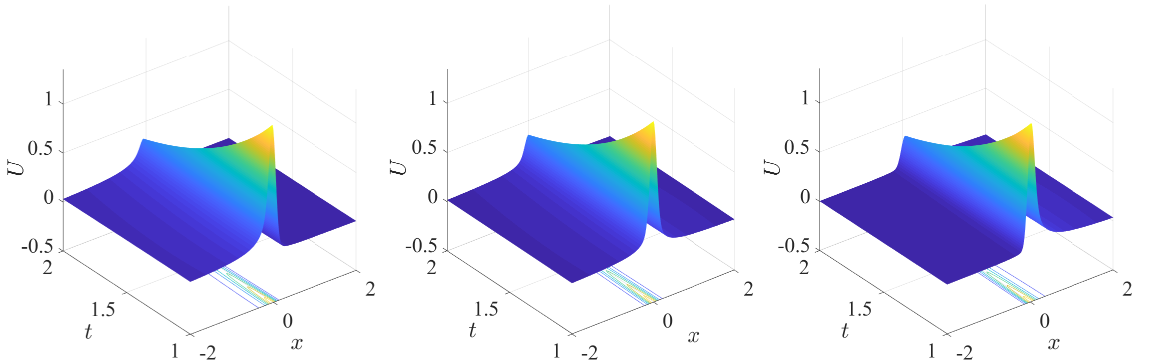

Fig. 5.8 Numerical solutions when the initial condition is (5.68) with $x_0 = 0$, $D = 1$, $\alpha = 0.2$ and as time changes from 1 to 2. Left: $p = -0.8$. Center: $p = 0$. Right: $p = 0.8$.

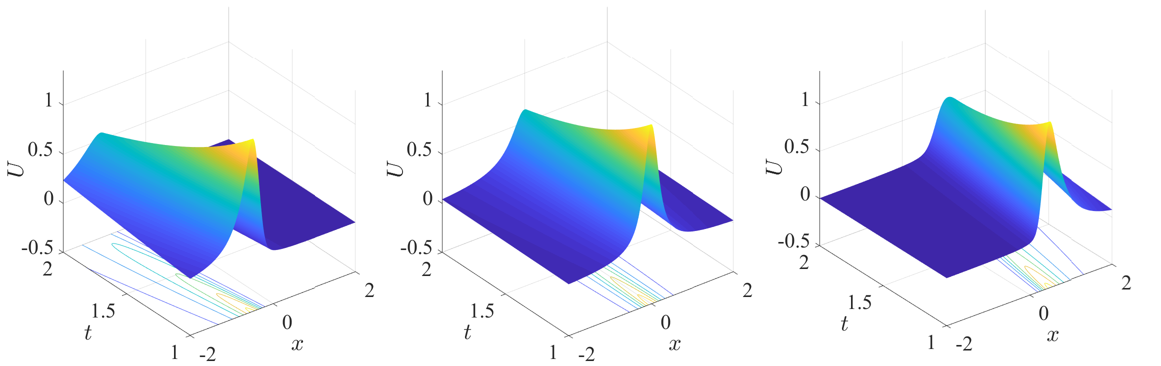

Fig. 5.9 Numerical solutions when the initial condition is (5.68) with $x_0 = 0$, $D = 1$, $\alpha = 0.8$ and as time changes from 1 to 2. Left: $p = -0.8$. Center: $p = 0$. Right: $p = 0.8$.

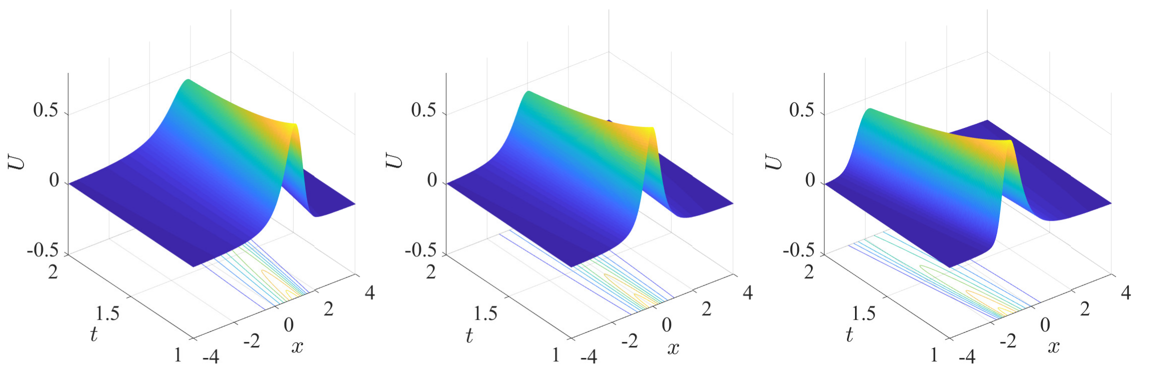

Fig. 5.10 Numerical solutions when the initial condition is (5.68) with $x_0 = 0$, $D = 1$, $\alpha = 1.2$ and as time changes from 1 to 2. Left: $p = -0.8$. Center: $p = 0$. Right: $p = 0.8$.

on the open domain regarding the influence of p and α: for $\alpha = 1.2$ the asymmetry is more noticeable and for $\alpha = 1.8$ the dispersion occurs faster.

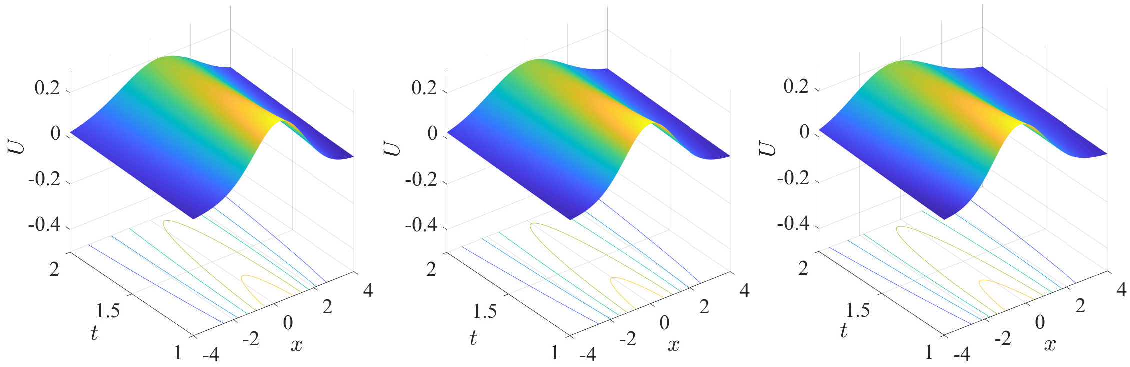

Fig. 5.11 Numerical solutions when the initial condition is (5.68) with $x_0 = 0$, $D = 1$, $\alpha = 1.8$ and as time changes from 1 to 2. Left: $p = -0.8$. Center: $p = 0$. Right: $p = 0.8$.

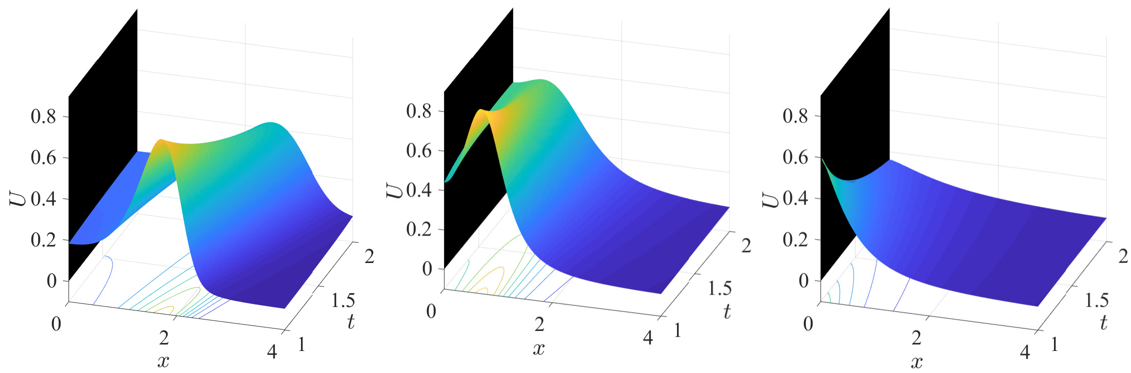

Fig. 5.12 Numerical solutions considering a reflecting wall when the initial condition is (5.68) with $x_0 = 0.7$, $D = 1$, $\alpha = 1.2$ and as time changes from 1 to 2. Left: $p = -0.8$. Center: $p = 0$. Right: $p = 0.8$.

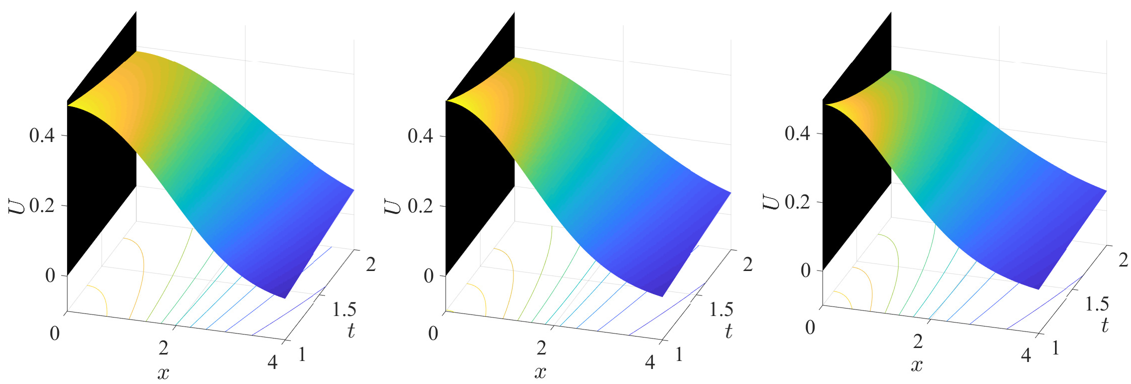

Fig. 5.13 Numerical solutions considering a reflecting wall when the initial condition is (5.68) with $x_0 = 0.7$, $D = 1$, $\alpha = 1.8$ and as time changes from 1 to 2. Left: $p = -0.8$. Center: $p = 0$. Right: $p = 0.8$.

In Figures 5.14, 5.15 and 5.16 we plot the numerical solutions for $t_M = 0.5$ for the problem with a reflecting wall at $x = 0$ (solid lines) versus the problem defined on the open domain (dashed lines) for $\alpha = 1.1, 1.5$ and 1.9, respectively, and for $p = -0.8, 0, 0.8$, in order to see the effect of having a reflecting condition. The initial condition is, once again, (5.68) with $x_0 = 0.7$ and $\varepsilon = 0.1$. We can observe that the area under the graph of the open domain solution for $(-\infty, 0)$ seems to accumulate under the graph of the reflecting wall solution, specially near the reflecting boundary. Therefore, the differences between the solutions with and without wall tend to escalate for higher values of α.

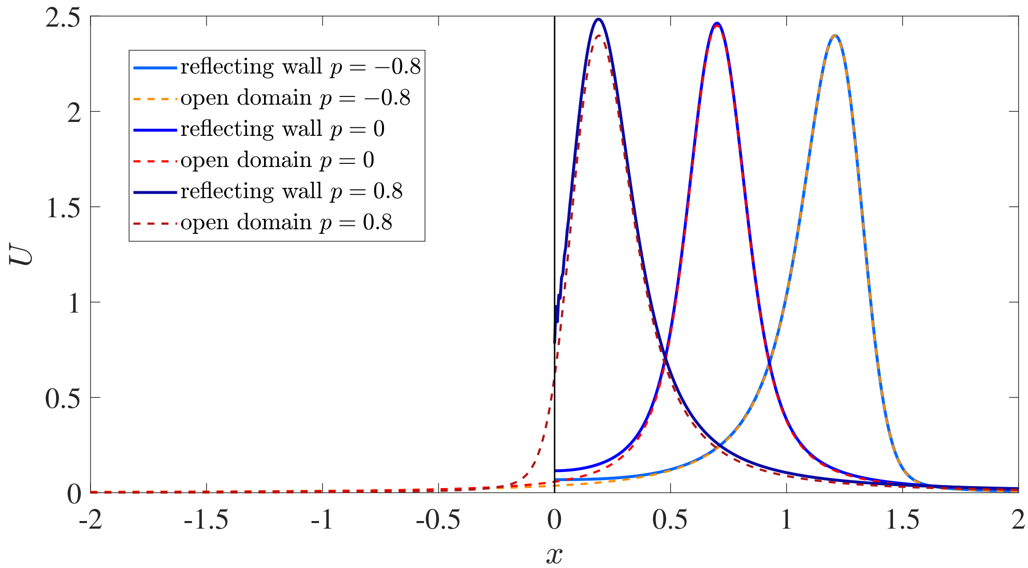

Fig. 5.14 Numerical solutions on the infinite domain (−−) versus on the semi-infinite domain with a reflecting wall at $x = 0$ (−) for $\alpha = 1.1$ and $p = -0.8, 0, 0.8$.

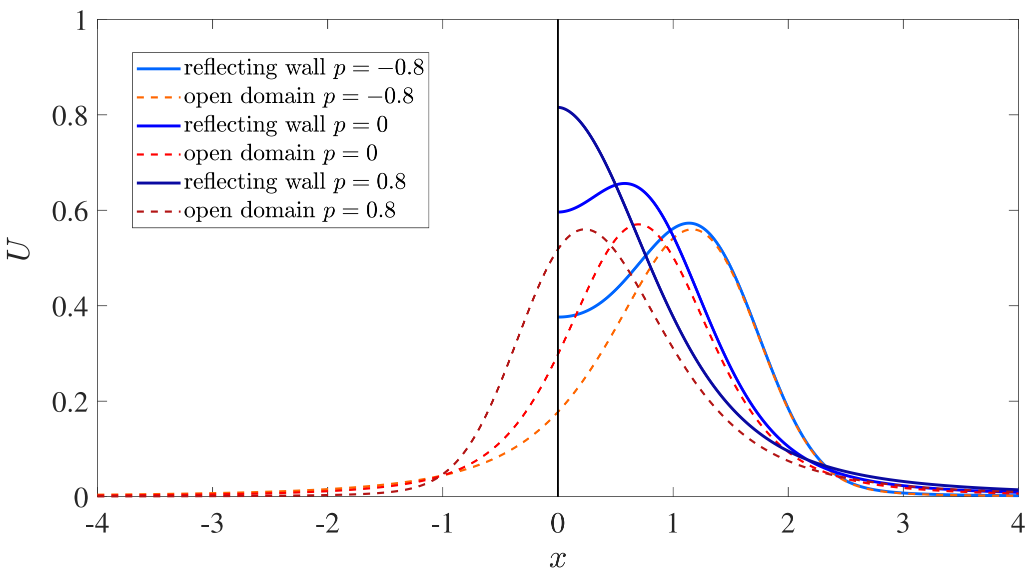

Fig. 5.15 Numerical solutions on the infinite domain (−−) versus on the semi-infinite domain with a reflecting wall at $x = 0$ (−) for $\alpha = 1.5$ and $p = -0.8, 0, 0.8$.

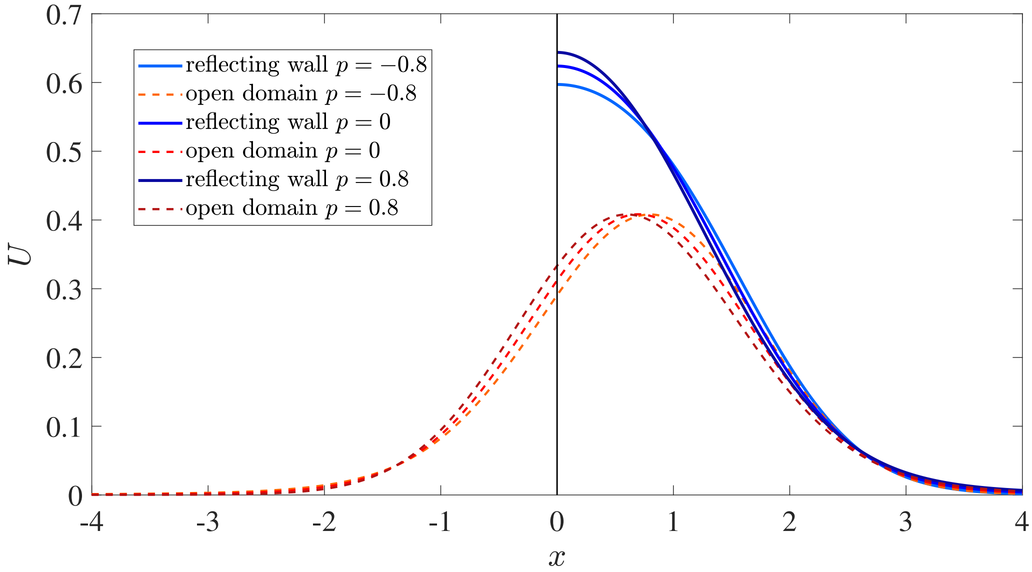

Fig. 5.16 Numerical solutions on the infinite domain (−−) versus on the semi-infinite domain with a reflecting wall at $x = 0$ (−) for $\alpha = 1.9$ and $p = -0.8, 0, 0.8$.

To finalize, we want to illustrate the differences between subdiffusion and superdiffusion, both considering $0 < \alpha < 1$. Therefore, we choose the parameters that equalize the approaches. For subdiffusion, we use the method derived in Chapter 4 for $\beta = 1$ and, for superdiffusion, we use the upwind second order method derived in Section 5.2.1 for $p = 0$ to preserve the spacial symmetry verified in the subdiffusive case. All the other parameters are the same for the two methods.

In Figure 5.17, we plot the solutions obtained for the subdiffusive model, in blue, and for the superdiffusive model, in orange. By observing the figure, we can identify the expected differences between the two models. For the Lévy flights (superdiffusion), we see that the solution peak remains higher for a longer period of time but, eventually, surpasses the subdiffusion solution. Additionally, we can spot the tails of the superdiffusive solution reaching a longer distance in a shorter period of time, illustrating the divergent second order moment of the displacement while for subdiffusion we can notice the tails tending to zero. Figure 5.18 is a cropped version of Figure 5.17 that makes more clear the previous conclusions.

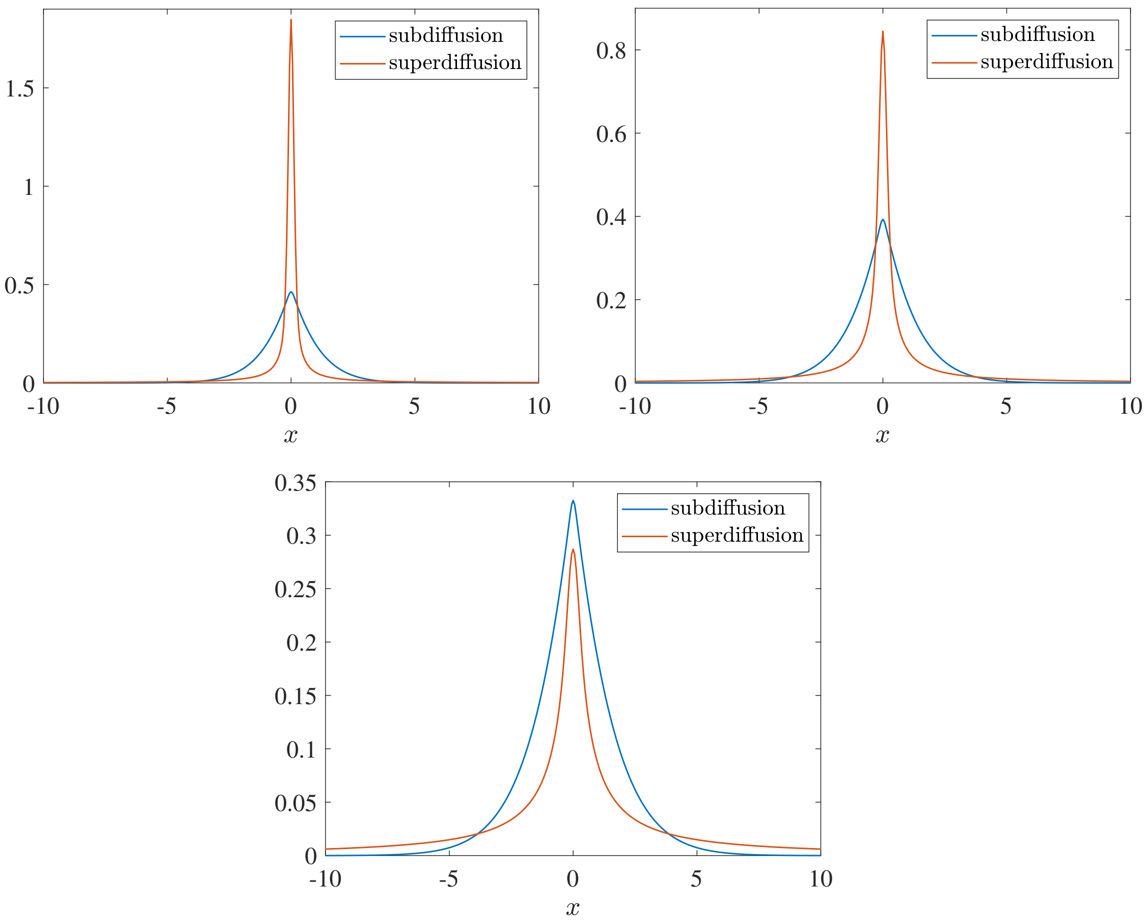

Fig. 5.17 Numerical solutions of the subdifusion and the superdiffusion problems when the initial condition is (5.68) with $x_0 = 0$ for $\alpha = 0.5$. Top left: $t = 0.5$. Top right: $t = 1$. Bottom: $t = 2$.

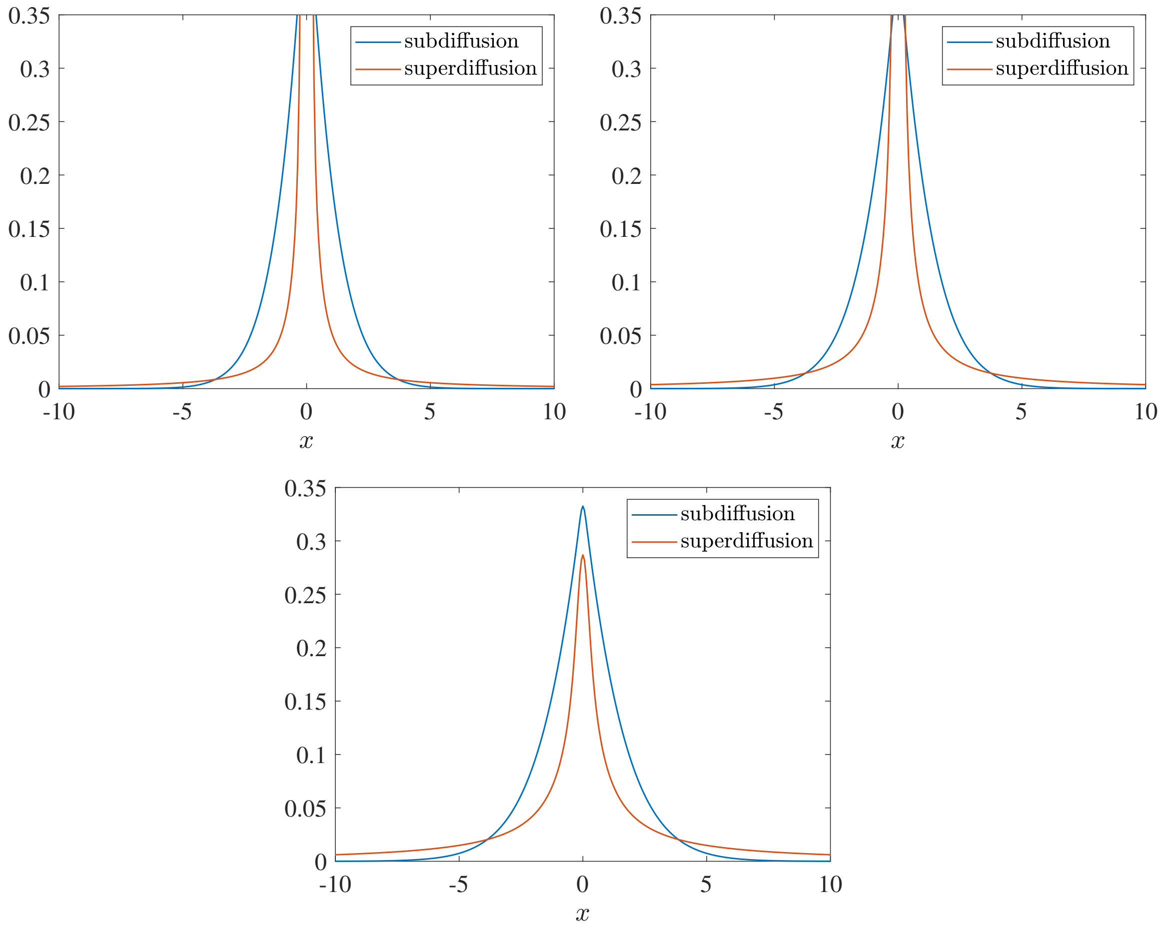

Fig. 5.18 Cropped plot of Figure 5.17 to enhance the different behaviour of the numerical solutions of the subdiffusion and the superdiffusion problems when the initial condition is (5.68) with $x_0 = 0$ for $\alpha = 0.5$. Top left: $t = 0.5$. Top right: $t = 1$. Bottom: $t = 2$.

Chapter 6

Conclusions and future work

In this thesis, we have investigated different problems in the field of anomalous diffusion, more specifically models related with subdiffusion and superdiffusion.

We have started, in Chapter 2, by presenting the definitions of B-splines and splines of fractional degree and then we have described the construction of the fractional B-splines on the real line, based on integer B-splines. Handling fractional splines is much more delicate than the classical ones, since the support of the functions is no longer compact and they are not always positive. We have focused our attention on splines with degree $0 < \beta \leqslant 2$. We have started by studying the splines of degree $0 < \beta \leqslant 1$, which are fully determined by the values on the knots of the function being interpolated. However, for the splines of degree $\beta > 1$, additional conditions are required. The most common condition is $s'(t_0) = u'(t_0)$. Nevertheless, this imposition originates an unstable scheme and therefore we have chosen the condition $s'(t_M) = u'(t_M)$, being t_M the last knot. Resorting to [85], we have seen that the fractional approximation is of order $\beta + 1$ for functions in $H^{\beta+1}(\mathbb{R})$. Furthermore, when the function has unbounded derivatives near the initial point of the time domain, that is, at $t = 0$, the order of convergence is affected. For functions such that $u = O(t^\gamma)$ as $t \to 0$, we have obtained that the order of accuracy of the approximation of a function by its spline interpolator of degree β is the minimum between $\beta + 1$ and $\gamma + 1/2$, for the L^2 norm. This result was illustrated by numerical tests. For the L^∞ norm, we have obtained a heuristic result for the order of accuracy of the approximation that is the minimum between $\beta + 1$ and γ. This result was supported by numerical experiments.

In Chapter 3, we have approximated the fractional integrals that are part of the definition of the Riemann-Liouville derivatives. These integrals are defined as the convolution of the function and a kernel. To approximate these integrals, we replace the function by a spline that is a polynomial. This allows us to compute exactly the integral for almost every point. For the points for which we cannot determine it exactly, we use the trapezoidal rule to approximate the integral. For the integral operator in time, we have used fractional splines of degree $0 < \beta \leqslant 2$. In all cases we have arrived to a recursive formula to compute the integral that involves the values of the replaced function on the knots. For $0 < \beta \leqslant 1$, the quadrature formula includes another recursive formula that expresses the entries of an inverse matrix by the values of the original lower triangular matrix, constructed using the B-splines. For $1 < \beta \leqslant 2$, such explicit recursive formula has not been obtained due to the change of structure of the matrix, that is no longer a triangular matrix. Furthermore, because the value of the derivative of u is needed but, in the scope of these problems, it is hardly available, we have included an approximation of the first order derivative considered in [39]. Using the error bounds for the spline approximation, we obtain the upper bound for the error norm when approximating the integral of order α. The upper bound tells us that the order of the approximation is the minimum between $\beta+1$ and $\gamma+\alpha+1/2$ for the L^2 norm and the minimum between $\beta+1$ and $\gamma+\alpha$ for the L^∞ norm, when $0<\beta\leqslant 1$. All the results have been corroborated by numerical tests represented by tables. For $1<\beta\leqslant 2$, the numerical experiments point out that the approximation of the first order derivative of u influence the rate of convergence of the method: for the L^2 discrete norm, we obtain as order of convergence the minimum between $\beta+1$, $\gamma+\alpha+1/2$ and $2+\alpha$; for the L^∞ discrete norm we obtain as order of convergence the minimum between $\beta+1$, $\gamma+\alpha$ and $2+\alpha$. All the results have been indicated by numerical tests displayed in tables. These conclusions have been obtained once again for functions $u=O(t^\gamma)$ as $t\to 0$. For the integral operator in space, we have only presented an approximation with the linear spline. This has been studied in [76] and it has been useful when approaching the problem of superdiffusion.

In Chapter 4, we have derived a numerical method for equation (4.1) by approximating the integral of order α, with $0<\alpha<1$, using a fractional spline of degree β, derived in Chapter 3. To discretize the second order spatial derivative, we have used the central second order difference formula. For $0<\beta\leqslant 1$, as we had the explicit values of the inverse matrix, we have been able to study the stability of the method and have concluded that the method was conditionally stable with a not very restrictive condition referred in Theorem 4.4(b). The order of convergence of the numerical method has been predicted from the error bounds derived for the fractional integral approximation. For $0\leqslant\beta\leqslant 1$, the order of convergence is the minimum between $\beta+1$ and $\gamma+\alpha+1/2$ for the L^2 discrete norm and the minimum between $\beta+1$ and $\gamma+\alpha$ for the L^∞ discrete norm. Furthermore, the results have pointed out that the fractional splines of degree $\beta=\alpha$ perform better for larger meshes. For $1<\beta\leqslant 2$, the order of convergence is the minimum between $\beta+1$, $\gamma+\alpha+1/2$ and $2+\alpha$ for the L^2 discrete norm and the minimum between $\beta+1$, $\gamma+\alpha$ and $2+\alpha$ for the L^∞ discrete norm. Once again, these results have been illustrated by numerical tests. At the end we have compared some figures with approximate solutions obtained by the numerical method with initial condition an approximation to the Dirac delta function. We have concluded that the process of subdiffusion is faster for higher values of α, this is, the peak values of the solution are lower for the same initial condition and final instant.

In Chapter 5, we have explored superdiffusion for $0<\alpha<1$ and for $1<\alpha<2$. For the case with $0<\alpha<1$, we have presented three different numerical methods to obtain numerical solutions for the problem involving the fractional differential equation (5.5). In order to approximate the derivative in time, we have used the Crank-Nicolson method. To approximate the integral operator in space, we used the linear spline, already proven to be of second order for sufficiently smooth function. To approximate the derivative of the integral, it has been considered a central approximation of second order (already studied in [75]) and two upwind approximations, one of first order and another of second order. The upwind schemes have been considered because the central method, despite being of second order, presented spurious oscillation for nonsymmetric cases for larger time steps. With the first order upwind method we extinguish the false oscillations, however it presents a lower order of accuracy. We have concluded that the upwind second order implicit method is the best choice since it is second order accurate and delivers solutions without unwanted oscillations. We have also studied the stability of the methods that have been proved to be unconditionally stable. We have presented tables with data obtained by the implementation of the numerical methods that illustrates the expected order of convergence for the three methods. For the superdiffusion with $1 < \alpha < 2$, we have presented briefly a second order numerical method based on the linear spline to approximate the solution of equation (5.7) that was derived in [76]. Then, we move forward to consider a reflecting boundary at $x = 0$. This resulted in considering equation (5.7) for $x > 0$ and $u(x,t) = u(-x,t)$ for $x > 0$, which led to a direct impact on the fractional operator. We have analyzed the stability and consistency of the new method, based on the proofs done in [76] for the open domain and have concluded that we had obtained a second order accurate and unconditionally stable method. This result was supported by numerical tests. The influence of the boundary condition has been illustrated by displaying the solution of the same model with and without boundary and we observed that the area that is under the open domain solution for $(-\infty, 0)$ accumulates under the solution of the problem with the reflecting wall defined in $(0, \infty)$, namely closer to $x = 0$. At the end, we show several numerical simulations for the three superdiffusive models with the initial condition once again being an approximation to the Dirac delta function. By observing these simulations, we have concluded that the asymmetry involved in all cases of superdiffusion considered in this thesis influences more the solutions for α near to 1. Furthermore, the spread of the solution seems to be faster for larger values of α. We conclude the chapter with a figure containing one solution of the subdiffusive model and another of the superdiffusive model, illustrating the characteristic behaviour of Lévy flights, with the tails becoming heavier as time evolves, while for the subdiffusive solutions the tails tend to zero.

Beyond the themes that we have approached in this thesis, there are still a lot of open problems related to anomalous diffusion. The open questions that are more closely correlated with our work are enumerated next. For the subdiffusion equation, it would be valuable to perform a more complete convergence analysis of the method proposed in Chapter 4 when using fractional splines of degree β with $1 < \beta \leqslant 2$. Furthermore, it may be of interest to apply the fractional splines approximation in space and therefore in problems of superdiffusion. The behaviour of the fractional splines approach the behaviour of the solution and we could expect that, to simulate superdiffusion of order α, the best tools would be splines of degree $\beta = \alpha$. Therefore, the study of fractional splines for $1 < \beta \leqslant 2$ is even more important since superdiffusion may contemplate the values of α between 1 and 2. Another question is how to include boundary conditions properly in superdiffusive models. The consideration of boundary conditions will remain one of the most important and challenging topics to be researched.

References

[1] Angstmann, C. N., Donnelly, I. C., Henry, B. I., Jacobs, B. A., Langlands, T. A. M., and Nichols, J. A. (2016). From stochastic processes to numerical methods: a new scheme for solving reaction subdiffusion fractional partial differential equations. *J. Comput. Phys.*, 307:508–534.

[2] Baeumer, B., Kovács, M., Meerschaert, M. M., and Sankaranarayanan, H. (2018). Boundary conditions for fractional diffusion. *J. Comput. Appl. Math.*, 336:408–424.

[3] Bai, Z.-Z. and Lu, K.-Y. (2020). Fast matrix splitting preconditioners for higher dimensional spatial fractional diffusion equations. *J. Comput. Phys.*, 404:109117.

[4] Behforooz, G. (1988). Quadratic spline. *Appl. Math. Lett.*, 1(2):177–180.

[5] Biebler, K.-E. and Wodny, M. (2013). *Splines and compartment models: an introduction*. World Scientific.

[6] Blu, T. and Unser, M. (1999). Quantitative Fourier analysis of approximation techniques: Part ii-wavelets. *IEEE Trans. Signal Process.*, 47:2796–2806.

[7] Böttcher, A. and Silbermann, B. (2012). *Introduction to large truncated Toeplitz matrices*. Springer Science & Business Media.

[8] Bueno-Orovio, A., Kay, D., Grau, V., Rodriguez, B., and Burrage, K. (2014). Fractional diffusion models of cardiac electrical propagation: role of structural heterogeneity in dispersion of repolarization. *J. R. Soc. Interface*, 11(97):20140352.

[9] Burch, N. and Lehoucq, R. B. (2011). Continuous-time random walks on bounded domains. *Phys. Rev. E*, 83(1):012105.

[10] Cartalade, A., Younsi, A., and Neel, M.-C. (2019). Multiple-relaxation-time lattice Boltzmann scheme for fractional advection–diffusion equation. *Comput. Phys. Commun.*, 234:40–54.

[11] Cartea, A. and del Castillo-Negrete, D. (2007). Fractional diffusion models of option prices in markets with jumps. *Phys. A: Stat. Mech. Appl.*, 374(2):749–763.

[12] Castillo, P. and Gómez, S. (2020). Conservative local discontinuous Galerkin method for the fractional Klein-Gordon-Schrödinger system with generalized Yukawa interaction. *Numer. Algorithms*, 84(1):407–425.

[13] Chen, C., Liu, F., Turner, I., and Ahn, V. (2007). A Fourier method for the fractional diffusion equation describing sub-diffusion. *J. Comput. Phys.*, 227:886–897.

[14] Cline, R., Plemmons, R., and Worm, G. (1974). Generalized inverses of certain Toeplitz matrices. *Linear Algebra Its Appl.*, 8(1):25–33.

[15] Cusimano, N., Burrage, K., Turner, I., and Kay, D. (2017). On reflecting boundary conditions for space-fractional equations on a finite interval: Proof of the matrix transfer technique. *Appl. Math. Modelling*, 42:554–565.

[16] Demaret, L., Dyn, N., and Iske, A. (2006). Image compression by linear splines over adaptive triangulations. *Signal Process.*, 86(7):1604–1616.

[17] Diethelm, K., Ford, N. J., and Freed, A. D. (2004). Detailed error analysis for a fractional Adams method. *Numer. Algorithms*, 36(1):31–52.

[18] Diethelm, K., Garrappa, R., Giusti, A., and Stynes, M. (2020). Why fractional derivatives with nonsingular kernels should not be used. *Fract. Calc. Appl. Anal.*, 23(3):610–634.

[19] Dipierro, S., Ros-Oton, X., and Valdinoci, E. (2017). Nonlocal problems with Neumann boundary conditions. *Rev. Mat. Iberoam.*, 33(2):377–416.

[20] Dybiec, B., Gudowska-Nowak, E., and Hänggi, P. (2006). Lévy-Brownian motion on finite intervals: Mean first passage time analysis. *Phys. Rev. E*, 73(4):046104.

[21] El Abd, A. E.-G. and Milczarek, J. J. (2004). Neutron radiography study of water absorption in porous building materials: anomalous diffusion analysis. *J. Phys. D: Appl. Phys.*, 37(16):2305.

[22] Ern, A. and Guermond, J.-L. (2004). *Theory and practice of finite elements*, volume 159. Springer.

[23] Gao, T., Duan, J., Li, X., and Song, R. (2014). Mean exit time and escape probability for dynamical systems driven by Lévy noises. *SIAM J. Sci. Comput.*, 36(3):A887–A906.

[24] Guo, B., Pu, X., and Huang, F. (2015). *Fractional partial differential equations and their numerical solutions*. World Scientific.

[25] Guo, S., Mei, L., Zhang, Z., Li, C., Li, M., and Wang, Y. (2020). A linearized finite difference/spectral-Galerkin scheme for three-dimensional distributed-order time–space fractional nonlinear reaction–diffusion-wave equation: Numerical simulations of gordon-type solitons. *Comput. Phys. Commun.*, 252:107144.

[26] Gustafsson, B., Kreiss, H.-O., and Oliger, J. (1995). *Time dependent problems and finite difference methods*. Wiley-Interscience.

[27] Heinsalu, E., Patriarca, M., Goychuk, I., and Hänggi, P. (2007). Use and abuse of a fractional Fokker-Planck dynamics for time-dependent driving. *Phys. Rev. Lett.*, 99:120602.

[28] Höllig, K. (2003). *Finite element methods with B-splines*. SIAM.

[29] Huang, C., Stynes, M., and An, N. (2018). Optimal $L^\infty(L^2)$ error analysis of a direct discontinuous Galerkin method for a time-fractional reaction-diffusion problem. *BIT Numer. Math.*, 58:661–690.

[30] Huang, Y.-C. and Lei, S.-L. (2020). Fast solvers for finite difference scheme of two-dimensional time-space fractional differential equations. *Numer. Algorithms*, 84(1):37–62.

[31] Jesus, C. and Sousa, E. (2020). Numerical method with fractional splines for a subdiffusion problem. *BIT Numer. Math.*, 60:1075–1111.

[32] Jesus, C. and Sousa, E. (2021a). Numerical solutions for asymmetric Lévy flights. *Numer. Algorithms*, 87:967–999.

[33] Jesus, C. and Sousa, E. (2021b). Superdiffusion in the presence of a reflecting boundary. *Appl. Math. Lett.*, 112:106742.

[34] Jin, B., Lazarov, R., and Zhou, Z. (2016). An analysis of the L1 scheme for the subdiffusion equation with nonsmooth data. *IMA J. Numer. Anal.*, 36:197–221.

[35] Kelly, J. F., Sankaranarayanan, H., and Meerschaert, M. M. (2019). Boundary conditions for two-sided fractional diffusion. *J. Comput. Phys.*, 376:1089–1107.

[36] Kilbas, A., Srivastava, H., and Trujillo, J. (2006). *Theory and applications of fractional differential equations*, volume 204. Elsevier.

[37] Klafter, J. and Sokolov, I. M. (2005). Anomalous diffusion spreads its wings. *Phys. World*, 18(8):29.

[38] Kopteva, N. (2019). Error analysis of the $L1$ method on graded and uniform meshes for a fractional-derivative problem in two and three dimensions. *Math. Comput.*, 88(319):2135–2155.

[39] Kreiss, H.-O., Petersson, N., and Yström, J. (2004). Difference approximations of the Neumann problem for the second order wave equation. *SIAM J. Numer. Anal.*, 42:1292–1323.

[40] Krepysheva, N., Pietro, L. D., and Néel, M.-C. (2006). Space-fractional advection-diffusion and reflective boundary condition. *Phys. Rev. E*, 73(2):021104.

[41] Kucerovsky, D., Mousavand, K., and Sarraf, A. (2016). On some properties of Toeplitz matrices. *Cogent Math.*, 3(1):1154705.

[42] Lakestani M., Dehghan M., I.-p. S. (2012). The construction of operational matrix of fractional derivatives using B-spline functions. *Commun. Nonlinear Sci. Numer. Simul.*, 17(3):1149–1162.

[43] Le, K., McLean, W., and Mustapha, K. (2016). Numerical solution of the time fractional Fokker-Planck equation with general forcing. *SIAM J. Numer. Anal.*, 54:1763–1784.

[44] Li, C. and Cai, M. (2019). *Theory and numerical approximations of fractional integrals and derivatives*. SIAM.

[45] Li, C., Deng, W., and Wu, Y. (2012). Finite difference approximations and dynamics simulations for the Lévy fractional Klein-Kramers equation. *Numer. Methods Partial Differ. Equ.*, 28:1944–1965.

[46] Li, C. and Zeng, F. (2015). *Numerical methods for fractional calculus (Vol. 24)*. CRC Press.

[47] Lighthill, M. J. (1958). *An introduction to Fourier analysis and generalised functions.* Cambridge University Press.

[48] Magdziarz, M., Gajda, J., and Zorawik, T. (2014). Comment on fractional Fokker-Planck equation with space and time dependent drift and diffusion. *J. Stat. Phys.*, 154:1242–1250.

[49] Marden, M. (1989). *Geometry of polynomials*. American Mathematical Society.

[50] Meerschaert, M. M. and Tadjeran, C. (2004). Finite difference approximations for fractional advection–dispersion flow equations. *J. Comput. Appl. Math.*, 172(1):65–77.

[51] Metzler, R. and Klafter, J. (2000). The random walk's guide to anomalous diffusion: a fractional dynamics approach. *Phys. Rep.*, 339:1–77.

[52] Miller, K. (1981). On the inverse of the sum of matrices. *Mathematics magazine*, 54(2):67–72.

[53] Mulholland, H. (1949). On generalizations of Minkowski's inequality in the form of a triangle inequality. 2(1):249–307.

[54] Narasimhan, T. (2009). The dichotomous history of diffusion. *Phys. Today*, 62(7):48–53.

[55] Narasimhan, T. N. (2004). Fick's insights on liquid diffusion. *Eos, Transactions American Geophysical Union*, 85(47):499–501.

[56] Nezza, E., Palatucci, G., and Valdinoci, E. (2012). Hitchhiker's guide to the fractional Sobolev spaces. *Bull. Sci. Math.*, 136:521–573.

[57] Nichols, J., Henry, B., and Angstmann, C. (2018). Subdiffusive discrete time random walks via Monte Carlo and subordination. *J. Comput. Phys.*, 372:373–384.

[58] Nikolski, N. (2020). *Toeplitz matrices and operators*, volume 182. Cambridge University Press.

[59] Padash, A., Chechkin, A., Dybiec, B., Pavlyukevich, I., Shokri, B., and Metzler, R. (2019). First-passage properties of asymmetric Lévy flights. *J. Phys. A: Math. Theor.*, 52(45):454004.

[60] Padash, A., Chechkin, A. V., Dybiec, B., Magdziarz, M., Shokri, B., and Metzler, R. (2020). First passage time moments of asymmetric Lévy flights. *J. Phys. A: Math. Theor.*, 53(27):275002.

[61] Patankar, S. V. (2018). *Numerical heat transfer and fluid flow*. CRC press.

[62] Pezza, L. and Pitolli, F. (2018). A fractional spline collocation-Galerkin method for the time fractional diffusion equation. *Commun. Appl. Ind. Math.*, 9:104–120.

[63] Pinto, L. and Sousa, E. (2017). Numerical solution of a time-space fractional Fokker Planck equation with variable force field and diffusion. *Commun. Nonlinear Sci. Numer. Simul.*, 50:211–228.

[64] Podlubny, I. (1998). *Fractional differential equations: an introduction to fractional derivatives, fractional differential equations, to methods of their solution and some of their applications*. Elsevier.

[65] Richtmyer, R. D. and Morton, K. W. (1994). *Difference methods for initial-value problems*. Malabar.

[66] Ross, B. (1977). The development of fractional calculus 1695–1900. *Hist. Math.*, 4(1):75–89.

[67] Saichev, A. and Zaslavsky, G. (1997). Fractional kinetic equations: solutions and applications. *Chaos*, 7(4):753–764.

[68] Samorodnitsky, G. and Taqqu, M. (2017). *Stable Non-Gaussian Random Processes: Stochastic Models with Infinite Variance: Stochastic Modeling*. Routledge.

[69] Shen, S. and Liu, F. (2004). Error analysis of an explicit finite difference approximation for the space fractional diffusion equation with insulated ends. *Anziam J.*, 46:C871–C887.

[70] Smith, G. D. (1985). *Numerical solution of partial differential equations: finite difference methods.* Oxford university press.

[71] Sokolov, I. M. (2012). Models of anomalous diffusion in crowded environments. *Soft Matter*, 8(35):9043–9052.

[72] Sousa, E. (2003). The controversial stability analysis. *Appl. Math. Comput.*, 145:777–794.

[73] Sousa, E. (2009). Finite difference approximations for a fractional advection diffusion problem. *J. Comput. Phys.*, 228(11):4038–4054.

[74] Sousa, E. (2011). Numerical approximations for fractional diffusion equations via splines. *Comput. Math. Appl.*, 62:938–944.

[75] Sousa, E. (2013). Numerical solution of a model for turbulent diffusion. *Int. J. Bifurcat. Chaos*, 23(10):1350166.

[76] Sousa, E. and Li, C. (2015). A weighted finite difference method for the fractional diffusion equation based on the Riemann–Liouville derivative. *Appl. Numer. Math.*, 90:22–37.

[77] Strichartz, R. S. (2003). *A guide to distribution theory and Fourier transforms*. World Scientific Publishing Company.

[78] Stynes, M. (2018). Fractional-order derivatives defined by continuous kernels are too restrictive. *Appl. Math. Lett.*, 85:22–26.

[79] Tang, T. (1993). A finite difference scheme for partial integro-differential equations with a weakly singular kernel. *Appl. Numer. Math.*, 11:309–319.

[80] Tilling, K., Macdonald-Wallis, C., Lawlor, D. A., Hughes, R. A., and Howe, L. D. (2014). Modelling childhood growth using fractional polynomials and linear splines. *Ann. Nutr. Metab.*, 65(2-3):129–138.

[81] Titchmarsh, E. C. (1948). *Introduction to the theory of Fourier integrals (Vol. 2)*. Oxford: Clarendon Press.

[82] Trench, W. F. (1964). An algorithm for the inversion of finite Toeplitz matrices. *Journal of the Society for Industrial and Applied Mathematics*, 12(3):515–522.

[83] Trench, W. F. (2009). Inverses of lower triangular Toeplitz matrices. *Unpublished.[Online].*

[84] Unser, M. (1999). Splines: A perfect fit for signal and image processing. *IEEE Signal Process. Mag.*, 16:22–38.

[85] Unser, M. and Blu, T. (2000). Fractional splines and wavelets. *SIAM Rev.*, 42:43–67.

[86] Wang, X., Duan, J., Li, X., and Song, R. (2018). Numerical algorithms for mean exit time and escape probability of stochastic systems with asymmetric Lévy motion. *Appl. Math. Comp.*, 337:618–634.

[87] Wang, Y. (2015). A compact finite difference method for solving a class of time fractional convection-subdiffusion equations. *BIT Numer. Math.*, 55:1187–1217.

[88] Xu, K. and Darve, E. (2020). Isogeometric collocation method for the fractional Laplacian in the 2d bounded domain. *Comput. Methods Appl. Mech. Eng.*, 364:112936.

[89] Yuste, S. and Acedo, L. (2005). An explicit finite difference method and a new von Neumann type stability analysis for fractional diffusion equations. *SIAM J. Numer. Anal.*, 42:1862–1874.

[90] Zahra, W. K. and Elkholy, S. M. (2012). Quadratic spline solution for boundary value problem of fractional order. *Numer. Algorithms*, 59(3):373–391.

[91] Zaky, M., Hendy, A., and Macías-Díaz, J. (2020). Semi-implicit Galerkin–Legendre spectral schemes for nonlinear time-space fractional diffusion–reaction equations with smooth and nonsmooth solutions. *J. Sci. Comput.*, 82(1):1–27.

[92] Zeng, F., Zhang, Z., and Karniadakis, G. (2016). Fast difference schemes for solving high-dimensional time-fractional subdiffusion equations. *J. Comput. Phys.*, 307:15–33.

[93] Zhao, S. (2007). On the spurious solutions in the high-order finite difference methods for eigenvalue problems. *Comput. Methods Appl. Mech. Eng.*, 196(49):5031–5046.

[94] Zhuang, P., Liu, F., Anh, V., and Turner, I. (2008). New solution and analytical techniques of the implicit numerical method for the anomalous subdiffusion equation. *SIAM J. Numer. Anal.*, 46:1079–1095.